Synthèse de polyuréthanes par polymérisation par ouverture de cycle anionique et auto-assemblage de copolymères amphiphiles à base de polyuréthane

Dapeng Zhang

THÈSE DE DOCTORAT
DE L'UNIVERSITÉ PSL

Préparée à l'École Nationale Supérieure de Chimie de Paris

Synthèse de polyuréthanes par polymérisation par ouverture de cycle anionique et auto-assemblage de copolymères amphiphiles à base de polyuréthane

Synthesis of polyurethanes by anionic ring opening polymerization and self-assembly of polyurethane-based amphiphilic copolymers

Soutenue par
Dapeng ZHANG
Le 08 Novembre 2018

Ecole doctorale n° 406
Ecole Doctorale de Chimie moléculaire de Paris Centre

Spécialité
Chimie moléculaire

Composition du jury :

M. Renaud NICOLAY Professeur des Universités, Université PSL, ESPCI Paris	*Président*
M. Daniel TATON Professeur des Universités, Université de Bordeaux-Bordeaux INP	*Rapporteur*
M. Christophe CHASSENIEUX Professeur des Universités, Le Mans Université	*Rapporteur*
Mme Sylvie POURCHET Maître de Conférences, Université Bourgogne Franche-Comté	*Examinateur*
Mme Min-Hui LI Directeur de Recherche CNRS, Université PSL, Chimie ParisTech	*CoDirecteur de thèse*
M. Christophe THOMAS Professeur des Universités, Université PSL, Chimie ParisTech	*Directeur de thèse*

Synthesis of polyurethanes by anionic ring opening polymerization and self-assembly of polyurethane-based amphiphilic copolymers

Dapeng ZHANG

Supervised by: Pr. Christophe THOMAS and Dr. Min-Hui LI

Table of Contents

Acknowledgement

Firstly, I would like to deeply thank my thesis supervisors, Prof. Christophe Thomas and Dr. Min-Hui Li for giving me the opportunity to do research for my PhD thesis at Chimie ParisTech, PSL University. I am very appreciated for their continuous support, assistance and encouragement during my three years PhD research in their groups. They not only teach me how to do the research, such as synthesis, polymerization and self-assembly, but also teach me how to think, design and analyze to be a research scientist. Prof. Christophe Thomas inspired me a lot by his optimistic attitude. Each time after talking with him, I felt very relaxed and confident. Dr. Min-Hui Li often helped me looking for solutions to solve problems in my experiments and sometimes even put on her lab coat to teach me how to do characterization by microscope herself in the lab.

Secondly, I would like to thank my committee members of defense, Prof. Daniel Taton, Prof. Christophe Chassenieux, Prof. Renaud Nicolaÿ and Dr. Sylvie Pourchet for being as my committee members. I want to thank you for letting my defense be an enjoyable moment, and for your brilliant comments and suggestions. Thank you very much.

In addition, I would like to thank all the former group members. Dr. Yang Zhang is thanked for helping me adapt to the lab and research environment when I firstly joined in the group. Also, I am thankful for his help in the synthesis and characterization of my products during the first few months in the lab. Dr. Lucie Fournier and Dr. Wei Qiang are thanked for being so helpful and kind to me as colleagues joining in the group in the same year. Dr. Paul Marin, Dr. Vincent Richard, Dr. Benoit Rhone, Dr. Malcolm Zimbron, Dr. Jiraya Kiriratnikom and Dr. Xinfeng Tao are thanked for their help and good suggestions to my research projects. I learned a lot from you.

Of course, the present members are also thanked very much. Dr. Carine Robert is thanked for the help of MALDI-TOF-MS measurement and good suggestions to my

A special thank to my girlfriend Yujiao Fan for always supporting me with her unconditional love and care, confidence, patience and encouragement during my three years PhD study in Paris.

Finally, I would to thank my family in China. My mother, father and little brother give their endless love, care, faith, support and understanding to me throughout my life. I would like to dedicate this thesis to my Family.

Dapeng Zhang

November 2018 in Paris

Table of Abbreviations

ACE	Activated chain-end
AIBN	2,2'-Azobis(isobutyronitrile)
AROP	Anionic ring opening polymerization
ATR-IR	Attenuated total reflectance-Infrared spectroscopy
ATRP	Atom transfer radical polymerization
BMC	Bis-methylcarbamate
n-BuLi	n-Butyllithium
CAT	Critical aggregation temperature
CD spectrum	Circular dichroism spectrum
CHU	5-Membered cyclohexane urethane monomer
CGC	Critical gelation concentration
ε-CL	ε-Caprolactone
CMC	Critical micelle concentration
CPP	Critical packing parameter
CRP	Controlled radical polymerization
CuAAC	Copper-catalyzed azide-alkyne cycloaddition
D_h	Hydrodynamic diameter
DBU	1,8-Diazabicyclo[5.4.0]undec-7-ene
DCM	Dichloromethane
DLS	Dynamic light scattering
DP	Degree of polymerization
DMAc	N,N-dimethylacetamide
DMAP	4-(Dimethylamino)pyridine
DMC	Dimethylcarbonate
DMCHA	Dimethylcyclohexylamine
DMEA	Dimethylethanolamine

DMF	N,N-Dimethylformamide
DSC	Differential scanning calorimetry
EDC•HCl	1-(3-Dimethylaminopropyl)-3-ethylcarbodiimide hydrochloride
cryo-EM	Cryo-electron microscopy
EO	Ethylene oxide
GC	Gas chromatography
GPC	Gel permeation chromatography
$H_{12}MDI$	Hydrogenated methylene diphenyl diisocyanate
HPLC	High-performance liquid chromatography
In situ IR	In situ infrared spectroscopy
LA	Lactide
LC	Liquid crystalline
LCM	Large compound micelle
LCST	Lower critical solution temperature
$LiN(TMS)_2$	Lithium bis(trimethylsilyl)amide
MALDI-TOF-MS	Matrix-assisted laser desorption ionization-time of flight mass spectrometry
MCC	Cholesteryl substituted trimethylenecarbonate monomer
MDI	Methylene diphenyl diisocyanate
N-ACL	*N*-acetylcaprolactam
NaH	Sodium hydride
NCA	*N*-carboxyanhydride
NDI	1,5-Naphthalene diisocyanate
NHC	*N*-heterocyclic carbene
NMP	Nitroxide-mediated polymerization
NMR	Nuclear magnetic resonance
PAA	Poly(acrylic acid)

PA6	Polyamide 6
PAChol	Cholesterol-based smectic LC polymer
PB-*b*-PEO	Poly(butadiene-*b*-ethylene oxide)
PBA	Poly(*n*-butyl acrylate)
PBLG	Poly(γ-benzyl-ʟ-glutamate)
PBO	Poly(butylene oxide)
PCL	Polycaprolactone or Poly(ε-caprolactone)
PDI	Polydispersity index
PDLA	Poly(ᴅ-(+)-*R*-lactide)
PEE-*b*-PEO	Poly(ethylethylene-*b*-ethylene oxide)
PEG	Polyethylene glycol
mPEG	Poly(ethylene glycol) monomethyl ether
mPEG-COOH	Carboxylic acid functionalized mPEG
mPEG-SH	Thiol-terminated mPEG
PEO	Polyethylene oxide
PHU	Polyhydroxyurethane
PLA	Polylactide
PLLA	Poly(ʟ-(−)-*S*-lactide)
PMMA	Poly(methyl methacrylate)
POM	Polarized optical microscopy
PPE	Polyphosphoester
PPG	Poly(propylene glycol)
PS	Polystyrene
PTHF	Poly(tetrahydrofuran)
PTU	Poly(trimethylene urethane)
PTeU	Poly(tetramethylene urethane)
PU	Polyurethane
PUP	Polyurethane phosphate ester
RAFT	Reversible addition-fragmentation chain transfer

ROMP	Ring-opening metathesis polymerization
ROP	Ring opening polymerization
SEM	Scanning electron microscopy
Sn(Oct)$_2$	Stannous octoate
TBD	1,5,7-Triazabicyclo[4.4.0]dec-5-ene
TEA	Triethylamine
TEM	Transmission electron microscopy
TDI	Toluene diisocyanate
TfOMe	Trifluoromethanesulfonate
TfOTf	Trifluoromethanesulfonic acid anhydride
T_g	Glass transition temperature
TGA	Thermogravimetric analysis
THF	Tetrahydrofuran
TMC	Trimethylene carbonate
TU	Trimethylene urethane
TeU	Tetramethylene urethane
XRD	X-Ray Diffraction
Y[N(TMS)$_2$]$_3$	Yttrium tris[N,N-bis(trimethylsilyl)amide]
Y(OiPr)$_3$	Yttrium tris(isopropoxide)
Y(OTf)$_3$	Yttrium trifluoromethanesulfonate

Synthèse de polyuréthanes par polymérisation par ouverture de cycle anionique et auto-assemblage de copolymères amphiphiles à base de polyuréthane

RÉSUMÉ

Le présent travail décrit la synthèse de polyuréthanes (PUs) sans isocyanate par la technique de polymérisation par ouverture de cycle anionique (AROP) et l'étude du comportement d'auto-assemblage de copolymères diblocs linéaires amphiphiles à base de PU et de copolymères greffés. Généralement, les PUs sont préparés par polyaddition de diols (ou polyols) sur des diisocyanates (ou polyisocyanates). Cette méthode nécessite des conditions drastiques pour conduire la réaction vers une conversion élevée et utilise des isocyanates très sensibles à l'humidité et toxiques, limitant ainsi leurs applications médicales. Dans ce travail, nous utilisons une nouvelle stratégie, basée sur la polymérisation par ouverture de cycle (ROP), pour obtenir des polyuréthanes aliphatiques à partir de carbamates cycliques. Une série d'homopolymères de PU ayant des poids moléculaires différents et des indices de polydispersité étroits ont été synthétisés. Par ailleurs, une série de copolymères séquencés linéaires amphiphiles à base de PU, PEG-*b*-PUs (polyéthylène glycol-*b*-polyuréthanes) et des copolymères greffés (PU-*g*-PEGs) ont été préparés. Les comportements d'auto-assemblage de ces copolymères amphiphiles à base de PU ont été étudiés en détails. La thèse se compose de cinq chapitres, dont le dernier est constitué par la partie expérimentale. Nous croyons que le présent travail fournira plus d'options et d'inspirations pour que les personnes puissent préparer des PUs sans isocyanate et des matériaux nanostructuraux fonctionnalisés à base de PU avec des applications potentielles.

Vous trouverez donc ci-dessous le résumé des quatre premiers chapitres.

Chapitre I. Introduction

1.1 Introduction générale des polyuréthanes

Les polyuréthanes (PU) sont une classe de polymères composés d'unités organiques reliées par des liaisons carbamate (uréthane, -NHCOO-) et font partie des matériaux polymères les plus importants et les plus polyvalents. Les PU sont découverts par Otto Bayer et ses collègues chez I.G. Farben Industrie, Allemagne, en 1937. La production industrielle de PU a commencé et a considérablement augmenté pendant la Seconde Guerre mondiale. En 1952, les propriétés élastomères du PU se sont nettement améliorées, car le polyisocyanate, en particulier le diisocyanate de toluène (TDI), devient disponible dans le commerce. Les élastomères thermoplastiques PU et les plastiques techniques PU ont été développés respectivement dans les années 1970 et 1980, ce qui a favorisé le développement rapide de l'industrie des polyuréthanes. Avec le développement continu des matériaux PU, leur production mondiale augmente d'année en année et est estimée à plus de 22 millions de tonnes en 2020, ce qui représente près de 5% en poids de la production mondiale totale de polymères.

$$n+m \quad O{=}C{=}N{-}R_1{-}N{=}C{=}O \; + \; n \; HO{-}R_2{\cdot}OH \; + \; m\,HO{\left(\!\!\begin{array}{c}H_2\\C\end{array}\!\!\right)}_x OH \longrightarrow$$

$$\left[\begin{array}{c}O\\ \| \\ C\end{array}{-}\begin{array}{c}H\\N\end{array}{-}R_1{-}\begin{array}{c}H\\N\end{array}{-}\begin{array}{c}O\\ \| \\ C\end{array}\left[O{\left(\!\!\begin{array}{c}H_2\\C\end{array}\!\!\right)}_x O{-}\begin{array}{c}O\\ \| \\ C\end{array}{-}\begin{array}{c}H\\N\end{array}{-}R_1{-}\begin{array}{c}H\\N\end{array}{-}\begin{array}{c}O\\ \| \\ C\end{array}\right]_{\frac{m}{n}}{-}O{-}R_2{\cdot}O\right]_n$$
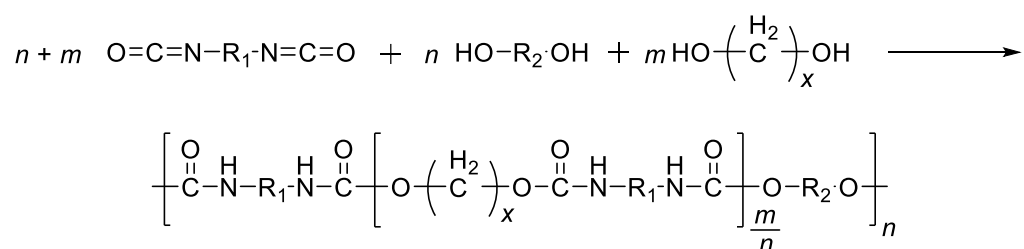
Figure 1. Structure générale des PU linéaires, monophasés (m = 0) et à phases séparées (m = 1, 2) à l'échelle micrométrique. Les segments rigides et flexibles sont distribués statistiquement.

Les PU sont des polymères contenant une répétition de liaisons uréthane dans leur structure (Figure 1). Dans l'industrie, les PU sont fabriqués par polyaddition de polyisocyanates (OCN-R$_1$-NCO) et de macropolyols (HO-R$_2$-OH) (Figure 1), où de nombreux groupes uréthane sont formés sur le squelette polymère. Lors de la production de matériaux en PU, les diols ou les diamines à chaîne courte sont

généralement ajoutés comme agents d'extension de chaîne pour ajuster précisément les propriétés des PU. Le premier réagit dans les liaisons uréthane comme les macropolyols tandis que le second réagit dans les liaisons urée. Ces deux liaisons sont appelées segment rigide dans la structure PU et les segments polyol sont appelés segments flexibles. Par conséquent, les PU sont en fait construits par de nombreux segments rigides et flexibles sous une forme modulaire.

En raison de leur structure très spécifique, les PU sont la seule classe de polymères pouvant présenter un comportement thermoplastique, élastomère et thermodurcissable en ajustant leur composition chimique et morphologique, ce qui leur permet d'être utilisés pour la production de mousses, sièges, roues élastomères et pneus, revêtements de performance, adhésifs.

Bien que les PU soient d'excellents matériaux polymères avec de nombreuses applications dans notre vie quotidienne, leur mise en œuvre peut entraîner des risques importants. Étant donné que les polyisocyanates sont synthétisés à partir de composés aminés et du phosgène hautement toxique ($COCl_2$), les matériaux finaux peuvent également être toxiques, ce qui limite leur utilisation dans des domaines liés au biomédical. En outre, le stockage du phosgène hautement toxique et volatil dans les usines de polyuréthane est également un problème important, ce qui représente un danger potentiel conséquent pour les personnes qui l'utilisent au quotidien ou vivent à proximité. Par conséquent, le développement de voies alternatives sans isocyanate pour préparer les PU devient de plus en plus primordial pour la recherche industrielle et universitaire.

À notre connaissance, il existe quatre types de voies sans isocyanate (Figure 2) : (1) la polyaddition de dicarbonates et de diamines cycliques (voie des carbonates cycliques) ; (2) la polycondensation de dicarbonates activés linéaires et de diamines (voie bis(dialkylcarbonate)) ; (3) polycondensation de carbamates et de diols activés linéaires (voie de transuréthanisation) ; (4) polymérisation par ouverture de cycle (ROP) des carbamates cycliques (voie ROP). La description détaillée de ces quatre voies sans isocyanate est résumée dans l'introduction.
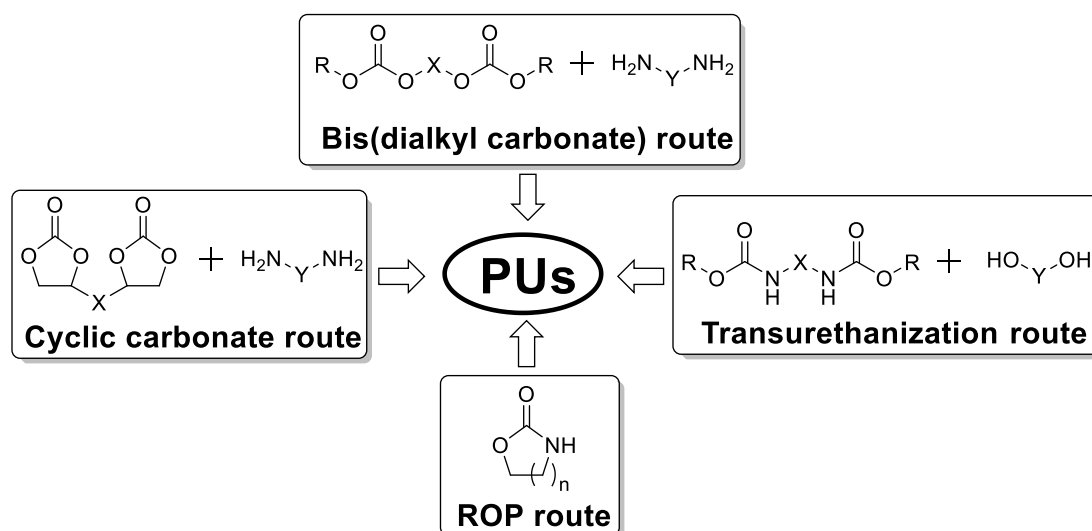
Figure 2. Principales voies sans isocyanate utilisées pour la synthèse des PU.

1.2 Auto-assemblage de copolymères amphiphiles à base de polyuréthane

L'auto-assemblage moléculaire est le processus par lequel les molécules se forment ou s'agrègent dans un arrangement défini sans aucune orientation ou gestion de la part de la source extérieure. Il est omniprésent dans la nature. Dans l'organisme vivant, presque tous les composants, de l'ADN, des protéines, des cellules à toutes sortes d'organes, sont construits par l'auto-assemblage de diverses biomolécules. Par exemple, les membranes cellulaires sont formées par l'auto-assemblage de phospholipides amphiphiles ; les doubles hélices d'ADN sont construits par auto-assemblage de paires de bases; l'auto-assemblage des protéines conduit à la formation de structures quaternaires. Inspirées par les systèmes biologiques de la nature, les études d'auto-assemblage moléculaire ont attiré de plus en plus l'attention ces dernières décennies pour concevoir et développer des assemblages artificiels avec des structures, propriétés et applications spécifiques, ainsi que la compréhension des principes et des théories.

Jusqu'à présent, de nombreux types de structures supramoléculaires sophistiquées ont été préparés par auto-assemblage de différentes molécules telles que des lipides, des tensioactifs de faible masse moléculaire, des polymères ayant des structures topologiques différentes, notamment. La force motrice d'auto-assemblage peut être une interaction hydrophobe, un empilement π-π, une liaison hydrogène ou une interaction électrostatique. Les tailles des auto-assemblages varient de l'échelle microscopique à

l'échelle macroscopique. Leurs différentes morphologies permettent la formation de micelles, vésicules, tubes, disques, bâtons, fibres, membranes par exemple.

Les polymères, et notamment les copolymères à structures amphiphiles, font preuve d'une excellente capacité d'auto-assemblage en masse ou en solution, basée sur des principes similaires à ceux rencontrés pour l'auto-assemblage de petites molécules, telles que les lipides ou les tensioactifs amphiphiles. Les polymères classiques comprennent les polymères linéaires, les copolymères à blocs linéaires, les polymères greffés, les polymères en étoile et les polymères dendritiques (Figure 3). Comparés aux agrégats définis de petites molécules, les agrégats de polymères présentent une stabilité et une durabilité supérieures en raison de leurs propriétés mécaniques et physiques. Par conséquent, l'auto-assemblage des polymères a attiré de plus en plus d'attention, non seulement pour son intérêt académique mais aussi pour leurs applications potentielles dans de nombreux domaines, tels que la biomédecine, les biomatériaux, les matériaux photoélectriques, la microélectronique et les catalyseurs.
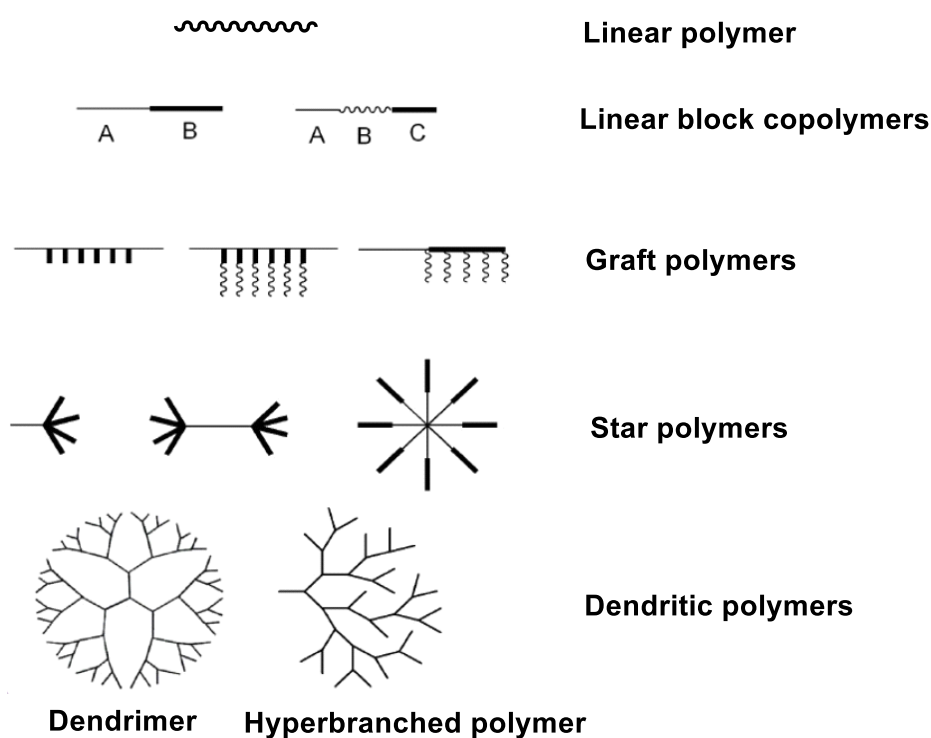
Figure 3. Polymères avec différentes topologies pour l'auto-assemblage.

Les copolymères à blocs linéaires, constitués de deux ou plusieurs séquences chimiquement distinctes et fréquemment non miscibles qui sont liées entre elles par

covalence, sont les systèmes les plus étudiés pour l'auto-assemblage. Parmi les différents types de copolymères à blocs disponibles (par exemple, les copolymères à blocs, les copolymères à trois blocs, les copolymères à blocs multiples, les copolymères à blocs coniques), les copolymères à blocs sont les plus étudiés en raison de leur structure relativement simple.

Selon la différence de solubilité des blocs dans l'eau, les copolymères diblocs peuvent être classés en systèmes amphiphiles, doubles hydrophiles et doubles hydrophobes. La plupart des études d'auto-assemblage sur les copolymères diblocs se concentrent sur les copolymères diblocs amphiphiles. En fonction de la différence de conformation des blocs, ils peuvent être classés en deux catégories : les copolymères à blocs tige-tige, bobine-bobine et tige-bobine. L'auto-assemblage des copolymères à blocs tige-tige a rarement été étudié, alors que les copolymères à blocs bobine-bobine et tige-bobine sont les objets représentatifs de l'auto-assemblage des copolymères diblocs linéaires.

Généralement, les copolymères diblocs « pelote-pelote » sont formés par des séquences polymères relativement souples qui sont chimiquement incompatibles. Ils peuvent donc permettre une séparation par microphases pour former de nombreux types de morphologies d'auto-assemblage. Pour l'auto-assemblage des copolymères diblocs « pelote-pelote », deux systèmes ont particulièrement attiré l'attention : les copolymères diblocs contenant des segments poly(éthylène glycol) (PEG) et les micelles de type « crew-cut » (littéralement micelles coupées en brosse), pour lesquelles la longueur de la chaîne hydrophobe est majoritaire.

L'auto-assemblage des copolymères diblocs « bâtonnet-pelote » n'est pas seulement affecté par la séparation des microphases mais également par l'anisotropie de forme et l'ordre supplémentaire dans le bloc en forme de bâtonnet, ce qui entraîne un comportement d'auto-assemblage plus compliqué que celui des copolymères. L'anisotropie de forme et l'ordre supplémentaire peuvent être introduits par des structures cristallines et cristallines liquides (LC) formées dans le bloc rigide, ou par des structures secondaires telles que l'hélice α ou le feuillet β dans le cas d'un peptide. Les exemples typiques de l'auto-assemblage de copolymères à blocs « pelote-pelote » et « bâtonnet-pelote » sont résumés dans l'introduction.

En tant que polymère ayant une bonne résistance et biocompatibilité, les polyuréthanes sont des matériaux polymères qui peuvent être potentiellement utilisés pour former des nanostructures ordonnées par auto-assemblage. Parallèlement, les progrès de la synthèse des polymères permettent de préparer des polyuréthanes biodégradables avec différentes structures et topologies pour l'auto-assemblage. Dans la littérature, de nombreuses études ont porté sur le développement de nanostructures de polyuréthane biodégradables avec diverses fonctionnalités pour des applications biomédicales telles que la délivrance de médicaments, en raison de leur bonne biocompatibilité, En outre, la conception et le développement d'auto-assemblages à base de polyuréthane pour des applications autres que les applications biomédicales sont également très intéressants. Les exemples typiques de l'auto-assemblage de copolymères amphiphiles à base de polyuréthane avec différentes topologies sont décrits dans l'introduction.

Chapitre II. Polymérisation par ouverture de cycle anionique contrôlée de carbamates cycliques à 5 chaînons en polyuréthanes

2.1 Introduction

La polymérisation par ouverture de cycle (ROP) est une polymérisation au cours de laquelle un monomère cyclique s'ouvre pour donner une unité monomère qui est acyclique ou contient moins de cycles que le monomère. Avec la polymérisation en chaîne (radicalaire et ionique) et la polymérisation par condensation, la ROP est l'une des trois voies importantes pour synthétiser les polymères. La force motrice de la ROP est libération de la tension de cycle des monomères. La polymérisabilité des monomères cycliques dépend des facteurs thermodynamiques et cinétiques mais les facteurs thermodynamiques sont les plus importants.

Les monomères cycliques communs pour ROP comprennent non seulement les alcanes cycliques, les alcènes mais également les hétérocycles, tels que les éthers, esters (lactones, lactides), les carbonates, les acétals, les anhydrides, les amines, les amides

(lactames), les *N*-carboxyanhydrides, les carbamates, les sulfures. Certaines réactions de ROP peuvent passer par un mécanisme similaire à celui d'une polymérisation en chaîne (ajout de monomère à l'extrémité d'une chaîne en croissance). Cependant, de nombreuses réactions de ROP sont différentes et procèdent par des mécanismes similaires à la polymérisation par condensation. Le centre de propagation est généralement radical, cationique ou anionique. Par conséquent, la ROP peut être de trois types : ROP radicalaire, ROP cationique et ROP anionique. Il convient également de noter que la ROP des oléfines cycliques se déroule *via* un autre type de mécanisme, à savoir la polymérisation par métathèse par ouverture de cycle (ROMP).

Dans ce chapitre, nous étudions principalement la ROP anionique (AROP) d'un monomère de type carbamate cyclique à 5 chaînons pour préparer sans isocyanate des polyuréthanes (PU) bien définis avec de nouvelles structures. Ce chapitre se divise en quatre parties : la synthèse des monomères, la polymérisation, le mécanisme ROP et la cinétique ROP.

2.2 Synthèse de monomères

La synthèse du monomère à 5 chaînons (CHU) comprend trois étapes, comme le montre la Figure 4. Tout d'abord, le 4-vinyl-1-cyclohexène-1,2-époxyde (**1**), qui est un mélange de deux types de diastéréoisomères confirmée par analyse RMN et GC, est mis à réagir avec un excès d'ammoniac pour synthétiser des aminoalcools (**2** et **3**). Indépendamment de l'énantiosélectivité des produits, il existe deux isomères de position ayant des positions vinyliques différentes sur le cycle cyclohexane produit à partir de cette étape. Ceci est dû au fait que les deux atomes de carbone de l'époxyde **1** avaient la même probabilité d'être attaqués par l'ammoniac. Deuxièmement, le mélange composé de **2** et **3** réagit avec le chloroformiate d'éthyle pour donner les composés **4** et **5**. Enfin, les carbamates cycliques **6** et **7** ont été obtenus par réaction de fermeture de cycle de **4** et **5** en présence d'un excès d'hydrure de sodium. Après purification par chromatographie sur colonne, on obtient **6** et **7** avec un rendement de 30% et 37% respectivement. Après caractérisation par RMN et HPLC, le CHU a été obtenu sous la forme d'un mélange de deux diastéréoisomères ou de quatre stéréoisomères et a été

utilisé sous cette forme pour synthétiser des PU.
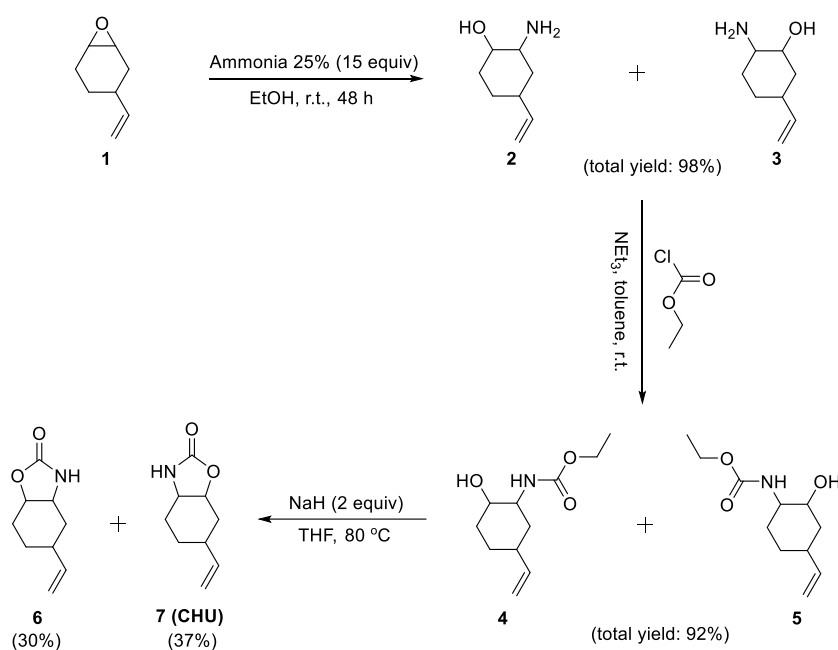
Figure 4. Voie de synthèse du monomère carbamate cyclique à 5 membres (CHU).

2.3 Polymérisation

Nous avons d'abord tenté de réaliser la ROP du monomère CHU en présence de catalyseurs de terres rares tels que le tris(isopropoxyde) d'yttrium (Y(O*i*Pr)$_3$), le tris[*N,N*-bis(triméthylsilyl)amide] d'yttrium (Y[N(TMS)$_2$]$_3$) et le trifluorométhanesulfonate d'yttrium (Y(OTf)$_3$) en utilisant également des alcools (*e.g.*, le néopentanol) comme amorceurs nucléophiles. Cependant, après de nombreux essais de polymérisation dans différentes conditions de réaction, des PU de poids moléculaires suffisants (> 2000 Da) n'ont pu être obtenus.

Par conséquent, nous avons essayé d'utiliser d'autres types de catalyseurs tels que les catalyseurs cationiques ou anioniques. Puis, par ajout de bases fortes (hydrure de sodium, *n*-butyllithium), nous avons constaté que des polymères ayant des poids moléculaires plus élevés (> 2000 Da) étaient obtenus. Cela a été confirmé par GPC (chromatographie par perméation de gel), ce qui indiquait que la ROP anionique du CHU pouvait représenter une bonne stratégie pour préparer des PU. Par la suite, nous nous sommes concentrés sur la ROP anionique de CHU pour trouver des conditions réactionnelles optimales.
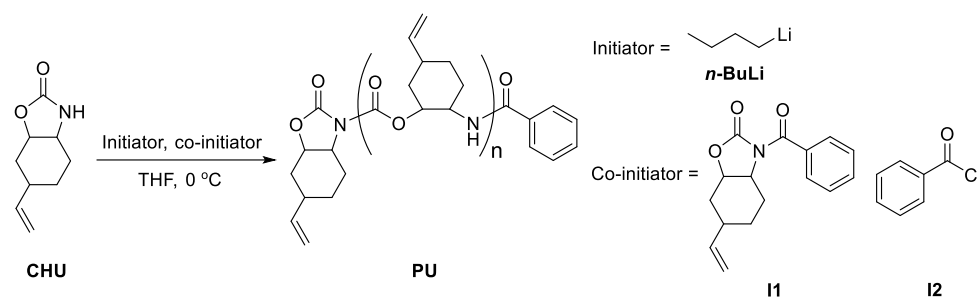
Figure 5. Schéma synthétique de PU par ROP anionique de CHU.

Tableau 1. ROP du monomère CHU pour préparer les PU.

Entry[a]	Initiator	Co-initiator	Monomer/ Initiator/ Co-initiator	Time /h	Conversion[b]	$M_{n,theory}$	$M_{n,NMR}$[b]	DP[b]	$M_{n,GPC}$[c]	PDI[c]
1	*n*-BuLi	-	20/1/1	5	8%	540	-	-	-	-
2	*n*-BuLi	I1	20/1/1	5	91%	3300	3900	23	5400	1.23
3	LiN(TMS)$_2$	I1	20/1/1	5	84%	2900	4600	27	4400	1.55
4	NaH	I1	20/1/1	5	47%	1700	3600	21	2100	1.50
5	*n*-BuLi	I2	20/2/1	5	73%	2600	2300	12	2800	1.33
6	*n*-BuLi	*N*-Acetylca-prolactam	20/1/1	5	79%	2800	-	-	5300	1.22
7	*n*-BuLi	I1	10/1/1	4	83%	1700	2400	14	3200	1.29
8	*n*-BuLi	I1	30/1/1	6	81%	4300	4400	26	6100	1.28
9[d]	*n*-BuLi	I1	50/1/1	24	81%	7100	7800	46	7500	1.32

a. Les concentrations de co-amorceurs étaient toutes de 0.0188 M ; *b*. La conversion des monomères, le degré de polymérisation (DP) et le $M_{n,RMN}$ ont été calculés par RMN ^{1}H ; *c*. $M_{n,GPC}$ et PDI ont été obtenus par GPC avec THF comme éluant et PS comme standards ; d. LiBr (1% en poids) a été ajouté dans la solution de polymérisation.

Le schéma de ROP anionique est présenté sur la Figure 5. Les résultats sont résumés dans le Tableau 1. Tout d'abord, une série d'essais de polymérisation a été effectuée pour trouver les conditions de polymérisation, en utilisant le *n*-butyllithium (*n*-BuLi) comme amorceur, en tant que co-amorceur, dans du THF à 0 °C (Figure 5). Ensuite, nous avons effectué plusieurs réactions ROP en utilisant différents rapports monomère/amorceur/co-amorceur. Après un certain temps de polymérisation, les conversions de monomères étaient supérieures à 80% ce qui a été confirmé par les spectres RMN ^{1}H du produit brut.

Des PU purs ont ainsi été obtenus en précipitant les produits bruts dans le *n*-hexane trois fois puis en séchant sous vide pendant 24 h. Ensuite, ils ont été caractérisés soigneusement par RMN et GPC. Comme le montre le Tableau 1, des PU ayant différents degrés de polymérisation (DP) et poids moléculaires ont été obtenus en faisant varier les rapports monomère/amorceur/co-amorceurs. Le DP a été calculé en comparant l'aire intégrée du pic proton du groupement vinyle sur la chaîne latérale des PU et celle du groupe benzyle en bout de chaîne dans les spectres RMN ^{1}H. Les poids moléculaires de la RMN étaient proches des poids théoriques et les PDI obtenus par GPC étaient relativement étroits (1.23-1.35). Tous ces résultats indiquaient que nous avions préparé des PU bien définis. Les PU obtenus ont également été caractérisés par spectrométrie MALDI-TOF, ATR-IR, TGA et DSC.

2.3 Mécanisme ROP

Suite aux résultats des expériences de polymérisation effectuées, nous avons proposé le mécanisme de ROP anionique représenté sur la Figure 6. La ROP anionique du monomère CHU comprend deux étapes d'initiation et de propagation. Pour l'initiation, le monomère réagit dans un premier temps avec l'amorceur pour former un monomère anionique. Puis, l'anion réagit avec le co-amorceur (**I1**) pour former un dimère présentant un nouveau centre *N*-acyle qui peut servir de centre de propagation. La propagation est la réaction continue du monomère anionique et du centre *N*-acyle à l'extrémité de la chaîne polymère avec transfert de protons entre la chaîne polymère et le monomère CHU pour régénérer du monomère anionique.
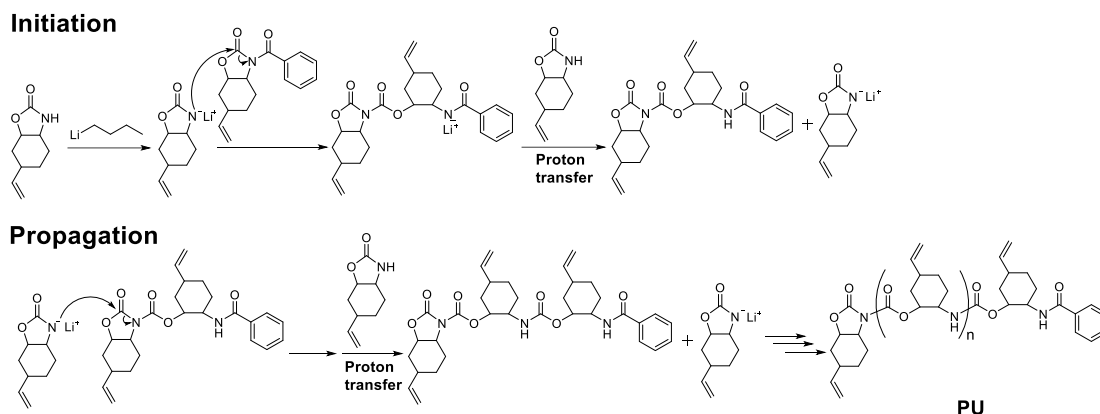
Figure 6. Mécanisme de ROP anionique de CHU avec **I1** comme co-amorceur.

Pour prouver ce mécanisme, la méthode la plus directe consistait à prouver la partie initiation de la ROP car la propagation était la même que celle de la deuxième étape de la partie initiation. En fait, linitiation est l'attaque nucléophile du monomère anionique sur le groupement carbonyle endocyclique du co-amorceurs. Certaines études de la littérature ont montré que les cycles carbamates cycliques *N*-acylés s'ouvraient à partir de la liaison C-N plutôt que de la liaison C-O lorsqu'ils étaient attaqués par des nucléophiles. Ici, nous nous attendions à synthétiser un dimère en utilisant un rapport molaire 1/1/1 entre le monomère, l'amorceur et le co-amorceur. Cependant, cela n'a pas fonctionné parce que le monomère avait tendance à se polymériser pour former un mélange de dimère, de trimère et d'oligomères.

Ensuite, nous avons essayé d'utiliser le spectromètre IR *in situ* pour suivre l'évolution de la réaction "1/1/1" (rapport molaire entre le monomère, l'amorceur et le co-amorceur). Enfin, le mécanisme a été prouvé par la caractérisation *in situ* IR et ^{13}C RMN, qui a clairement montré que le PU était préparé par le mécanisme proposé sur la Figure 6.

2.4 Cinétique ROP

Après avoir exploré le mécanisme de polymérisations, nous nous sommes intéressés à la cinétique de la ROP du monomère CHU. En utilisant un suivi IR *in situ*, nous avons pu observer clairement la variation des concentrations en monomère au cours du processus de polymérisation. Afin d'étudier la relation entre le taux de polymérisation

et la concentration en monomère, nous avons suivi trois polymérisations par IR in situ avec les mêmes concentrations en amorceur et en co-amorceur (**I1**) mais une concentration différente en monomère . Les résultats ont montré que lorsque le rapport molaire entre le monomère et l'amorceur était élevé, la vitesse de polymérisation du monomère CHU pouvait avoir une dépendance de premier ordre sur la concentration en CHU. Lorsque le rapport molaire entre le monomère et l'amorceur était faible, la vitessede polymérisation et la concentration en monomère présentaient des relations mathématiques compliquées. La raison pourrait être que lorsque le rapport molaire entre le monomère et l'initiateur est faible, certaines réactions secondaires pourraient être plus susceptibles de se produire.

Enfin, l'étude préliminaire des propriétés des PU obtenus a montré qu'ils pouvaient présenter des propriétés d'émission déclenchée par regroupement après traitement thermique.

Chapitre III. Synthèse et auto-assemblage de copolymères diblocs linéaires amphiphiles à base de polyuréthane

3.1 Introduction

Les copolymères à blocs linéaires représentent le type de copolymères à blocs le plus courant et le plus étudié en raison de l'architecture relativement simple par rapport aux autres types. Les copolymères diblocs linéaires amphiphiles constitués de deux séquences chimiquement distinctes souvent non miscibles et liées de manière covalente sont particulièrement intéressants car ils peuvent former une multitude de nanostructures définies par auto-assemblage.

L'immiscibilité des deux blocs conduit à l'auto-assemblage de copolymères diblocs linéaires amphiphiles lorsqu'ils sont dissous dans un solvant sélectif qui est un solvant thermodynamiquement bon pour un bloc mais un mauvais solvant pour l'autre. Plus précisément, les chaînes de copolymères s'associent spontanément dans des structures micellaires constituées d'un cœur plus ou moins gonflé et formé par les blocs insolubles

13

entourés d'une couronne souple constituée par des blocs solubles. Les morphologies et tailles des agrégats micellaires sont influencées par de nombreux facteurs, tels que la composition du polymère et son poids moléculaire, le solvant utilisé, la concentration, et les additifs notamment. Lorsque les deux éléments constitutifs sont hydrophobes et hydrophiles, les copolymères diblocs linéaires amphiphiles peuvent s'auto-assembler en solution aqueuse pour former diverses nanostructures, ce qui a suscité un intérêt considérable non seulement en raison de leurs propriétés uniques mais aussi en particulier pour des applications dans le domaine biomédical.

Dans ce chapitre, plusieurs copolymères diblocs linéaires amphiphiles PEG-*b*-PU dans lesquels un bloc est du polyuréthane (PU) hydrophobe et l'autre un poly(éthylène glycol) (PEG) hydrophile ont été préparés en présence de co-amorceurs macromoléculaires à base de mPEG (poly(éthylène glycol) monométhyléther) (mPEG-CHU). Ceci nous a permis de développer la synthèse de co-amorceurs macromoléculaires à base de mPEG, la synthèse de copolymères diblocs linéaires amphiphiles en PEG-*b*-PU et l'auto-assemblage de copolymères diblocs linéaires amphiphiles en PEG-*b*-PU.

3.2 Synthèse de co-amorceurs macromoléculaires à base de mPEG

Nous avons constaté que les co-amorceurs à base de petites molécules contenant des groupements *N*-acylimides ou chlorures d'acyle (Figure 7) sont nécessaires pour synthétiser des PU avec des poids moléculaires élevés et des PDI étroits. De plus, les groupes benzéniques des co-amorceurs se retrouvent en bout de chaine dans les PU finaux. Ces résultats nous ont donné l'idée que des polymères contenant des groupements *N*-acylimides ou des groupements chlorure d'acyle à une extrémité de la chaîne pouvaient être utilisés comme co-amorceurs macromoléculaires pour préparer des copolymères séquencés à base de PU (Figure 7). Comme le PEG est un polymère hydrophile commun avec une structure relativement simple, la synthèse de co-amroceurs macromoléculaires à base d'éther monométhylique de PEG (mPEG) a été proposée, qui pourrait être utilisée pour synthétiser des copolymères diblocs linéaires PEG-*b*-PU amphiphiles.
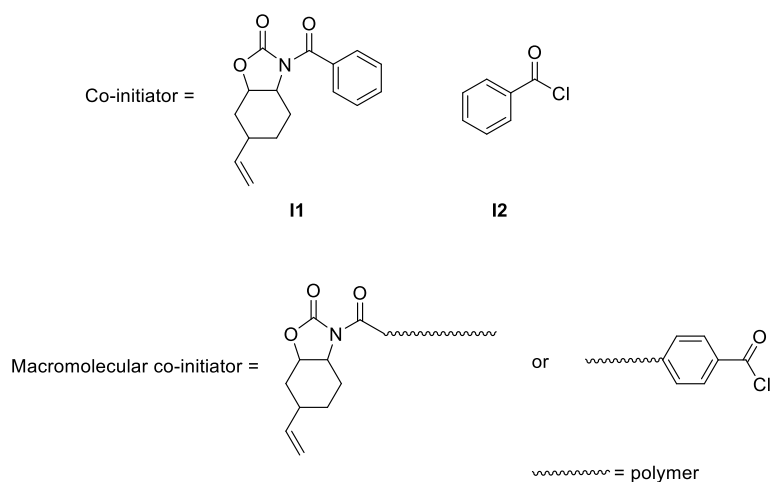
Figure 7. Co-initiateurs à petites molécules et co-initiateurs macromoléculaires.
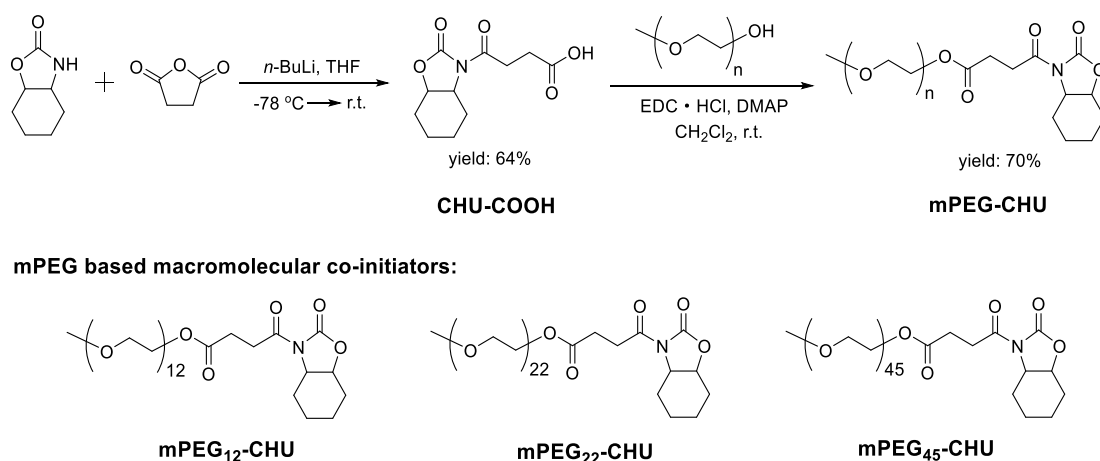
Figure 8. Synthèse des co-amorceurs macromoléculaires à base de mPEG et structures moléculaires des co-amorceurs macromoléculaires de mPEG-CHU préparés avec différentes masses moléculaires de mPEG.

Néanmoins, la synthèse de co-amorceurs macromoléculaires à base de mPEG s'est avérée ardue. Nous avons conçu plusieurs voies de synthèse, mais une seule a fonctionné comme le montre la Figure 8. Dans cette voie, un intermédiaire CHU (CHU-COOH) fonctionnalisé avec un acide carboxylique a d'abord été synthétisé en faisant réagir du CHU avec de l'anhydride succinique en présence de n-butyllithium. Après recristallisation, le CHU-COOH a été obtenu avec un rendement de 64%. Ensuite, le co-amorceur macromoléculaire à base de mPEG, mPEG-CHU a été prépare par estérification entre CHU-COOH et mPEG-OH en présence de chlorhydrate de 1-(3-

diméthylaminopropyl)-3-éthylcarbodiimide (EDC•HCl) et de 4-(diméthylamino)pyridine (DMAP). Après purification par chromatographie sur colonne, du mPEG-CHU pur a été obtenu avec un rendement d'environ 80%.

Sur la base de cette voie de synthèse, trois types de mPEG-CHU ont été préparés avec succès, à savoir : mPEG$_{12}$-CHU ($M_{n,PEG}$ = 550 Da), mPEG$_{22}$-CHU ($M_{n,PEG}$ = 1000 Da) and mPEG$_{45}$-CHU ($M_{n,PEG}$ = 2000 Da).

3.3 Synthèse de copolymères diblocs linéaires amphiphiles en PEG-*b*-PU

Le schéma de synthèse des copolymères diblocs linéaires amphiphiles PEG-*b*-PU est présenté sur la Figure 9. Les copolymères ont été synthétisés *via* la ROP anionique de monomères CHU avec le mPEG-CHU en tant que co-amorceurs macromoléculaires, conformément à la synthèse développée pour les homopolymères de PU dans le deuxième chapitre. Différents paramètres de polymérisation tels que la température, la concentration, la nature des amorceurs et les co-amorceurs ont d'abord été évalués. Après plusieurs tentatives, nous avons constaté que les conditions optimales consistaient à utiliser le *n*-butyllithium (*n*-BuLi) comme amorceur à 40 °C. Enfin, nous avons obtenu quatre copolymères avec des rapports hydrophiles différents ($f_{PEG, \% en poids}$ de 17% à 35%) dans chaque série de PEG$_{12}$-*b*-PU et PEG$_{22}$-*b*-PU, tandis que seuls deux copolymères séquencés avec des rapports hydrophiles supérieurs à 49.1 % ont été obtenus pour le PEG$_{45}$-*b*-PU. Les résultats caractéristiques sont résumés dans le Tableau 2.
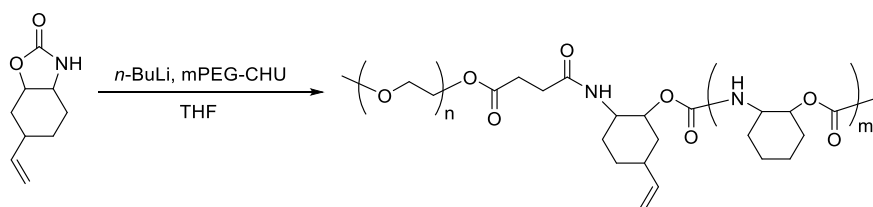
Figure 9. Synthèse des copolymères diblocs linéaires amphiphiles de type PEG-*b*-PU.

Tableau 2. Synthèse de copolymères diblocs linéaires amphiphiles en PEG-*b*-PU en utilisant des co-amorceurs macromoléculaires à base de mPEG.

Entry[a]	Co-initiator	Monomer/ *n*-BuLi/Co-initiator	T/°C	Time/h	Conversion[b]	$M_{n,\ theory}$	$M^b_{n,\ NMR}$	DP[b]	PDI[c]	$f_{PEG,wt\%}$
1	mPEG$_{12}$-CHU	18.6/1/1	40	20	80%	1500	3100	14	1.57	17.7%
2	mPEG$_{12}$-CHU	10/1/1	40	20	81%	2100	2800	12	1.49	19.8%
3	mPEG$_{12}$-CHU	8/1/1	40	20	80%	1800	2100	8	1.64	26.1%
4	mPEG$_{12}$-CHU	9.3/1/1	0	6	57%	1700	1600	5	1.42	34.2%
5	mPEG$_{22}$-CHU	50/1/1	40	20	81%	8000	5600	26	1.44	17.9%
6	mPEG$_{22}$-CHU	30/1/1	40	20	80%	5200	4400	19	1.46	22.7%
7	mPEG$_{22}$-CHU	22.5/1/1	40	20	82%	4300	3200	12	1.47	30.9%
8	mPEG$_{22}$-CHU	18.6/1/1	40	20	80%	3700	2900	10	1.39	34.5%
9	mPEG$_{45}$-CHU	30/1/1	40	20	81%	6300	4100	11	1.20	49.1%
10	mPEG$_{45}$-CHU	50/1/1	40	20	81%	9300	3200	6	1.27	61.8%

a. Pour les entrées 1-4, la concentration en monomères était de 0.375 M; pour les entrées 5-10, la concentration de *n*-BuLi était de 0.02 M; *b*. La conversion des monomères, $M_{n,RMN}$ et le degré de polymérisation (DP) ont été calculés par RMN ^{1}H; *c*. La PDI a été obtenue par GPC avec du THF comme éluant et PS comme standards.

Pour obtenir des copolymères diblocs purs de type PEG-*b*-PU, nous avons soigneusement isolé les produits bruts par précipitation dans un mélange *n*-hexane / éther diéthylique (l'éther diéthylique était un bon solvant pour les oligomères de PU) pour éliminer les oligomères de PU. Ainsi, des copolymères diblocs linéaires amphiphiles en PEG-*b*-PU ayant différents rapports hydrophiles ont été obtenus avec succès, ce qui a été confirmé par les résultats de RMN et de GPC. Étant donné que les copolymères PEG$_{45}$-*b*-PU ayant de faibles rapports hydrophiles (< 30%) n'ont pas été obtenus, nous avons concentré l'étude d'auto-assemblage sur les copolymères PEG$_{12}$-*b*-PU et PEG$_{22}$-*b*-PU.

3.3 Auto-assemblage de copolymères diblocs linéaires amphiphiles en PEG-*b*-PU

Après la synthèse de copolymères diblocs linéaires amphiphiles de type PEG-*b*-PU, leur auto-assemblage dans l'eau a ensuite été étudié. Deux échantillons de PEG$_{12}$-*b*-PU et deux échantillons de PEG$_{22}$-*b*-PU présentant différents rapports hydrophiles ont été choisis pour effectuer l'auto-assemblage. Leurs poids moléculaires et leurs distributions

de poids moléculaires sont résumés dans le Tableau 3. La nanoprécipitation a été utilisée comme technique d'auto-assemblage pour les quatre échantillons (Figure 10).

Tableau 3. Distribution des poids moléculaires et des masses moléculaires des copolymères diblocs linéaires PEG$_{12}$-*b*-PU et PEG$_{22}$-*b*-PU pour l'étude d'auto-assemblage.

Sample	DP of PU[a]	M_n[a]	PDI[b]	$f_{PEG,wt\%}$
PEG$_{12}$-*b*-PU$_{14}$	14	3100	1.57	17.7%
PEG$_{12}$-*b*-PU$_8$	8	2100	1.64	26.1%
PEG$_{22}$-*b*-PU$_{26}$	26	5600	1.44	17.9%
PEG$_{22}$-*b*-PU$_{10}$	10	2900	1.39	34.5%

a. DP et M_n ont été calculés par RMN ^{1}H; *b*. PDI a été obtenu par GPC avec du THF comme éluant.
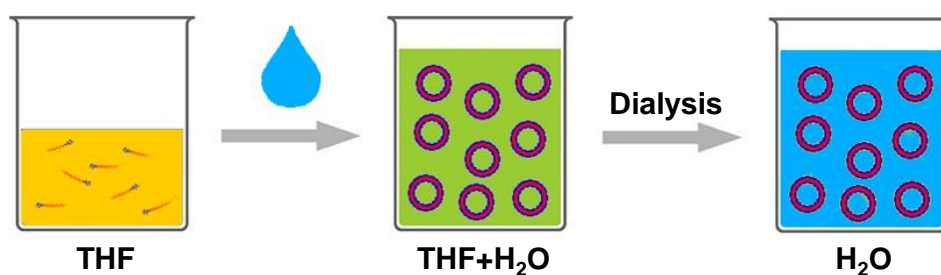
Figure 10. Schéma de principe du processus d'auto-assemblage des copolymères PEG-*b*-PU par des techniques de nanoprécipitation et de dialyse.

Dans une expérience typique d'auto-assemblage, le PEG-*b*-PU a d'abord été dissous dans du THF (concentration 2.5 mg/mL), bon solvant pour le PEG et le PU. Ensuite, de l'eau désionisée a été ajoutée lentement (environ 3 µL/min) jusqu'à ce qu'elle atteigne 50% en poids de la solution totale. La solution a été agitée doucement pendant l'addition d'eau. Le THF a ensuite été éliminé par dialyse contre de l'eau désionisée pendant 3 jours dans un sac de cellulose de 3500 Da. Enfin, la solution aqueuse des auto-

assemblages de PEG-*b*-PU a été obtenue à une concentration d'environ 2 mg/mL dans le sac de dialyse.

Les auto-assemblages des quatre échantillons de PEG-*b*-PU ont été soigneusement caractérisés par des mesures DLS, SEM et cryo-EM. Les caractérisations Cryo-EM montrent que les copolymères diblocs PEG$_{12}$-*b*-PU avec différents rapports hydrophiles peuvent s'auto-assembler sous forme de vésicules ou de micelles solides sphériques (Figures 11a,b) dans l'eau. De plus, les copolymères diblocs PEG$_{22}$-*b*-PU avec différents rapports hydrophiles peuvent s'auto-assembler sous forme de micelles solides avec des morphologies polygonales ou de micelles solides sphériques (Figure 11c, d) dans l'eau. De plus, les auto-assemblages des copolymères diblocs PEG$_{22}$-*b*-PU peuvent émettre une forte fluorescence bleu-cyan lorsqu'ils sont excités par la lumière UV. En résumé, les copolymères diblocs linéaires PEG-*b*-PU préparés peuvent s'auto-assembler en nanoparticules pouvant émettre une fluorescence, ce qui pourrait avoir des applications potentielles pour l'administration de médicaments ou la bioimagerie.
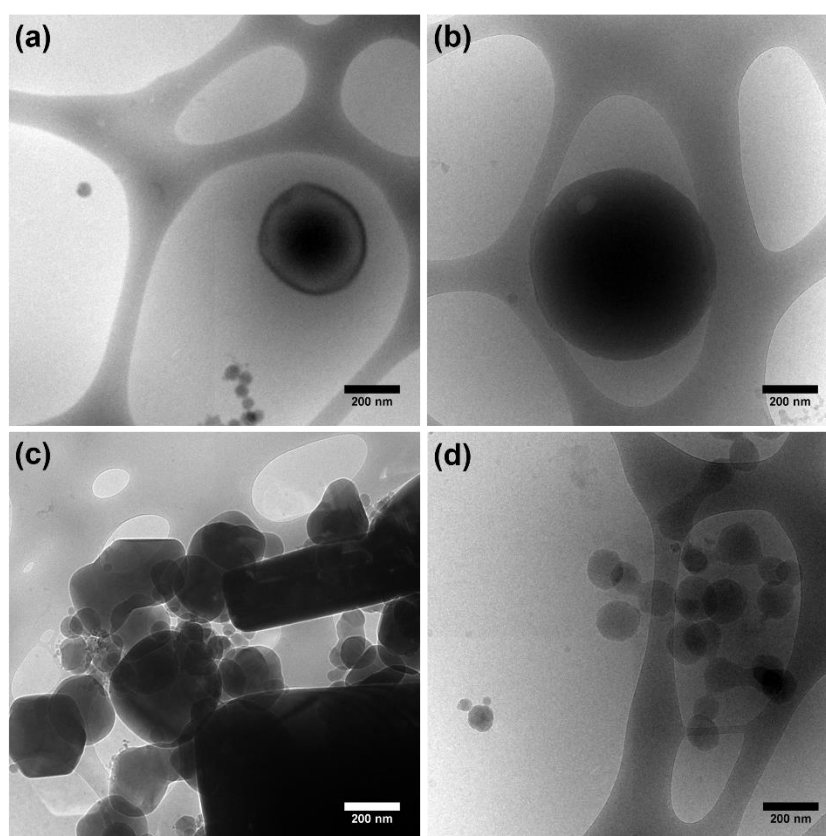
Figure 11. Images Cryo-EM des auto-assemblages de copolymères diblocs PEG$_{12}$-*b*-PU (a, b) et de copolymères diblocs PEG$_{22}$-*b*-PU (c, d).

Chapitre IV. Synthèse et auto-assemblage de copolymères greffés amphiphiles à base de polyuréthane

4.1 Introduction

Les copolymères greffés, également connus sous le nom de brosses polymères cylindriques ou de polymères en brosse, sont une sorte de polymère à topologie unique. Composés d'une grande quantité de chaînes latérales liées chimiquement à squelette linéaire, les copolymères greffés possèdent des propriétés fascinantes : ils peuvent notamment adopter une conformation « worm-like », présenter une dimension moléculaire compacte et avoir des effets de fin de chaîne spécifiques. Le développement de macromolécules artificielles en forme de brosse est donc important et nécessaire pour explorer leurs fonctionnalités et propriétés potentielles. C'est pourquoi, les études sur les copolymères greffés ont suscité beaucoup d'intérêt et sont principalement axées sur le contrôle des structures moléculaires, la compréhension de la relation entre leur architecture et leurs propriétés.
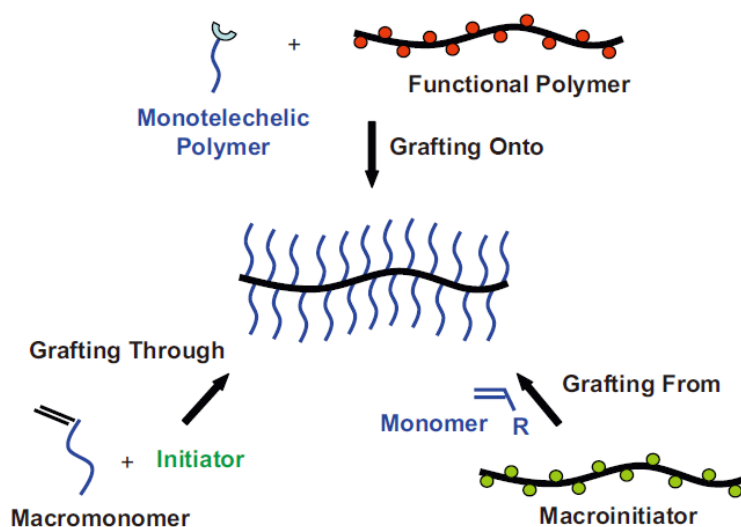
Figure 12. Trois stratégies principales développées pour synthétiser les copolymères greffés.

Trois stratégies principales ont été développées pour synthétiser des copolymères greffés: " grafting onto " (par ajout de chaînes latérales préalablement préparées à un

squelette), " grafting through " (par polymérisation de macromonomères) et " grafting from " (par polymérisation de chaînes latérales sur la chaîne principale linéaire qui sert de macro-amorceur), comme le montre la Figure 12.

Les copolymères greffés amphiphiles constitués d'un squelette linéaire non miscible et de chaînes latérales pendantes sont des architectures de polymères intéressantes pour les études d'auto-assemblage. Par rapport aux copolymères à blocs linéaires, les copolymères greffés présentent un comportement d'auto-assemblage distinct dû à l'effet des densités de greffage et des longueurs moléculaires des chaînes latérales. Par exemple, les copolymères greffés peuvent être sous la forme de molécule sphérique, lorsque la longueur du squelette est similaire à celle des chaînes latérales ; ou en forme de ver, lorsque la longueur du squelette est nettement plus longue que celle des chaînes latérales. Par conséquent, il est important d'étudier l'auto-assemblage des copolymères greffés, en particulier des copolymères greffés amphiphiles, pour explorer en détail la relation entre les architectures complexes et les propriétés correspondantes ainsi que leurs applications potentielles.

Dans ce chapitre, de nouveaux copolymères greffés amphiphiles de type PU-*g*-PEG ont été préparés par couplage de type thiol-ène de l'homopolymère de PU préparé par AROP du CHU comportant des groupements vinyle sur chaque motif de répétition avec des mPEG à terminaison thiol (mPEG-SH). Leur auto-assemblage dans l'eau a été étudié. Le chapitre se divise en trois parties : synthèse de mPEG à terminaison thiol (mPEG-SH), synthèse de copolymères greffés amphiphiles PU-*g*-PEG et auto-assemblage de copolymères greffés amphiphiles PU-*g*-PEG.

4.2 Synthèse de mPEG à terminaison thiol (mPEG-SH)

La thiolation du poly(éthylène glycol) monométhyléther linéaire de poids moléculaire 550 Da ($mPEG_{12}$-OH) a été réalisée par réaction avec de l'acide thioglycolique en utilisant de l'acide sulfurique comme catalyseur (Figure 13). L'eau produite dans la réaction a été éliminée par distillation azéotropique avec du toluène pour augmenter le rendement. Le mPEG-SH pur a ensuite été obtenu par recristallisation du produit brut dans un mélange THF / éther diéthylique. Le degré de

fonctionnalisation du mPEG-SH obtenu peut alors être calculé en comparant la zone d'intégration du pic d avec celle du pic a dans le spectre RMN ^{1}H du mPEG$_{12}$-SH, et il est déterminé qu'il est d'environ 99% (Figure 13).
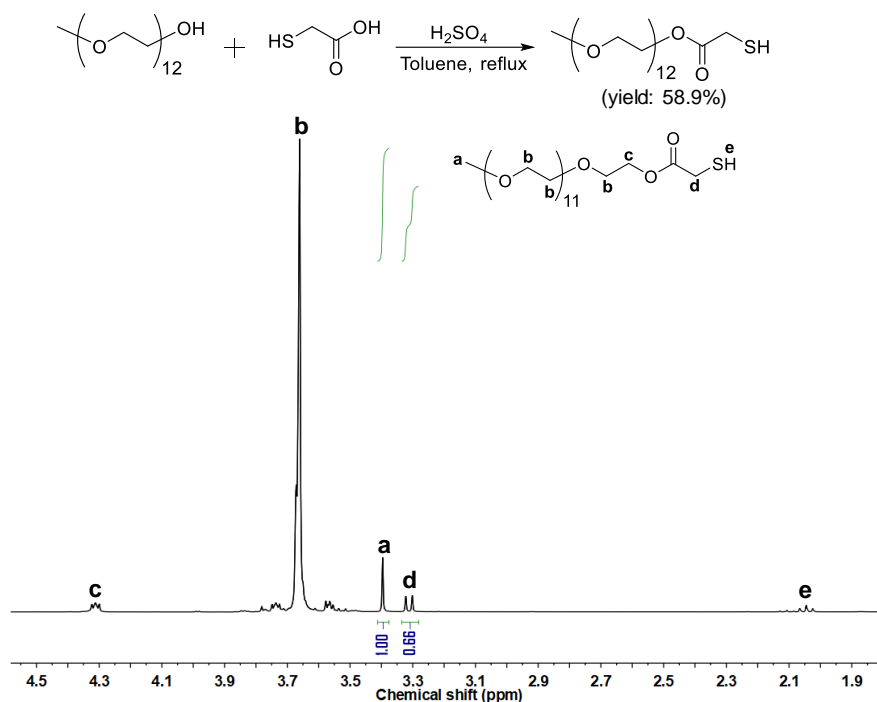
Figure 13. Schéma synthétique et spectre RMN ^{1}H du mPEG$_{12}$-SH.

4.3 Synthèse de copolymères greffés amphiphiles PU-*g*-PEG
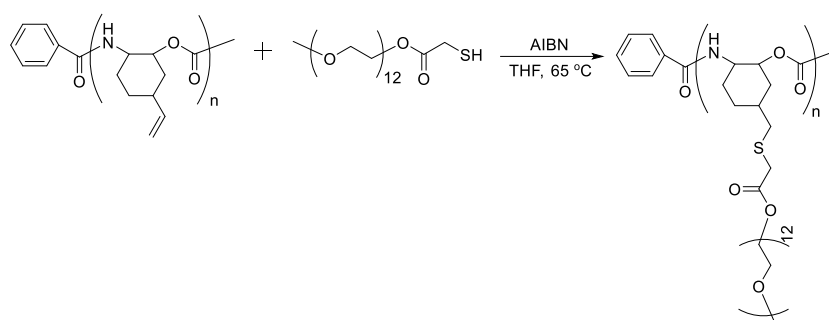
Figure 14. Synthèse de copolymères greffés amphiphiles PU-*g*-PEG par couplage de type thiol-ène. Le PU a été préparé par AROP de monomères CHU.

Les copolymères greffés amphiphiles PU-*g*-PEG ont été préparés par réaction thiol-ène à médiation radicalaire d'un homopolymère de PU linéaire fonctionnalisé avec des groupements vinyle avec du mPEG-SH, en utilisant une stratégie « grafting onto » (Figure 14). L'homopolymère de PU a été préparé par AROP du monomère de CHU

comme décrit dans le deuxième chapitre. La réaction de couplage thiol-ène a été effectuée en utilisant de l'AIBN (2,2'-azobis (isobutyronitrile)) comme amorceur radicalaire dans du THF à 65 °C. Un excès de mPEG-SH (4 fois plus en pourcentage molaire que les groupements vinyle) a été ajouté au mélange réactionnel afin d'obtenir une haute densité de greffage des chaînes de PEG et d'éviter une éventuelle réaction de réticulation provoquée par une réaction de couplage radicalaire. Une fois la réaction terminée, le produit brut a été purifié par dialyse contre de l'éthanol dans un sac en cellulose de 3500 Da pendant 5 jours pour éliminer le mPEG-SH n'ayant pas réagi et la solution d'éthanol a été changée deux fois par jour.
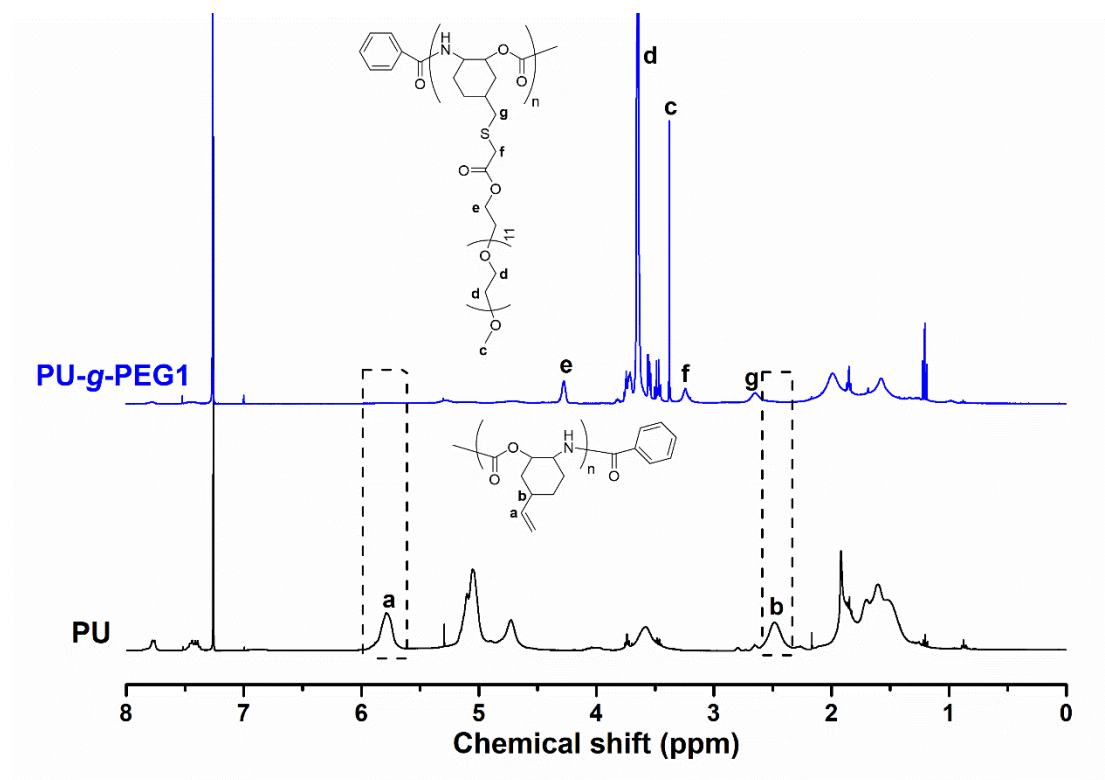
Figure 15. Spectres RMN ^{1}H du copolymère greffé amphiphile PU-*g*-PEG1 et du squelette PU.

Le produit pur a ensuite été caractérisé par ^{1}H RMN et GPC. En comparant les spectres RMN ^{1}H de PU avec PU-*g*-PEG (Figure 15), les signaux des protons à δ 5.78 (pic a) et 2.48 ppm (pic b) attribués aux groupes "CH" sur le fragment vinyle et le fragment cyclohexane ont complètement disparu après la réaction. Ce résultat indique bien que le taux de greffage des chaînes latérales de PEG est quantitatif. De plus, la

courbe GPC du copolymère PU-*g*-PEG montre une distribution monomodale avec un temps de rétention décalé vers la gauche par rapport à la courbe GPC du PU. Tous ces résultats de caractérisation confirment que le copolymère greffé amphiphile pur PU-*g*-PEG ayant une densité de greffage élevée a été obtenu par la réaction de couplage thiol-ène de PU avec mPEG-SH.

Tableau 4. Synthèse de copolymères greffés amphiphiles à base de PU PU-*g*-PEG avec une densité de greffage de 100%.

Sample[a]	DP of PU[b]	$M_{n,PU}$[b]	M_n[b]	PDI[c]	$f_{PEG,wt\%}$
PU-*g*-PEG1	14	2400	13600	1.41	56.6%
PU-*g*-PEG2	24	4000	19100	1.60	69.1%

a. Tous les copolymères greffés ont été synthétisés par la réaction de couplage thiol-ène entre PU et mPEG$_{12}$-SH dans du THF à 65 °C; temps de réaction: 24 h; Purification: dialyse contre éthanol pendant 5 jours.

b. La conversion des monomères, le degré de polymérisation (DP) et le M_n ont été calculés par RMN ^{1}H;

c. La PDI a été obtenue par GPC avec du THF comme éluant et PS comme standards.

En utilisant cette stratégie, deux copolymères amphiphiles de PU-*g*-PEG ayant des longueurs de squelette et des poids moléculaires différents ont été préparés en utilisant du PU avec des poids moléculaires différents (Tableau 4). De plus, les copolymères de PU-*g*-PEG obtenus ont présenté un comportement d'auto-assemblage différent dans l'eau, comme décrit ci-dessous.

4.4 Auto-assemblage de copolymères greffés amphiphiles PU-*g*-PEG

Etant donné que les copolymères de type PU-*g*-PEG obtenus ont des rapports hydrophiles relativement élevés (Tableau 4), ils peuvent avoir une bonne solubilité dans l'eau si leurs concentrations ne sont pas trop élevées. Il est alors possible de mesurer leur concentration micellaire critique (CMC) en suivant le changement des propriétés

de la solution de polymère avec l'augmentation de la concentration. Ici, nous avons choisi la technique de fluorescence pour mesurer les CMC des copolymères greffés PU-*g*-PEG, car leur solution aqueuse pouvait émettre une fluorescence lorsqu'elle était excitée par la lumière UV.

L'intensité de fluorescence de la solution aqueuse de PU-*g*-PEG1 a augmenté progressivement à mesure que la concentration en PU-*g*-PEG1 augmentait. Une intersection est apparue à environ 2.1 mg/mL, ce qui indique un changement de l'état d'agrégation des unimères de surfactant en micelles. La raison possible de la diminution de la pente après l'intersection pourrait être due aux changements environnementaux des molécules de PU-*g*-PEG, c'est-à-dire allant de molécules simples entourées de molécules d'eau à des agrégats entourés de molécules de copolymère. Ainsi, la propriété luminescente comme l'intensité de la fluorescence a également changé. Sur la base de l'intersection du tracé intensité-concentration de fluorescence, nous avons obtenu une CMC du copolymère greffé PU-*g*-PEG1 dans l'eau de 2.1 mg/mL. La CMC de PU-*g*-PEG2 est de 0.19 mg/mL mesurée par la même méthode.

Après les mesures CMC des deux copolymères greffés PU-*g*-PEG, leur auto-assemblage dans l'eau a été réalisé en utilisant la technique de nanoprécipitation. Les auto-assemblages des deux échantillons de PU-*g*-PEG ont été caractérisés avec soin par DLS, SEM et cryo-EM. Les caractérisations SEM et cryo-EM ont montré que le copolymère greffé PU-*g*-PEG avec un rapport hydrophile de 56.6% pouvait s'auto-assembler en micelles à surfaces rugueuses et irrégulières (Figures 16a, b) éventuellement issues de l'agrégation de petites micelles. Les auto-assemblages de copolymère greffé PU-*g*-PEG avec un rapport hydrophile de 69.1% étaient des micelles en forme de disque de grand diamètre et de faible épaisseur (Figure 16c, d). La caractérisation par microscopie de fluorescence des micelles en forme de disque montre des nanoparticules circulaires bleues avec un phénomène d'émission de fluorescence hétérogène (Figures 16e, f), indiquant que les micelles en forme de disque obtenues pouvaient être hétérogènes.
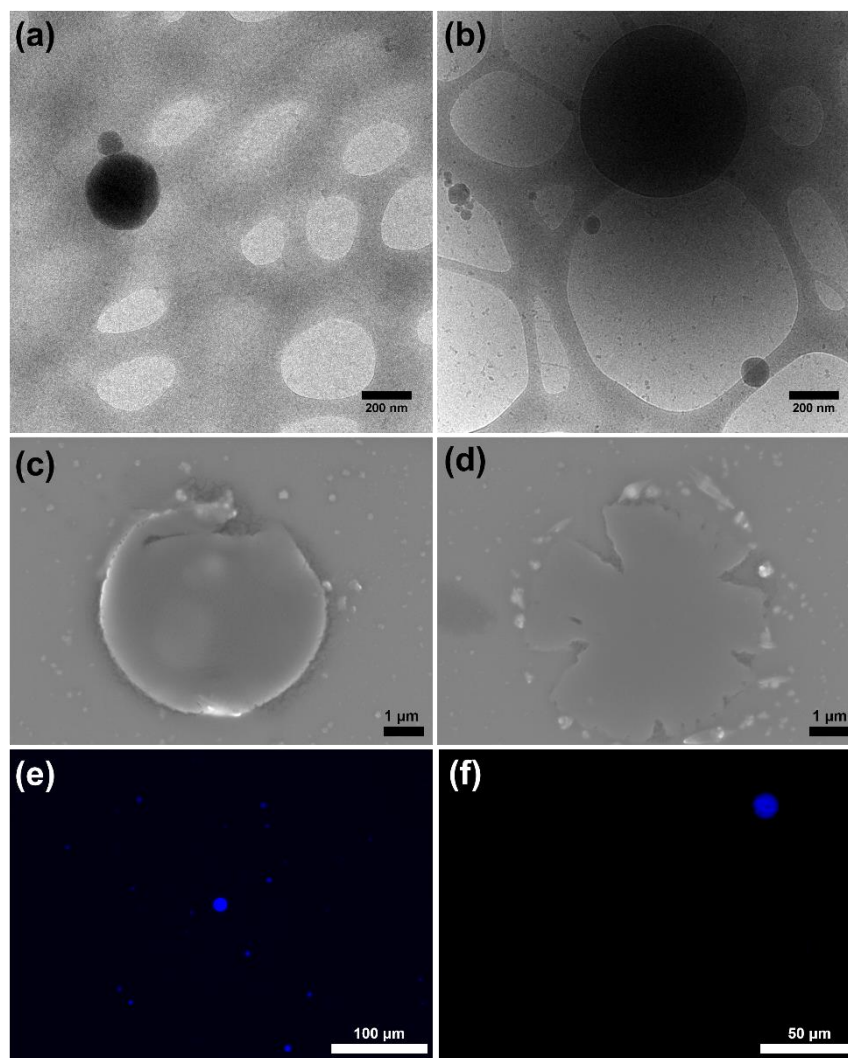
Figure 16. Images Cryo-EM (a, b) et SEM (c, d) des auto-assemblages de copolymères greffés amphiphiles PU-*g*-PEG. Images de microscopie à fluorescence (e, f) des micelles en forme de disque.

En résumé, nous avons synthétisé des micelles analogues à des disques qui peuvent émettre de la fluorescence sous lumière UV par auto-assemblage de copolymères greffés PU-*g*-PEG avec une composition spécifique, ce qui enrichit nos connaissances sur l'auto-assemblage de copolymères greffés amphiphiles et fournit plus de nouveaux matériaux nanostructuraux fonctionnalisés avec des applications potentielles.

Synthesis of polyurethanes by anionic ring opening polymerization and self-assembly of polyurethane-based amphiphilic copolymers

ABSTRACT

The present work describes the synthesis of isocyanate-free polyurethanes (PUs) through the anionic ring opening polymerization (AROP) technique and the self-assembly behavior of PU based amphiphilic linear diblock copolymers and graft copolymers. Generally, PUs are prepared by the polyaddition of diols (or polyols) with diisocyanates (or polyisocyanates). This method requires drastic conditions to drive the reaction toward high conversion and uses highly moisture sensitive and toxic isocyanates, thus limiting their medical applications. In this work, we use a new strategy, based on ring opening polymerization (ROP), to obtain aliphatic polyurethanes from cyclic carbamates. A series of PU homopolymers with different molecular weights and narrow polydispersity indexes has been synthesized. Also, a series of PU based amphiphilic linear block copolymers PEG-*b*-PUs (polyethylene glycol-*b*-polyurethanes) and graft copolymers (PU-*g*-PEGs) has been prepared. The self-assembly behaviors of these PU based amphiphilic copolymers have been studied carefully. The present thesis manuscript consists of five chapters, in which the first chapter is "Introduction" and the fifth chapter is "Materials and methods". The main research contents can be divided into three parts:

I. Controlled anionic ring opening polymerization of 5-membered cyclic carbamates to polyurethanes

In this part, isocyanate-free and well-defined PUs with novel structures have been prepared *via* the AROP of a 5-membered cyclic carbamate bearing a vinyl group

(termed as CHU) by using *n*-butyllithium (*n*-BuLi) as the initiator and CHU-derived imide as the co-initiator. The cyclic carbamate monomer has been carefully designed and synthesized. The prepared PUs have relatively narrow polydispersity indexes (PDI = 1.2-1.3) and the experimental molecular weights are close to the theoretical ones. The AROP mechanism has been proposed and characterized by *in situ* IR and ^{13}C NMR, which reveals that the origin of the polymerization activity of our system is very likely to be caused by the formation of highly active anionic species. The study of the ROP kinetics shows that the polymerization can present the characteristics of the first order kinetics in some cases. The preliminary study of the properties of the obtained PUs shows that they could emit blue fluorescence upon UV irradiation after thermal treatment. In summary, the present work will provide more options and inspirations for people to prepare isocyanate-free and well-defined PUs.

II. Synthesis and self-assembly of polyurethane-based amphiphilic linear diblock copolymers

In this part, a series of amphiphilic PEG-*b*-PU linear diblock copolymers with different sequence lengths of PEG and PU has been prepared *via* the AROP of CHU in the presence of mPEG (poly(ethylene glycol) monomethyl ether) based macromolecular co-initiators (mPEG-CHU). Three kinds of mPEG-CHU with different molecular weights of PEG have been synthesized successfully through the esterification between mPEG-OH and carboxylic acid functionalized CHU (CHU-COOH). Two types of PEG$_{12}$-*b*-PU diblock copolymers and two types of PEG$_{22}$-*b*-PU diblock copolymers with different hydrophilic ratios are chosen for the self-assembly study using the nanoprecipitation technique. Cryo-EM characterization shows that PEG$_{12}$-*b*-PU diblock copolymers with different hydrophilic ratios can self-assemble into vesicles or spherical solid micelles in water. Also, PEG$_{22}$-*b*-PU diblock copolymers with different hydrophilic ratios can self-assemble into solid micelles with polygonal morphologies or spherical solid micelles in water. In addition, the self-assemblies of the PEG$_{22}$-*b*-PU diblock copolymers can emit strong cyan fluorescence when they are excited by UV light. In summary, the prepared PEG-*b*-PU linear diblock copolymers

can self-assemble into nanoparticles that can emit fluorescence, which might have potential applications in biomedical areas such as drug delivery or bioimaging.

III. Synthesis and self-assembly of polyurethane-based amphiphilic graft copolymers

In this part, novel PU based amphiphilic PU-*g*-PEG graft copolymers have been prepared *via* the thiol-ene coupling reaction of PU homopolymer which is prepared by AROP of CHU having vinyl groups attached on each repeating unit and thiol-terminated mPEG (mPEG-SH) based on the grafting onto strategy. mPEG-SH has been prepared by the esterification catalyzed by sulfuric acid of mPEG-OH (M_n = 550 Da) and thioglycolic acid. Two PU-*g*-PEG graft copolymers with different backbone lengths and hydrophilic ratios have been prepared. The critical micelle concentration (CMC) of the amphiphilic PU-*g*-PEG graft copolymers in water has been measured by fluorescence technique. The self-assembly of PU-*g*-PEG graft copolymers is performed using the nanoprecipitation technique. SEM and cryo-EM characterizations show that PU-*g*-PEG graft copolymers with different backbone lengths and hydrophilic ratios can self-assemble into spherical micelles or disk-like micelles in water. The fluorescence microscopy characterization of the disk-like micelles shows blue circular nanoparticles with heterogeneous fluorescence emission phenomenon, indicating that the obtained disk-like micelles might be heterogeneous. In summary, we have prepared disk-like micelles that could emit fluorescence under UV light by self-assembly of PU-*g*-PEG graft copolymers with specific composition, which enriches our knowledge about the self-assembly of amphiphilic graft copolymers and provides novel functionalized nanostructural materials with potential applications.

Chapter I. Introduction

1.1 General introduction to polyurethanes

1.1.1 Discovery history of polyurethanes

Polyurethanes (PUs) are a class of polymers composed of organic units joined by carbamate (urethane, -NHCOO-) linkages. As one of the most important and versatile polymeric materials, PUs were discovered by Otto Bayer and his coworkers at I.G. Farben industrie, Germany in 1937.[1] At first, the research and development of PUs were the response to the competitive challenge arising from Carother's work on polyamides, or nylons, at E.I. Dupont. But the further research on this subject revealed that they were new polymeric materials with interesting properties.[2] The industrial production of PU started and grew significantly during World War II. In 1952, there was a noticeable improvement of the elastomeric properties of PU when polyisocyanate, especially toluene diisocyanate (TDI), has become commercially available. In 1952-1954, polyester-polyisocyanate systems were developed by Bayer. After that, all kinds of PU products such as Lycra, Estane, Texin and Pallethane as well as the polyether polyols based PUs have been developed by different companies in USA or Europe.[2]
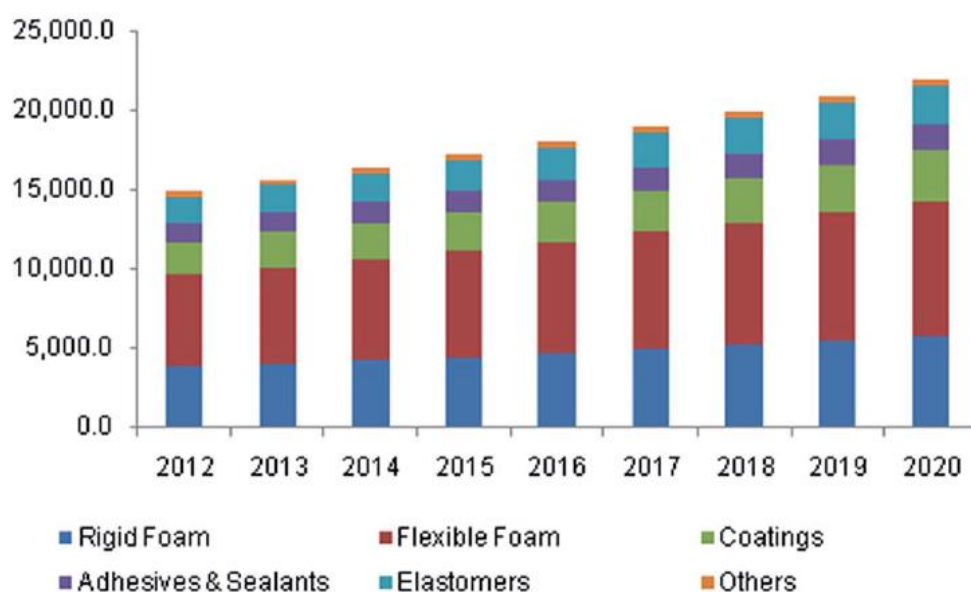
Figure 1.1. Worldwide PU production and an estimated forecast up to 2020 (unit: kilotons).[3]

Thermoplastic PU elastomers and PU engineering plastics were respectively developed in 1970s and 1980s, which promoted the fast development of PU industry. Their worldwide production is now estimated to exceed 22 million tons in 2020 (Figure 1.1),[3] which accounts for nearly 5 wt % of total worldwide polymer production.

1.1.2 Structures, properties and applications of polyurethanes

PUs are polymers containing a repetition of urethane linkages in their structure (Figure 1.2). In industry, PUs are made by the polyaddition of polyisocyanates (OCN-R_1-NCO) with macropolyols (HO-R_2-OH) (Figure 1.2), thereby allowing the formation of many urethane groups.[4] During the production of PU materials, short-chain diols (HO-$(CH_2)_x$-OH) or diamines (NH_2-$(CH_2)_x$-NH_2) are usually added as chain extenders to adjust the properties of PUs precisely. The former give urethane linkages like the macropolyols while the latter allow access to urea linkages. The urethane and urea linkages are rigid segments in the PU structure and the polyol segments are flexible ones. Therefore, PUs are actually constructed by numerous rigid and flexible segments in a modular-like form. The plastic and strength properties of PUs are mainly dictated by the rigid segments, while the rubber and elastomer properties of PUs originate from the flexible segments. By changing the chemical composition and feeding ratios of starting materials, we can produce PUs with diverse and versatile properties and applications.

$$n + m \quad O=C=N-R_1-N=C=O \; + \; n \; HO-R_2 \cdot OH \; + \; m \, HO \left(C^{H_2} \right)_x OH \longrightarrow$$

$$\left[\overset{O}{\underset{\parallel}{C}}-\overset{H}{\underset{}{N}}-R_1-\overset{H}{\underset{}{N}}-\overset{O}{\underset{\parallel}{C}} \left[O \left(C^{H_2} \right)_x O - \overset{O}{\underset{\parallel}{C}}-\overset{H}{\underset{}{N}}-R_1-\overset{H}{\underset{}{N}}-\overset{O}{\underset{\parallel}{C}} \right]_{\frac{m}{n}} O-R_2 \cdot O \right]_n$$

Figure 1.2. General structure of linear, single-phase (m=0) and phase-separated (m=1, 2) PUs on the micrometer scale. Rigid segments (urethane linkages) and flexible segments (polyols) are distributed statistically.[4]

Owing to this very specific structure, PUs can display thermoplastic, elastomeric, and thermoset behavior by tuning their chemical and morphological makeup, which makes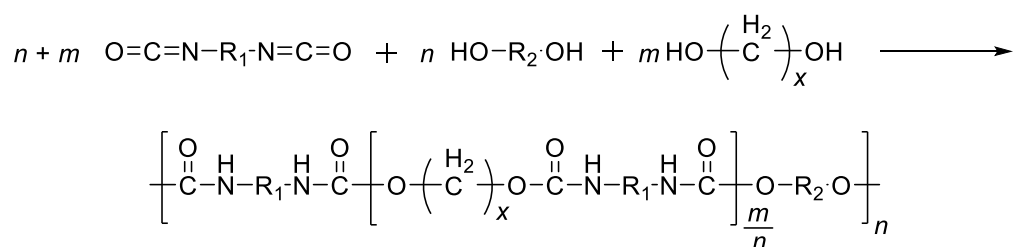 them useful for various applications (*e.g.*, foams, seats, elastomeric wheels and tires, high-performance coatings, adhesives) (Figure 1.3). As far as we know, PUs belong to one of the few classes of polymers which have applications in the area of plastics, rubbers, foams, fibers, coatings, adhesives and functional polymers. They are widely used in different industry sectors such as construction, light industry, automobile industry, textile industry, petrochemical industry, metallurgical industry, *etc*.

POLYURETHANES

Thermoplastic PU	Flexible PU	Rigid PU	PUI	Water-borne PU
Examples: Keyboard protector for laptop, outer cases of mobile electronic devices, automotive instrument panels, caster wheels, power tools, sporting goods, medical devices, drive belts, footwear, inflatable rafts, and a variety of extruded film, sheet and profile applications.	Examples: Cushion materials, carpet underlays, furniture, bedding, automotive interior parts, packaging, biomedicine and nanocomposites	Examples: Thermal and sound insulators	Examples: Artificial hearts, connector tubing for heart pacemakers and haemodialysis tubes	Examples: Coatings, adhesives, sealants, binders

Figure 1.3. Important types of PUs and common examples of their applications.[3]

It is noteworthy that more than 66% of PU raw materials (polyisocyanates/polyols) go into foam applications. The basic step to produce PU foams is the reaction between isocyanates and water. As shown in Figure 1.4, the corresponding unstable carbamic acid forms firstly, which spontaneously decomposes into an amine and carbon dioxide. The amine reacts with additional isocyanate to form a urea, while the resulting CO_2 serves as the blowing agent. Additional physical blowing agents can be incorporated if necessary.[4]

$$R-NCO \xrightarrow{H_2O} R-\overset{O}{\underset{H}{N}}-OH \longrightarrow R-NH_2 + CO_2 \xrightarrow{R-NCO} R-\overset{O}{\underset{H}{N}}-\overset{}{\underset{H}{N}}-R$$

Figure 1.4. Formation of PU foams through the reaction between isocyanate and water.

1.1.3 Traditional method to prepare polyurethanes

Generally, most PUs are synthesized through the polyaddition of diols (or polyols) onto diisocyanates (or polyisocyanates), forming repeating urethane groups along the polymer chain, in the presence of chain extenders, catalysts and/or other additives. The isocyanates and polyols should necessarily contain two or more isocyanate groups (R_1–$(N=C=O)_{n\geq2}$) and hydroxyl groups (R_2–$(OH)_{n\geq2}$), respectively. The types o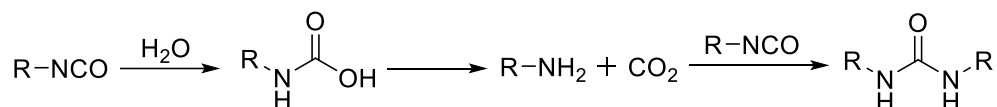f polyols and polyisocyanates have important impact on the exhibited physical and chemical properties of the PUs.[5] Generally, soft elastic PUs can be produced from polyols with flexible long chains, whereas rigid and tough PUs can be obtained through a high degree of cross-linking. Stretchy PU materials can be produced from long polymer chains with low degree of cross-linking, whereas hard PU materials can be obtained from short polymer chains with high degree of cross-linking. Besides, PUs with high degree of cross-linking often possess an infinite molecular weight with a three-dimensional (3D) network build-up, which usually will not turn soft or melt when they are heated. The incorporation of different additives alongside the polyisocyanates and polyols, as well as the modification of the processing conditions, makes it possible to produce PU materials with a wide range of characteristic features and various applications.[6]

1.1.3.1 Isocyanates

The isocyanates used to prepare PUs usually contain two or more isocyanate groups, so they are called diisocyanates or polyisocyanates. They can be aromatic, aliphatic or cycloaliphatic and have a molecular weight less than 200 Da. In industry, the most commonly used isocyanates are aromatic diisocyanates. The representative ones are toluene diisocyanate (TDI), comprising the isomers 2,4-TDI (**1**) and 2,6-TDI (**2**), and methylene diphenyl diisocyanate (MDI), comprising 4,4'-MDI (**3**) and 2,4'-MDI (**4**) (Figure 1.5). In addition, there are a few special other aromatic polyisocyanates used, such as 1,5-naphthalene diisocyanate (NDI) (**5**) (Figure 1.5). The aromatic diisocyanates are generally used to make flexible foams, rigid foams, elastomers and so on. For the aliphatic and cycloaliphatic isocyanates, they are used in small quantities

to make coatings or other materials in which color and transparency are important since PUs made with aromatic isocyanates tend to darken on exposure to light. The representative aliphatic and cycloaliphatic isocyanates are hexamethylene diisocyanate (HDI, **6**), isophorone diisocyanate (IPDI, **7**), and hydrogenated MDI (H$_{12}$MDI, **8**) (Figure 1.5).
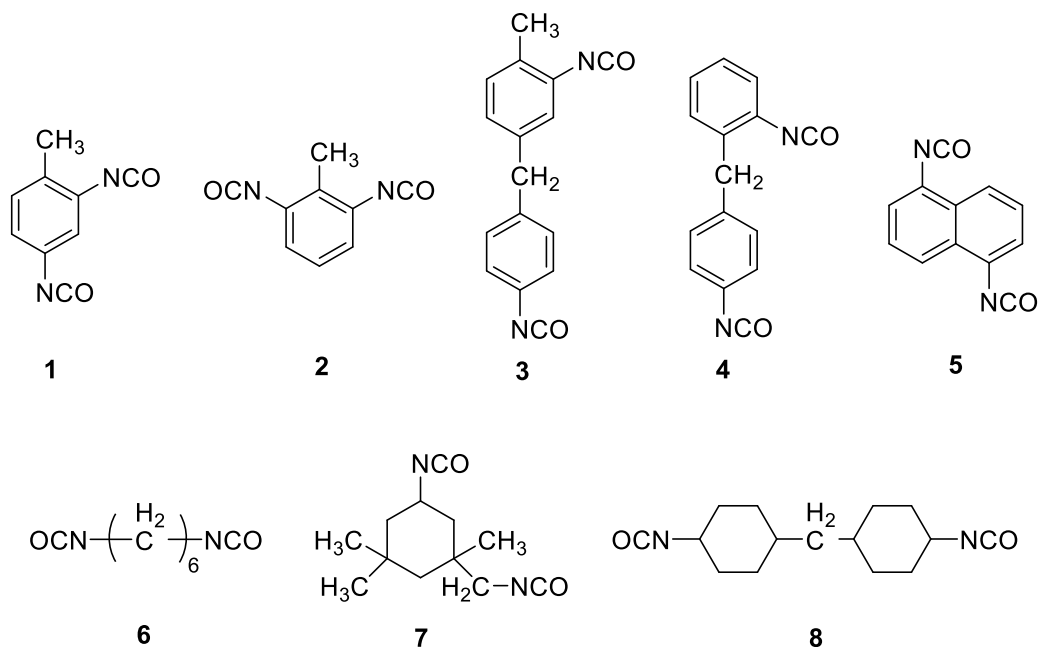
Figure 1.5. Diisocyanates used in the industry.

1.1.3.2 Polyols

Polyols used for PU synthesis usually contain two or more hydroxy groups. There are different types of polyols used to make PUs with good flexibility, stability or resistance. Meanwhile, the molecular weights of the polyols used have also a crucial role. For example, rigid PUs are made from polyols with low molecular weights (a few hundred units), whereas flexible PUs are produced from polyols with high molecular weights (more than ten thousand units).[7] Among the polyols with high molecular weights, polyethers like polyethylene glycol (PEG) or poly(tetrahydrofuran) (PTHF) are the most common polyols, but polyesters, polycarbonates or polybutadienes are also used (Figure 1.6).

The most widely used polyether polyols have molecular weights between 500 and 3000 Da, and they generally have hydroxyl groups per molecule equal to two for

elastomers, three for flexible foams, and up to six for more rigid foams. Polyester polyols are generally more expensive and are used with more specific constraints. They are more sensitive to water because of the potential hydrolysis of the ester group. This specific property allows them to be used as biodegradable PUs for applications such as absorbable sutures. Also, there are some kinds of polyols prepared from renewable sources such as vegetable oils, derivatives of vegetable oils, sorbitol and cellulose. They are reported for the production of eco-friendly polyurethane coatings.[8]
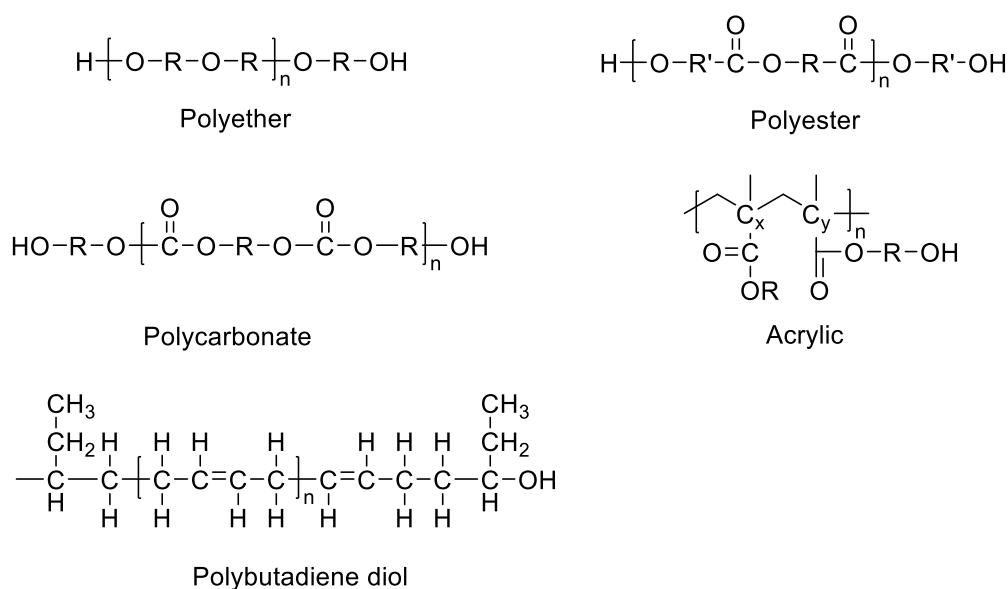
Figure 1.6. Some polyols with high molecular weights to prepare PUs.[3]

1.1.3.3 Catalysts

The reaction between diisocyanates and polyols is slow at room temperature under catalyst-free conditions due to the phase incompatibility between the polar and less dense polyol phase and the relatively non-polar and denser isocyanate phase. Also, the molecular weight of synthesized PU is not high without catalyst. It is therefore necessary to add some suitable surfactants and catalysts during the PU synthesis. The catalyst can take effect by activating the alcohol (nucleophilic activation) (Figure 1.7b) or the isocyanate (electrophilic activation) (Figure 1.7c). It is worth noting that an electrophilic mechanism involving the activation of isocyanate *via* hydrogen bonding to the O atom or the N atom can also occur.[9]

Tin-based complexes, such as dibutyltin dilaurate (DBTDL) and dibutyltin diacetate (DBTDA), are classical catalysts in the PUs production. They are typical Lewis acidic catalysts and can activate the isocyanate to accelerate the formation of PUs. Tertiary amine catalysts, such as triethylenediamine (TEDA, also called DABCO, 1,4-diazabicyclo[2.2.2]octane), dimethylcyclohexylamine (DMCHA) or dimethylethanolamine (DMEA) are also widely used because of their good performance in enhancing the nucleophilicity of the diols. Recently, organocatalysis attracted much interest when organic bases,[10] such as N-heterocyclic carbenes (NHCs),[11] amidines/guanidines, or organic acids[12] or latent organic[13] compounds have been reported to effectively catalyze the PU formation. This field is expected to grow and could provide an alternative tool to the traditional metal-based catalysts in a near future.[9]
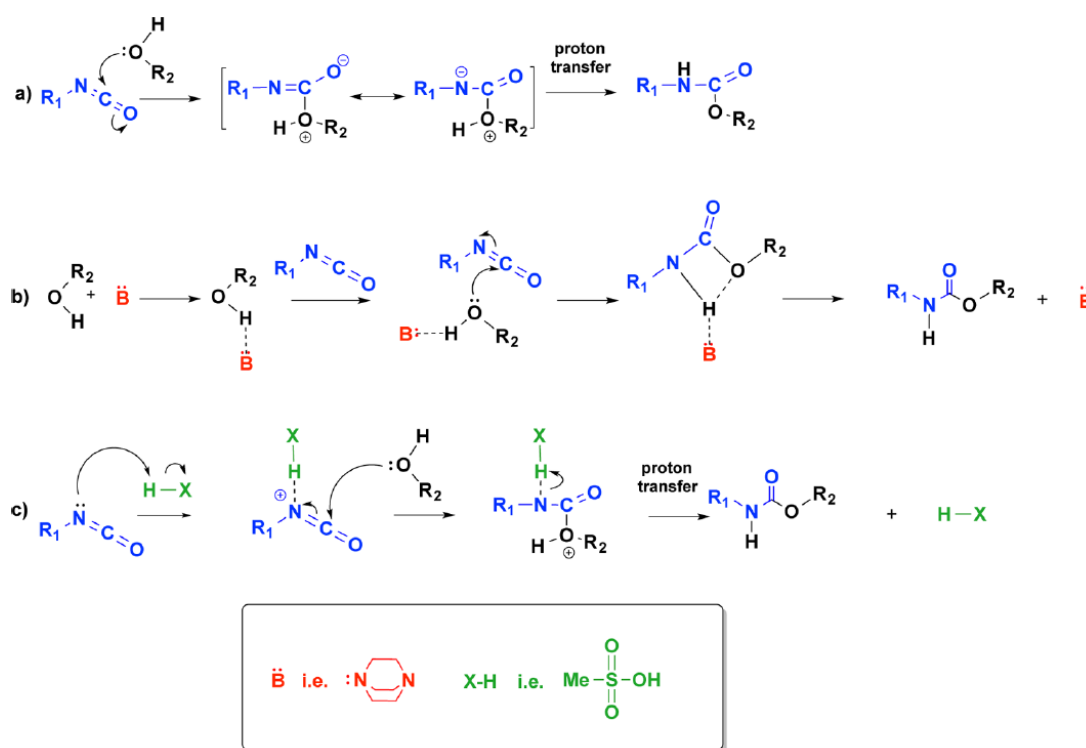

Figure 1.7. General mechanism of isocyanate/alcohol reaction (a) in the absence of catalyst, (b) in the presence of a base or nucleophilic activator, and (c) in the presence of an acid or electrophilic activator.[9]

1.1.3.4 Chain extenders and cross linkers

Chain extenders and cross linkers play an important role in modification of the final properties of the PUs. They are generally multi-functional hydroxyl and amine terminated compounds with low molecular weights (40-300 Da). The commonly used chain extenders are ethylene glycol, 1,4-butanediol, 1,6-hexanediol, cyclohexane dimethanol and hydroquinone bis(2-hydroxyethyl) ether. All of these glycols can be used to form PUs that have well-defined hard segment domains, good phase separation, and are melt processable. Diethanolamine and triethanolamine are often used in flex molded foams to increase firmness/rigidity and increase the activity of catalysts.

1.1.3.5 Surfactants

Surfactants are used to modify the properties of both foam and non-foam PUs and improve the production process. The typical representatives are polydimethylsiloxane-polyoxyalkylene block copolymers, silicone oils and nonylphenol ethoxylates. In foams, they are used to emulsify the liquid components, regulate cell size, and stabilize the cell structure to prevent collapse and sub-surface voids. In non-foam PUs, they play a key role to act as air release and antifoaming agents or as wetting agents. Additionally, they can be used to eliminate surface defects such as pin holes, orange peel, and sink marks in the final PU materials.

1.2 Isocyanate-free methods to prepare polyurethanes

Although PUs are excellent polymeric materials with many applications in our daily life, there are still some concerns about them. Because one of the starting materials (*i.e.*, polyisocyanates) is synthesized from the corresponding amine and highly toxic phosgene ($COCl_2$, other names like carbonyl chloride, carbon oxychloride, chloroformyl chloride) compounds, the final PU materials may also be toxic, which limits their use in biomedical applications. In addition, the storage of the highly volatile phosgene in the PU factories is also a major problem,[14] which represents a huge potential safety hazard for people who work in the factories or live nearby. Therefore,

developing alternative isocyanate-free pathways to prepare PU becomes more and more attractive for industry and academic research. To the best of our knowledge, there are four types of isocyanate-free routes reported (Figure 1.8): (1) polyaddition of cyclic di-carbonates and diamines (*i.e.*, cyclic carbonate route); (2) polycondensation of linear activated dicarbonates and diamines (*i.e.*, bis(dialkyl carbonate) route); (3) polycondensation of linear activated carbamates and diols (*i.e.*, transurethanization route); (4) ring opening polymerization (ROP) of cyclic carbamates (*i.e.*, ROP route).
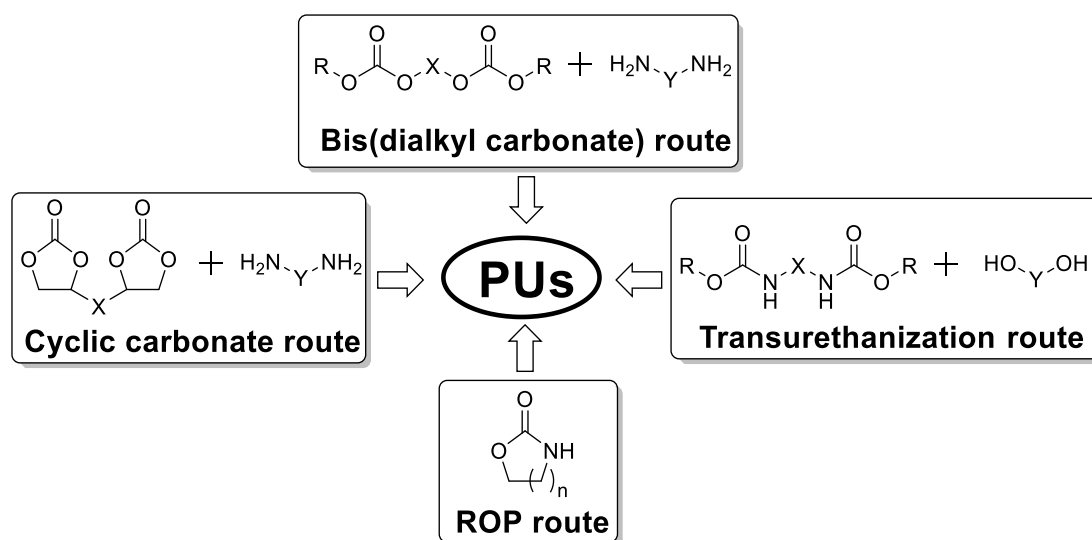
Figure 1.8. Most employed isocyanate-free routes to PUs.

1.2.1 Polyaddition of cyclic di-carbonates and diamines (cyclic carbonate route)

Among the isocyanate-free approaches, polyaddition of cyclic di-carbonates and diamines is the most efficient and popular one.[15-20] The pioneering work of this approach can date back to 1957, when Groszos and coworkers patented the synthesis of oligo hydroxyl-urethanes through the reaction between cyclic carbonates, amine compounds, and ureas.[21] After that, Whelan,[22] Mikheev,[23] and Rokicki and Czajkowska[24] reported the preparation of polyhydroxyurethanes (PHUs) using the polyaddition of bis cyclic carbonates and diamines, which cannot be prepared by the polyaddition of diisocyanates and diols. In 1993, Endo and coworkers described the polyaddition between bis five-membered cyclic carbonates and diamines to prepare PHUs.[25] The authors systematically studied the polymerization and found that the most

significant feature of this polyaddition is its high chemoselectivity. For example, it can be performed in the presence of water, alcohol, and esters, which is impossible for the polyaddition between diisocyanates and diols. Bis cyclic carbonate compounds bearing ester group can also be used as monomers. In addition, the property and reactivity of the produced PHUs were also studied in detail.
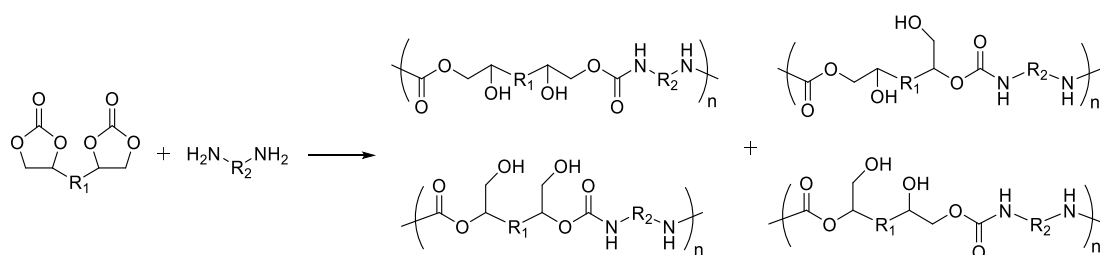

Figure 1.9. Synthetic route of polyhydroxyurethanes from bis 5-membered cyclic carbonates and diamines.

As illustrated in Figure 1.9, the typical synthetic route is the polyaddition of bis-5-membered cyclic carbonates and diamines which produces linear PHUs with primary or secondary alcohols along the polymer chains. Based on this strategy, various PHUs with different structures and properties can be synthesized by changing the R_1 group on the bis-5-membered cyclic carbonates or R_2 group on the diamines. For example, Endo and co-workers have prepared optically active PHUs by the polyaddition of bis five-membered cyclic carbonates monomers derived from bisphenol A and L-lysine derivatives in the presence of base such as 1,8-diazabicyclo[5.4.0]undec-7-ene (DBU) (Figure 1.10).[26] The synthesized PHUs was able to react with cupric acetate, sodium tetrahydroborate, and titanium tetraisopropoxide to afford the corresponding crosslinked gels immediately, which are expected to be novel optically active catalysts, optically active supports for HPLC or biodegradable materials.

Guillaume and coworkers have reported a simple isocyanate-free method to synthesize poly(trimethylene carbonate hydroxyurethane)s (PTMCHUs) containing polycarbonate segments of tunable length/molar mass from the ring-opening polyaddition of α,ω-di(cyclic carbonate) telechelic polycarbonate precursors synthesized by ROP of trimethylene carbonates with cyclic carbonate alcohols as the

chain transfer agent, and diamines (Figure 1.11).[27] Taking into account the biodegradability of the synthesized PTMCHUs, the biomass (glycerol) origin of the starting materials, the initial preparation of the polycarbonates from "immortal" ring opening polymerization (iROP), the absence of toxic isocyanates and of any tin catalyst during the PU formation, this strategy presents a more environmentally friendly approach to prepare poly(carbonate-urethane)s.
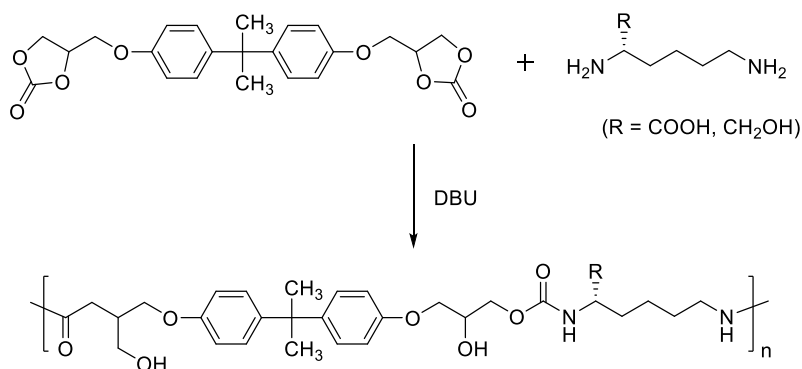

Figure 1.10. Synthetic route of optically active PHUs from bis 5-membered cyclic carbonates and diamines.[26]

Also, 6- and 7- membered dicyclic carbonates were used for the polyaddition reaction with diamines to form PHUs.[28-30] For example, Cramail and coworkers have prepared bis 6-membered cyclic carbonates from methyl 10-undecenoate, which was produced from ricinoleic acid, a main constituent of castor oil (Figure 1.12).[31] Kinetic studies of these novel fatty acid based 6-membered cyclic carbonates revealed that they had higher reactivity toward hexylamines than their analogues, 5-membered ones (30 times). This result was also confirmed by the work of Tomita and coworkers,[28,32] who found that 6-membered cyclic carbonates reacted quantitatively with hexylamines at 30 °C over a period of 24 h, whereas the conversion of 5-membered cyclic carbonates was much lower (*e.g.*, 34%). Thermoplastic isocyanate free PHUs were then synthesized from the polyaddition of bis 6-membered cyclic carbonates and dodecane-1,12-diamines at a temperature as low as room temperature in solution or bulk. At higher conversion, a chemical gel was obtained possibly due to the ring opening of cyclic carbonates by the formed hydroxides on PHUs. Quenching with a large excess of

hexylamines could break the network in the gel along with the formation of urea linkages.
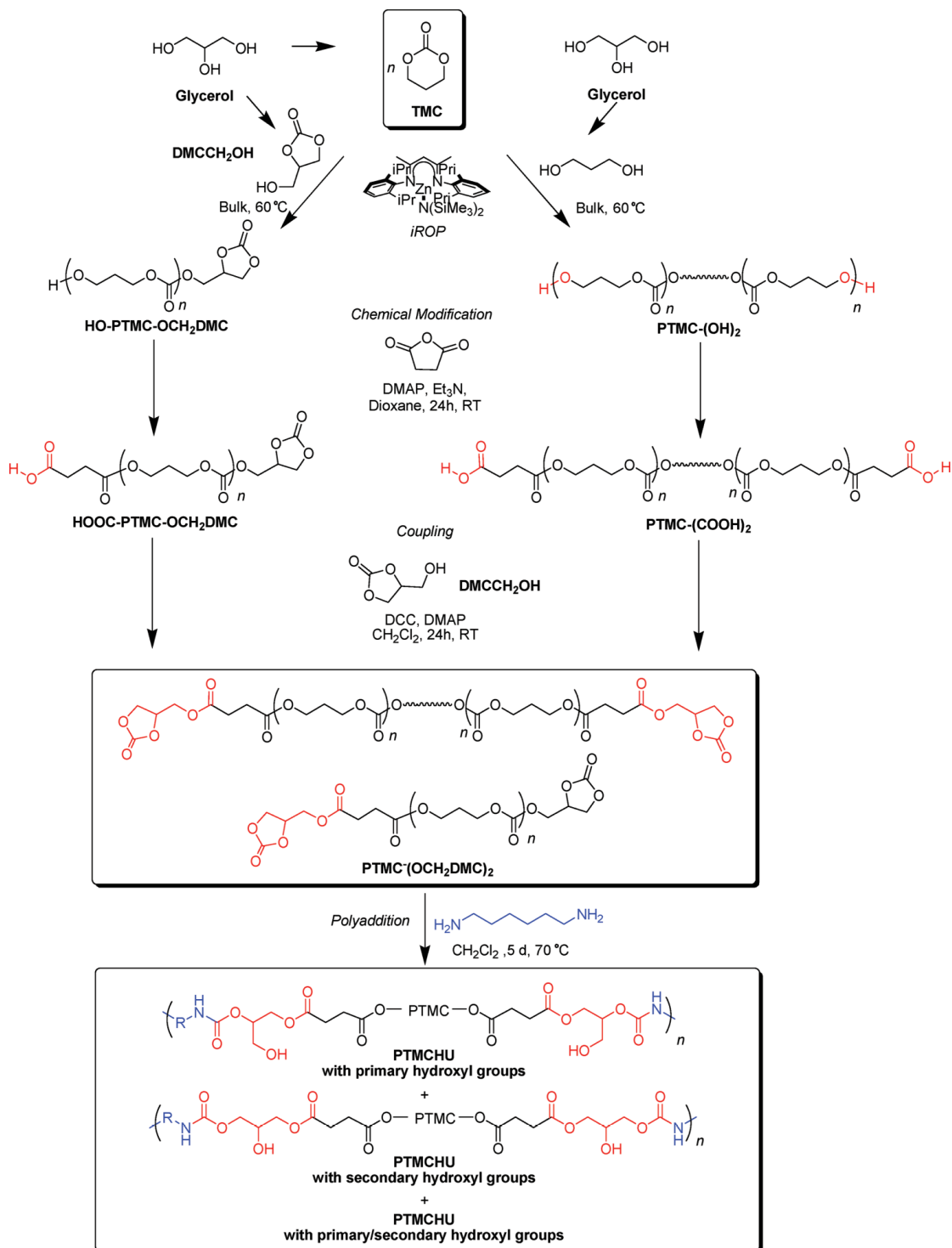
Figure 1.11. Representation of the general approach for the synthesis of poly(trimethylene carbonate hydroxyurethane)s (PTMCHUs) starting from trimethylene carbonate (TMC).[27]
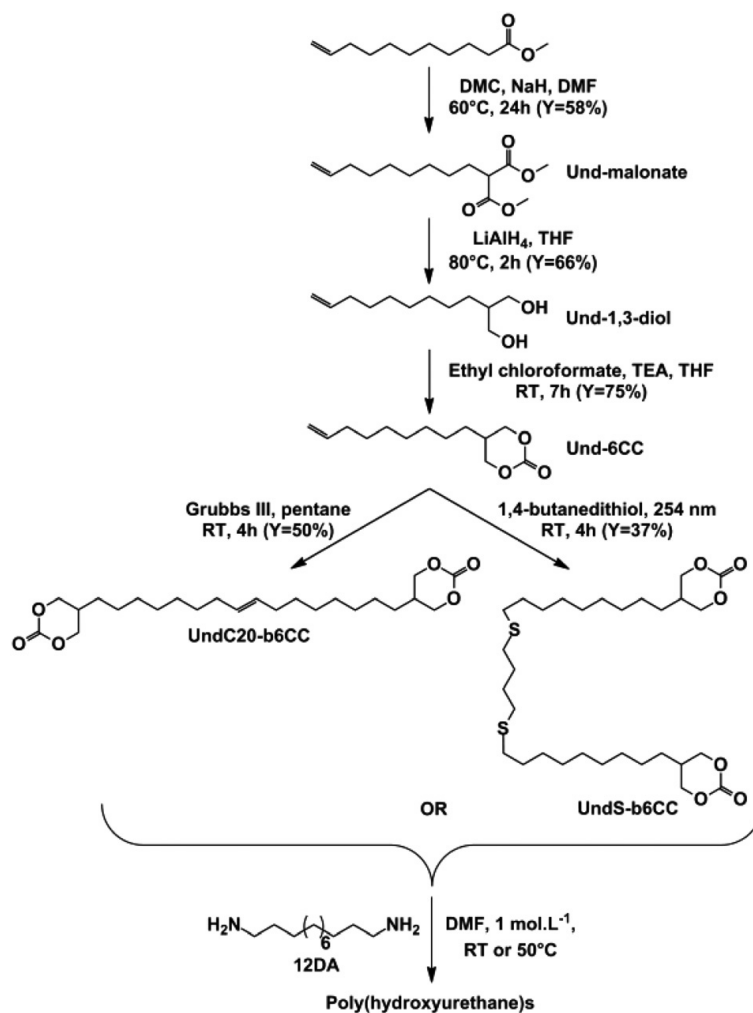
Figure 1.12. General synthetic route to bis 6-membered cyclic carbonates and poly(hydroxyurethane)s.[31]

Recently, Matsukizono and Endo have reported the synthesis of multifunctional 6-membered cyclic carbonates (6-CCs) comprising acetal structures *via* phosgene-free routes, which could be utilized to fabricate reworkable networked poly(acetal-hydroxyurethane)s (PAHUs) films (Figure 1.13).[33] The authors found that dibenzoyl-protected di-(trimethylolpropane) (DTMP) reacted with multifunctional aldehydes derived from non-expensive alcohols to form protected multifunctional DTMPs, which were then deprotected to react with diphenyl carbonates to afford multifunctional 6-CCs. The polyaddition of the 6-CCs and diamines (1,3-diaminopropanes, DAPs) effectively proceeded in DMF to produce networked PAHU films with good transparency and flexibility. These films exhibited a self-healing ability due to acid-

catalyzed reversibility of acetal linkages. Particularly, the film fabricated using excess hexa-functional 6-CCs could reform reproducibly with maintaining its mechanical properties to some degree.

Tri-DTMPC **Tetra-DTMPC** **Hexa-DTMPC** **1,3-diaminopropane (DAP)**
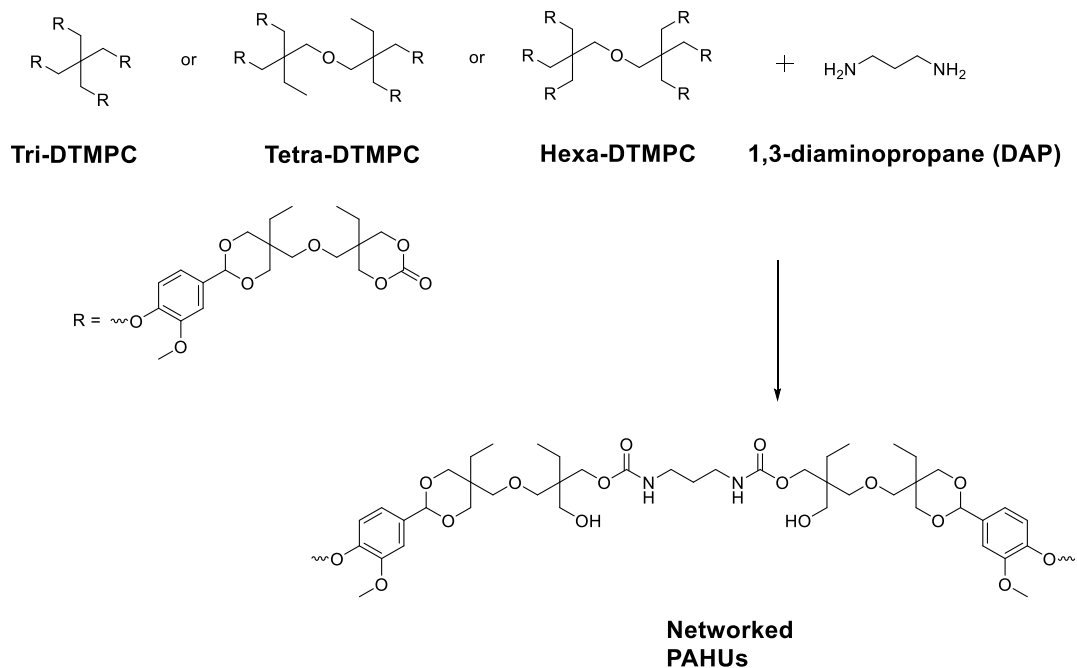
Networked PAHUs

Figure 1.13. Synthesis of networked poly(acetal-hydroxyurethane)s (PAHUs) by the ring-opening polyaddition of multifunctional 6-membered cyclic carbonates (6-CCs) and 1,3-diaminopropanes (DAPs) (DTMPC: di(trimethylolpropane) based 6-CCs).[33]

In summary, the stepwise polyaddition of bicyclic carbonates and polyamines represents a new isocyanate-free method to synthesize PUs, although the PUs obtained are PHUs actually. The PHUs obtained from this route possess various advantages such as the bypass of isocyanates and phosgene derivatives making the synthetic process safer and the capture of CO_2 in some cases. The insensitivity to moisture is also an advantage of this pathway. Moreover, there is no particular caution needed for the storage processes of raw materials and the formation of irreversible side products (urea and CO_2) as produced in the classical isocyanate/ployol route.[17] In addition, the possibility of this route to prepare PU materials with no release of volatile organic compounds allows its use for coating applications.[34] The presence of abundant hydroxyl groups in the polymer structure brings specific properties to the material. For example,

the hydroxyl groups enable the formation of intramolecular and intermolecular hydrogen bonds, which combine with the nonporous structure of the material and absence of thermally labile biuret and allophanate groups improve thermal stability and chemical resistance to nonpolar solvents.[17,35] In addition, the reactive pendant hydroxyl groups make it easy to perform the post functionalization of PHUs with chemical or biological functionalities. However, they may cause higher water absorption owing to the higher hydrophilicity of the polymer in some cases.[28] The other problems such as getting control of the reaction conditions and achieving high molecular weights are also needed to be addressed to make this route more applicable.

1.2.2 Polycondensation of linear activated dicarbonates and diamines (bis(dialkyl carbonate) route)

Synthesis of PUs through the polycondensation of bifunctional linear activated carbonates which are commercially available and diamines represents an alternative access to isocyanate-free PUs.[36,37] Recently, Sardon and coworkers reported an efficient and environmentally friendly method (catalyst- and isocyanate- free) to synthesize PUs *via* nucleophilic polycondensation of activated dicarbonates and diamines in aqueous solution (Figure 1.14).[38] They firstly converted 1,6-hexanediols or poly(ethylene glycol)s to activated dicarbonates by reaction with bis(pentafluorophenyl)carbonates. In the second step, polyurethanes were synthesized in aqueous media through the reaction of the activated carbonate and a linear diamine (JEFFAMINE). The condensation reaction was performed in the presence of a weak organic base, such as triethylamine (TEA) to facilitate the nucleophilic attack of the amine. By varying the 1,6-hexanediol/PEG ratio, the authors prepared five different polyurethanes, which were biodegradable PEG-like polymers with different thermal and mechanical properties. The obtained PUs in aqueous media had relatively high molecular weight (M_n = 15-16.5 kDa) because of the reactivity of the employed activated carbonates, which allowed the urethane linkage formation before the carbonate decomposition in aqueous solution.

However, the presence of toxic pentafluorophenol which is produced as a side product adds limitation to this reaction. The synthesized polymers must be purified carefully before the final application. To solve this problem, Pan and coworkers and Koning and co-workers proposed to use dimethyl carbonates and diphenyl carbonates instead.[39,40] In their work, polyureas were prepared *via* the reaction of primary amines and carbonates in the presence of TBD catalyst.
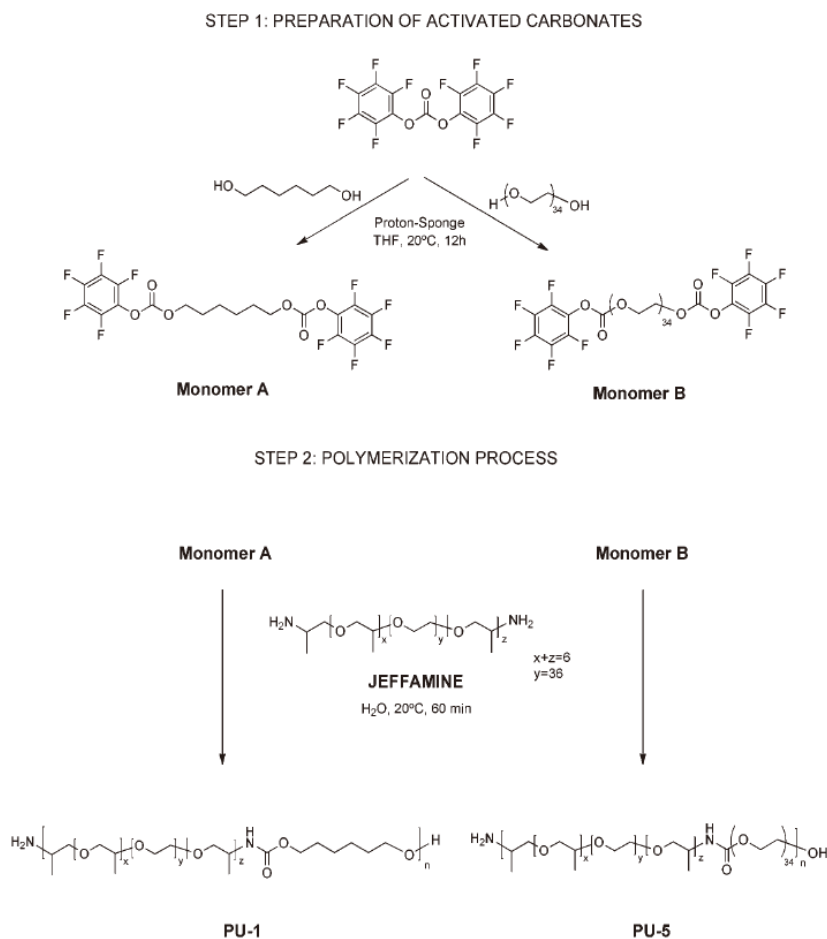
Figure 1.14. Isocyanate- and catalyst-free synthesis of polyurethanes in aqueous media.[38]

1.2.3 Polycondensation of linear activated carbamates and diols (transurethanization route)

In organic chemistry, the condensation reaction between an alcohol and a carbamate molecule can lead to a new carbamate molecule, which is called transurethane reaction, transurethanization or transcarbamoylation. When plurifunctional monomers are used,

PUs can be synthesized, and this represents another isocyanate-free route to PUs (Figure 1.15). The side products generated from this reaction are alcohols, usually with low molecular weights.

The activated dicarbamates used to prepare PUs in this route are usually bis-alkylcarbamates, which can be prepared *via* the reaction between dialkylcarbonates and diamines. The most widely studied dialkylcarbonates are dimethylcarbonates (DMCs), which were originally produced industrially by phosgenation of methanol. Nowadays, several phosgene-free routes are developed with ether using carbon monoxide, methanol, and dioxygen, or carbon dioxide and methanol as starting materials.[41,42] The synthesis of isocyanate-free PUs using this method has been mainly studied with bis-methylcarbamate (BMC) and bis-phenylcarbamate monomers.
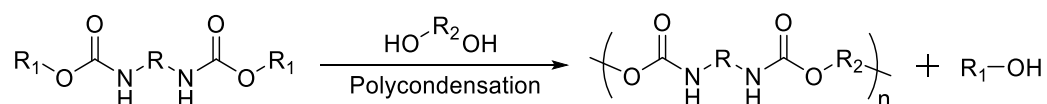
Figure 1.15. Synthesis of isocyanate-free PUs through transurethanization route.
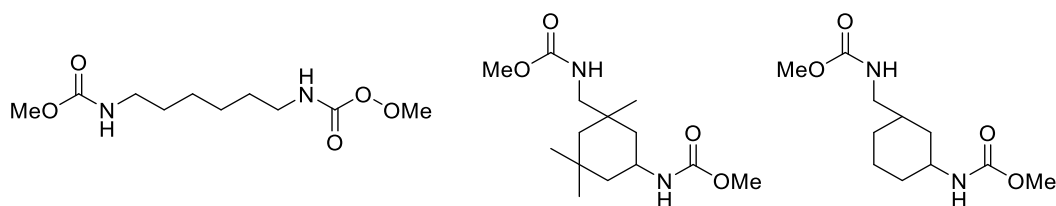
Figure 1.16. Bis-methylcarbamates BMCs.

Jayakannan and coworkers have studied the polycondensation of BMCs (Figure 1.16) with various aliphatic, cyclic, or polymeric diols in detail.[36,43,44] In their studies, the polymerization process started by heating the monomers in bulk at 150 °C for 4 h under nitrogen in the presence of Ti(OBu)$_4$ (titanium butoxide) in catalytic amount. Then the reaction continued for another 2 h under reduced pressure. After characterization of the polymer products, they found that the properties of the synthesized PUs varied with the BMC monomers and diols used; the T_g varied from 31 to 120 °C and M_w varied from 3.9 to 47.7 kDa. They also determined that primary alcohols exhibited higher reactivity

than the secondary ones under identical conditions, thus leading to PUs with higher molecular weights. In addition, BMCs with different molecular structures did not show any significant difference in reactivity when polymerized with the same diols.

For this isocyanate-free route to PUs, polymerizations are usually carried out at high temperatures (above 150 °C) with a two-step procedure. The first step is the formation of PU oligomers under air or nitrogen. Then, reduced pressure is applied to remove the alcohol generated from the reaction and shift the reaction toward the polymerization. It is worth noting that a highly reactive catalyst is mandatory due to the low reactivity of diols compared with diamines. Additionally, dicarbamate monomers are generally difficult to synthesize using isocyanate-free methods, making this route less popular.

1.2.4 Ring opening polymerization (ROP) of cyclic carbamates (ROP route)

Ring opening polymerization (ROP) of cyclic carbamate monomers to prepare PUs is a highly effective and convenient method because ROP has important advantages over conventional polymerization such as atom economy, waste reduction and energy consumption.[45] This new kind of isocyanate-free method is promising as it allows the preparation of non-toxic PUs. Nevertheless, the high stability of the carbamate ring and the reactive hydrogen on the ring add difficulties to control the polymerization, such as the existence of some side reactions. Up to now, only 6- and 7- membered cyclic carbamates have been reported to prepare PUs by cationic ring opening polymerization.

Höcker and coworkers reported the cationic ROP of trimethylene and tetramethylene urethane monomers (TU and TeU, 6- and 7- membered cyclic carbamates respectively) in the melt with methyl trifluoromethanesulfonate (TfOMe) as initiator.[46-49] For the cationic ROP of TU, the polymerization was performed between 100-120 °C for 24 h (Figure 1.17a).[46] They found that the polymerization was homogeneous in the beginning, but the polymer precipitated from the melt later. The polymerization was terminated by dissolution of the product in *N,N*-dimethylacetamide (DMAc) and polymer was purified by precipitation in methanol. The yield of poly(trimethylene urethane)s (PTUs) was about 70% and polymers exhibited a uniform microstructure

without carbonate or urea fragments in the polymer as deduced from NMR spectroscopic analysis. The authors proposed an activated chain-end (ACE) mechanism to explain the cationic ROP of TU monomer. They claimed that a nucleophilic attack of the carbonyl oxygen at the methylene group adjacent to the oxygen atom on the ring was able to occur during the chain growth reaction (Figure 1.17b).
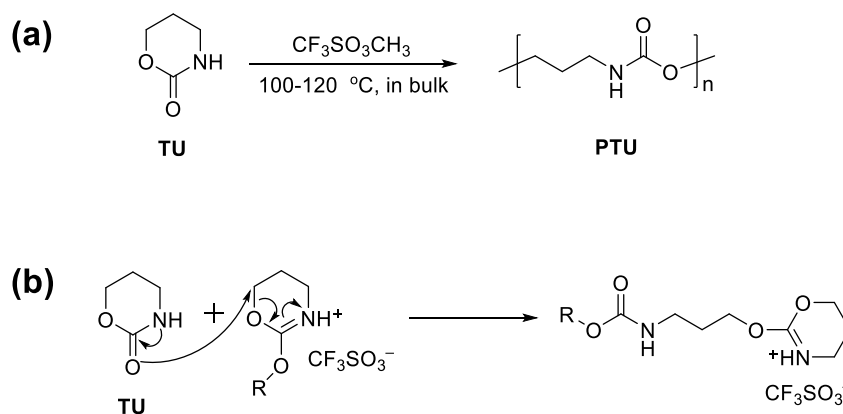
Figure 1.17. Cationic ROP of trimethylene urethane (TU) to poly(trimethylene urethane) (PTU). (a) ROP scheme; (b) proposed activated chain-end (ACE) mechanism of ROP.[46]

After the successful synthesis of PTU homopolymers, the authors prepared di- and triblock copolymers with tetramethyleneoxy and trimethylene urethane repeating units by sequential cationic ROP of tetrahydrofuran (THF) and TU, using the monofunctional initiator TfOMe and bifunctional initiator trifluoromethanesulfonic acid anhydride (TfOTf), respectively (Figure 1.18).[47] They found that the prepared block copolymers PTU-*b*-PTHF after purification showed a uniform A-B or A-B-A microstructure as confirmed by NMR and GPC analyses. The block copolymers were semicrystalline materials with distinct melting points of the poly(THF) and the poly(TU) domains.
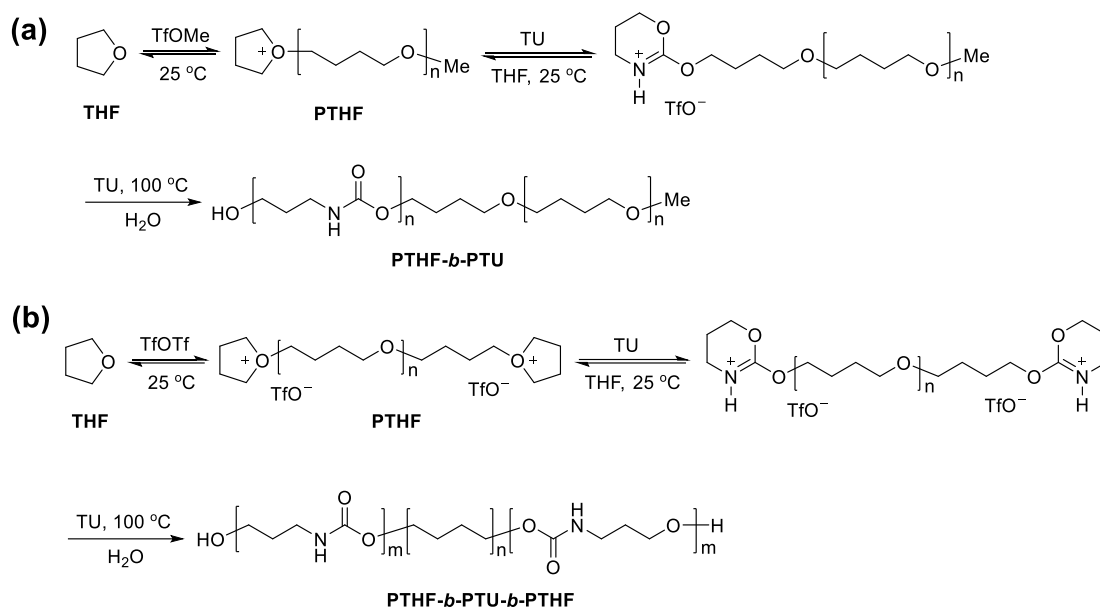
Figure 1.18. Synthesis of PTHF-PTU block copolymers. (a) A-B diblock copolymer; (b) A-B-A triblock copolymer.[47]
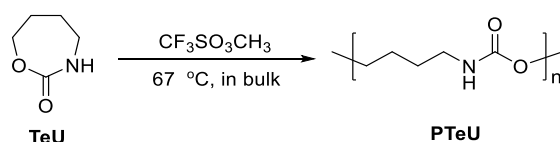
Figure 1.19. Cationic ROP scheme of tetramethylene urethane (TeU) to poly(tetramethylene urethane) (PTeU).[49]

For the cationic ROP of TeU monomer, the polymerization process was similar except that the polymerization temperature was lower (67 °C) because of the lower melting point of TeU compared with TU (Figure 1.19).[49] The polymerization was terminated by cooling the reaction mixture to room temperature followed by maceration of the crushed product with dichloromethane (DCM). After characterization of the obtained PTeU carefully, the authors found that the polymer was a semicrystalline material with a T_g of 47 °C and a T_m of 209.5 °C with a regular microstructure. The polymerization proceeded *via* an active chain-end mechanism with a protonated cyclic endo iminocarbonate as the active species, which was similar to the one obtained for the cationic ROP of TU monomer. As shown in Figure 1.20, the propagation step involved nucleophilic attack of the carbonyl oxygen of the monomer at the endocyclic

methylene group adjacent to the oxygen atom of the active species. They also studied the ROP kinetics and calculated the propagation rate constant, that was, 4.2×10^{-4} mol·L^{-1}·s^{-1}. In addition, the polymerization of TeU was accompanied by termination reactions, although transfer reactions and backbiting reactions were not observed. Thermodynamic analysis also supported the ROP mechanism and the thermal stability of prepared PTeUs.
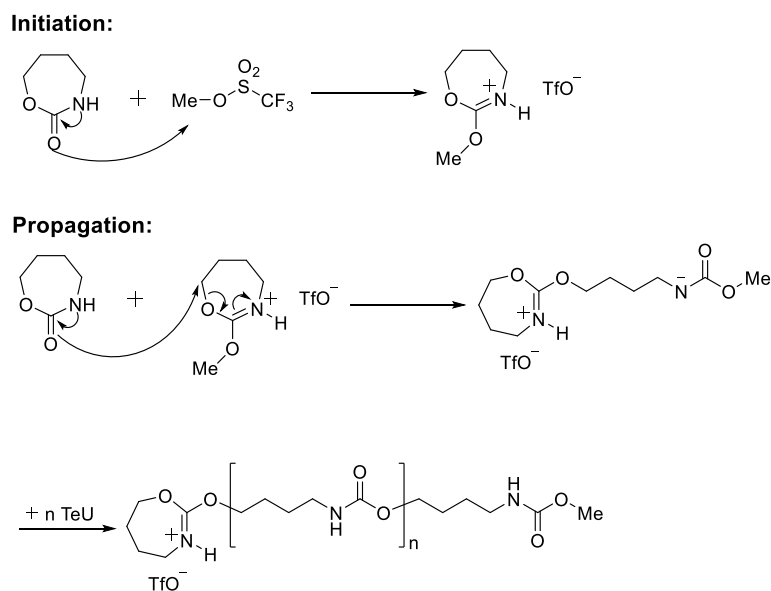
Figure 1.20. Cationic ROP mechanism of tetramethylene urethane (TeU) to poly(tetramethylene urethane) (PTeU).[49]

In summary, ROP of cyclic carbamate monomers is an effective approach to synthesize isocyanate-free PUs according to the literature. However, there are still major drawbacks for the cationic ROP$_S$ mentioned above. For example, these polymerizations are not well-controlled: PDIs are relatively broad (about 2) and the experimental molecular weights are different from the theoretical ones. In addition, the low solubility of the synthesized PUs hampers the characterization by NMR or GPC. Therefore, there is still a great need and importance to control the ROP of cyclic carbamates to prepare PUs.

1.3. Self-assembly of polyurethane-based amphiphilic copolymers

1.3.1 Molecular self-assembly

Molecular self-assembly is the process in which molecules self-organize into a defined arrangement without any role of the outside source. Generally, there are two types of molecular self-assembly: intramolecular self-assembly and intermolecular self-assembly. The intermolecular self-assembly is more typical and common, which is equal to molecular self-assembly in most cases; while the intramolecular self-assembly is sometimes called folding.

Molecular self-assembly is ubiquitous in nature. In the living organism, almost all the components, from DNA, proteins, cells to al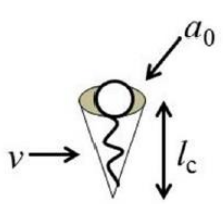l kinds of organs, are constructed by the self-assembly of various biomolecules. For example, cell membranes are formed by the self-assembly of amphiphilic phospholipids; double helical DNAs are constructed through the self-assembly of the base pairs; the self-assembly of proteins can lead to the formation of secondary, tertiary and quaternary structures. Inspired by the biological systems in nature, the studies of molecular self-assembly to design and develop artificial assemblies with specific structures, properties and applications as well as understanding of their principles and theories have attracted more and more attention in recent decades.[50,51]

Up to now, many kinds of sophisticated supramolecular structures have been prepared through the molecular self-assembly. Their sizes range from microscale to macroscale level. Their various morphologies allow the formation of micelles,[52] vesicles,[53] tubes,[54] disks,[55] sticks,[56] fibers,[57] membranes[58] for instance. To our knowledge, most of these self-assemblies are obtained from the intermolecular interactions such as hydrophobic interaction, π-π stacking, hydrogen bonding and electrostatic interaction of amphiphilic molecules containing hydrophobic and hydrophilic parts simultaneously. The common amphiphilic molecules for self-assembly include lipids, surfactants with low molecular masses and polymers with different architectures. For the morphology of the self-assemblies, it is primarily determined by the packing parameter of the amphiphilic molecules, $p = v/a_o l_c$, where v

is the volume of the hydrophobic segment, a_o is the optimized interfacial area of the hydrophilic group, and l_c is the length of the hydrophobic segment (Figure 1.21). In general, when $p < 1/3$, spheres are formed; when $1/3 < p < 1/2$, cylinders; when $1/2 < p < 1$, flexible lamellae or vesicles; finally, when $p = 1$, planar lamellae are obtained. If $p > 1$, inverted structures can be observed.[59,60]
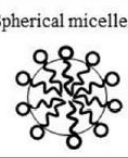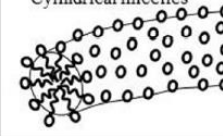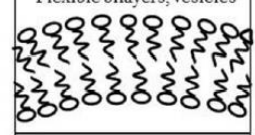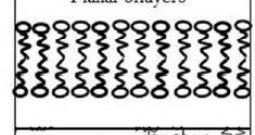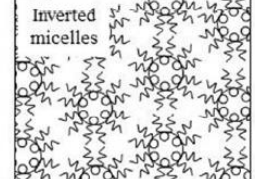
Figure 1.21. Critical packing parameter (CPP, also called packing parameter, p) of molecules for self-assembly and the morphologies of the formed assemblies.[59]

Analogous to the self-assembly of small molecule amphiphiles such as lipids or surfactants, (co)polymers with amphiphilic characteristics also exhibit excellent self-assembly ability in bulk and in solution, based on the similar principles to those found in the self-assembly of small molecules. These amphiphilic polymers include linear polymers, linear block copolymers, graft polymers, star polymers and dendritic polymers, as shown in Figure 1.22.[52,60] Compared with the self-assemblies of small

molecules, polymer self-assemblies present higher stability and robustness owing to their polymeric nature and viscoelastic properties. Therefore, the self-assembly of polymers has attracted more and more attention, not only for academic interest but also for their potential applications in many fields, such as biomedicine, biomaterials, photoelectric materials, microelectronics and catalysts.[52,60,61]
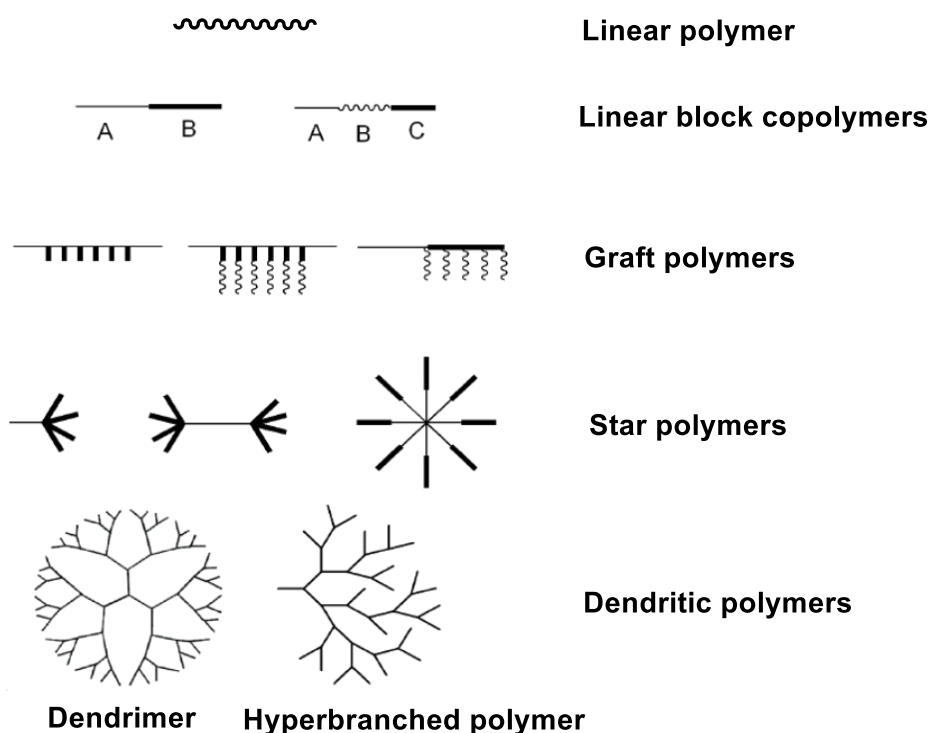
Figure 1.22. Polymers with different topologies for self-assembly.

1.3.2 Self-assembly of linear diblock copolymers

Linear block copolymers, consisting of two or more chemically distinct and frequently immiscible blocks, are the most extensively studied systems for self-assembly. Among different types of block copolymers, diblock copolymers, triblock copolymers, multiblock copolymers and tapered block copolymers are particularly important.[60]

According to the solubility difference of the blocks in water, diblock copolymers can be classified into amphiphilic, double hydrophilic and double hydrophobic systems. Most of the self-assembly studies about diblock copolymers focus on the amphiphilic diblock copolymers. Depending on the difference of block conformation, they can be

categorized into rod-rod, coil-coil and rod-coil block copolymers further.[62] The rod block is a relatively rigid block and the coil block is a relatively flexible one, which exhibits rod and random coil conformation in the free state separately. Coil-coil and rod-coil block copolymers are the most studied linear diblock copolymers for self-assembly (Figure 1.23).
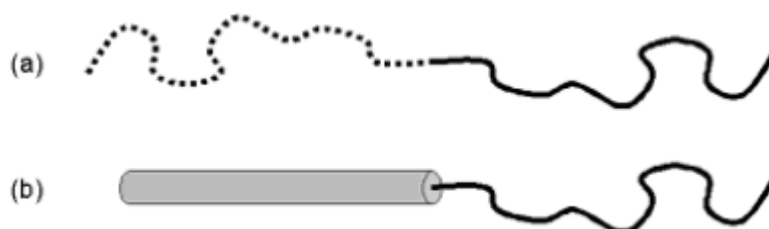
Figure 1.23. Typical linear diblock copolymers for self-assembly. (a) coil-coil diblock copolymers; (b) rod-coil diblock copolymers.[62]

1.3.2.1 Self-assembly of coil-coil diblock copolymers

Generally, coil-coil diblock copolymers are formed by relatively flexible polymer blocks that are chemically incompatible. They can undergo microphase separation to form many kinds of self-assembly morphologies.[63,64] Two emblematic amphiphilic coil-coil diblock copolymers are poly(butadiene-*b*-ethylene oxide) (PB-*b*-PEO) and poly(ethylethylene-*b*-ethylene oxide) (PEE-*b*-PEO). Discher and Bates reported giant wormlike micelles, giant vesicles and three-dimensional networks containing a preponderance of loops and Y-junctions from the self-assembly of these two diblock copolymers (Figure 1.24).[65-67]

Eisenberg and coworkers also conducted a lot of research on the self-assembly of amphiphilic coil-coil diblock copolymers, such as polystyrene-*b*-poly(acrylic acid) (PS-*b*-PAA) and polystyrene-*b*-poly(ethylene oxide) (PS-*b*-PEO). They found that these copolymers in which the hydrophobic blocks were much longer than the hydrophilic segments could form self-assemblies with large hydrophobic regions and small hydrophilic coronas, which were called "crew-cut" aggregates. By contrast, copolymers having longer hydrophilic blocks and shorter hydrophobic blocks usually formed aggregates in which the coronas were much larger than the core regions, which

were called "star-like" aggregates.[71] Moreover, Eisenberg and coworkers found that "crew-cut" aggregates have more morphologies. For example, in the case of the self-assembly of PS-*b*-PAA, a series of thermodynamically controlled morphologies ranging from spheres, rods, bicontinuous rods, bilayers (lamellae and vesicles), to inverse rods and large spheres were observed (Figure 1.25).[72] The factors that had effect on the morphologies included copolymer composition and concentration, ratio of each block, water content in the solution, nature of the common solvent, presence of additives such as ions or homopolymers.[60]
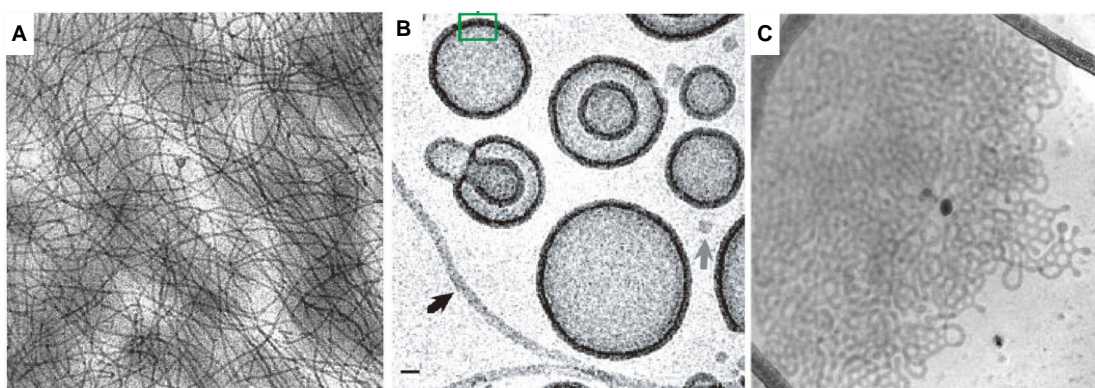
Figure 1.24. Self-assembly morphologies of PB-*b*-PEO and PEE-*b*-PEO diblock copolymers. (A) giant wormlike micelles (PB-*b*-PEO); (B) giant vesicles (PEE-*b*-PEO); (C) three-dimensional networks containing a preponderance of loops and Y-junctions (PB-*b*-PEO).[65-67]
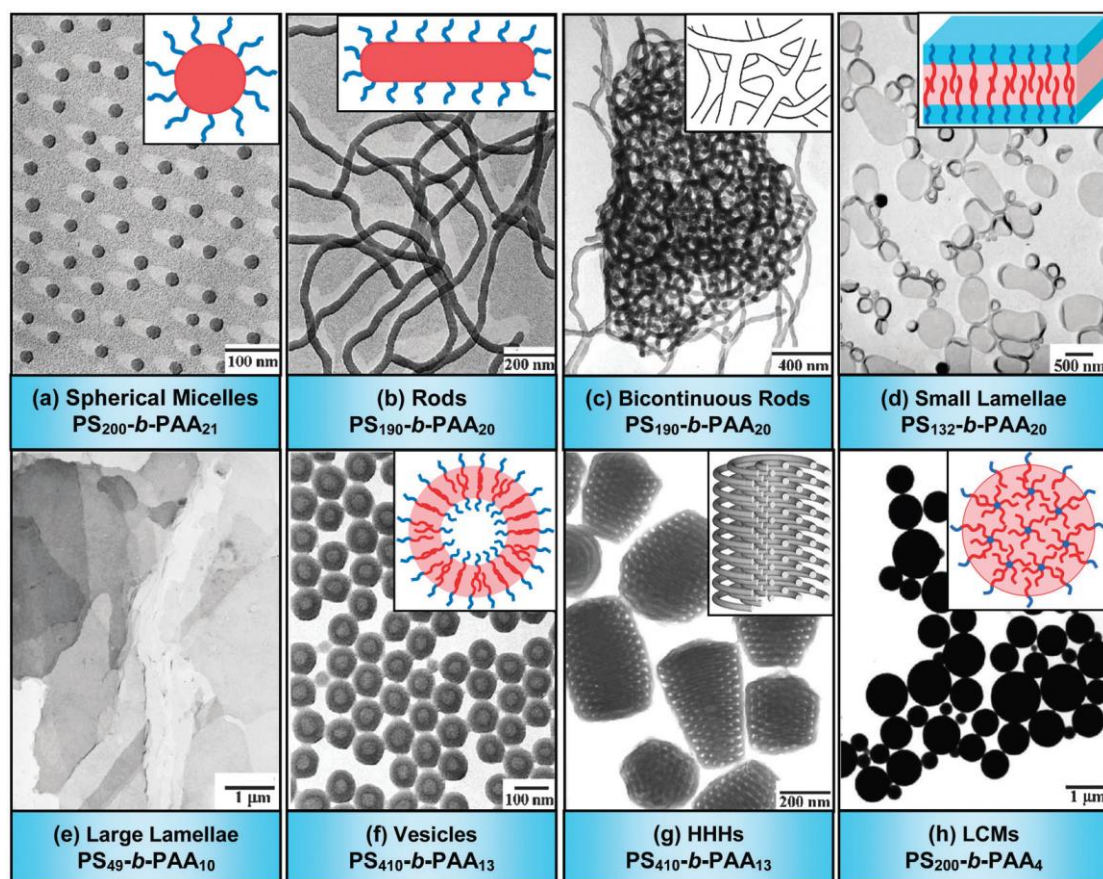
Figure 1.25. Transmission electron microscopy (TEM) photographs and corresponding schematic diagrams of various morphologies formed from amphiphilic PS_m-b-PAA_n copolymers. Note: m and n are the degrees of polymerization of PS and PAA, respectively. In the schematic diagrams, the red represents hydrophobic PS parts, while the blue denotes hydrophilic PAA segments. HHHs: hexagonally packed hollow hoops; LCMs: large compound micelles, in which inverse micelles are composed by a PAA core surrounded by PS coronal chains. Generally, the hydrophilic segments of the "crew-cut" aggregates cannot be seen in TEM images if they are not stained.[72]

1.3.2.2 Self-assembly of rod-coil diblock copolymers

Self-assembly of rod-coil diblock copolymers is affected not only by the relative sizes of the two constituting blocks, but also by the shape anisotropy and additional order in the rod-like block, which results in a more sophisticated self-assembly behavior than that of coil-coil diblock copolymers.[73,74] The shape anisotropy and additional order can be introduced by crystalline and liquid crystalline (LC) structures formed in the

rigid block, or by secondary structures such as α-helix or β-sheet in the case of a peptide.[75-77] For example, M.-H. Li and coworkers have introduced various LC orders in the rod-like block and studied extensively the self-assembly behaviors of the liquid crystalline amphiphilic rod-coil diblock copolymers.[74,76,78-83]
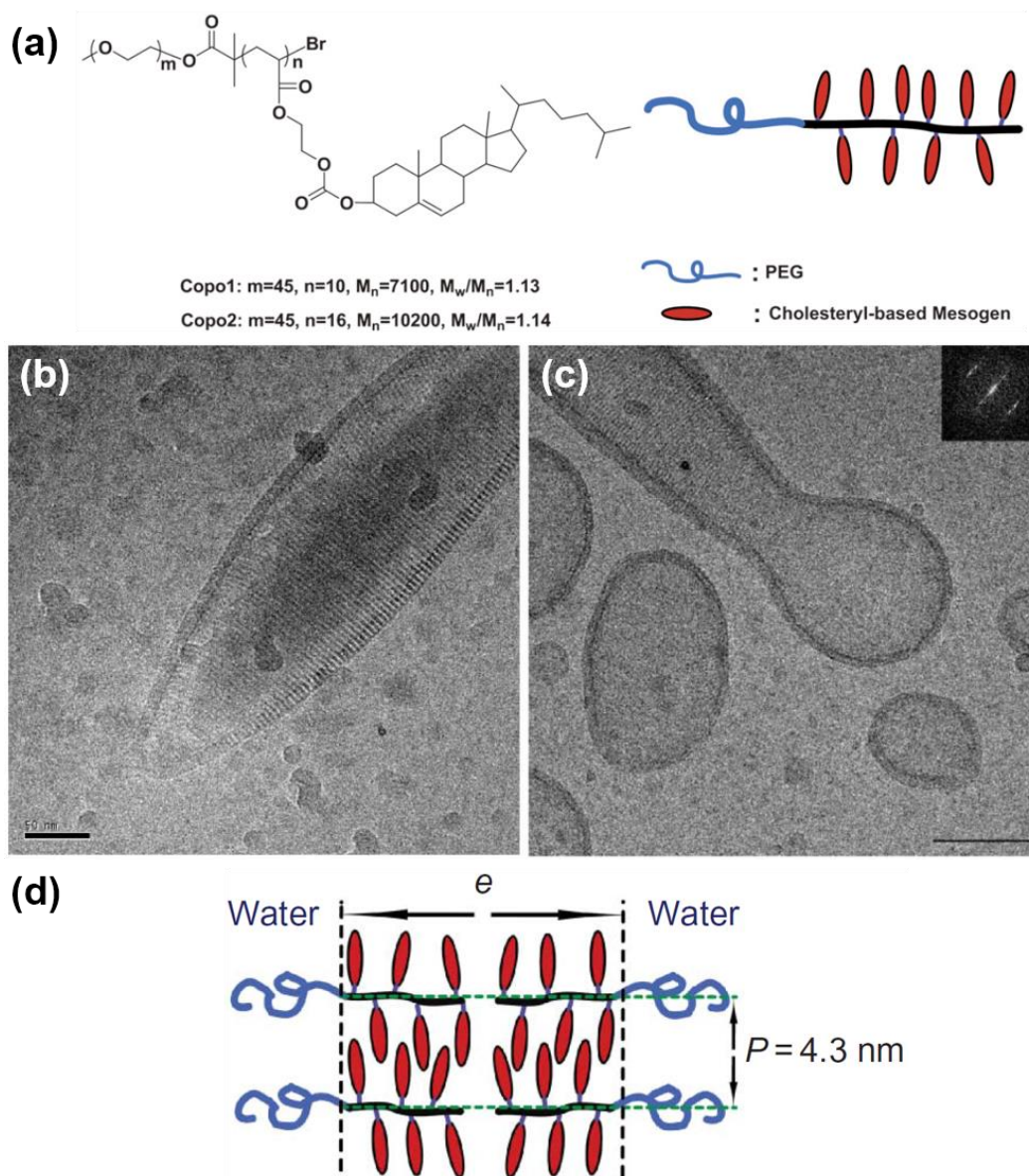
Figure 1.26. (a) Amphiphilic LC block copolymers containing a cholesteryl-based mesogen PEG-*b*-PAChol. Cryo-transmission electron micrographs of smectic polymer vesicles of (b) PEG$_{45}$-*b*-PAChol$_{16}$ (scale bar = 50 nm) and (c) PEG$_{45}$-*b*-PAChol$_{10}$, (scale bar = 100 nm). Inset in (c) is Fourier transform of representative areas of the vesicles. (d) Schematic model of the smectic molecular stacking within a cross section of the membrane of PEG-*b*-PAChol polymersome.[80]

Figure 1.26 showed non-spherical polymersomes formed by an amphiphilic liquid crystal block copolymer consisting of a cholesterol-based smectic LC polymer block (PAChol) and poly(ethylene glycol) (PEG) block (PEG-*b*-PAChol).[80] M.-H. Li and coworkers studied the effects of copolymer composition, hydrophilic/hydrophobic weight ratios and the type of organic solvent on the self-assembly of diblock copolymers in detail. They found that ellipsoidal smectic polymer vesicles and/or nanofibers were formed by adding water into a dilute solution of copolymers in dioxane. If THF was used as the co-solvent, solid spherical aggregates were obtained upon water addition for PEG$_{45}$-*b*-PAChol series, while macroscopic precipitation occurred for PEG$_{114}$-*b*-PAChol series. The mesomorphic properties and microphase segregation structures of the diblock copolymers in bulk were studied by X-ray scattering, DSC (differential scanning calorimetry) and POM (polarized optical microscopy). They found that the interdigital smectic A phase with a lamellar period of 4.3 nm was detected in all diblock copolymers. Also, lamellar type of microphase segregation was observed in some PEG$_{114}$-*b*-PAChol copolymers. Owing to their stable and rigid liquid crystal structures, these polymer vesicles and nanofibers obtained from biocompatible cholesterol-containing diblock copolymers have potentially interesting applications in drug delivery and material science.[80]

1.3.3 Self-assembly of polyurethane-based amphiphilic copolymers

Self-assembly of amphiphilic block copolymers allowed the formation of ordered supramolecular aggregates with better stability and durability than those from small molecules. However, in some specific areas such as drug delivery, the use of polymer nanostructures (*e.g.*, polymer capsules, polymer micelles and polymer vesicles) as drug carriers still has some challenges and issues needed to be solved. For example, how to minimize the side effect induced by the polymer transporter itself, how to increase the drug encapsulation yield and the drug bioavailability over time, how to enhance the targeting efficiency and how to achieve controlled release of drug into the target cells. To address these challenges, new biocompatible and biodegradable polymers need to

be synthesized; efficient targeting groups should be introduced; smart nanostructures with stimuli-responsive properties should be developed; the nanostructures should be well characterized *in vitro* and in *vivo*. Therefore, development of novel self-assembly systems from new biocompatible and biodegradable polymers is a very important research topic.

As polyurethanes display interesting features such as good strength and biocompatibility, these materials can potentially be used to form ordered nanostructures by self-assembly. Advances in polymer synthesis make it possible to prepare biodegradable polyurethanes with different structures and topologies for self-assembly. Consequently, polyurethanes, especially polyurethane-based amphiphilic copolymers, became very promising candidates for drug carriers in drug delivery research. Numerous studies focused on the development of biodegradable polyurethane nanostructures with various functionalities for biomedical applications, due to their good biocompatibility, excellent molecular tailor ability, and convenience to incorporate functional moieties.[84-87] Also, design and development of polyurethane-based self-assemblies for applications other than drug delivery is also very attractive. The self-assembly of polyurethane-based amphiphilic copolymers with different topologies will be introduced briefly in the following part.

1.3.3.1 Self-assembly of polyurethane-based linear block copolymers

Similar to traditional amphiphilic diblock or triblock copolymers that can perform self-assembly to form polymeric nanoaggregates as vehicles for delivering drugs, imaging probes or other agents, polyurethane-based linear block copolymers can also form micellar self-assemblies in aqueous solution, driven by hydrophobic interactions.[84] Biodegradable PUs for micelle preparation were readily synthesized through a two-step reaction using polycaprolactone (PCL) and PEG or methoxyl-poly(ethylene glycol)-PCL (mPEG-PCL) diblock copolymer coupled with a chain extender such as L-lysine methyl ester diisocyanate (LDI), isophorone diisocyanate (IPDI) or hexamethylene diisocyanate (HMDI) (Figure 1.27).[88-90] The PEG-PCL-PEG

based PUs could self-assemble into core-shell spherical nanoparticles in water like the traditional triblock copolymers. The formed spherical micelles were able to encapsulate hydrophobic anticancer drugs into their hydrophobic cores and release the cargo in a sustained and controlled manner.[88] Moreover, these nanocarriers are nontoxic by intravenous administration and can act as safe candidates for hydrophobic drug delivery.
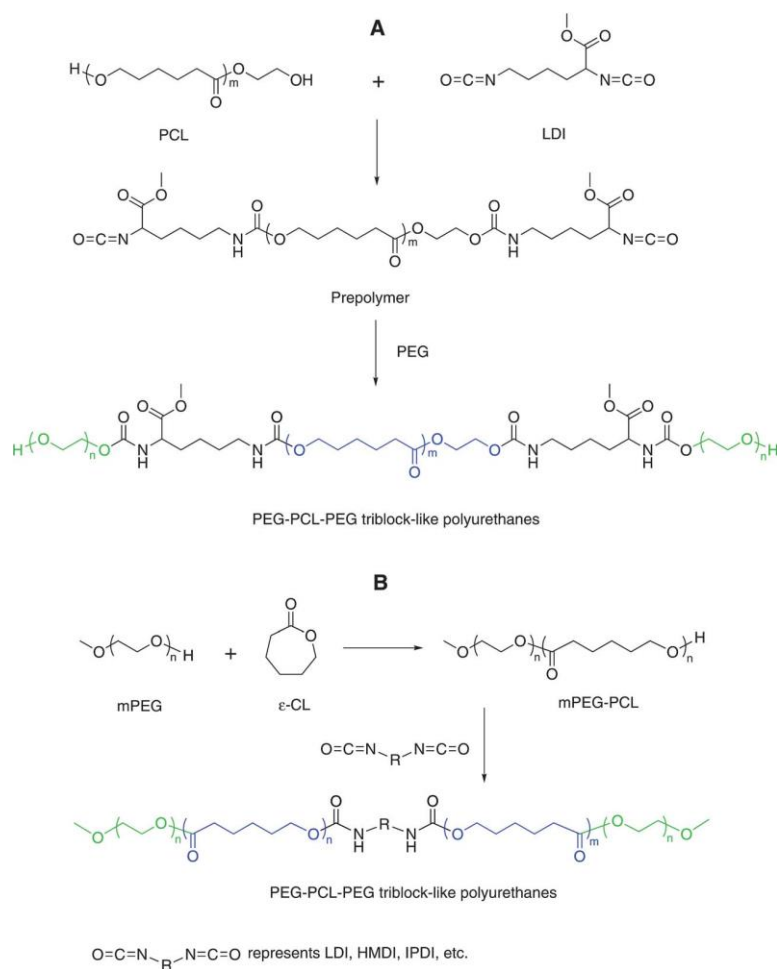
Figure 1.27. Synthetic scheme of polyurethane-based block copolymers containing PEG and PCL segments. [88]

Alternatively, Jin and coworkers reported the preparation and self-assembly of an amphiphilic polyurethane phosphate ester (PUP) polymer having similar architecture to phospholipid (Figure 1.28).[91] Polymers consisting of a hydrophilic phosphate head and two amphiphilic PPG-IPDI-MPEG (PPG = poly(propylene glycol)) based PU tails were synthesized *via* coupling and phosphorylation reactions in sequence. These

amphiphilic multiblock PU copolymers self-assembled into various nanostructures in water, such as spheres, worm-like micelles, vesicles and large compound vesicles, depending on the hydrophobic chain length of PU tails and the initial polymer concentrations in water. The authors found that the morphology transition was not only caused by the molecular structures of amphiphilic PUs, but also influenced by the additional hydrophobic phosphate groups incorporated, which can affect the force balance governing the aggregation structures.
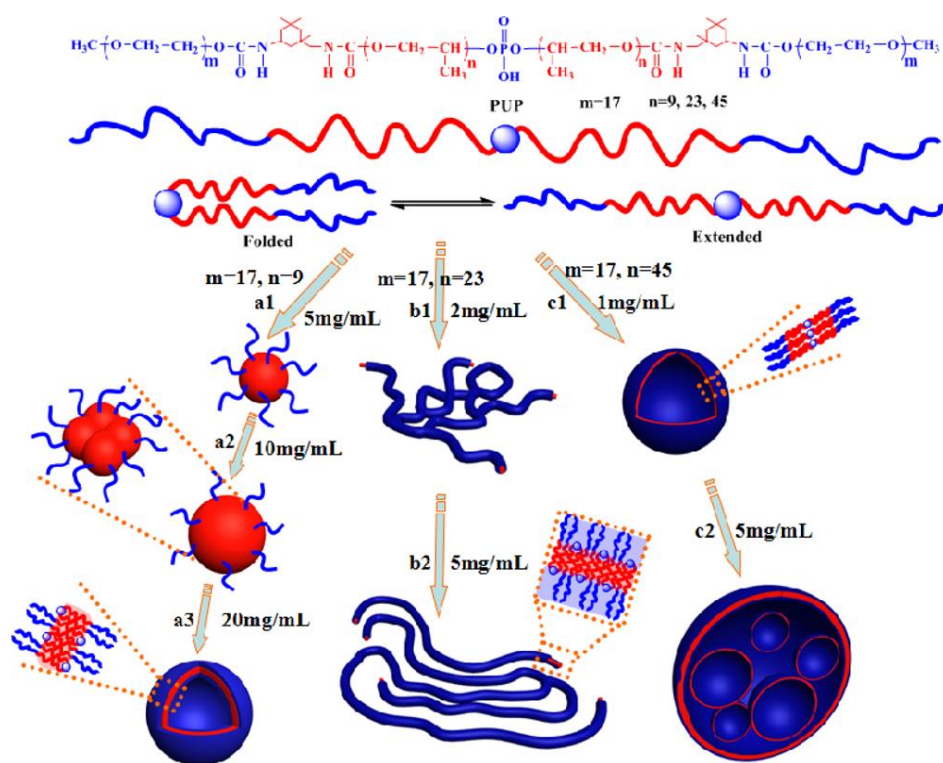
Figure 1.28. Chemical structures of phospholipid-like polyurethane phosphate ester (PUP) polymers and the schematic diagram of their self-assembly in water.[91]

1.3.3.2 Self-assembly of polyurethane-based graft copolymers

Rodriguez-Hernandez and coworkers reported the preparation and self-assembly behavior of a polyurethane-based graft copolymer combining soft lateral poly(*n*-butyl acrylate) (PnBuA) chains with rigid and crystallizable polycaprolactone (PCL) segments in its structure (Figure 1.29).[92] Segmented PUs could microphase separate into hard PCL domains with high-glass transition temperature and soft PnBuA domains with low-glass transition temperature. The relationship between the microstructure and
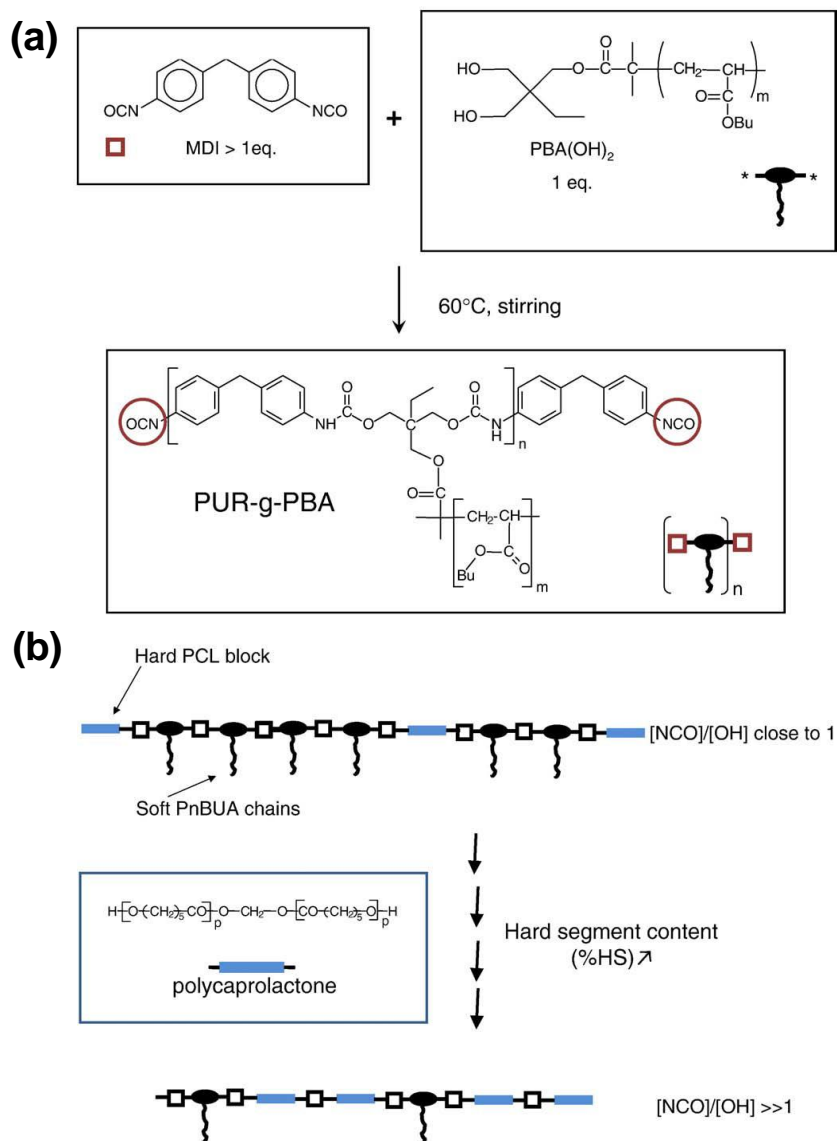
Figure 1.29. Synthetic scheme of graft polyurethanes containing both crystallizable polycaprolactone blocks and soft poly(*n*-butyl acrylate) (PBA, or PnBuA) segments. (a) Reaction scheme to prepare diisocyanate terminated graft PUs. (b) Chain extension of the diisocyanate terminated PUs using polycaprolactone diol. Decrease of the initial chain length of the prepolymer (high [NCO]/[OH] ratio) will produce PUs with a higher content of hard segment within the structure.[92]

the content of hard segment (ratio between hard to soft segments) within the structure has been studied by atomic force microscopy. They observed lamellar planes (multilayered "terrace-like" morphology) in the graft PU films and they found that the increase of the hard segment (PCL) content in the graft PU chains favored the

62

microphase separation to occur in a longer extent. Additionally, they determined that the crystallization mechanism appeared to be related to the properties of the substrates since parallel lamellar structures were formed on hydrophilic substrates while perpendicular lamellae structures were formed on hydrophobic substrates.[92]

1.3.3.3 Self-assembly of polyurethane-based hyperbranched copolymers

Zhibo Li and coworkers reported the preparation and self-assembly of a novel hyperbranched amphiphilic multiblock polyurethane copolymer containing poly(propylene glycol) (PPG), poly(ethylene glycol) (PEG) and polycaprolactone (PCL) segments (Figure 1.30).[93] The hyperbranched poly(PPG/PEG/PCL urethane)s, shortened as HBPEC copolymers, were synthesized from PPG diols, PEG diols and PCL triols using 1,6-hexamethylene diisocyanate (HMDI) as the coupling agent (Figure 1.30a). The authors found that HBPEC copolymers exhibited thermoresponsive micelle formation and aggregation behaviors. As shown in Figure 1.30b, the morphology and size distributions of the HBPEC copolymer micelles in response to temperature were characterized by TEM and DLS. The results showed that the size of the copolymer micelles at 60 °C was significantly larger than the one obtained at 25 °C. It was because PPG behaved more favorably in hydrophilicity at low temperature (25 °C) and the incorporated PCL in the micelles provided the main driving force for self-assembly, while at 60 °C, the PPG segments became dehydrated and hydrophobic. Therefore, the driving force for self-assembly, hydrophobic interaction, was highly enhanced owing to the increase in polymer hydrophobicity resulting from PPG blocks in the copolymer structures. Consequently, PPG chains collapsed with each other, leading to the formation of more densely aggregated and larger micelles with only PEG as the corona.[93]
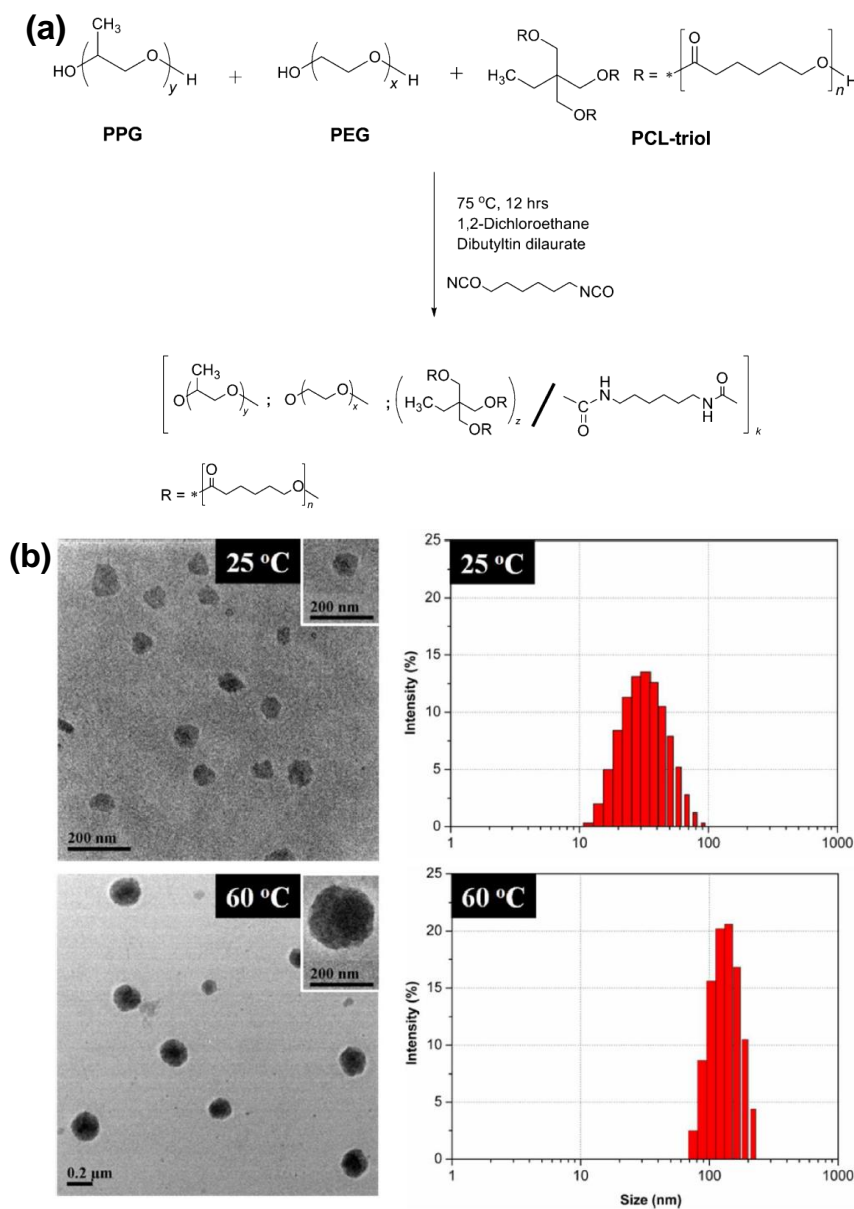
Figure 1.30. (a) Synthetic scheme of hyperbranched poly(PPG/PEG/PCL urethane) (HBPEC) block copolymers. (b) TEM micrographs (left) and size distribution by intensity (right) of micelles formed by HBPEC3 copolymer at different temperatures.[93]

In addition, the authors found that the lower critical solution temperature (LCST) of the copolymers was significantly affected by the copolymer structure. HBPEC copolymers showed much lower LCST than their linear counterparts with the same block composition but different topology of the final copolymer. They determined that the effect of hyperbranched architecture was more prominent in the gelation of the

copolymers. The aqueous solution of HBPEC copolymers showed thermogelling behaviors at critical gelation concentrations (CGCs) ranging from 4.3 to 7.4 wt%, which were much lower than those of PCL-containing linear thermogelling copolymers. More interestingly, at high temperature, HBPEC copolymer formed a dehydrated gel rather than turbid sol which was usually formed by other linear thermogelling copolymers. The authors thought that these phenomena were caused by the hyperbranched structure of HBPEC copolymers, which could enhance the interaction among copolymer branches and improve the chain association through synergetic hydrogen bonding effect.[93]

1.4 Research novelty

In the present thesis work, aliphatic isocyanate-free PUs were synthesized through the anionic ring opening polymerization (AROP) technique for the first time. A series of PU homopolymers with different molecular weights and narrow polydispersity indexes has been synthesized. Based on this AROP method, a series of PU based amphiphilic linear block copolymers PEG-*b*-PUs and graft copolymers (PU-g-PEGs) has also been synthesized. The self-assembly behaviors of these PU based amphiphilic copolymers have been studied carefully. Interestingly, we found that the synthesized PU homopolymers without conjugated structures could emit blue fluorescence upon UV irradiation after thermal treatment. The self-assemblies of the PEG_{22}-*b*-PU diblock copolymers could emit strong cyan fluorescence when they were excited by UV light. In addition, disk-like micelles that could emit fluorescence under UV light were obtained by self-assembly of PU-*g*-PEG graft copolymers with specific composition. The main research contents of the present thesis manuscript focus on chapters II, III and IV, which cover the synthesis of PU homopolymers, linear block copolymers and graft copolymers as well as the self-assembly study of the copolymers. We will discuss them in detail in the following part.

65

References

1. Bayer, O. *Angew. Chem.* **1947**, *59*, 257-272.

2. Chattopadhyay, D. K.; Raju, K. V. S. N. *Prog. Polym. Sci.* **2007**, *32*, 352-418.

3. Akindoyo, J. O.; Beg, M. D. H.; Ghazali, S.; Islam, M. R.; Jeyaratnam, N.; Yuvaraj, A. R. *RSC Adv.* **2016**, *6*, 114453-114482.

4. Engels, H.-W.; Pirkl, H.-G.; Albers, R.; Albach, R. W.; Krause, J.; Hoffmann, A.; Casselmann, H.; Dormish, J. *Angew. Chem. Int. Ed.* **2013**, *52*, 9422-9441.

5. Charlon, M.; Heinrich, B.; Matter, Y.; Couzigné, E.; Donnio, B.; Avérous, L. *Eur. Polym. J.* **2014**, *61*, 197-205.

6. Pauzi, N. N. P. N.; Majid, R. A.; Dzulkifli, M. H.; Yahya, M. Y. *Composites Part B-Engineering* **2014**, *67*, 521-526.

7. Petrović, Z. S. *Polym. Rev.* **2008**, *48*, 109-155.

8. Rajput, S. D.; Hundiwale, D. G.; Mahulikar, P. P.; Gite, V. V. *Progress in Organic Coatings* **2014**, *77*, 1360-1368.

9. Sardon, H.; Pascual, A.; Mecerreyes, D.; Taton, D.; Cramail, H.; Hedrick, J. L. *Macromolecules* **2015**, *48*, 3153-3165.

10. Alsarraf, J.; Ammar, Y. A.; Robert, F.; Cloutet, E.; Cramail, H.; Landais, Y. *Macromolecules* **2012**, *45*, 2249-2256.

11. Coutelier, O.; El Ezzi, M.; Destarac, M.; Bonnette, F.; Kato, T.; Baceiredo, A.; Sivasankarapillai, G.; Gnanou, Y.; Taton, D. *Polym. Chem.* **2012**, *3*, 605-608.

12. Sardon, H.; Chan, J. M. W.; Ono, R. J.; Mecerreyes, D.; Hedrick, J. L. *Polym. Chem.* **2014**, *5*, 3547-3550.

13. Alsarraf, J.; Robert, F.; Cramail, H.; Landais, Y. *Polym. Chem.* **2013**, *4*, 904-907.

14. Pyo, S.-H.; Persson, P.; Mollaahmad, M. A.; Sorensen, K.; Lundmark, S.; Hatti-Kaul, R. *Pure Appl. Chem.* **2012**, *84*, 637-661.

15. Hahn, C.; Keul, H.; Möller, M. *Polym. Int.* **2012**, *61*, 1048-1060.

16. Guan, J.; Song, Y.; Lin, Y.; Yin, X.; Zuo, M.; Zhao, Y.; Tao, X.; Zheng, Q. *Ind. Eng. Chem. Res.* **2011**, *50*, 6517-6527.

17. Kathalewar, M. S.; Joshi, P. B.; Sabnis, A. S.; Malshe, V. C. *RSC Adv.* **2013**, *3*, 4110-

4129.

18. Pyo, S.-H.; Persson, P.; Mollaahmad, M. A.; Sörensen, K.; Lundmark, S.; Hatti-Kaul, R. *Pure Appl. Chem.* **2011**, *84*, 411-860.

19. Nohra, B.; Candy, L.; Blanco, J.-F.; Guerin, C.; Raoul, Y.; Mouloungui, Z. *Macromolecules* **2013**, *46*, 3771-3792.

20. Blattmann, H.; Fleischer, M.; Bähr, M.; Mülhaupt, R. *Macromol. Rapid Commun.* **2014**, *35*, 1238-1254.

21. Groszos, S. J.; Drechsel, D. a. E. K. U.S. Patent US2802022, 1957. *Chem. Abstr.* **1957**, *51*, 99381.

22. Whelan, J. M., Jr.; Hill, M.; Cotter, R. J. U.S. Patent US3072613, 1963.

23. Mikheev, V. V.; Svetlakov, N. V.; Sysoev, V. A.; Brus'ko, N. V. Deposited Document SPSTL 41 Khp-D82, 1982; *Chem. Abstr.* **1983**, *98*, 127745a.

24. Rokicki, G.; Czajkowska, J. *Polimery* **1989**, *34*, 141-147.

25. Kihara, N.; Endo, T. *J. Polym. Sci. Part A: Polym. Chem.* **1993**, *31*, 2765-2773.

26. Kihara, N.; Kushida, Y.; Endo, T. *J. Polym. Sci. Part A: Polym. Chem.* **1996**, *34*, 2173-2179.

27. Helou, M.; Carpentier, J.-F.; Guillaume, S. M. *Green Chem.* **2011**, *13*, 266-271.

28. Tomita, H.; Sanda, F.; Endo, T. *J. Polym. Sci., Part A: Polym. Chem.* **2001**, *39*, 860-867.

29. Matsukizono, H.; Endo, T. *RSC Adv.* **2015**, *5*, 71360-71369.

30. Tomita, H.; Sanda, F.; Endo, T. J. *Polym. Sci., Part A: Polym. Chem.* **2001**, *39*, 4091-4100.

31. Maisonneuve, L.; Wirotius, A.-L.; Alfos, C.; Grau, E.; Cramail, H. *Polym. Chem.* **2014**, *5*, 6142-6147.

32. Tomita, H.; Sanda, F.; Endo, T. *J. Polym. Sci., Part A: Polym. Chem.* **2001**, *39*, 162-168.

33. Matsukizono, H.; Endo, T. *J. Am. Chem. Soc.* **2018**, *140*, 884-887.

34. Delebecq, E.; Pascault, J.-P.; Boutevin, B.; Ganachaud, F. *Chem. Rev.* **2013**, *113*, 80-118.

35. Figovsky, O.; Shapovalov, L.; Leykin, A.; Birukova, O.; Potashnikova, R. *Chem. Chem. Technol.* **2013**, *7*, 79-87.

36. Deepa, P.; Jayakannan, M. *J. Polym. Sci., Part A: Polym. Chem.* **2008**, *46*, 2445-2458.

37. Zahn, H.; Dominik, M. *Makromol. Chem.* **1961**, *44-46*, 290-311.

38. Sardon, H.; Engler, A. C.; Chan, J. M. W.; Coady, D. J.; O'Brien, J. M.; Mecerreyes, D.; Yang, Y. Y.; Hedrick, J. L. *Green Chem.* **2013**, *15*, 1121-1126.

39. Pan, W. C.; Lin, C.-H.; Dai, S. A. *J. Polym. Sci., Part A: Polym. Chem.* **2014**, *52*, 2781-2790.

40. Tang, D.; Mulder, D.-J.; Noordover, B. A. J.; Koning, C. E. *Macromol. Rapid Commun.* **2011**, *32*, 1379-1385.

41. Romano, U.; Tesel, R.; Mauri, M. M.; Rebora, P. *Ind. Eng. Chem. Prod. Res. Dev.* **1980**, *19*, 396-403.

42. Peng, W.; Zhao, N.; Xiao, F.; Wei, W.; Sun, Y. *Pure Appl. Chem.* **2011**, *84*, 603-620.

43. Deepa, P.; Jayakannan, M. *J. Polym. Sci., Part A: Polym. Chem.* **2007**, *45*, 2351-2366.

44. Deepa, P.; Jayakannan, M. *J. Polym. Sci., Part A: Polym. Chem.* **2008**, *46*, 5897-5915.

45. Dechy-Cabaret, O.; Martin-Vaca, B.; Bourissou, D. *Chem. Rev.* **2004**, *104*, 6147-6176.

46. Neffgen, S.; Keul, H.; Höcker, H. *Macromol. Rapid Commun.* **1996**, *17*, 373-382.

47. Neffgen, S.; Keul, H.; Höcker, H. *Macromol. Rapid Commun.* **1999**, *20*, 194-199.

48. Neffgen, S.; Kusan, J.; Fey, T.; Keul, H.; Höcker, H. *Macromol. Chem. Phys.* **2000**, *201*, 2108-2114.

49. Kusan, J.; Keul, H.; Höcker, H. *Macromolecules* **2001**, *34*, 389-395.

50. Lasic, D. D. *Trends Biotechnol.*, **1998**, *16*, 307-321.

51. Fong, C.; Le T.; Drummond C. J. *Chem. Soc. Rev.*, **2012**, *41*, 1297-1322.

52. Riess, G. *Prog. Polym. Sci.* **2003**, *28*, 1107-1170.

53. Antonietti, M.; Forster, S. *Adv. Mater.* **2003**, *15*, 1323-1333.

54. Shimizu, T.; Masuda, M.; Minamikawa, H. *Chem. Rev.* **2005**, *105*, 1401-1443.

55. Zemb, T.; Dubois, M.; Deme, B.; Gulik-Krzywicki, T. *Science* **1999**, *283*, 816-819.

56. Hartgerink, J. D.; Beniash, E.; Stupp, S. I. *Science* **2001**, *294*, 1684-1688.

57. Wang, X.; Guerin, G.; Wang, H.; Wang, Y.; Manners, I.; Winnik, M. A. *Science* **2007**, *317*, 644-647.

58. Israelachvili, J. N.; Mitchell, D. J.; Ninham, B. W. *J. Chem. Soc. Faraday Trans.* **1976**, *72*, 1525-1568.

59. Salim, M.; Minamikawa, H.; Sugimura, A.; Hashim, R. *Medchemcomm* **2014**, *5*, 1602-1618.

60. Mai, Y.; Eisenberg, A. *Chem. Soc. Rev.* **2012**, *41*, 5969-5985.

61. Alexandridis, P.; Lindman, B. *Amphiphilic Block Copolymers: Self-Assembly and Applications*, Elsevier, Amsterdam, **2000**.

62. Klok, H.; Lecommandoux, S. *Adv. Mater.* **2001**, *13*, 1217-1229.

63. Bates, F. S.; Fredrickson, G. H. *Phys. Today* **1999**, *52*, 32-38.

64. Förster, S.; Plantenberg, T. *Angew. Chem., Int. Ed.* **2002**, *41*, 688-714.

65. Won, Y. Y.; Davis, H. T.; Bates, F. S. *Science* **1999**, *283*, 960-963.

66. Discher, B. M.; Won, Y. Y.; Ege, D. S.; Lee, J. C. M.; Bates, F. S.; Discher, D. E.; Hammer, D. A. *Science* **1999**, *284*, 1143-1146.

67. Jain, S.; Bates, F. S. *Science* **2003**, *300*, 460-464.

68. Zhang, L.; Eisenberg, A. *Science* **1995**, *268*, 1728-1731.

69. Zhang, L.; Yu, K.; Eisenberg, A. *Science* **1996**, *272*, 1777-1779.

70. Zhang, L.; Eisenberg, A. *J. Am. Chem. Soc.* **1996**, *118*, 3168-3181.

71. Zhang, L.; Eisenberg, A. *Polym. Adv. Technol.* **1998**, *9*, 677-699.

72. Cameron, N. S.; Corbierre M. K.; Eisenberg, A. *Can. J. Chem.* **1999**, *77*, 1311-1326.

73. Jenekhe, S. A.; Chen, X. L. *Science* **1998**, *279*, 1903-1907.

74. Jia, L.; Cao, A.; Lévy, D.; Xu, B.; Albouy, P.-A.; Xing, X.; Bowick, M. J.; Li, M.-H. *Soft Matter* **2009**, *5*, 3446-3451.

75. Jenekhe, S. A.; Chen, X. L. *Science* **1999**, *283*, 372-375.

76. Yang, J.; Piñol, R.; Gubellini, F.; Lévy, D.; Albouy, P.-A.; Keller, P.; Li, M.-H.

Langmuir **2006**, *22*, 7907-7911.

77. Bellomo, E. G.; Wyrsta, M. D.; Pakstis, L.; Pochan, D. J.; Deming, T. J. *Nat. Mater.* **2004**, *3*, 244-248.

78. Yang, J.; Lévy, D.; Deng, W.; Keller, P.; Li, M.-H. *Chem. Commun.* **2005**, 4345-4347.

79. Piñol, R.; Jia, L.; Gubellini, F.; Lévy, D.; Albouy, P.-A.; Keller, P.; Cao, A.; Li, M.-H. *Macromolecules* **2007**, *40*, 5625-5627.

80. Jia, L.; Albouy, P.-A.; Di Cicco, A.; Cao, A.; Li, M.-H. *Polymer* **2011**, *52*, 2565-2575.

81. Zhang, X.; Boissé, S.; Bui, C.; Albouy, P.-A.; Brûlet, A.; Li, M.-H.; Rieger, J.; Charleux, B. *Soft Matter* **2012**, *8*, 1130-1141.

82. Jia, L.; Cui, D.; Bignon, J.; Di Cicco, A.; Wdzieczak-Bakala, J.; Liu, J.; Li, M.-H. *Biomacromolecules* **2014**, *15*, 2206-2217.

83. Zhou, L.; Zhang, D.; Hocine, S.; Pilone, A.; Trépout, S.; Marco, S.; Thomas, C. M.; Guo, J.; Li, M.-H. *Polym. Chem.* **2017**, *8*, 4776-4780.

84. Ding, M.; Li, J.; Tan, H.; Fu, Q. *Soft Matter* **2012**, *8*, 5414-5428.

85. Bil, M.; Ryszkowska, J.; Woźniak, P.; Kurzydłowski, K. J.; Lewandowska-Szumieł, M. *Acta Biomater.* **2010**, *6*, 2501-2510.

86. Li, Z.; Li, J. J. *Phys. Chem. B* **2013**, *117*, 14763-14774.

87. Ding, M.; He, X.; Wang, Z.; Li, J.; Tan, H.; Deng, H.; Fu, Q.; Gu, Q. *Biomaterials* **2011**, *32*, 9515-9524.

88. Zhang, Y.; Zhuo, R. X. *Biomaterials* **2005**, *26*, 6736-6742.

89. Gong, C.; Wei, X.; Wang, X.; Wang, Y.; Guo, G.; Mao, Y.; Luo, F.; Qian, Z. *Nanotechnology* **2010**, *21*, 215103.

90. Gong, C.; Wang, Y.; Wang, X.; Wei, X.; Wu, Q.; Wang, B.; Dong, P.; Chen, L.; Luo, F.; Qian, Z. *J. Nanopart. Res.* **2011**, *13*, 721-731.

91. Cheng, X. F.; Jin, Y.; Fan, B. Z.; Qi, R.; Li, H. P.; Fan, W. H. *Acs Macro Letters* **2016**, *5*, 238-243.

92. Ibarboure, E.; Baron, A.; Papon, E.; Rodriguez-Hernandez, J. *Thin Solid Films* **2009**,

517, 3281-3286.

93. Li, Z.; Zhang, Z.; Liu, K. L.; Ni, X.; Li, J. *Biomacromolecules* **2012**, *13*, 3977-3989.

Chapter II. Controlled anionic ring opening polymerization of 5-membered cyclic carbamates to polyurethanes

2.1 Introduction

Ring opening polymerization (ROP) is a type of polymerization in which a cyclic monomer opens to yield a monomeric unit which is acyclic or contains fewer cycles than the monomer (Figure 2.1).[1] Together with chain polymerization (radical, ionic and coordination polymerization) and condensation polymerization, ROP is one of the three important paths to synthesize polymers.[2] The typical characteristics of ROP are: only opening of monomer rings is performed in the polymerization process; the connection manner of hydrocarbon groups or heteroatoms varies from intramolecular connection to intermolecular connection; there is no new chemical bonds or groups produced.

$$n \underset{}{\overset{R-Z}{\boxed{}}} \xrightarrow{\text{ROP}} \left[R-Z\right]_n$$
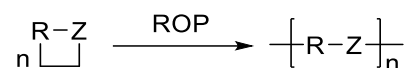
Figure 2.1. General ROP equation of cyclic monomers. R represents hydrocarbon groups and Z represents heteroatoms in the ring. Notably, there is no Z in the case of cyclic alkane or alkene monomers.

The driving force for the ROP of cyclic monomers is the relief of ring strain or steric repulsions between atoms on the ring. The polymerizability of cyclic monomers is dependent on thermodynamic and kinetic factors, among which thermodynamic factors are predominant. From the viewpoint of thermodynamics, the change of Gibbs free energy from cyclic monomers to polymers in ROP should be negative, which is decided by the thermodynamic stability of monomers and polymers.[3]

The common cyclic monomers for ROP include not only cyclic alkanes, alkenes but also heterocyclic ethers, esters (lactones, lactides), carbonates, acetals, anhydrides, amines, amides (lactams), *N*-carboxyanhydrides, carbamates, sulfides, phosphates, and siloxanes. The polymerizability of these cyclic monomers with different ring sizes is summarized in table 2.1 according to the literature.[2,4] From the table we can see that only 6- and 7- membered cyclic carbamates are useful monomers for ROP (up to now).

The polymerizability of cyclic carbamates with other ring sizes is still unknown.

Table 2.1. Polymerizability of cyclic monomers.[2,4]

Cyclic monomers	Ring size						
	3	4	5	6	7	8	≥9
alkanes		+	+	−	+	+	+
olefins		+	+	−	+	+	+
ethers	+	+	+	−	+		
esters		+	−	+	+	+	+
carbonates			−	+	+	+	
acetals			+	−	+	+	+
anhydrides		+	+	−			
amides		+	+	+	+	+	+
imides	+	+	−	−	+		
carbamates				+	+		
ureas			+	−	+		
sulfides	+	+	−	−			
disulfides		+	+	+	+	+	+
thioethers	+	+					
thiolactones		+	+	+	+	+	

+ : monomers can perform ROP; − : monomers cannot perform ROP.

The mechanism of ROP is complicated. Some ROP can proceed *via* a mechanism similar to the chain polymerization (addition of monomer to a growing chain end). However, many ROP reactions are different and proceed *via* mechanisms similar to condensation polymerization or both chain polymerization and condensation polymerization.[2] In ROP, the propagating center can be radical, cationic or anionic. Therefore, ROP could be classified into three types: radical ROP, cationic ROP and anionic ROP. In addition, it is noteworthy that the ROP of cyclic olefins proceeds *via*

another type of mechanism, that is, ring-opening metathesis polymerization (ROMP).[5] As my research subject is anionic ROP of cyclic carbamate monomers to prepare polyurethanes, the anionic ROP will only be introduced in the following part.

2.1.1 Anionic ROP

Anionic ring opening polymerization (AROP) is a kind of ROP in which a nucleophilic and anionic polymer chain end attacks the heterocyclic monomers. The cyclic monomers that can be used for AROP include epoxides, aziridines, episulfides, lactones, lactams, siloxanes and cyclic phosphates. These cyclic monomers usually have an electron-deficient carbon atom on the ring resulting from the presence of an adjacent heteroatom (such as oxygen, nitrogen, sulfur and phosphorous). The AROP of cyclic monomers is very important for many practical applications. For example, the AROP of ε-caprolactam is an important industrial process to produce Nylon 6 (polyamide 6, PA6).

The initiators for AROP are usually nucleophilic reagents, including radical anions, carbanions, alkoxides, silanolates, carboxylates, thiolates, lactam anions, amines and Al-trialkoxides. Generally, AROP is triggered by the nucleophilic attack of the initiator on the electron-deficient carbon atom of the monomer ring, producing a new species that will act as a new "initiator" to react with another monomer.

For the propagation of AROP, the general mechanism is the continuous nucleophilic attack of the growing polymer chain end on the monomer. For example, the AROP of epoxides and lactones proceeds with this mechanism. The typical AROP process of ε-caprolactone initiated by alkoxides is shown in Figure 2.2.[6]
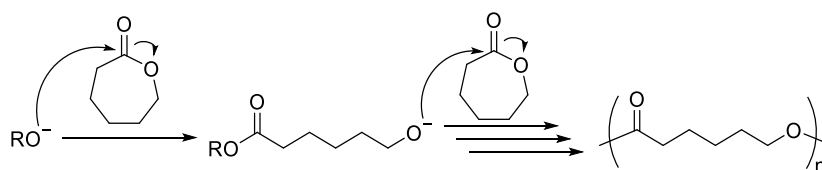
Figure 2.2. The AROP of ε-caprolactone initiated by alkoxides.

2.1.2 Anionic ROP mechanism of ε-caprolactams

Another possible mechanism of AROP is the continuous nucleophilic attack of an activated monomer on the growing polymer chain end. For example, the AROP of lactams and *N*-carboxyanhydrides proceeds with this mechanism.[7-10] The typical AROP process of ε-caprolactams initiated by sodium hydride is shown in Figure 2.3. Other strong bases such as alkali metals, metal amides, metal alkoxides and organometallic compounds can also initiate the AROP of lactam monomers by forming the lactam anions.

I. Initiation

II. Propagation
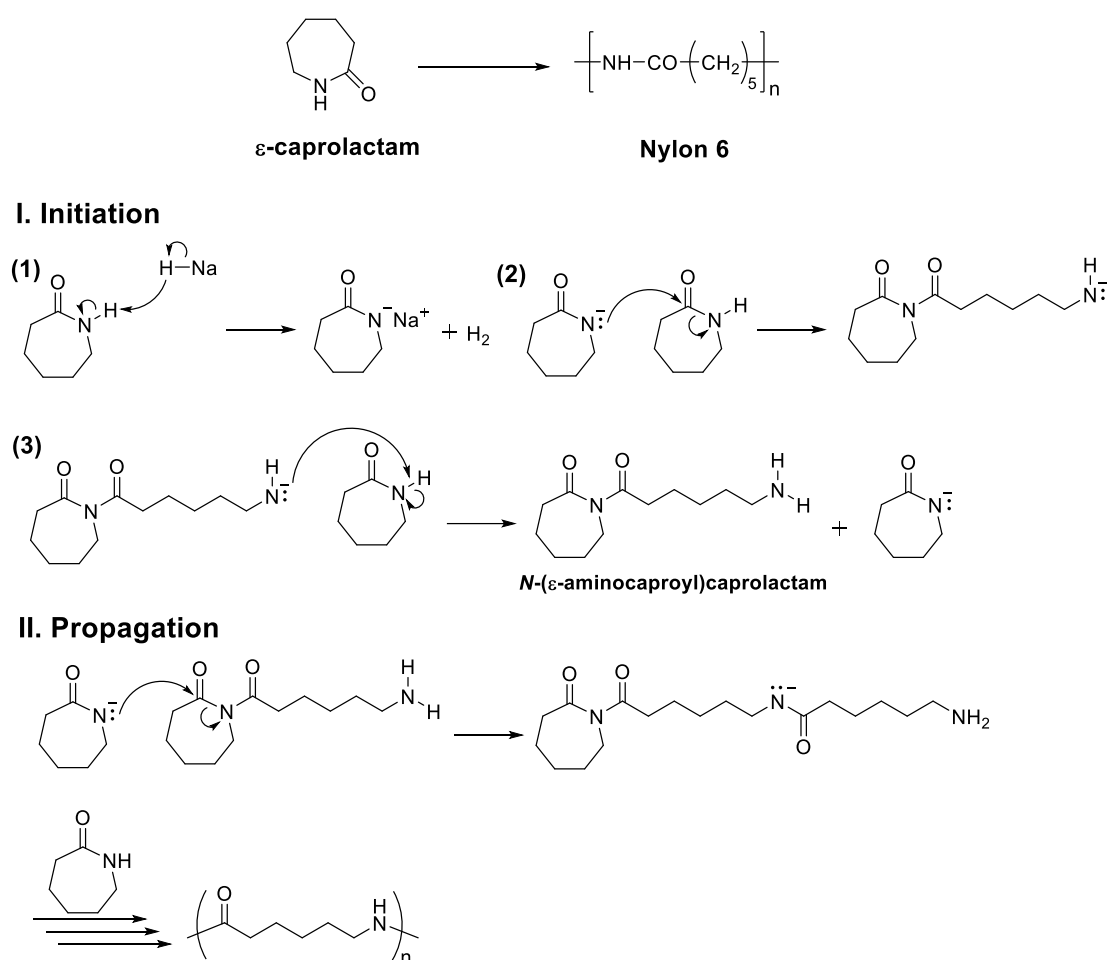
Figure 2.3. The AROP of ε-caprolactams initiated by sodium hydride.

For the AROP initiation of ε-caprolactams by sodium hydride (Figure 2.3, I), the first step is the deprotonation of lactams to produce lactam anions. In the second step, the lactam anions react with ε-caprolactam monomers through a ring opening

transamidation reaction to produce the primary amine anions. Unlike the lactam anion, the highly reactive linear primary amine anion is not stable by conjugation with a carbonyl group. Thus, in the third step, it rapidly abstracts a proton from another ε-caprolactam monomer to form the stable imide dimer, *N*-(ε-aminocaproyl)caprolactam and the lactam anions are regenerated simultaneously. In the further propagation steps (Figure 2.3, II), the highly reactive linear second amine anion replaces the linear primary amine anion in initiation to regenerate the lactam anions (*i.e.*, activated monomer).

This imide dimer has already been isolated and is the actual initiating species of the following ROP.[11,12] AROP of lactams is characterized by an initial induction period with low reaction rate since the formation of imide dimers is slow. The imide dimer is necessary for the propagation because the amide bond in the lactam ring is not sufficiently reactive toward transamidation by lactam anions. The presence of the *exo*-carbonyl group attached to the nitrogen in the *N*-acyllactam structure increases the electron deficiency of the amide linkage, which improves the reactivity of the amide ring structure toward nucleophilic attack by lactam anions. Propagation proceeds in the same manner as the reaction of the imide dimers and lactam anions, followed by fast proton exchange with other ε-caprolactams to regenerate the lactam anions and propagating polymer chains.

The AROP of lactam monomers proceeds through an activated monomer mechanism. The propagation center is the cyclic amide linkage with a *N*-acyl structure. It is the monomer anions (lactam anions), often referred to as activated monomers, rather than monomers that add to the propagating polymer chain. The propagation rate depends on the concentrations of lactam anions and *N*-acyllactams, both of which are determined by the concentrations of lactam monomers and base.

In addition, the use of strong base alone for initiating the AROP of lactams is limiting because of the long induction period to produce *N*-acyllactams. Generally, a *N*-acyllactam compound like *N*-acetylcaprolactam can be synthesized by reaction of lactam and an acylating agent such as acid chloride, anhydride, isocyanate,

monocarbodiimide or others. The addition of this *N*-acyllactam compound to the reaction system can reduce the initiation time efficiently and increase the polymerization rate as well as the molecular weight of final polymer.[13]

For the transfer and termination of AROP, it is relatively fast as the active centers of AROP such as alkoxides or carboxylates are nucleophilic species which can act as bases to abstract protons from monomers, waters, other polymer chains and so on.[2] Therefore, it is necessary to remove water and impurities in the AROP systems to produce well-defined polymers with high molecular weights.

2.2 Research subjects

In this work, we have prepared polyurethanes (PUs) with novel structures *via* the anionic ring opening polymerization (AROP) of a 5-membered cyclic carbamate monomer. The cyclic monomer was carefully designed and synthesized. The ROP was performed at low temperature using specific initiator and co-initiator, which was well controlled. The prepared PUs had relatively narrow polydispersity indexes (PDI = 1.2-1.3) and the experimental molecular weights were close to the theoretical ones. The AROP mechanism was proposed and proved, which was a new mechanism for the synthesis of PU. The study of the ROP kinetics showed that the polymerization can present the characteristics of the first order kinetics in some cases. The preliminary study of the properties of the obtained PUs showed that they can emit blue fluorescence upon UV irradiation after thermal treatment.

2.3 Results and Discussion

2.3.1 Monomer Synthesis

2.3.1.1 Design of appropriate cyclic carbamate monomer

In a previous study on the ROP of cyclic carbamates in our lab, several carbamate monomers have been prepared, as depicted in Figure 2.4. Most of them are 5-membered cyclic carbamates due to the use of epoxides such as propylene oxide, styrene oxide, cyclohexene oxide or aminoalcohols such as ethanolamine, 2-aminophenol as the

starting materials to synthesize the target monomers. However, monomers **a-d** did not perform ROP at all or displayed very low conversions from room temperature to 150 °C in the presence of various catalysts or initiators such as boron trifluoride (BF_3), sodium hydride (NaH) and yttrium tris(isopropoxide) (Y(O*i*Pr)$_3$). According to the literature, ROP of dimethylene urethane (monomer **a**, Figure 2.4) was thermodynamically allowed but slightly hindered since the change of Gibbs free energy of the polymerization was not so negative (c.a. -1 kJ/mol) that the equilibrium polymer concentrations were low.[14] These results seemed to indicate that 5-membered cyclic carbamates were not good choice to synthesize PUs *via* ROP.
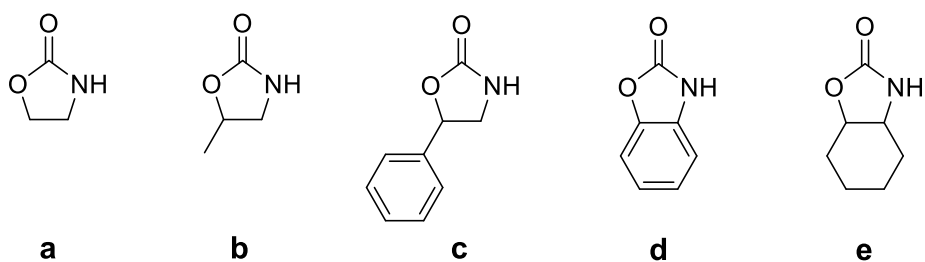
Figure 2.4. Cyclic carbamates prepared for ROP.

Nevertheless, in the ROP trials of monomer **e** (Figure 2.4), it was found that it could polymerize to produce PUs in the presence of Y(O*i*Pr)$_3$, confirmed by ^{1}H NMR and MALDI-TOF-MS (Matrix-assisted laser desorption ionization-time of flight mass spectrometry). The cyclohexane molecule can present different conformations such as boat conformation and chair conformation. They might have important impact on the ring strain of the 5-membered cyclic carbamate which shares two carbon atoms with the cyclohexane. Consequently, the opening of the cyclic carbamate ring might be easier compared to dimethylene urethane (monomer **a**).

But the problems were also that the obtained PUs were not soluble in many common organic solvents like chloroform, THF or DMF and their molecular weights were relatively low (c.a. 1000 Da). The possible reason might be that there were numerous hydrogen bonds formed between the PU chains prepared from monomer **e**, which led to the bad solubility of PUs in organic solvents. In the NMR characterization of PU, good spectra were obtained only by adding one or two drops of trifluoroacetic acid into

the CDCl$_3$ solution to break the hydrogen bonds in PU as well as promote its solubility. Moreover, precipitation of PUs in THF or DMF during the polymerization possibly resulted in the embedding of the active chain ends in the precipitates and the low molecular weights of the obtained PUs.

Based on these results, we envisaged to design and synthesize new cyclohexane-based 5-membered cyclic carbamate monomers with pendant functional groups on the cyclohexane ring, which would provide steric hindrance and alleviate the hydrogen bonding interactions among the PU chains prepared by ROP. Thus, the PUs might have better solubility in organic solvents and their molecular weights might also be improved. Therefore, we prepared a 5-membered cyclic carbamate monomer bearing a vinyl group on the cyclohexane ring. As expected, the obtained PUs had very good solubility in organic solvents such as THF, chloroform and DMF. Meanwhile, the presence of vinyl groups on the prepared PUs made it possible to easily perform the post-functionalization of PUs by "thiol-ene" coupling reaction, olefin metathesis, *etc*. So, we chose this kind of 5-membered cyclic carbamate with a vinyl group as the monomer to prepare non-isocyanate PUs *via* ROP. For convenience, it was named as CHU since it had the cyclohexane urethane structure.

2.3.1.2 Synthesis of CHU monomer

In the method reported in the literature, the synthesis of cyclic carbamates such as trimethylene urethane (TU) can be achieved upon nucleophilic addition of aminoalcohols with carbonate compounds under catalytic conditions and at high temperatures (Figure 2.5).[15] Moreover, the side products of the reaction were usually difficult to remove. Accordingly, we developed an easier route for the synthesis of CHU in high yield. This route was more convenient because the cyclic carbamates can be synthesized at relatively lower temperature (80 °C) with a good yield and the side products can be easily removed.
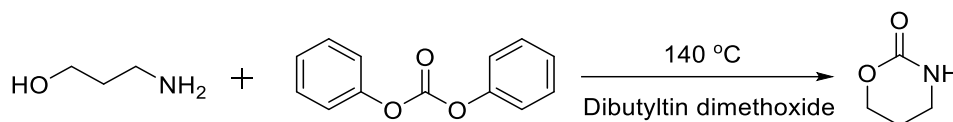
Figure 2.5. Conventional synthetic route to trimethylene urethane (TU).[15]

As shown in Figure 2.6, the synthesis of CHU included three steps. Firstly, 4-vinyl-1-cyclohexene-1,2-epoxide (**1**) reacted with excess ammonia to give amino alcohols (**2**) and (**3**). They were constitutional isomers having different vinyl positions on the cyclohexane ring. It was because the two carbon atoms of the epoxide **1** had the same probability to be attacked by ammonia, which led to the formation of two constitutional isomers. Secondly, the mixture of **2** and **3** reacted with ethyl chloroformate to yield compounds (**4**) and (**5**). Finally, cyclic carbamates (**6**) and (**7**) were obtained by the ring-closing reaction of **4** and **5** in the presence of excess sodium hydride. After purification by column chromatography, **6** and **7** with a yield of 30 % and 37% respectively were obtained.

Figure 2.6. Synthetic route to 5-membered cyclic carbamate monomer with vinyl group (CHU).

80

Figure 2.7. ^{1}H NMR (a) and ^{13}C NMR (b) spectra of CHU monomer. CDCl$_3$, 300 MHz, 297 K.
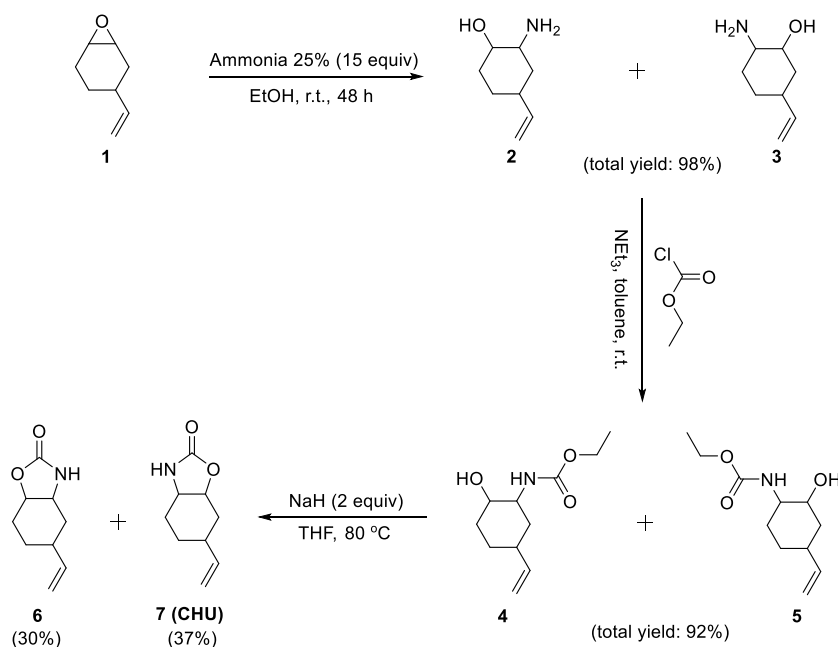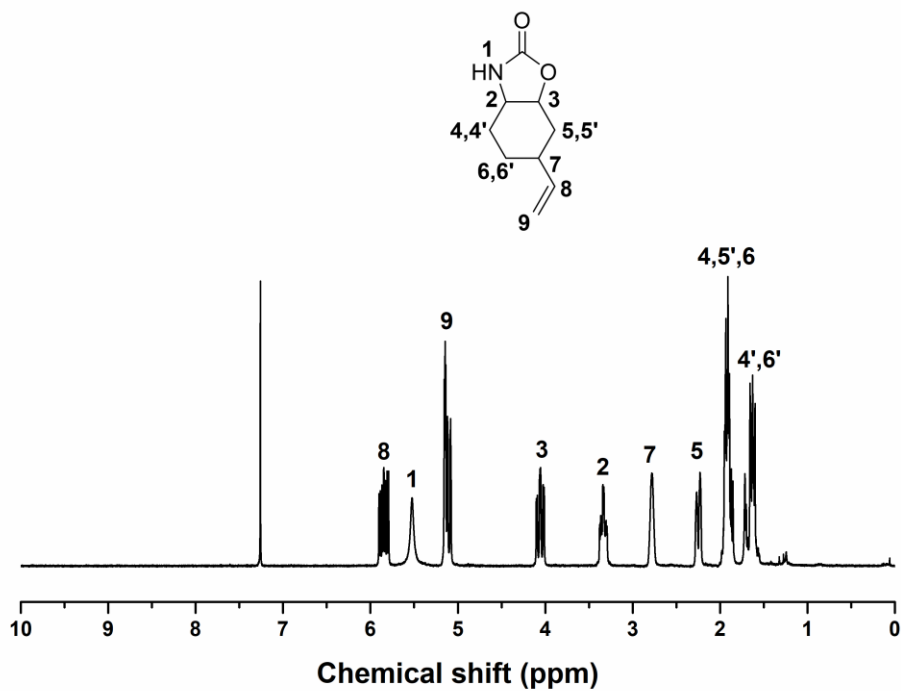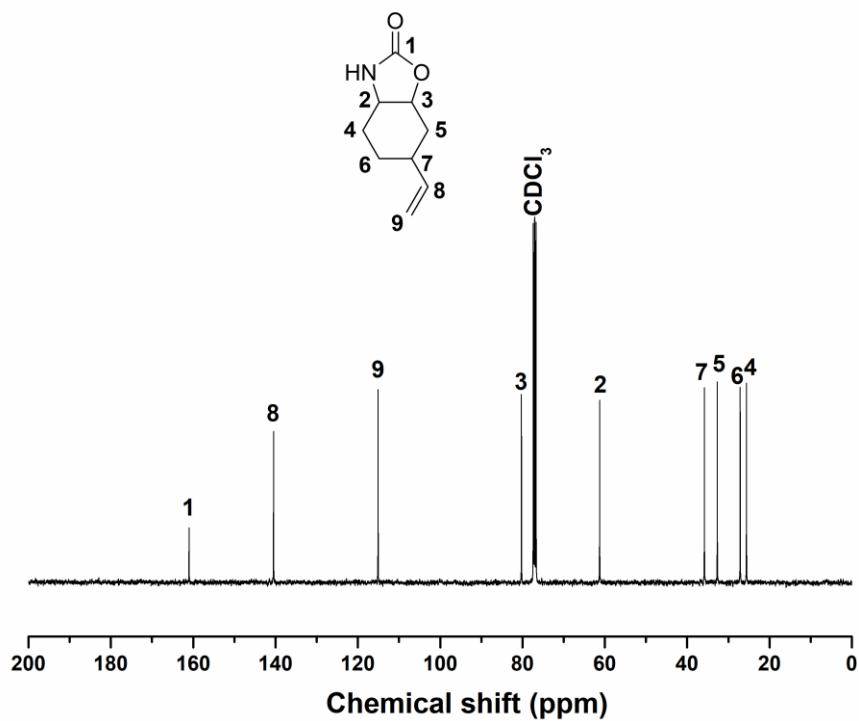
The two constitutional isomers **6** and **7** were all interesting precursors to polymerize and did not show different ROP phenomena in our tests. The obtained polymers might

have different chemical or physical properties because of the different structures, but it was not our current subject and would be studied later. Here, we chose isomer **7** (CHU) as the monomer to perform the ROP. CHU was characterized by ^{1}H NMR and ^{13}C NMR spectroscopy (Figure 2.7). It was also characterized by 2D NMR (COSY, NOESY, HSQC and HMBC) spectra (see Chapter V for the details) to confirm the position of the vinyl group on the cyclohexane ring.

2.3.1.3 Stereochemistry of CHU monomer

For CHU synthesis, it is important to know more about the stereoselectivity of the reaction. Stereochemistry of CHU is complicated because there are three chiral stereogenic centers in its molecular structure and the whole synthetic steps from 4-vinyl-1-cyclohexene-1,2-epoxide to the final CHU are non-stereoselective. If we consider that all configuration are possible for the three chiral centers in CHU, it is a mixture of eight stereoisomers. Although it is not our current research subject to resolve these stereoisomers, we need to know the possible types and ratios of stereoisomers in CHU monomer. So, we have carried out a preliminary study on that.

The starting material, 4-vinyl-1-cyclohexene-1,2-epoxide, was purchased from chemical supplier as a mixture of isomers. It can exist as eight stereoisomers at most since it had three chiral centers. However, GC (gas chromatography) characterization showed only two signal peaks with a ratio of about 6:4 (see Chapter V for the details). So, we speculated that it might be a mixture of four stereoisomers or two racemic mixtures of diastereomers (Figure 2.8). This explained why there were two signal peaks in the GC spectrum. ^{13}C NMR characterization of 4-vinyl-1-cyclohexene-1,2-epoxide also showed two signals for the methine carbon atoms with a ratio of about 6:4, which further confirmed it was a mixture of two racemic mixtures of diastereomers.

The reaction between 4-vinyl-1-cyclohexene-1,2-epoxide and ammonia in ethanol gave rise to two constitutional isomers (**2** and **3**, Figure 2.8). Considering that this reaction is a S_N2 nucleophilic reaction,[16,17] the addition of ammonia on the epoxide ring was a *trans* addition and the produced NH_2 group and OH group in compound **2** or **3**

should have opposite orientation *versus* the cyclohexane ring. So, **2** and **3** existed as four stereoisomers. After the following two non-stereoselective synthetic steps from **3**, CHU was synthesized as a mixture of four stereoisomers in which the orientation of C-O and C-N bonds connected to the cyclohexane ring kept consistent with those in **2** and **3**, as shown in Figure 2.8. Similarly, the four stereoisomers were also two pairs of diastereomers. To confirm this, the pure CHU was characterized by HPLC (high-performance liquid chromatography) but we were not able to detect it as the detector of HPLC was a UV detector. So, we used a CHU derivative that substituted the H atom on the NH group with a benzoyl group (co-initiator **I1** for the AROP, see the polymerization part for the details) for the HPLC characterization. The result showed two signal peaks with a ratio of about 6:4 (see Chapter V for the details), which confirmed our previous results. In the following work, CHU was considered as a mixture of stereoisomers to synthesize PUs by AROP.
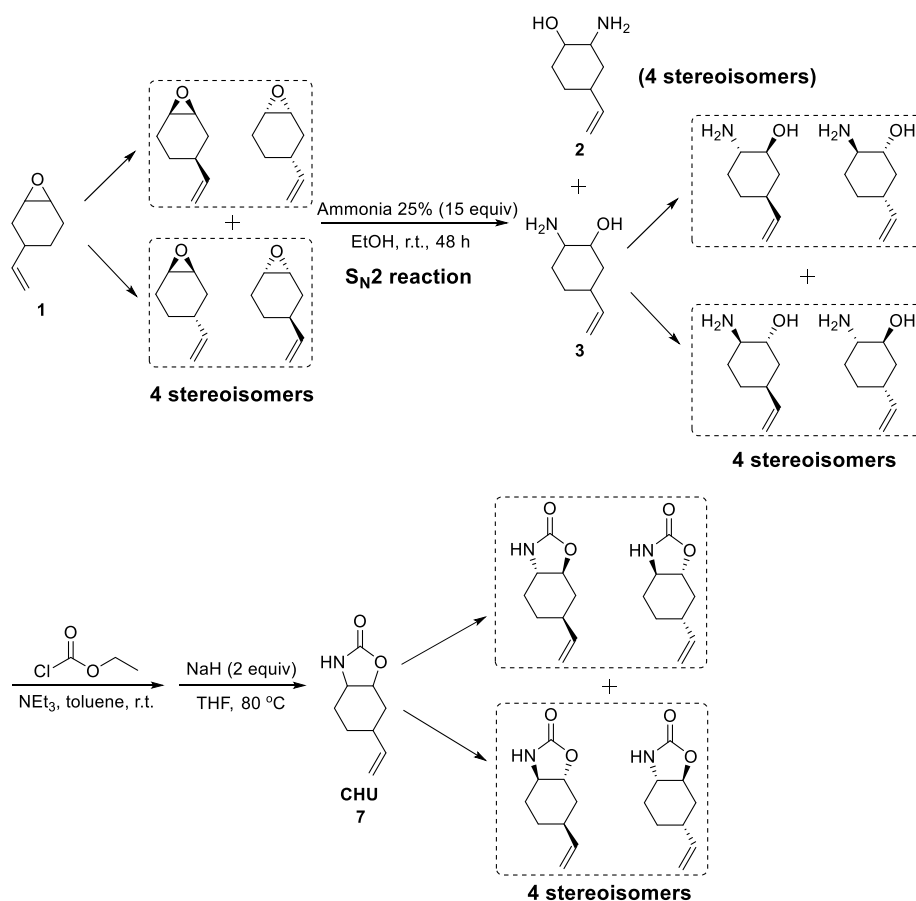

Figure 2.8. Stereochemistry study of CHU monomer.

2.3.2 Polymerization

In the preliminary study of the ROP of CHU, I have tried to carry out the ROP in the presence of rare earth catalysts such as yttrium(III) isopropoxide ($Y_5(OiPr)_{13}$), yttrium tris[*N,N*-bis(trimethylsilyl)amide] ($Y[N(TMS)_2]_3$) and yttrium trifluoromethanesulfonate ($Y(OTf)_3$) and neopentyl alcohol as a nucleophilic initiator. However, after a lot of polymerization attempts at different reaction conditions, PUs with high molecular weight (> 2000 Da) could not be obtained. Typical results are shown in Figure 2.9 and Table 2.2.
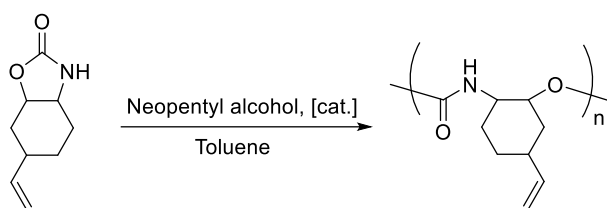
Figure 2.9. ROP of CHU in the presence of rare earth catalysts and neopentyl alcohol.

Table 2.2. Typical ROP results of CHU in the presence of rare earth catalysts and neopentyl alcohol.

Entry[a]	[cat.]	Monomer/ [cat.]/[alcohol]	T/ °C	Time/h	Conversion[b]	M_n[c]	PDI[c]
1	$Y_5(OiPr)_{13}$	80/1/0	120	24	80%	868	1.02
2	$Y[N(TMS)_2]_3$	70/1/10	120	24	82%	578	1.02
3	$Y(OTf)_3$	32/1/1	80	20	16%	850	1.13
4	$Y(OTf)_3$	32/1/1	80	24	21%	1170	1.15
5	$Y(OTf)_3$	32/1/1	80	48	90%	780	1.40

a. The monomer concentrations were all 0.5 M;

b. Conversion of monomers was calculated by ^{1}H NMR;

c. M_n and PDI were obtained by GPC with THF as eluent and PS as standards.

Then, I tried to use cationic catalysts such as methyl trifluoromethanesulfonate to perform the ROP, which also failed to prepare PUs with high molecular weights. After

careful examination of the literature, I thought that the AROP process of ε-caprolactams might be applicable to the ROP of cyclic carbamates because of some structural analogy between the two cyclic monomers.

Therefore, I tried to perform the AROP of CHU. After the addition of strong bases (*e.g.*, sodium hydride, *n*-butyllithium), I observed that polymers with higher molecular weights (> 2000 Da) were obtained. This was confirmed by GPC (gel permeation chromatography), which indicated that the AROP of CHU might be a good strategy to prepare PUs. Thereafter, I focused on the AROP of CHU to find the optimal ROP conditions.

The AROP scheme is shown in Figure 2.10. The results are summarized in Table 2.3. Firstly, the polymerization temperature was optimized at 0 °C and THF was chosen as the solvent. Secondly, strong base like *n*-butyllithium (*n*-BuLi) that can abstract a proton from a CHU molecule to produce a monomer anion was used as the initiator. Although *n*-BuLi can be nucleophilic, it showed better ROP results (entry 2) compared with some non-nucleophilic bases such as lithium bis(trimethylsilyl)amide (entry 3) or sodium hydride (entry 4). The reaction solution kept clear throughout the polymerization process and the polymers obtained had narrower PDIs. Therefore, we decided to use *n*-BuLi as the initiator for the ROP.

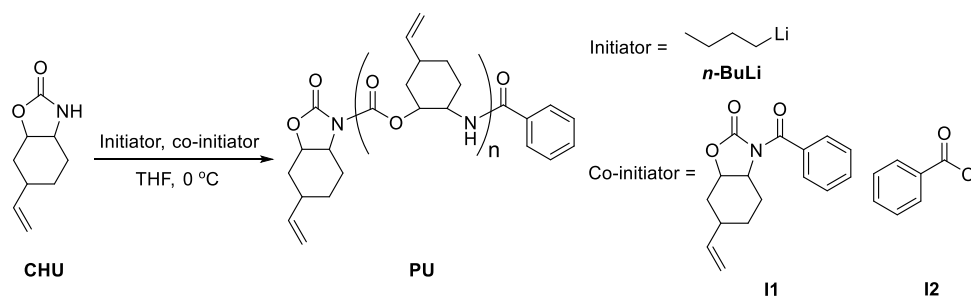**Figure 2.10**. Synthetic scheme of PU by AROP of CHU.

The co-initiator **I1** was synthesized by a one-step reaction between CHU and benzoyl chloride. Addition of co-initiator increased the conversion of monomers significantly in the anionic ROP of CHU at 0 °C (Table 2.3, entries 1 and 2). Benzoyl chloride was also used as an efficient co-initiator (**I2**), since it could react with CHU monomer to

produce **I1** in situ. To compare the effect of **I1** and **I2**, we performed a reaction using a clean combination of 1 equiv benzoyl chloride (**I2**) with 2 equiv of *n*-BuLi in order to *in situ* generate the imide **I1** (entry 5). These results showed that benzoyl chloride could act as a co-initiator but was less efficient than **I1**. Indeed, we observed that *n*-BuLi/**I2** system reacted more slowly and produced polymers with lower molecular weights (entry 5). As *N*-acetylcaprolactam was already used for the anionic ROP of caprolactam, it was interesting to observe that it was also active in the presence of *n*-BuLi (entry 6) but less efficient than **I1** (entry 2). Therefore, the optimal ROP conditions are the ones with *n*-BuLi as the initiator, CHU-derived imide **I1** as the co-initiator, in THF at 0 °C.

Table 2.3. ROP of CHU monomer to prepare PUs.

Entry[a]	Initiator	Co-initiator	Monomer/ Initiator/ Co-initiator	Time /h	Conve -rsion[b]	$M_{n,theory}$	$M_{n,NMR}$[b]	DP[b]	$M_{n,GPC}$[c]	PDI[c]
1	*n*-BuLi	-	20/1/1	5	8%	540	-	-	-	-
2	*n*-BuLi	I1	20/1/1	5	91%	3300	3900	23	5400	1.23
3	LiN(TMS)₂	I1	20/1/1	5	84%	2900	4600	27	4400	1.55
4	NaH	I1	20/1/1	5	47%	1700	3600	21	2100	1.50
5	*n*-BuLi	I2	20/2/1	5	73%	2600	2300	12	2800	1.33
6	*n*-BuLi	*N*-Acetylca-prolactam	20/1/1	5	79%	2800	-	-	5300	1.22
7	*n*-BuLi	I1	10/1/1	4	83%	1700	2400	14	3200	1.29
8	*n*-BuLi	I1	30/1/1	6	81%	4300	4400	26	6100	1.28
9[d]	*n*-BuLi	I1	50/1/1	24	81%	7100	7800	46	7500	1.32

*a*. The concentration of co-initiators were all 0.0188 M;

b. Conversion of monomers, degree of polymerization (DP) and $M_{n,NMR}$ were calculated by ^{1}H NMR;

c. $M_{n,GPC}$ and PDI were obtained by GPC with THF as eluent and PS as standards;

d. LiBr (1 wt%) was added in the polymerization solution.

Then, we performed several ROP reactions using different monomer/initiator/co-initiator ratios but the same initial concentrations of initiator and co-initiator (**I1**). Monomer conversions were always higher than 80%, as confirmed by the ^{1}H NMR spectra of the crude product. Notably, addition of lithium bromide (LiBr, 1 wt%) allowed to increase the monomer conversion (entry 9). When no LiBr was added, the monomer conversion was less than 50 %, even after 60 h of polymerization and the molecular weight of the obtained PUs was lower than 5000 Da. The possible reason might be that when the polymer chain was longer than a certain value, the cationic lithium ions might be blocked in the polymer chains which hampered the lithium transfer between polymer chain and monomer and the formation of monomer anions (see the ROP mechanism part).

The pure PUs were obtained by precipitating three times the crude products into *n*-hexane and then drying under vacuum for 24 h. Then they were characterized by NMR spectroscopy (Figure 2.11) and GPC (Figure 2.12). As shown in table 2.3, PUs with different degrees of polymerization (DPs) and molecular weights were obtained with different monomer/initiator/co-initiator ratios. DP was calculated by comparing the integrated area of the proton signal from the vinyl group on the side chain of PUs with the one from the benzene group at the polymer chain end in the ^{1}H NMR spectrum (Figure 2.11a). The molecular weights from NMR were close to the theoretical ones. PDIs observed by GPC ranged from 1.23 to 1.32 (entries 2, 7, 8 and 9), which were narrower than those of PUs prepared by cationic ROP of cyclic carbamate monomers.[18] All these results indicated that we had prepared well-defined PUs.

(a)
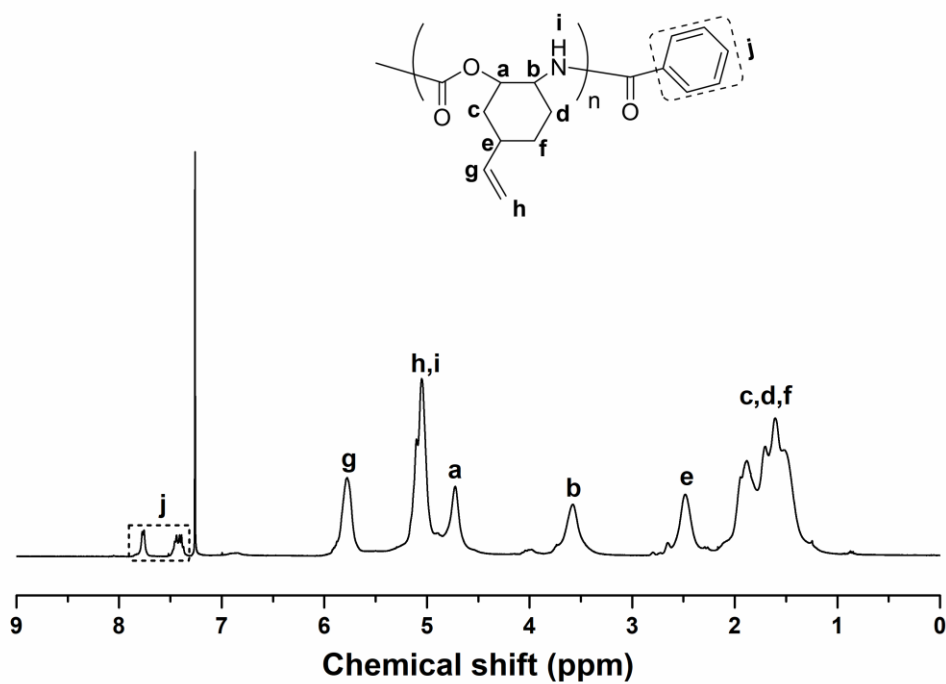
(b)
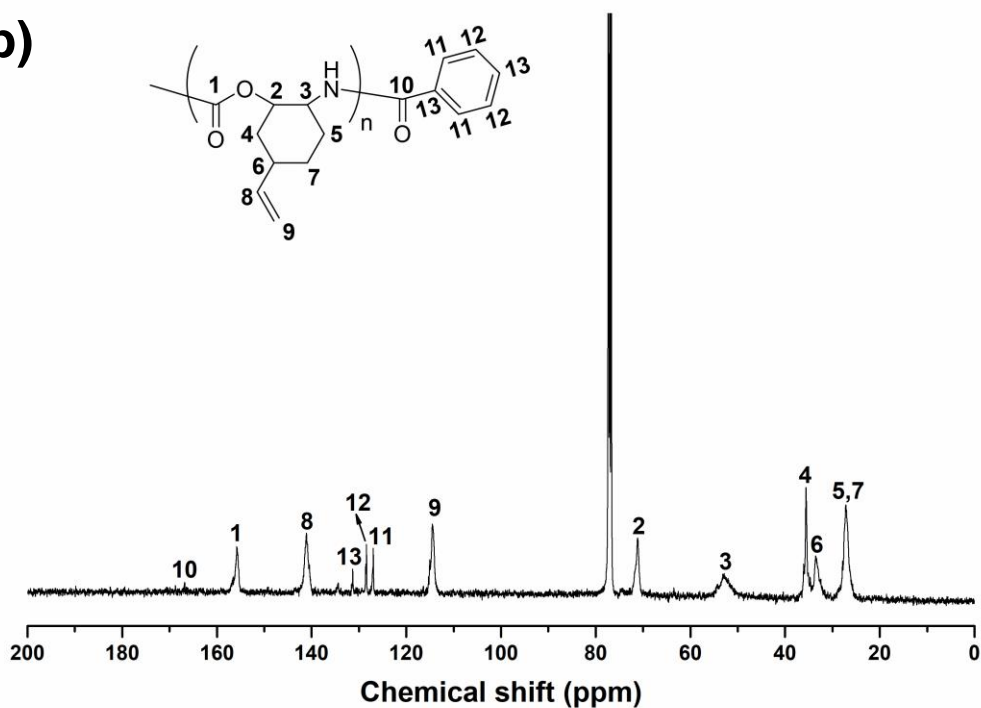
Figure 2.11. ^{1}H NMR (a) and ^{13}C NMR (b) spectra of PU (polymer from entry **7** in
Table 2.3). CDCl$_3$, 400 MHz, 297 K.

Figure 2.12. GPC traces of PUs from Table 2.3 with THF as the eluent.

Figure 2.13. MALDI-TOF-MS spectra of PU (polymer from entry 2 in Table 2.3).

The molecular structures of PUs were also characterized by MALDI-TOF-MS and ATR-IR (attenuated total reflectance-infrared spectroscopy). From the MALDI-TOF-MS spectra of PU from entry 2 (Figure 2.13), we firstly observed that the interval of

89

two adjacent peaks was 167.1 Da, which corresponded to the molecular weight of CHU monomer. Secondly, we were able to determine the end groups of the PU prepared *via* AROP (Figure 2.10). In addition, ATR-IR spectra of the synthesized PUs (Figure 2.14) showed the characteristic peaks of carbonyl groups and secondary amines, which were similar to the reported ones from the traditional PUs.[19]

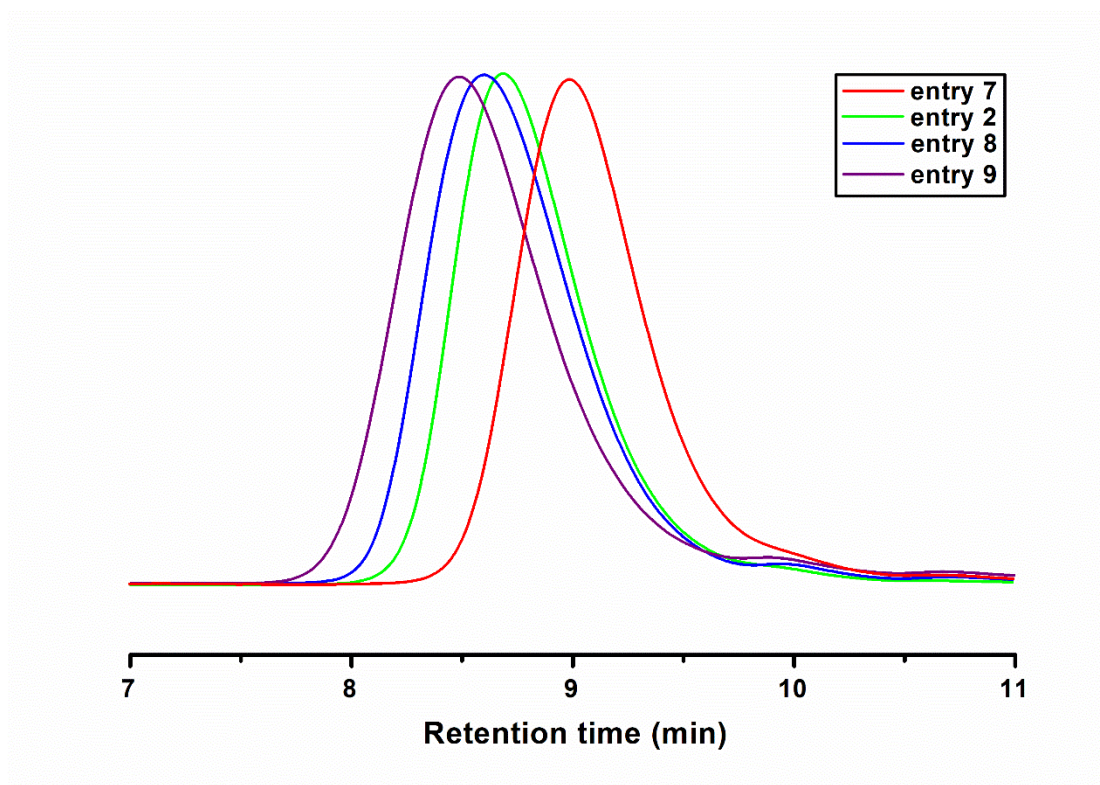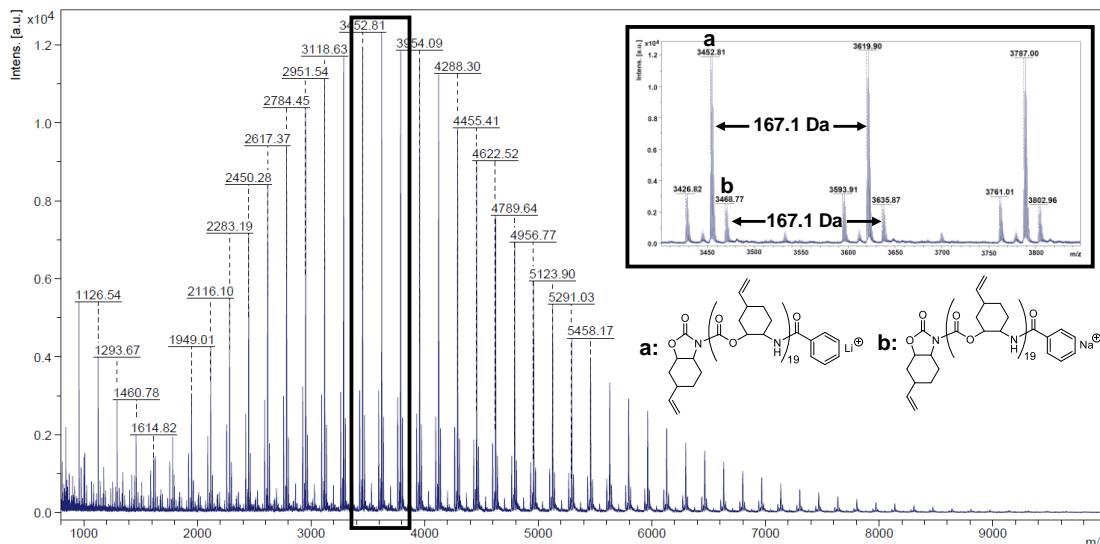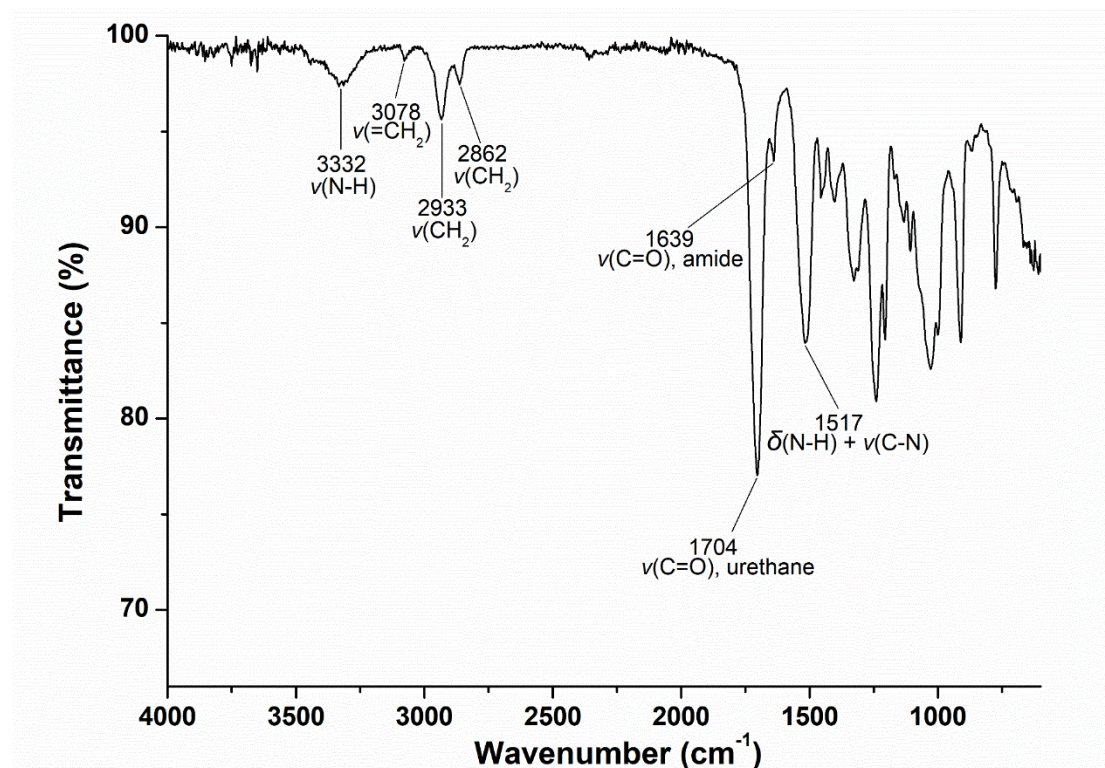**Figure 2.14**. ATR-IR spectrum of PU (polymer from entry 2 in Table 2.3).

2.3.3 AROP mechanism of CHU polymerization

I have succeeded in the CHU polymerization using conditions similar to the ones used for ε-caprolactam. However, there is a major difference between cyclic lactam and cyclic carbamate. This ester group presented in the latter can also be a cleavable bond for the ring opening. Therefore, it is necessary to study in detail the real AROP mechanism of CHU polymerization.

In a preliminary study, I tried several ROP experiments by using catalysts known for the ROP of lactone monomers such as stannous octoate (Sn(Oct)$_2$) or yttrium triflate (Y(OTf)$_3$) in combination with alcohols as initiators. Nevertheless, either no polymers or only oligomers were produced under these conditions. Then I hypothesized that the

monomer might perform ROP as lactam monomers. So, I tried to use some strong bases such as *n*-BuLi or sodium hydride to initiate the AROP of CHU monomers. This time, polymers were produced but the oberved PDIs were relatively broad. Then I added some *N*-acetylcaprolactam (*N*-ACL) as a co-initiator. The conversion increased and the PDIs were narrower than before (entry 6 in Table 2.3). Next, I synthesized **I1** inspired by the structure of *N*-ACL as the co-initiator and continuously optimized the polymerization conditions. Finally, well-defined PUs were synthesized.

According to the above observations, we found that the AROP of CHU monomer was similar to the one of lactam. Therefore, we hypothesized that the AROP of CHU includes two parts (Figure 2.15), namely the initiation and the propagation. In the initiation part, monomer reacts with the initiator to form the monomer anion. Then this anion can react with the co-initiator (**I1**) to form the dimer which has a new *N*-acyl center to serve as the propagation center. The propagation part is the subsequent reaction of the monomer anion with the *N*-acyl center at the polymer chain end. Then the proton transfer occurs between the polymer chain and the CHU monomer to regenerate the monomer anion.

To prove this mechanism, the most direct method was to determine the initiation part of the AROP because the propagation part was the same as the second step of the initiation part. In fact, the initiation part is the nucleophilic attack of the monomer anion on the endocyclic carbonyl group of the co-initiator. Some studies in the literature reported that the rings of the *N*-acyl cyclic carbamates opened from the C-N bond rather than the C-O bond when they were attacked by nucleophiles.[20,21] Here, we expected to synthesize a dimer using a 1/1/1 molar ratio between the monomer, initiator and co-initiator (Figure 2.16). But it did not work because the monomer tended to polymerize to form a mixture of dimer, trimer and oligomers. We could not separate them even by using column chromatography.
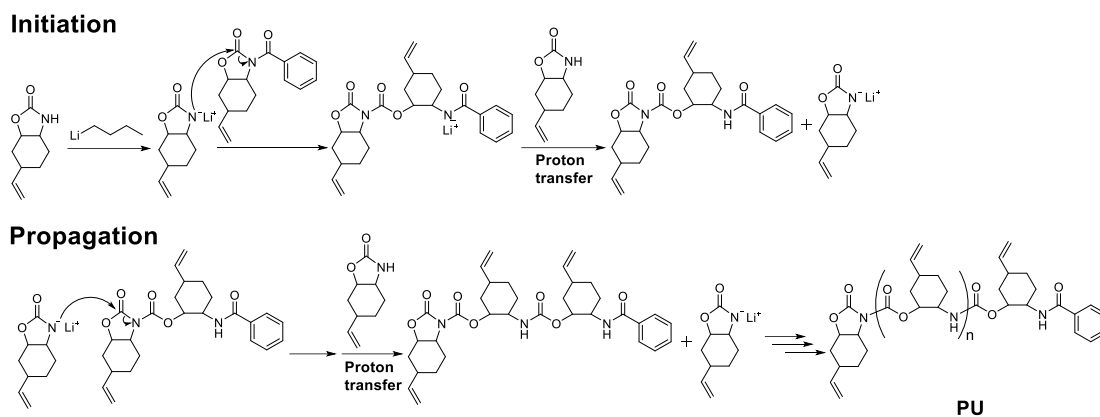
Initiation

Propagation

Figure 2.15. AROP mechanism of CHU polymerization with **I1** as the co-initiator.
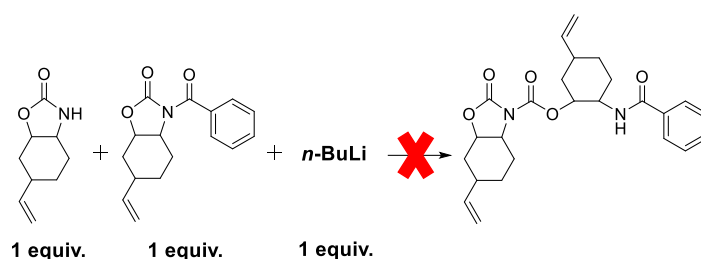
Figure 2.16. Attempt to synthesize the imide dimer with a *N*-acyl structure.

Then we tried to use the *in situ* IR spectrometer to monitor the "1/1/1" (molar ratio of monomer, initiator and co-initiator) reaction (Figure 2.17). Figure 2.17b shows the temporal evolution of the polymerization mixture during 16 h. The stretching vibration peaks of carbonyl groups from the monomer (carbonyl group **1** in Figure 2.17a, 1776 cm^{-1}) and co-initiator (carbonyl groups **2** and **3** in Figure 2.17a, 1798 cm^{-1} and 1690 cm^{-1} respectively) decreased regularly with time. The carbonyl groups **2** and **3** from the co-initiator disappeared completely after 16 h, which indicated that all the co-initiator had been consumed and transformed to products. New IR peaks are also observed at 1723 cm^{-1} (peaks **4**) and 1642 cm^{-1} (peak **5**). After analyzing the peak value and possible product structure, we think they can be attributed to the stretching vibration of carbonyl groups from urethane functions on the PU chains and amide groups at the chain end. The evolution of some characteristic IR peaks *versus* time (Figure 2.18) clearly shows the decrease of the signals from reactants and the increase of the signals from products.
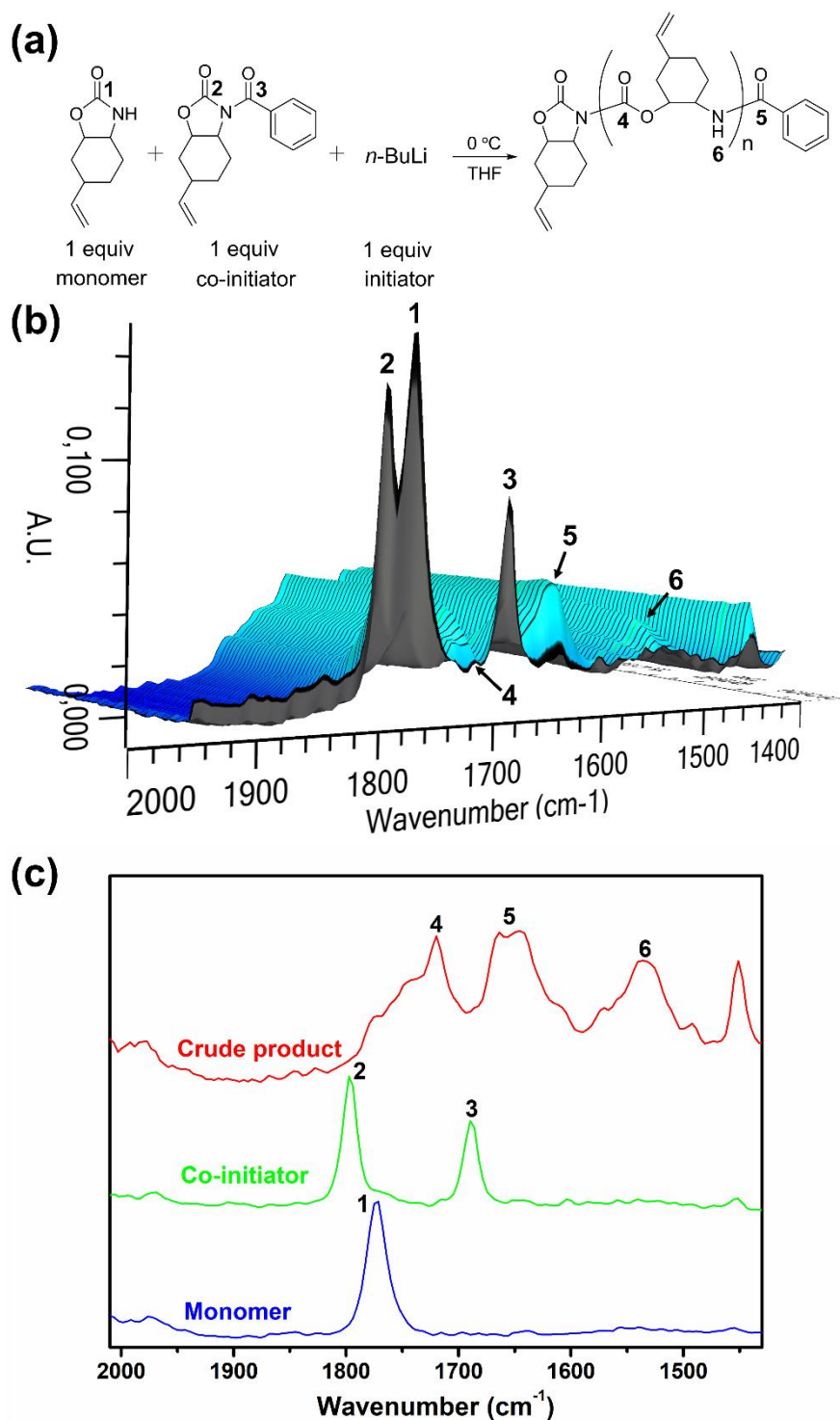
Figure 2.17. *In situ* IR experiments to prove AROP mechanism. (a) Model reaction equation with the molar ratio of monomer, initiator and co-initiator being 1/1/1. (b) *In situ* IR spectra of the reaction mixture from 0-16 h. (c) IR spectra of monomer, co-initiator and the crude product.
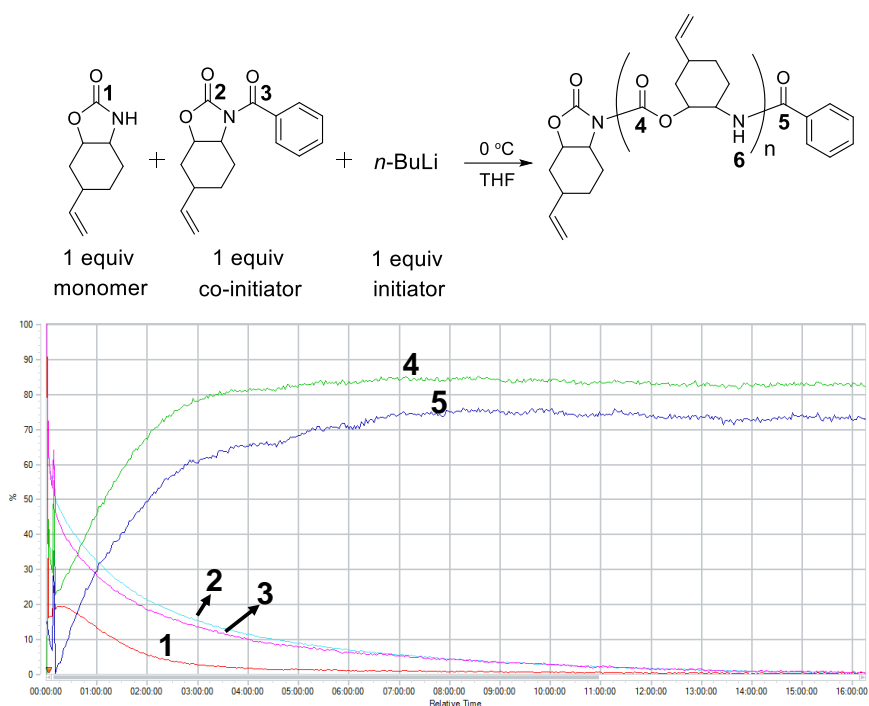
Figure 2.18. Evolutions of characteristic IR peaks *versus* time by *in situ* IR experiment.

In addition, by comparing the spectra of monomer, co-initiator and the crude product after *in situ* IR experiment (Figure 2.17c), we could clearly see the disappearance of co-initiator signals in the crude product and appearance of signals attributed to the PU oligomers. The ^{13}C NMR spectra showed the same phenomena (Figure 2.19). Comparing the ^{13}C NMR spectra of monomer, co-initiator and the crude product, we could see the appearance of new carbonyl signals (**d** and **e** in the spectra of crude product, Figure 2.19) attributed to the PU oligomers.

In conclusion, *in situ* IR and ^{13}C NMR characterization evidenced that PU was synthesized by the AROP mechanism postulated in Figure 2.15, which is a new mechanism for the synthesis of PU.
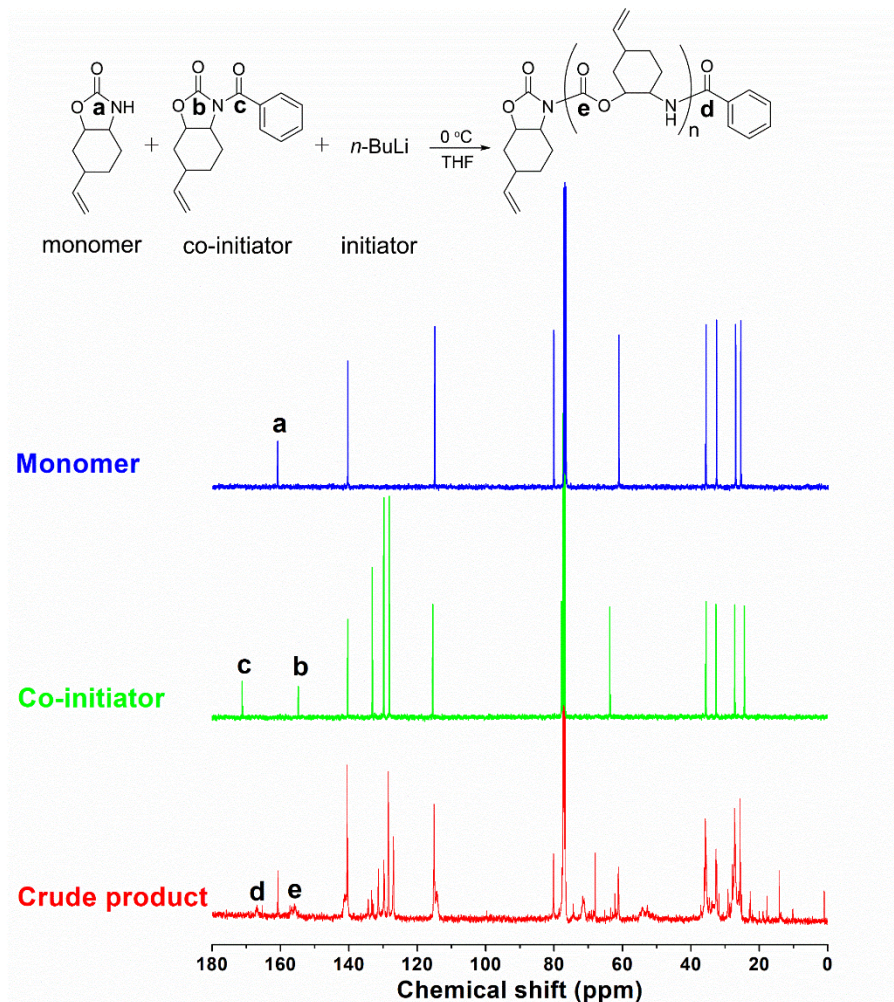
Figure 2.19. ^{13}C NMR spectra of monomer, co-initiator and the crude product in the *in situ* IR experiment to monitor the "1/1/1" (molar ratio of monomer, initiator and co-initiator) reaction.

2.3.4 ROP kinetics

We then studied the kinetics of the ROP of CHU monomer by *in situ* IR. It was reported that the absorbance intensity of the characteristic peaks in IR spectrum is closely related to the concentrations of the monomer and polymer.[22] The absorbance intensity exhibited approximatively linear relationship with compound concentrations in a wide concentration range.[23,24] So, we could obtain the real-time concentration values by knowing the real-time absorbance intensities of the carbonyl group attributed to CHU (1776 cm^{-1} in the *in situ* IR spectra) and the initial monomer concentration. In order to explore the relationship between polymerization rate and monomer

95

concentration, we monitored three ROP experiments with the same initiator and co-initiator (**I1**) but different monomer concentration (Figure 2.20).
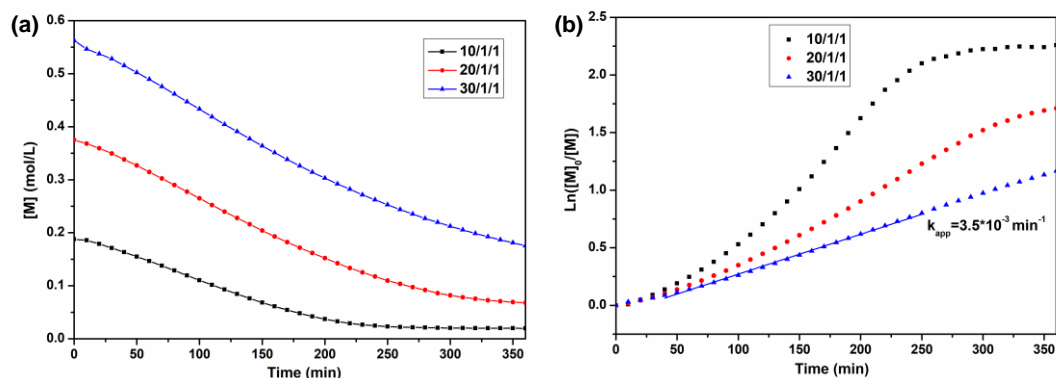
Figure 2.20. (a) Monomer concentration as a function of time with the molar ratio of monomer, initiator and co-initiator being 10/1/1, 20/1/1 and 30/1/1 monitored by *in situ* IR. The initial monomer concentrations were 0.188 M, 0.376 M and 0.564 M respectively. Initial concentrations of initiator and co-initiator were 0.0188 M. (b) Semilogarithmic plot of the data used to generate part (a).

The variation of monomer concentration *versus* time monitored is shown in Figure 2.20a. Figure 2.20b represents the semilogarithmic plot of the data to generate Figure 2.20a. We can see that in the ROP experiment with the molar ratio of monomer, initiator and co-initiator 30/1/1, the $\ln([M]_0/[M])$ displays a linear relationship with time, which indicates that the monomer concentration decreases at a rate proportional to its current value. However, for the other two experiments (*i.e.*, molar ratios of 10/1/1 and 20/1/1), the $\ln([M]_0/[M])$ corresponds to a more complicated mathematical relationship with time. These results suggest that when the molar ratio between monomer and initiator is high, the AROP rate of CHU might have a first-order dependence on the CHU concentration. When the molar ratio between monomer and initiator is low, some side reactions might be more inclined to occur or the linear relationship between the IR absorbance intensity and monomer concentration possibly has deviations. The first reason is more plausible since the PDIs of the prepared PUs were higher than 1.2, which tends to indicate that there might be side reactions in the ROP process.

In addition, the apparent ROP rate constant (k_{app}) can be calculated from the linear

fitting equation of $\ln([M]_0/[M])$ and t in the "30/1/1" ROP experiment, which is the slope of the fitting line actually. The observed k_{app} is $3.5*10^{-3}\,min^{-1}$, and represents the kinetic characteristic of the AROP of CHU for this specific ROP experiment.

2.3.5 Material properties of the PU homopolymers

2.3.5.1 Thermal properties

The thermal properties of PU were characterized by TGA (thermogravimetric analysis) and DSC (differential scanning calorimetry) measurements (Figure 2.21, 2.22). The curve of TGA of PU (entry 2 in Table 2.3, Figure 2.21) showed that the polymer did not decompose below 200 °C. Meanwhile, DSC curves (Figure 2.22) of the same sample showed the presence of a high glass transition temperature (T_g) at around 150 °C.
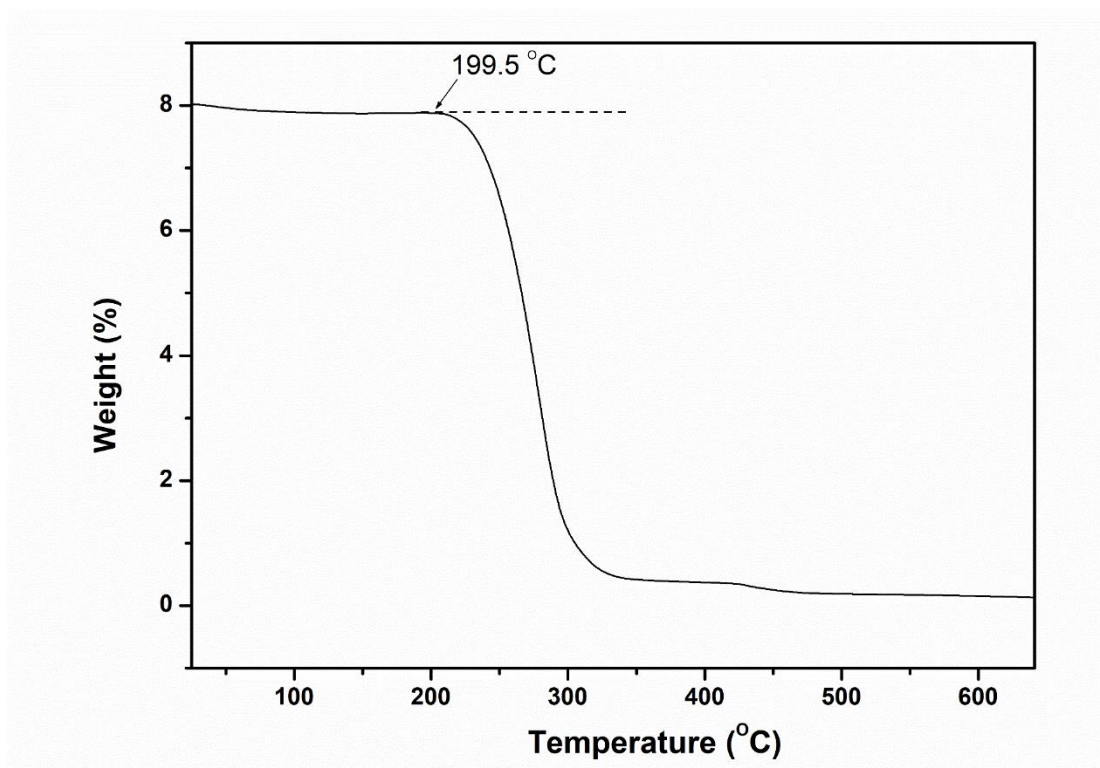
Figure 2.21. TGA curve of PU (polymer from entry 2 in Table 2.3).

97
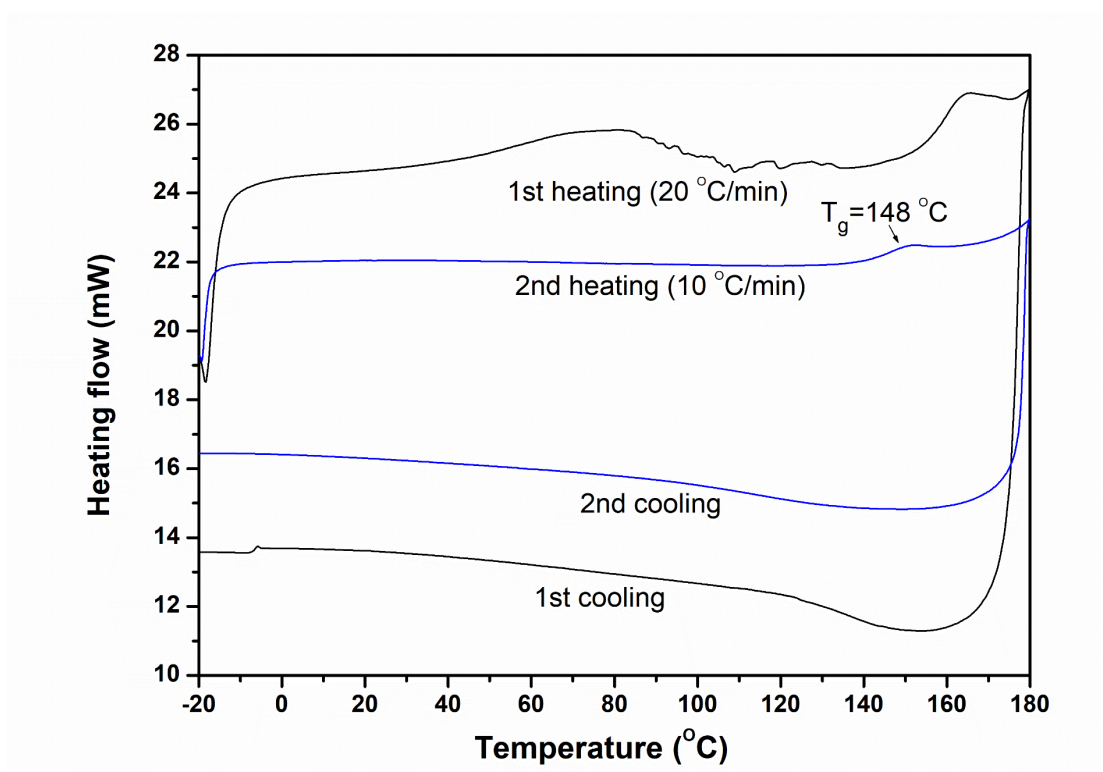
Figure 2.22. DSC curves of PU (polymer from entry 2 in Table 2.3).

2.3.5.2 Fluorescence properties

Very interestingly, we found that the PU samples (M_n = 4000 Da) collected from the DSC sample pan after DSC measurement could emit blue fluorescence under the UV lamp with a wavelength of 365 nm. However, the original PU products obtained from precipitation in *n*-hexane did not exhibit any fluorescence under the same UV lamp, as shown in Figure 2.23.
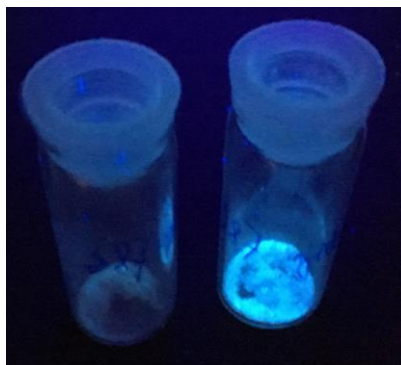
Figure 2.23. Photographs of PU samples (M_n = 4000 Da) under UV lamp (λ = 365 nm). Left: PU obtained from precipitation in *n*-hexane; Right: PU collected from the DSC measurement.

This special phenomenon is difficult to understand as there is no conjugated group in our PU structure as the conventional fluorescent dyes. Moreover, the original PU samples that were not melted by DSC did not have this phenomenon. To explain that, we had done some preliminary research, which might be not completed, and more work was needed.

Firstly, we noted that the main difference between the original PU samples and PU samples collected from DSC measurement was that in DSC experiment PU had been heated to 180 °C under inert atmosphere (N_2). So, we repeated this thermal treatment outside DSC and prepared some PU samples (M_n = 4000 Da) by heating to 180 °C and then cooling to room temperature (r.t.) slowly under argon. Compared with the soft and viscous original PU powder products, the thermally treated PUs were hard solid products, which also could emit blue fluorescence under UV lamp (λ = 365 nm).

Secondly, the two PU samples were observed carefully by POM (polarized optical microscopy) (Figure 2.24). As shown in Figure 2.24a, the POM photographs of the original non-heated PU sample did not show any birefringence phenomenon and we could observe many soft solid fragments. While in Figure 2.24b-d, many small hard and "glass-like" fragments were observed by POM for the thermally treated PUs, although they did not show any birefringence phenomenon either. This morphology difference indicated that the PUs formed more compact structure after thermal treatment under inert atmosphere, which might contain more complicated three-dimensinoal structures/networks owing to the appearance of more intermolecular hydrogen bonding interactions.

The thermally treated PU samples were also characterized by fluorescence microscopy. As shown in Figure 2.24e-f, blue fragments were observed under the excitation of UV light (λ = 365 nm) from the fluorescence microscopy. From the pictures we could see that the fluorescence was not emitted by the PU fragments homogenously. The edges of the fragments seemed to emit stronger fluorescence than the central parts. The reason might be that the central part was too thick to prevent UV light from penetrating into the interior of the fragments to excite the blue fluorescence.
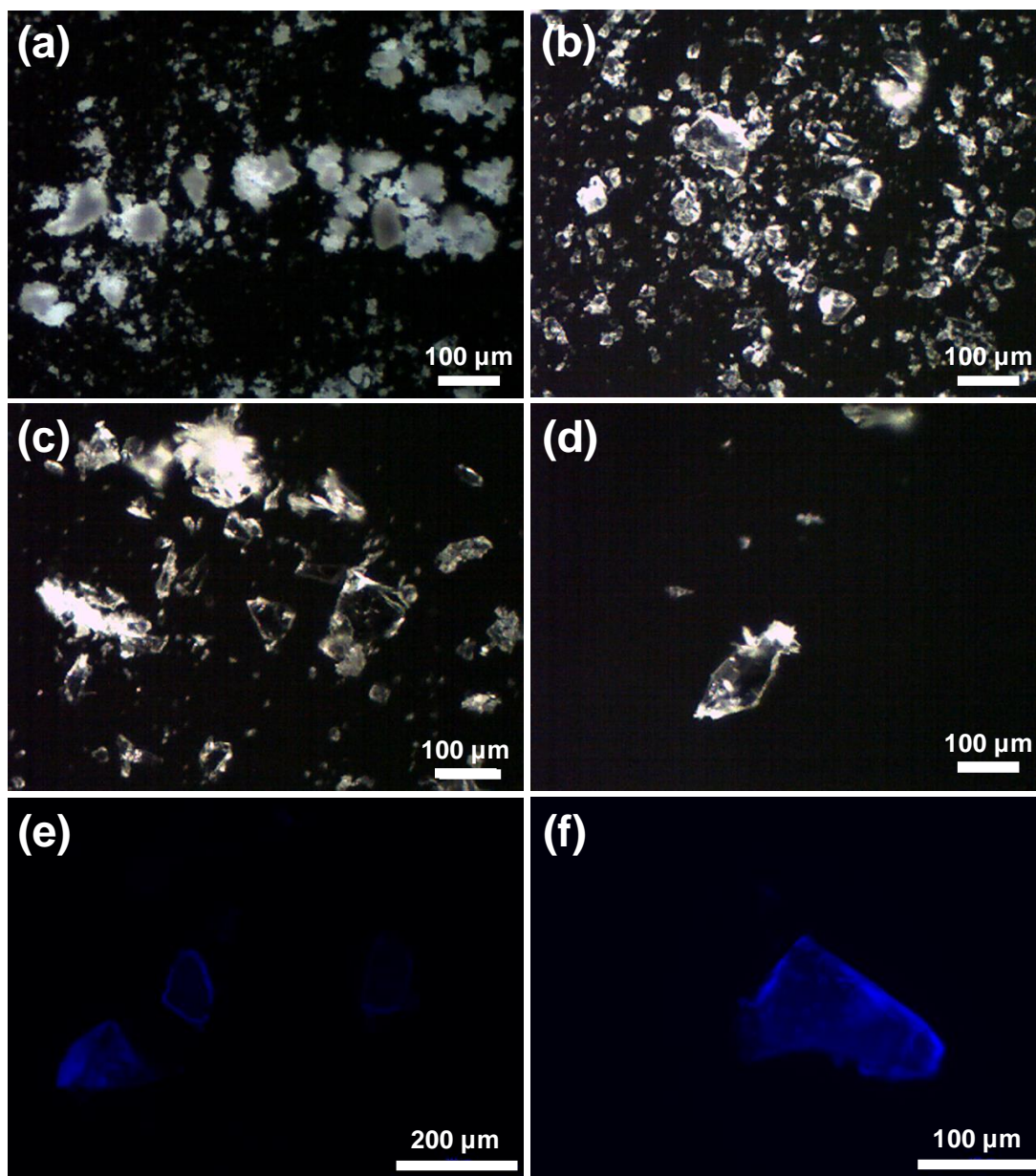
Figure 2.24. Photographs captured by POM (a-d) and Fluorescence microscopy (e,f). (a) original PU samples (M_n = 4000 Da) without being heated; (b-f) PU samples after heated to 180 °C and cooled to r.t. slowly under argon.

Finally, we have also tried to characterize the two PU samples by ^{1}H NMR, ATR-IR and XRD (X-ray diffraction). The ^{1}H NMR spectra of PU polymer (M_n = 4000 Da) and thermally treated PUs did not show significant difference (Figure 2.25a). The ATR-IR spectra of the two samples did not show significant difference either except there was a small split peak appearing on the stretching vibration peak of carbonyl group of PUs

(Figure 2.25b). The reason might be that there were more hydrogen bonding interactions formed between oxygen atoms from "C=O groups" and H atoms from "-NH- groups" in the PU samples after thermal treatment. The XRD spectra (Figure 2.26) of the two samples did not show any peak in the range of 20-60° (q = 14.2–40.8 nm^{-1}), indicating that neither of them had crystal structures.
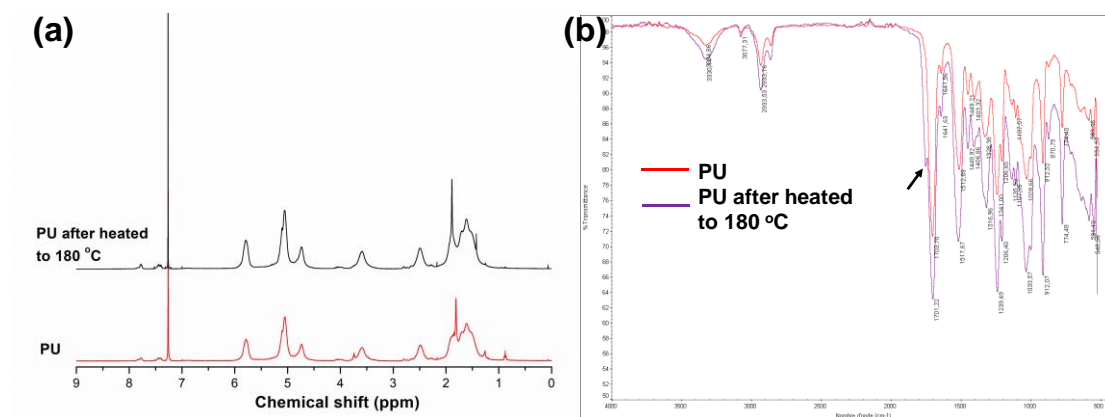
Figure 2.25. ^{1}H NMR (a) and ATR-IR (b) spectra of PU polymer (M_n = 4000 Da) and PU after heated to 180 °C and cooled to r.t. slowly under argon.
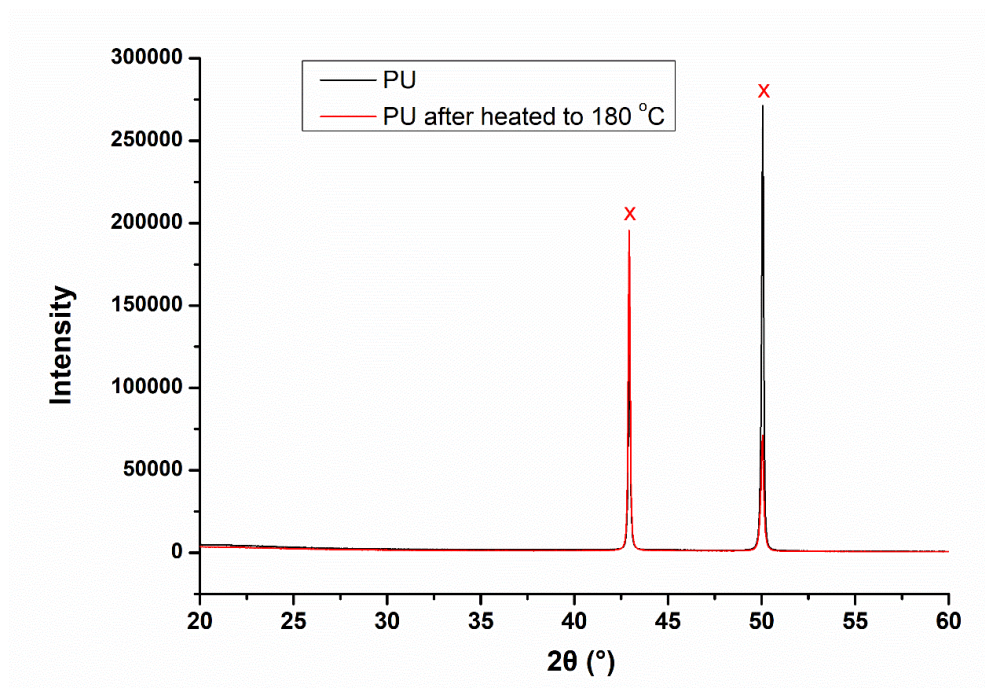
Figure 2.26. XRD spectra of PU polymer (M_n = 4000 Da) and PU after heated to 180 °C and cooled to r.t. slowly under argon. The two diffraction peaks (x) are from the sample support made of copper.

Very recently, Ben Zhong Tang and coworkers reported that some non-conjugated polymers without aromatic building blocks were luminescent under certain conditions, as shown in Figure 2.27.[25] These polymers usually contain aliphatic tertiary amines, cyanos, amides, carbonyls structures *et al.* (Figure 2.27a). For example, the solid powders of polyacrylonitrile (PAN) and poly(*N*-hydroxysuccinimide methacrylate) (PNHSMA) emitted visible blue emission upon UV irradiation (Figure 2.27b,c). In addition, bright blue emission was observed from starch, cellulose, and BSA protein (Figure 2.27d). These phenomena are similar to what we observed in PU sample after thermal treatment. Tang and coworkers proposed the clustering-triggered emission mechanism to explain these phenomena. It is a through-space conjugation mechanism. In detail, the emission is caused by the electron cloud overlap due to the clustering of electron-rich subgroups (N, O, S, P (phosphorus) with lone pair electrons), together with conformation rigidification.[25] We speculate that the fluorescence of our PU sample after thermal treatment is triggered by the clustering of urethane groups which contain electron-rich atoms N and O due to the closer spatial distance of these atoms after heating. This phenomenon will be studied further in the future.
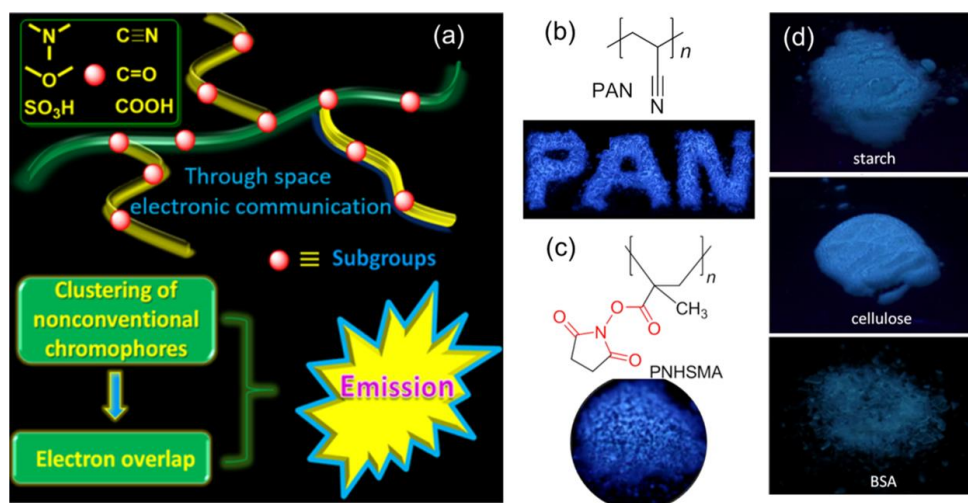
Figure 2.27. (a) Schematic illustration of the clusters constructed by through-space conjugated subgroups. (b) Molecular structure of polyacrylonitrile (PAN) and fluorescent photograph of its blue solid powders. (c) Molecular structure of PNHSMA and fluorescent photograph of its blue solid powders. (d) Fluorescent photographs of starch, cellulose, and bovine serum albumin (BSA) solid powders.[25]

2.4 Conclusion

In conclusion, a new isocyanate-free method to prepare PUs has been reported. Non-isocyanate and well-defined PUs with novel structures were prepared *via* the AROP of a 5-membered cyclic carbamate bearing a vinyl group (CHU) by using *n*-butyllithium as the initiator and CHU-derived imide as the co-initiator. The monomer was synthesized in three steps at 80 °C in a good yield. A series of PUs with different molecular weights was synthesized by changing the feeding ratios of monomer, initiator and co-initiator. The AROP mechanism was proposed and proved by *in situ* IR and ^{13}C NMR spectroscopies, which revealed that the origin of the polymerization activity of our system was very likely to be caused by the formation of highly active anionic species. The ROP kinetics in the polymerization system was studied and the polymerization could present the characteristics of the first order kinetics in some cases. The preliminary study of the properties of the obtained PUs showed that they could emit blue fluorescence upon UV irradiation after thermal treatment, possibly due to the clustering-triggered emission. The other properties and applications for the synthesized PUs will be studied in the future. We believe the present work will provide more options and inspirations for people to prepare isocyanate-free PUs.

References

1. Penczek, S.; Moad, G. *Pure Appl. Chem.* **2008**, *80*, 2163-2193.

2. Nuyken, O.; Pask, S. D. *Polymers* **2013**, *5*, 361-403.

3. Allcock, H. R. *J. Macromol. Sci. Revs. Macromol. Chem.* **1970**, *C4*, 149.

4. Hall, H. K.; Schneider, A. K. *J. Am. Chem. Soc.* **1958**, *80*, 6409-6412.

5. Bielawski, C. W.; Grubbs, R. H. *Prog. Polym. Sci.* **2007**, *32*, 1-29.

6. Hamitou, A.; Ouhadi, T.; Jerome, R.; Teyssié, P. *J. Polym. Sci., Part A: Polym. Chem.* **1977**, *15*, 865-873.

7. Hashimoto, K. *Prog. Polym. Sci.* **2000**, *25*, 1411-1462.

8. Sebenda, J.; Hauer, J. *Polym. Bull.* **1981**, *5*, 529-534.

9. Kricheldorf, H. In *Pencze S (ed) Models of biopolymers by ring opening polymerization*; CRC, Boca Raton, 1990, pp 1-132.

10. Cheng, J. J.; Deming, T. J. In *Peptide-Based Materials*; Deming, T., Ed. 2012; Vol. 310, pp 1-26.

11. Hall, H. K. *J. Am. Chem. Soc.* **1958**, *80*, 6404-6409.

12. Rothe, V. M.; Reinisch, G.; Jaeger, W.; Schopov, I. *Makromol. Chem.* **1962**, *54*, 183-204.

13. Luisier, A.; Bourban, P. E.; Manson, J. A. E. *J. Polym. Sci., Part A: Polym. Chem.* **2002**, *40*, 3406-3415.

14. Lebedev, B.; Veridusova, V.; Höcker, H.; Keul, H. *Macromol. Chem. Phys.* **2002**, *203*, 1114-1125

15. Neffgen, S.; Kusan, J.; Fey, T.; Keul, H.; Höcker, H. *Macromol. Chem. Phys.* **2000**, *201*, 2108-2114.

16. McManus, S. P.; Larson, C. A.; Hearn, R. A. *Synth. Commun.* **1973**, *3*, 177-180.

17. Hawkins, L. R.; Bannard, R. A. B. *Can. J. Chem.* **1958**, *36*, 220-227.

18. Kusan, J.; Keul, H.; Höcker, H. *Macromolecules* **2001**, *34*, 389-395.

19. Chiono, V.; Mozetic, P.; Boffito, M.; Sartori, S.; Gioffredi, E.; Silvestri, A.; Rainer, A.; Giannitelli, S. M.; Trombetta, M.; Nurzynska, D.; Di Meglio, F.; Castaldo, C.; Miraglia, R.; Montagnani, S.; Ciardelli, G. *Interface Focus* **2014**, *4*: 20130045.

20. Oishi, S.; Yoshimoto, J.; Saito, S. *J. Am. Chem. Soc.* **2009**, *131*, 8748-8749.

21. Bouzide, A.; Sauve, G. *Tetrahedron Letters* **2002**, *43*, 1961-1964.

22. Deng, H.; Shen, Z.; Li, L.; Yin, H.; Chen, J. *J. Appl. Polym. Sci.* **2014**, *131*, 40503.

23. Messman, J. M.; Storey, R. F. *J. Polym. Sci., Part A: Polym. Chem.* **2004**, *42*, 6238-6247.

24. Schwartz, T. J.; Lyman, S. D.; Motagamwala, A. H.; Mellmer, M. A.; Dumesic, J. A. *ACS Catal.* **2016**, *6*, 2047-2054.

25. He, Z.; Ke, C.; Tang, B. Z. *ACS Omega* **2018**, *3*, 3267-3277.

Chapter III. Synthesis and self-assembly of polyurethane-based amphiphilic linear diblock copolymers

3.1 Introduction

3.1.1 General introduction of amphiphilic linear diblock copolymers

Block copolymers are a specific class of copolymers which contain discrete blocks formed by different monomer units along the polymer chain.[1] From the viewpoint of molecular architecture, they can be linear, branched (graft and star) or cyclic.[2] Linear block copolymers are the most common and extensively studied type of block copolymers due to the relatively simple architecture compared with other types. Amphiphilic linear diblock copolymers consisting of two chemically distinct and frequently immiscible blocks linked through a covalent manner are particularly interesting as they can form a plethora of defined nanostructures by self-assembly.[3]

The immiscibility of the two blocks leads to the self-assembly of amphiphilic linear diblock copolymers when they are dissolved in a selective solvent that is a thermodynamically good solvent for one block but a counter solvent for the other. More precisely, the copolymer chains associate spontaneously into micellar structures consisting of a more or less swollen core formed by the insoluble blocks surrounded by a flexible corona formed by the soluble blocks.[3,4] The morphologies and sizes of the micellar aggregates are influenced by many factors, such as the polymer composition and molecular weight, the solvent used, concentration and additives.[5] When the two building blocks are hydrophobic and hydrophilic, amphiphilic linear diblock copolymers can self-assemble in aqueous solution to form various nanostructures, which has attracted considerable interest not only owing to their unique properties but also due to their potential widespread applications in technical and biomedical areas. In this chapter, the amphiphilic PEG-*b*-PU linear diblock copolymers prepared belong to this kind of diblock copolymers in which one block is hydrophobic polyurethane (PU) and the other is hydrophilic poly(ethylene glycol) (PEG).

PEG, also known as PEO (polyethylene oxide), is a biocompatible polyether useful

for many applications. It is usually used as the hydrophilic block linked with various hydrophobic blocks like PPO (poly(propylene oxide)), PBO (poly(butylene oxide)), PS (polystyrene), PMMA (poly(methyl methacrylate)) to produce amphiphilic linear diblock copolymers for self-assembly. PEG is generally prepared by ROP of ethylene oxide (EO) from a suitable (anionic) initiator. Functionalized PEGs are obtained by using a specific initiator or through post-functionalization.

3.1.2 Synthetic techniques of amphiphilic linear diblock copolymers

For the synthesis of amphiphilic linear diblock copolymers, the advancement of polymer synthetic strategies makes it available to prepare various amphiphilic linear diblock copolymers with precisely controlled molecular weights and defined molecular structures.[6] As far as we know, the main synthetic strategies include: (1) the sequential addition of different monomers *via* "living" / controlled polymerization techniques; (2) the polymerization of specific monomers using macromolecular initiators; (3) the coupling reactions between two polymer segments with active chain ends.[2,7] Among these strategies, the first and second ones are the most studied thanks to the higher efficiency of both synthesis and purification.

Sequential addition of different monomers *via* "living" / controlled radical polymerization (CRP) techniques represent one facile and versatile approach to synthesize amphiphilic linear diblock copolymers. A number of CRP methods have been developed and the three most promising ones are: atom transfer radical polymerization (ATRP), reversible addition-fragmentation chain transfer (RAFT) radical polymerization and nitroxide-mediated polymerization (NMP).[8-10] All these methods rely on establishing a dynamic equilibrium between the active propagating chains with a low concentration and dormant chains with a predominant amount, leading to the formation of polymers with narrow polydispersity indexes (PDIs) and well-defined molecular structures.[11]

Other polymerization methods, such as cationic or anionic polymerization, ring opening polymerization (ROP), ring-opening metathesis polymerization (ROMP) and

combination of these different polymerization techniques can also be used to prepare amphiphilic linear diblock copolymers through the strategy of sequential addition of two different monomers. All these approaches can also be applied to the second strategy where linear homopolymers bearing functional groups at one chain end are used as the macromolecular initiators to initiate the polymerization of only one type of monomers. For example, poly(ethylene glycol) monomethyl ether (mPEG) functionalized with an alkyl halide could be used as the macromolecular initiator for ATRP of vinyl monomers to prepare PEG-based amphiphilic linear diblock copolymers.

In this chapter, we mainly studied the ROP of 5-membered cyclic carbamate monomers using mPEG derivatives as the macromolecular initiators to prepare amphiphilic PEG-*b*-PU linear diblock copolymers. The following part will introduce several PEG based amphiphilic linear diblock copolymers prepared through the ROP of heterocycles using mPEG or mPEG derivatives as macromolecular initiators.

3.1.2.1 Synthesis and self-assembly of amphiphilic PEG-b-Polyester linear diblock copolymers

Poly(ε-caprolactone) (PCL) is a biodegradable, semi-crystalline and hydrophobic polyester, which is usually prepared by ROP of ε-caprolactone (ε-CL) using a catalyst such as stannous octoate ($Sn(Oct)_2$). It has been used in a variety of biomedical applications as diverse as controlled drug release, gene therapy, regenerative medicine, or implants. However, PCL degrades rather slowly and is less biocompatible with soft tissue due to its high degree of crystallinity and hydrophobicity.[12] Therefore, the modification of PCL with PEG will allow the formation of amphiphilic linear PEG-*b*-PCL diblock copolymers, which can improve the hydrophilicity, biodegradability and mechanical properties of the resulting polymer significantly.[13] Moreover, the corresponding amphiphilic diblock copolymer can form various nanostructures in water by self-assembly, allowing various applications of PCL in biomedical areas.

The most widely used method to synthesize PEG-*b*-PCL diblock copolymers is the ROP of ε-CLs with mPEG as a macromolecular initiator (Figure 3.1).[12] In a typical

polymerization, mPEG is firstly distilled with dry toluene to remove residual water in
the solvent. Then predetermined amounts of ε-CL and catalysts (*e.g.*, Sn(Oct)$_2$, stannous
chloride, GeO$_2$, SnO$_2$) are added and the mixture is refluxed for a certain time at an
appropriate temperature. Copolymers with different PCL block lengths can be obtained
by changing the molar ratio of ε-CL and mPEG. During the polymerization, the
moisture in the solvent and catalyst concentration have important influence on the yield
and molecular weight of block copolymers, which requires the drying of mPEG and ε-
CL before use. Also, the polymerization is supposed to be performed under inert
atmosphere or high vacuum.[12]
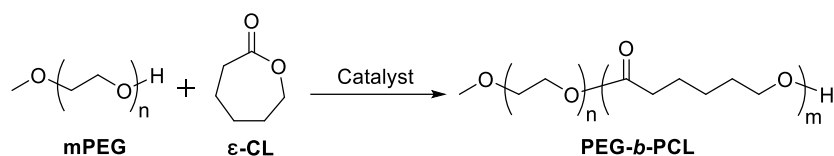
Figure 3.1. Synthesis of amphiphilic PEG-*b*-PCL linear diblock copolymer.[12]
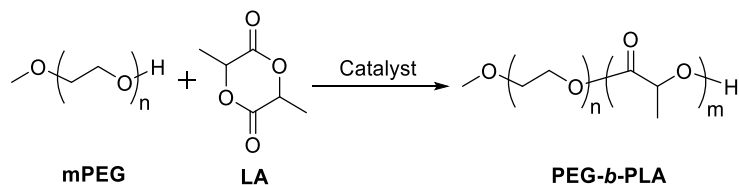
Figure 3.2. Synthesis of amphiphilic PEG-*b*-PLA linear diblock copolymer.[15]

Polylactide (PLA) is a hydrophobic polyester which is biocompatible, FDA-
approved for clinical use and biodegradable by enzyme and hydrolysis under
physiological conditions. There are three types of PLA stereoisomers: optically
active/isotactic poly(L-(−)-*S*-lactide) (PLLA) and poly(D-(+)-*R*-lactide) (PDLA), and
racemic/atactic PDLLA.[14] PLA and amphiphilic PEG-*b*-PLA linear diblock copolymer
are usually synthesized by ROP of LA using hydroxy- or amine- functionalized
initiators. For example, Li and coworkers have prepared a series of PEG-*b*-PLA diblock
copolymers *via* the ROP of L- or D- lactide with mPEG as the macromolecular initiator
and nontoxic zinc lactate as the catalyst (Figure 3.2).[15] Micelles were formed by direct
dissolution of PEG-*b*-PLA diblock copolymers in water without heating or using any

organic solvents.

The authors found that the obtained micelles were large anisotropic micelles instead of conventional spherical ones. The structure of the novel micelles was influenced by various parameters, such as the copolymer chain structure, molecular weights of copolymers, PEG fraction, copolymer concentration and stereocomplexation (*i.e.*, stereocomplexation results from stereoselective interactions, mainly van der Waals forces, between two stereoregular polymers which interlock to form a new material with altered physical properties as compared to the parent polymers) between L- or D-PLA blocks. The morphology of the micelles is not spherical but elliptical, cylindrical, or acicular. The length of the anisotropic micelles varies from 150 to 500 nm and the width is in the range of 30 to 100 nm. Moreover, it was found that the anisotropic micelles were susceptible to further self-assemble into more organized and complicated aggregates at appropriately high concentrations.[15]

3.1.2.2 Synthesis and self-assembly of amphiphilic PEG-b-Polyphosphoester linear diblock copolymers

Polyphosphoesters (PPEs) are an important class of biocompatible and biodegradable polymers for biomedical applications.[16,17] With numerous repeating phosphoester linkages in the backbone, PPEs have the structural similarity to naturally occurring nucleic and teichoic acids. PPEs and PPE based copolymers are usually prepared from the ROP of 5-membered cyclic phosphoester monomers with $Sn(Oct)_2$ as the catalyst. Thanks to the pentavalence of the central phosphorous, PPEs with different side groups can be easily prepared by using cyclic phosphoesters bearing different functional groups.[18]

PPE based amphiphilic linear diblock copolymers such as PEG-*b*-PPE are also promising materials for biomedical applications due to their self-assembly and degradability. For example, Wang and coworkers have prepared the amphiphilic PEG-*b*-PPE linear diblock copolymers with various molecular weights and compositions through the ROP of 2-ethoxy-2-oxo-1,3,2-dioxaphospholane (EEP) and 2-isopropoxy-

2-oxo-1,3,2-dioxaphospholane (PEP) monomers using mPEG as the macromolecular initiator and Sn(Oct)$_2$ as the catalyst (Figure 3.3).[19] The obtained block copolymers exhibited thermo-induced self-assembly behavior and the critical aggregation temperature (CAT) of the block copolymers could be conveniently adjusted by changing the PEG fraction or the hydrophobicity of the cyclic phosphoester monomer. The authors observed that the copolymers showed low *in vitro* toxicity and a presumed autocatalytic degradation behavior at neutral pH, which was explained by the generation of an ionic phosphate polymer that might catalyze the degradation further. Therefore, thanks to their good biocompatibility and thermoresponsiveness, these biodegradable block copolymers were thought to be promising materials for biomedical applications.
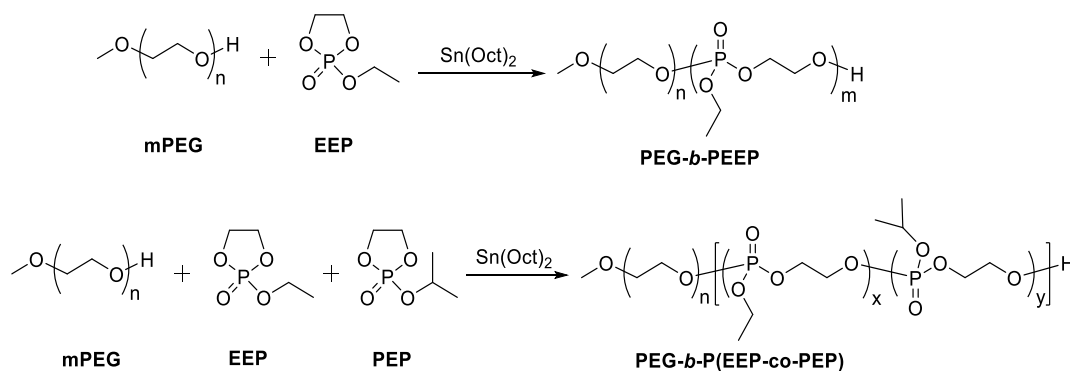
Figure 3.3. Synthesis of amphiphilic PEG-*b*-PPE linear diblock copolymer.[19]

3.1.2.3 Synthesis and self-assembly of amphiphilic PEG-b-Polycarbonate linear diblock copolymers

Polycarbonates have important applications in our daily life as engineering, construction or electronic materials. Generally, they are prepared from the polycondensation of bisphenol A (BPA) and phosgene (COCl$_2$) in industry. Recently, biocompatible and biodegradable aliphatic polycarbonates and their copolymers have received much interest because of their potential applications in biomedical fields. They can be synthesized by ROP of cyclic carbonate monomers in the presence of (organo)catalysts.

For example, Guo, Li, Thomas and coworkers have prepared the amphiphilic PEG-

b-PMCC linear diblock copolymers through the ROP of a methyl and cholesteryl substituted trimethylenecarbonate monomer (MCC) with mPEG as the macromolecular initiator in the presence of rare-earth La[N(SiMe$_3$)$_2$]$_3$ (C1) or alkaline-earth Ca[N(SiMe$_3$)$_2$]$_2$ (C2) complexes, which are among the most reactive species in the ROP of cyclic heterocycles (Figure 3.4).[20] The authors found that smectic ellipsoidal vesicles and nanofibers were obtained by self-assembly of PEG-*b*-PMCC block copolymers. For the first time they observed the transition from rod-to-lamellae-to-vesicle in liquid crystalline (LC) block copolymers. This indicated that the PEG-*b*-PMCC block copolymers self-assembled into ellipsoidal vesicles in water following the following mechanism: amphiphilic block copolymers rapidly form small spherical micelles, which then slowly evolved into cylindrical micelles and open disc-like micelles by collision; the large disc-like micelles then gradually close to form vesicles. Their findings highlighted the interplay of complicated hierarchical structures in the nanostructures of amphiphilic LC block copolymers and offered a new family of polymersomes that might have high loading efficiency for hydrophobic molecules used in drug delivery.
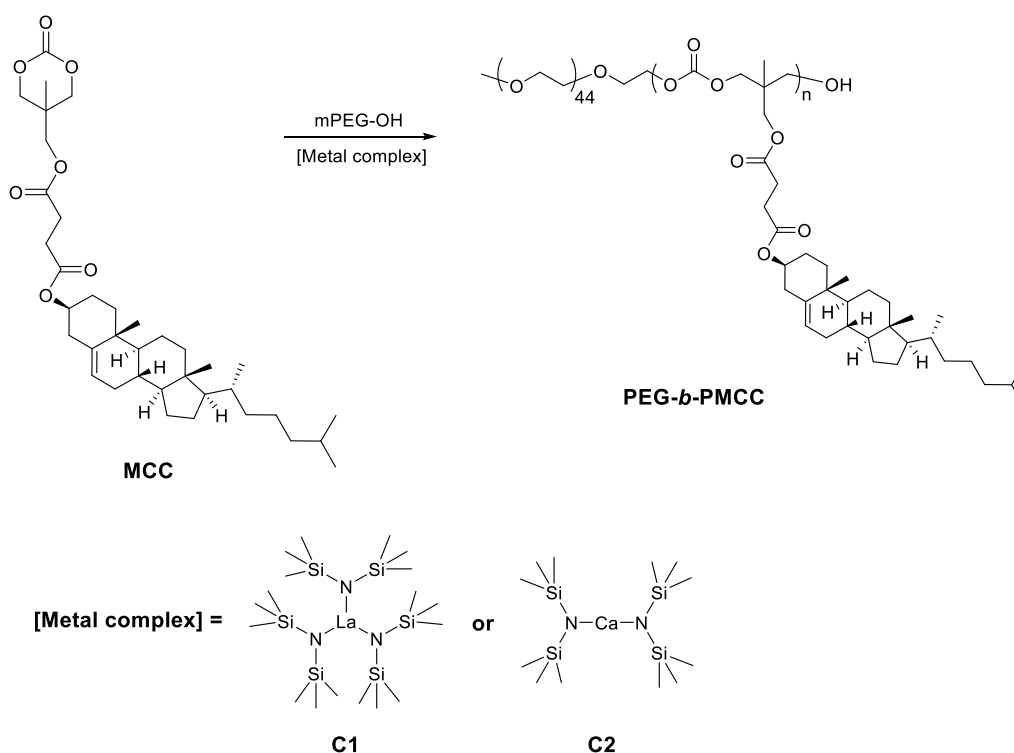

Figure 3.4. Synthesis of amphiphilic PEG-*b*-PMCC linear diblock copolymer.[20]

Yang and coworkers have also prepared a series of cholesterol-functionalized amphiphilic polycarbonate diblock copolymers mPEG$_{113}$-b-P(MTC-Chol)$_n$ through the organocatalytic ROP of a cholesterol-functionalized aliphatic cyclic carbonate monomer (MTC-Chol).[21] The polymerization was accomplished by using metal-free organic catalyst N-(3,5-trifluoromethyl)phenyl-N'-cyclohexylthiourea (TU) in combination with 1,8-diazabicyclo[5.4.0]undec-7-ene (DBU) with mPEG$_{113}$-OH (M_n = 5000 Da) as the macroinitiator (Figure 3.5a). The authors found that the amphiphilic mPEG$_{113}$-b-P(MTC-Chol)$_n$ diblock copolymers had unique self-assembly behaviors in aqueous solution. Disk-like micelles (n = 4) and stacked-disk-like morphology (n = 11) were observed by TEM (Figure 3.5b). These cholesterol-containing PEGylated polycarbonate block copolymers could serve as unique building blocks to self-assemble into unique nanostructures for the development of drug delivery vehicles.[21]

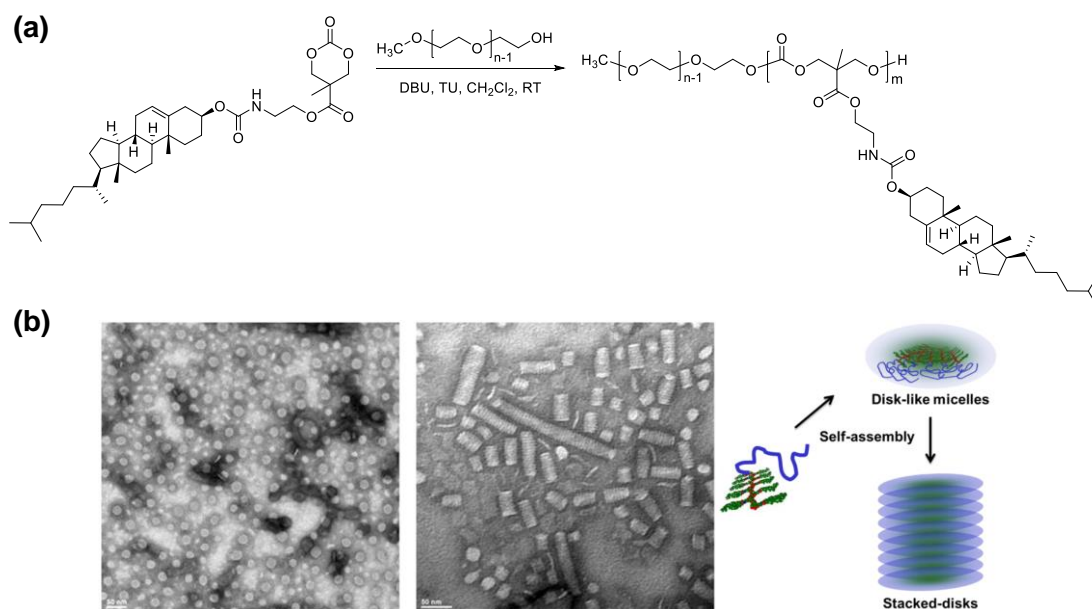**Figure 3.5**. (a) Synthesis of cholesterol-functionalized amphiphilic polycarbonate diblock copolymer mPEG$_{113}$-b-P(MTC-Chol)$_n$ *via* organocatalytic ROP. (b) TEM images and schematic illustration of disk-like micelles and stacked-disk-like aggregates formed by the self-assembly of mPEG$_{113}$-b-P(MTC-Chol)$_n$ copolymers.[21]

*3.1.2.4 Synthesis and self-assembly of amphiphilic PEG-b-Polypeptide linear diblock
copolymers*

Among the self-assembly of amphiphilic block copolymers, polypeptide-based self-
assembly has received much interest because polypeptide segments can adopt various
conformations such as random coil, α-helix and β-sheet, which have a significant
impact on the self-assembly behavior of the copolymers in solution.[22,23] For example,
Mai and coworkers have reported the self-assembly of amphiphilic poly(ethylene
glycol)-*b*-poly(γ-benzyl-L-glutamate) (PEG-*b*-PBLG) linear diblock copolymers in
water.[24] These copolymers were prepared by the ROP of γ-benzyl-L-glutamate-*N*-
carboxyanhydrides (BLG-NCA) using methoxy poly(ethylene glycol)amine (mPEG-
NH$_2$) as a macromolecular initiator (Figure 3.6). For the first time the authors found
two-dimensional (2D) disk-like micelles with cylindrical pores which were obtained by
self-assembly of PEG-*b*-PBLG in water (Figure 3.7). Their research revealed that the
α-helical conformation of PBLG blocks played a key role in the formation of disk-like
micelles. Moreover, other self-assembly structures like micelles, vesicles and large
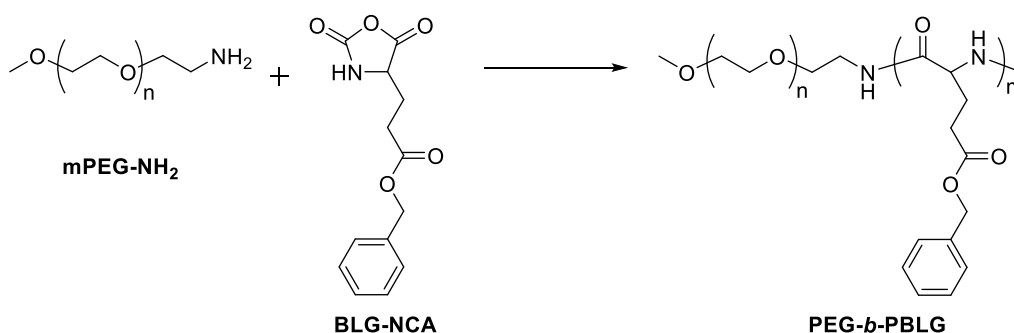vesicles could be achieved by tuning the ratio between PEG and PBLG segments in the
copolymers.[24]

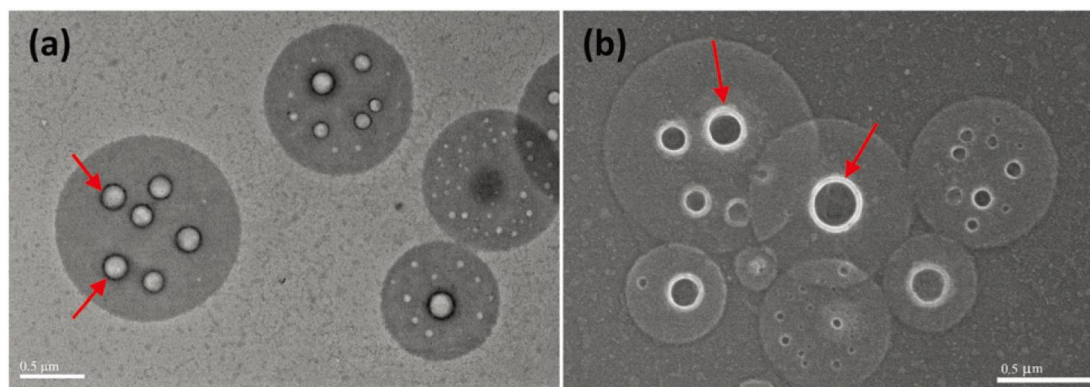**Figure 3.6**. Synthesis of amphiphilic PEG-*b*-PBLG linear diblock copolymer.[24]

Figure 3.7. Typical TEM (a) and SEM (b) images of the aggregates obtained from self-assembly of PEG$_{45}$-*b*-PBLG$_{150}$ block copolymer. Scale bars: 0.5 μm.[24]

3.1.3 Self-assembly techniques of amphiphilic linear diblock copolymers

Similar to small molecular amphiphiles, block copolymers with low molecular weights and short insoluble blocks such as the family of Pluronic (*e.g.*, PEO-*b*-PPO-*b*-PEO) can be self-assembled directly in a selective solvent which is "good" for one block but "poor" for another one.[4] Thermal annealing or ultrasonic agitation may be necessary in some cases to assist the self-assembling process.[2] However, this technique is not suitable for block copolymers with high molecular weights. We can then use the techniques by changing the solvent quality from good to bad.[2,4] In general, the copolymer is firstly dissolved in a common good solvent for both blocks. Then the conditions such as temperature or composition of the solvent are changed gradually in the way that leads to the formation of self-assemblies. The self-assembly by temperature change is only applicable in the case of thermo-responsive copolymers where the solubility of one block is temperature-dependent with a critical aggregation temperature. The self-assembly by solvent exchange is usually achieved by adding slowly a selective bad solvent for one of the blocks such as water, followed by removing the common solvent using the dialysis against the bad solvent or water. This technique by solvent exchange is also known as "nanoprecipitation", and is widely used in the preparation of polymer nanoparticles.

3.2 Research subjects

We have prepared amphiphilic PEG-*b*-PU linear diblock copolymers *via* the anionic ring opening polymerization (AROP) of the 5-membered cyclic carbamate monomer (CHU) in the presence of mPEG based macromolecular co-initiators (mPEG-CHU). Three mPEG-CHU with different PEG molecular weights (M_n = 550, 1000 and 2000 Da) were synthesized. A series of PEG-*b*-PU linear diblock copolymers with various sequence lengths of PEG and PU were therefore prepared. Then we selected two types of PEG$_{12}$-*b*-PU diblock copolymers and two types of PEG$_{22}$-*b*-PU diblock copolymers for the self-assembly study in water using the nanoprecipitation technique. The self-assemblies thus obtained were carefully characterized by DLS (dynamic light scattering), SEM (scanning electron microscopy) and cryo-EM (cryo-electron microscopy).

3.3 Results and Discussion

3.3.1 Synthesis of mPEG based macromolecular co-initiators

In the second chapter, we have found that co-initiators containing *N*-acyl imide groups or acyl chlorides (Figure 3.8) are necessary to synthesize PUs with high molecular weights and narrow PDIs. Moreover, the benzene group of the co-initiator is one of the end groups in the final PUs. These results gave us the idea that polymers containing *N*-acyl imide groups or acyl chloride groups at one chain end could be used as macromolecular co-initiators to prepare PU based block copolymers (Figure 3.8). Since PEG is a common hydrophilic polymer with relatively simple structure, synthesis of PEG monomethyl ether (mPEG) based macromolecular co-initiators was proposed, which could be used to synthesize amphiphilic PEG-*b*-PU linear diblock copolymers.

Nevertheless, the synthesis of mPEG based macromolecular co-initiators was not easy. We have designed four different synthetic routes, but the first three ones in the preliminary attempts were not successful (Figure 3.9). Note that the 5-membered cyclic carbamate monomer without vinyl group was used in the synthesis of macromolecular co-initiators. This cyclohexyl urethane compound can also be used to perform AROP,

but only oligomer PUs were obtained due to their bad solubility in most organic solvents. However, we found that the corresponding co-initiator with a *N*-acyl imide group synthesized from the urethane compound was efficient for the AROP of CHU monomers as well as CHU based co-initiators. Therefore, we chose it to synthesize mPEG based macromolecular co-initiators. For convenience, we also called it CHU and the obtained macromolecular co-initiator as mPEG-CHU.
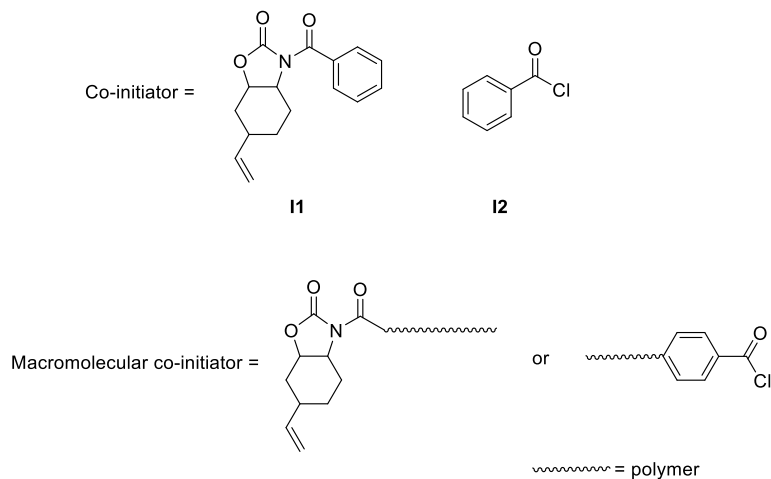

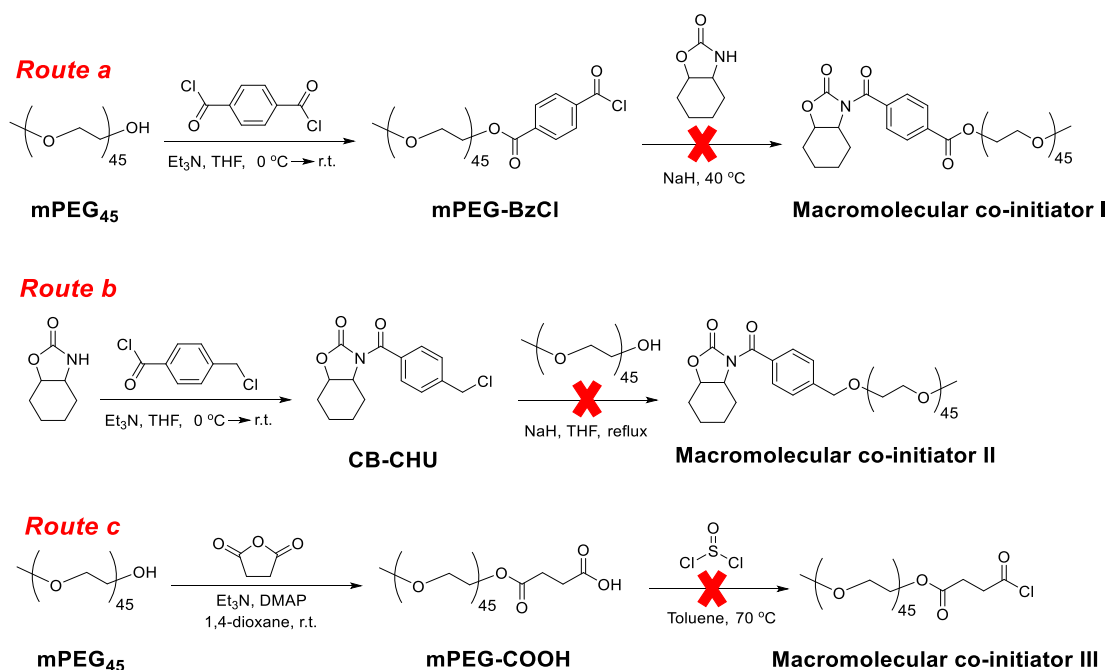**Figure 3.8**. Small-molecule co-initiators and macromolecular co-initiators.

Figure 3.9. Unsuccessful synthesis of mPEG based macromolecular co-initiators.

For route a, the starting materials were mPEG$_{45}$ (M_n = 2000 Da), terephthaloyl chloride and triethylamine (Et$_3$N). Although the first step was thorough (grafting ratio was almost 100% according to the ^{1}H NMR spectrum), the yield of the second step was very modest (grafting ratio was lower than 10% according to the ^{1}H NMR spectrum). In addition, PEG dimers were present according to the GPC characterization of the crude product. So, we designed to try another route.

For route b, the first step was also successful and pure imide derivative containing chloromethylbenzoyl group (CBCHU) was obtained. However, there was almost no reaction for the second step even if the reaction temperature was increased to 70 °C (*i.e.*, reflux in THF) as confirmed by the ^{1}H NMR spectrum.

For route c, carboxylic acid functionalized mPEG (mPEG-COOH) was synthesized successfully with a high yield (97%). Then in the second step, mPEG-COOH was treated with thionyl chloride (SOCl$_2$) to convert the carboxylic group into an acyl chloride function. The reaction performed well, but the obtained mPEG-COCl could not be purified as it was unstable and could be hydrolyzed easily by the ambient moisture. After several attempts of AROP using the mPEG-COCl as the macromolecular co-initiator, we found that the conversion of cyclic carbamate monomers was not high, and the molecular weights of the obtained PEG-*b*-PU copolymers were relatively low.
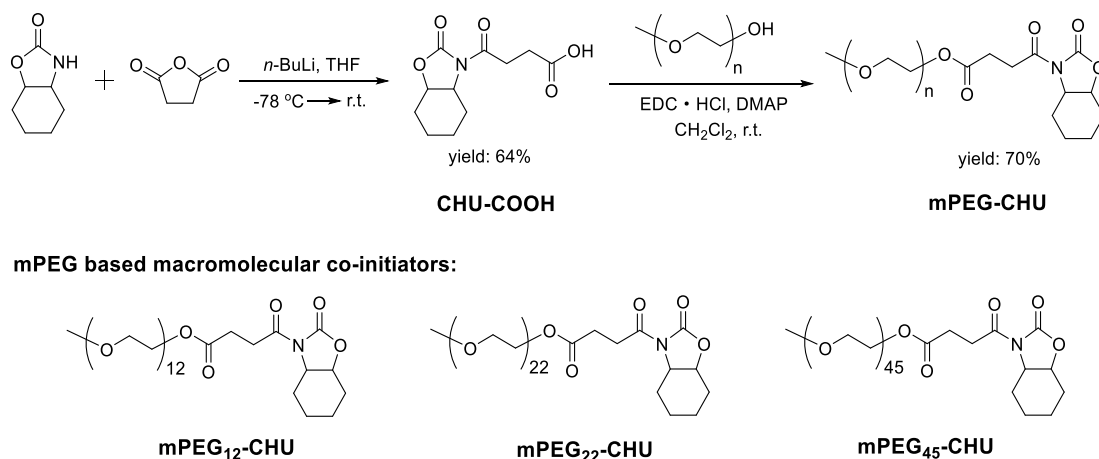
Figure 3.10. Successful synthetic route to mPEG based macromolecular co-initiators and the molecular structures of the prepared mPEG-CHU macromolecular co-initiators with different molecular weights of mPEG.

The last successful route is shown in Figure 3.10, which is a variant of the route c by changing the order of reaction steps. As shown in Figure 3.10, a carboxylic acid functionalized CHU (CHU-COOH) intermediate was firstly synthesized by reacting CHU with succinic anhydride in the presence of n-butyllithium. After recrystallization, CHU-COOH was obtained with a yield of 64%. ^{1}H NMR and ^{13}C NMR spectra are shown in Figure 3.11. Then mPEG based macromolecular co-initiator mPEG-CHU was prepared through the esterification between CHU-COOH and mPEG-OH in the presence of 1-(3-dimethylaminopropyl)-3-ethylcarbodiimide hydrochloride (EDC•HCl) and 4-(dimethylamino)pyridine (DMAP). After purification by column chromatography using methanol and dichloromethane as eluents, pure mPEG-CHU was obtained with a yield of about 80%.
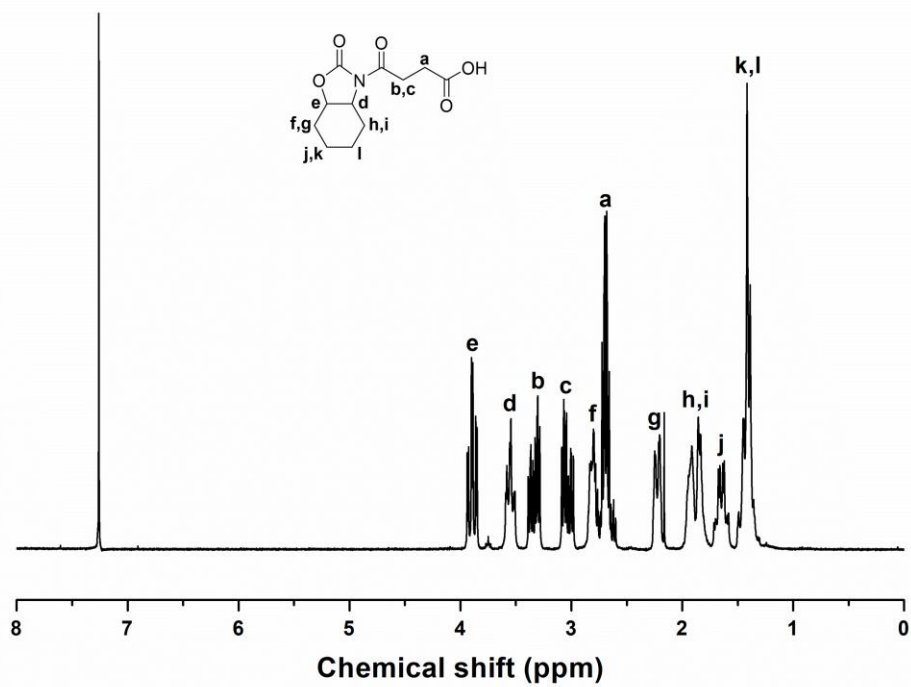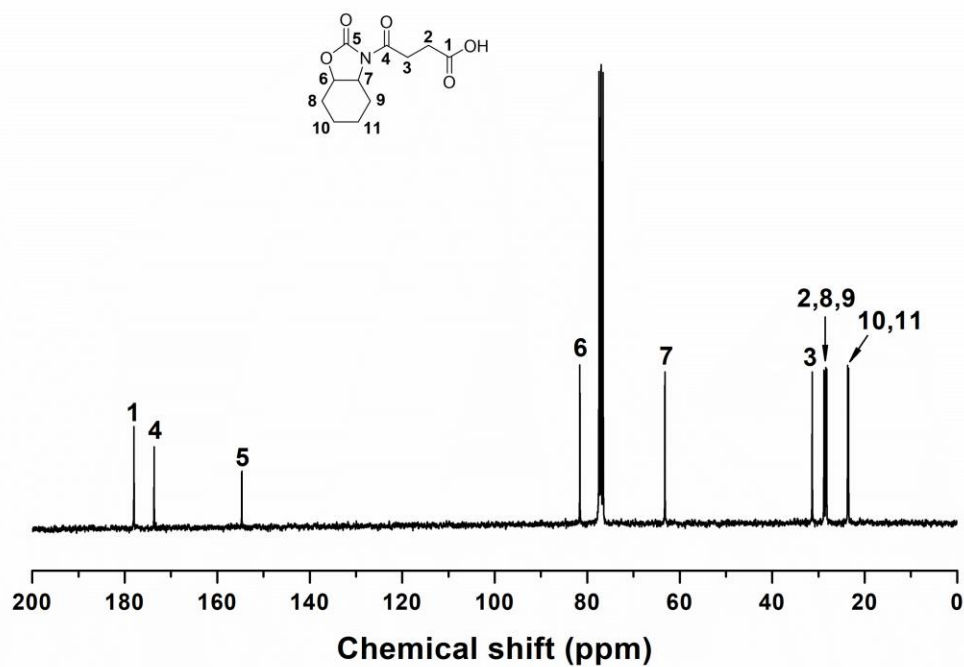
Figure 3.11. ^{1}H NMR (a) and ^{13}C NMR (b) spectra of CHU-COOH. CDCl$_3$, 400 MHz, 297 K.
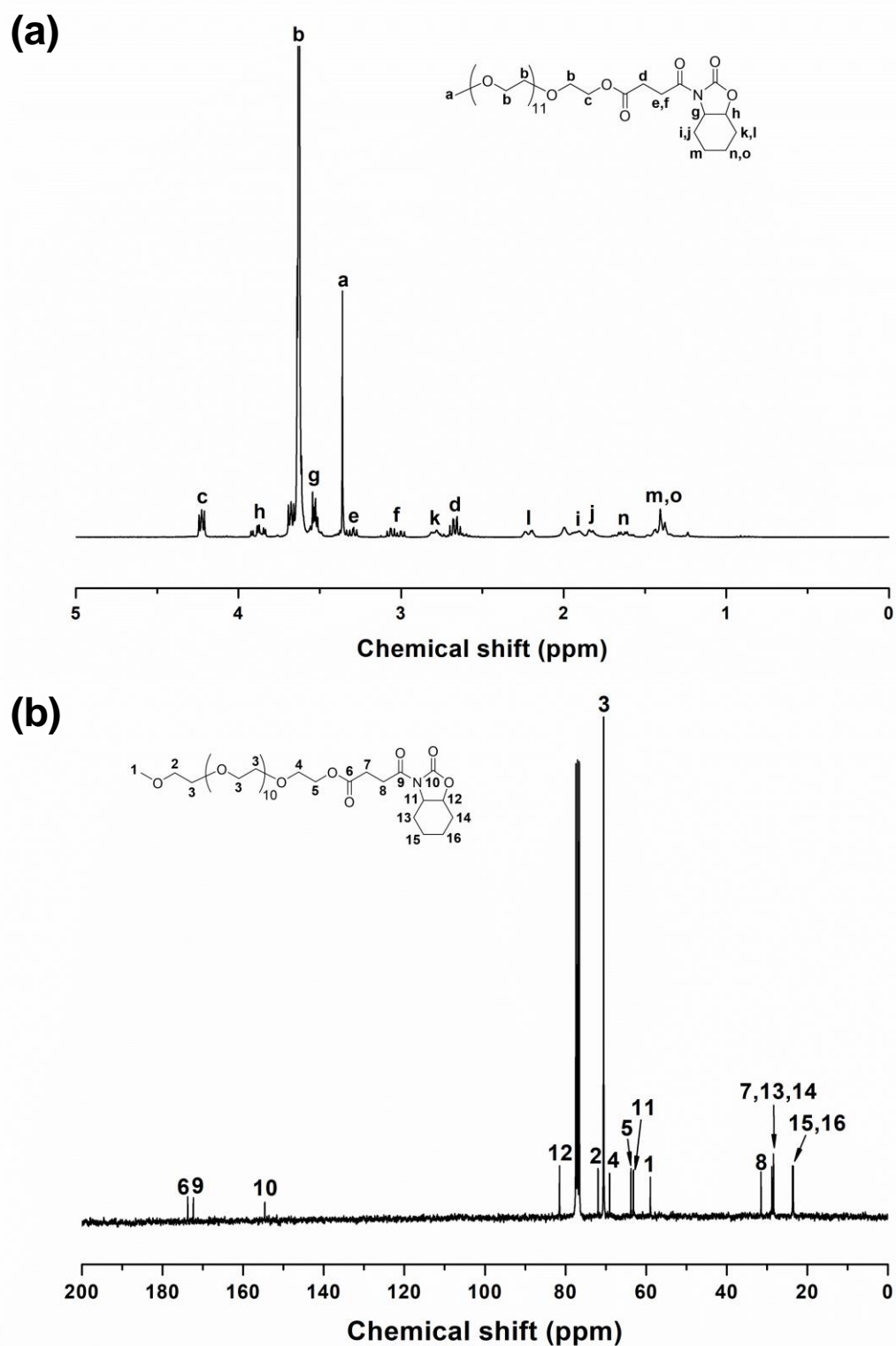
Figure 3.12. ^{1}H NMR (a) and ^{13}C NMR (b) spectra of mPEG$_{12}$-CHU. CDCl$_3$, 400 MHz,
297 K.
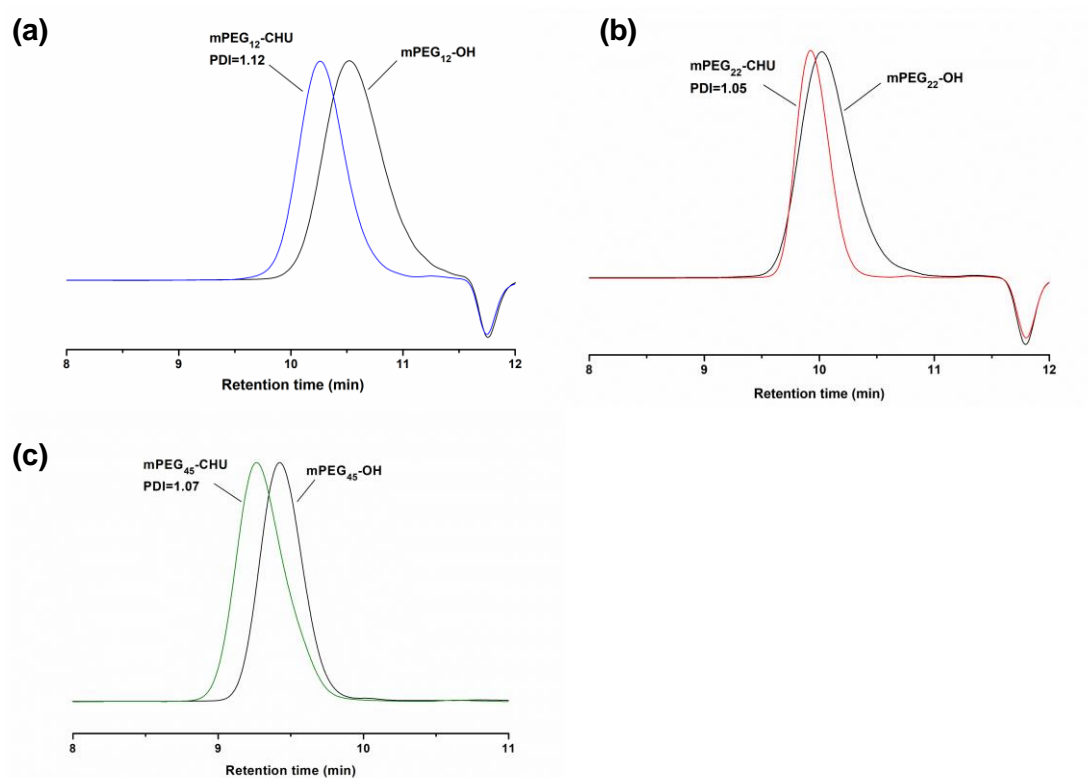
Figure 3.13. GPC traces of mPEG$_{12}$-OH and mPEG$_{12}$-CHU (a), mPEG$_{22}$-OH and mPEG$_{22}$-CHU (b) and mPEG$_{45}$-OH and mPEG$_{45}$-CHU (c) with THF as the eluent.

Using this synthetic route, we have prepared three different mPEG-CHUs, namely mPEG$_{12}$-CHU ($M_{n,PEG}$ = 550 Da), mPEG$_{22}$-CHU ($M_{n,PEG}$ = 1000 Da) and mPEG$_{45}$-CHU ($M_{n,PEG}$ = 2000 Da). The ^{1}H NMR and ^{13}C NMR spectra of mPEG$_{12}$-CHU are shown in Figure 3.12. The GPC curves of mPEG$_{12}$-CHU, mPEG$_{22}$-CHU and mPEG$_{45}$-CHU are shown in Figure 3.13. They all indicated that pure mPEG-CHUs without any mPEG-OH were obtained.

3.3.2 Synthesis of amphiphilic PEG-*b*-PU linear diblock copolymers

The synthetic scheme of amphiphilic PEG-*b*-PU linear diblock copolymers is shown in Figure 3.14. The copolymers were synthesized *via* the AROP of CHU monomers with mPEG-CHU as macromolecular co-initiators, in accordance to the synthesis developed for PU homopolymers in the second chapter. Different polymerization parameters such as temperature, concentration, initiators and co-initiators were firstly

evaluated. After several attempts, we found that the optimal conditions were at 40 °C

with n-butyllithium (n-BuLi) as initiator at a concentration higher than 0.02 M. Finally,

we have obtained four copolymers with different hydrophilic ratios ($f_{PEG,wt\%}$ from 17%

to 35%) in each series of PEG_{12}-b-PU and PEG_{22}-b-PU, while only two block

copolymers with hydrophilic ratios higher than 49.1% were obtained for PEG_{45}-b-PU.

The typical AROP results are listed in Table 3.1.
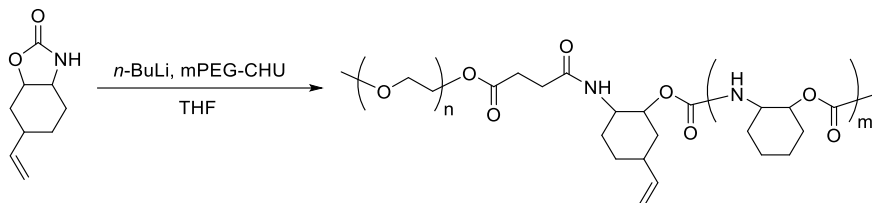
Figure 3.14. Synthetic scheme of amphiphilic PEG-b-PU linear diblock copolymers.

Table 3.1. Synthesis of amphiphilic PEG-b-PU linear diblock copolymers by using
mPEG based macromolecular co-initiators.

Entry[a]	Co-initiator	Monomer/ n-BuLi/Co-initiator	T/°C	Time/h	Conversion[b]	$M_{n,\,theory}$	$M^b_{n,\,NMR}$	DP[b]	PDI[c]	$f_{PEG,wt\%}$
1	mPEG$_{12}$-CHU	18.6/1/1	40	20	80%	1500	3100	14	1.57	17.7%
2	mPEG$_{12}$-CHU	10/1/1	40	20	81%	2100	2800	12	1.49	19.8%
3	mPEG$_{12}$-CHU	8/1/1	40	20	80%	1800	2100	8	1.64	26.1%
4	mPEG$_{12}$-CHU	9.3/1/1	0	6	57%	1700	1600	5	1.42	34.2%
5	mPEG$_{22}$-CHU	50/1/1	40	20	81%	8000	5600	26	1.44	17.9%
6	mPEG$_{22}$-CHU	30/1/1	40	20	80%	5200	4400	19	1.46	22.7%
7	mPEG$_{22}$-CHU	22.5/1/1	40	20	82%	4300	3200	12	1.47	30.9%
8	mPEG$_{22}$-CHU	18.6/1/1	40	20	80%	3700	2900	10	1.39	34.5%
9	mPEG$_{45}$-CHU	30/1/1	40	20	81%	6300	4100	11	1.20	49.1%
10	mPEG$_{45}$-CHU	50/1/1	40	20	81%	9300	3200	6	1.27	61.8%

a. For entries 1-4, the monomer concentration was 0.375 M; for entries 5-10, the

concentration of n-BuLi was 0.02 M; b. Conversion of monomers, $M_{n,NMR}$ and degree

of polymerization (DP) were calculated by ^{1}H NMR; c. PDI was obtained by GPC with

THF as eluent and PS as standards.

In Table 3.1, we can see that the monomer conversion is approximately 80% for most

entries except for entry 4 in which the ROP temperature is lower (*i.e.*, 0 °C). We can

also observe that the polymerization was not well controlled since the experimental molecular weights are different from the theoretical ones. The possible reason might be that the ROP was conducted at 40 °C, thus enabling the nucleophilic attack of the CHU-derived anions on CHU monomers rather than on macromolecular co-initiators. As a result, PU oligomers were produced at this polymerization temperature.

To obtain pure PEG-*b*-PU diblock copolymers, we isolated the crude products carefully by precipitation in a *n*-hexane/diethyl ether mixture (diethyl ether was a good solvent for PU oligomers) to remove PU oligomers. Finally, amphiphilic PEG-*b*-PU linear diblock copolymers with different hydrophilic ratios were obtained successfully, which was confirmed by the NMR and GPC results. The ^{1}H NMR spectrum of a typical PEG$_{22}$-*b*-PU$_{26}$ copolymer (entry 5 in Table 3.1) is shown in Figure 3.15. The GPC traces of PEG$_{12}$-*b*-PU (entries 1-4 in Table 3.1) and PEG$_{22}$-*b*-PU (entries 5-8 in Table 3.1) linear diblock copolymers are shown in Figure 3.16. Since PEG$_{45}$-*b*-PU copolymers with low hydrophilic ratios (< 30%) were not obtained, we focused the self-assembly study on PEG$_{12}$-*b*-PU and PEG$_{22}$-*b*-PU copolymers.
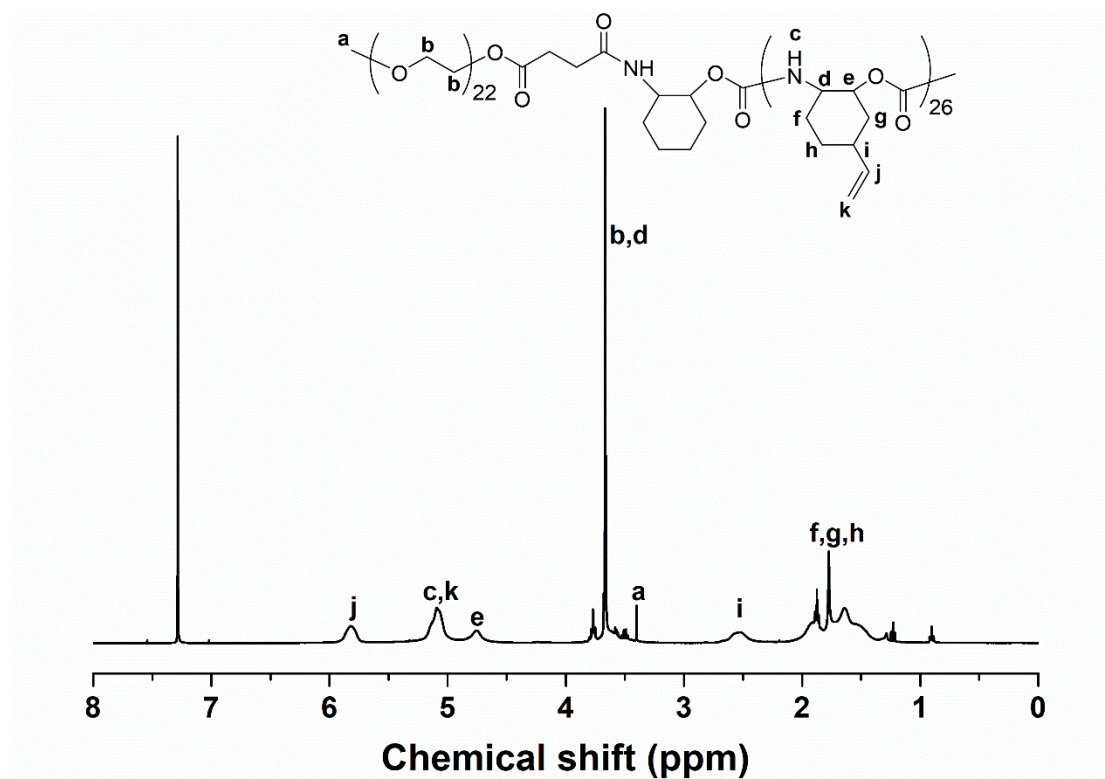
Figure 3.15. ^{1}H NMR spectrum of PEG$_{22}$-*b*-PU$_{26}$ (entry 5 in Table 3.1). CDCl$_3$, 400 MHz, 297 K.
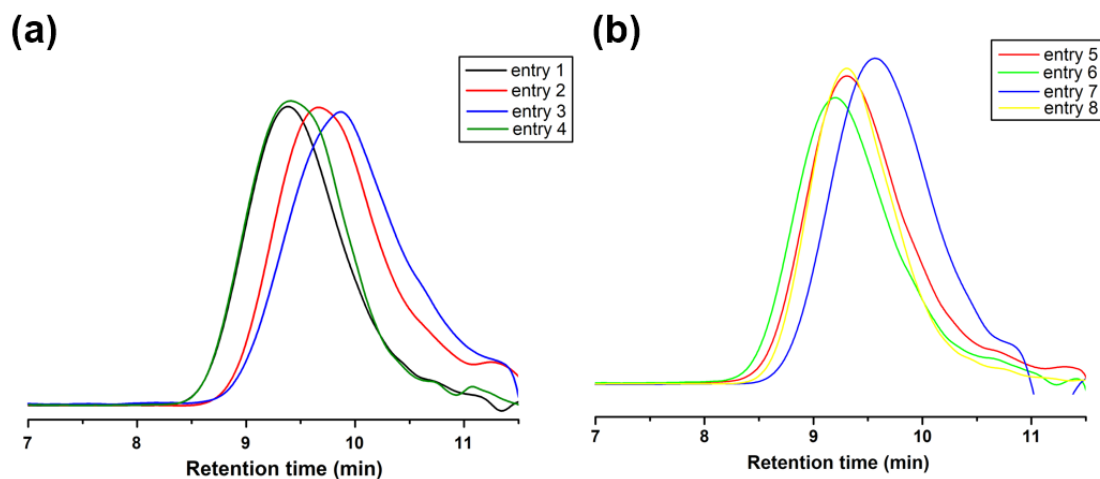
Figure 3.16. GPC traces of PEG$_{12}$-*b*-PU (entries 1-4 in Table 3.1, **a**) and PEG$_{22}$-*b*-PU (entries 5-8 in Table 3.1, **b**) with THF as the eluent.

3.3.3 Self-assembly of amphiphilic PEG-*b*-PU linear diblock copolymers

After the synthesis of amphiphilic PEG-*b*-PU linear diblock copolymers, their self-assembly behaviors in water were studied. We have chosen two samples of PEG$_{12}$-*b*-PU and two samples of PEG$_{22}$-*b*-PU with different hydrophilic ratios, respectively, to perform the self-assembly. Their molecular weights and molecular weight distributions are summarized in Table 3.2. Nanoprecipitation was used as the self-assembly technique for all the four samples (Figure 3.17).

Table 3.2. Molecular weights and molecular weight distributions of the PEG$_{12}$-*b*-PU and PEG$_{22}$-*b*-PU linear diblock copolymers for self-assembly study.

Sample	DP of PU[a]	M_n[a]	PDI[b]	$f_{PEG,wt\%}$
PEG$_{12}$-*b*-PU$_{14}$	14	3100	1.57	17.7%
PEG$_{12}$-*b*-PU$_8$	8	2100	1.64	26.1%
PEG$_{22}$-*b*-PU$_{26}$	26	5600	1.44	17.9%
PEG$_{22}$-*b*-PU$_{10}$	10	2900	1.39	34.5%

a. Degree of polymerization (DP) and M_n were calculated by ^{1}H NMR;

b. PDI was obtained by GPC with THF as eluent.
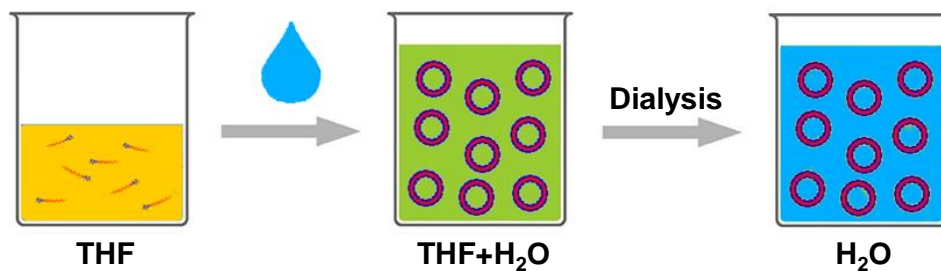
Figure 3.17. Schematic diagram of the self-assembly process of PEG-*b*-PU copolymers by nanoprecipitation and dialysis techniques.

In a typical self-assembly experiment, PEG-*b*-PU was firstly dissolved in THF (concentration 2.5 mg/mL), which is a good solvent for both PEG and PU. Then deionized water was added slowly (around 3 uL/min) until it reached 50 wt% of the whole solution. The solution was shaked gently during the addition of water. THF was removed by dialysis against deionized water for 3 days in a 3500 Da cut off cellulose bag. Finally, an aqueous solution of the self-assemblies of PEG-*b*-PU with a concentration of about 2 mg/mL in the dialysis bag was obtained.
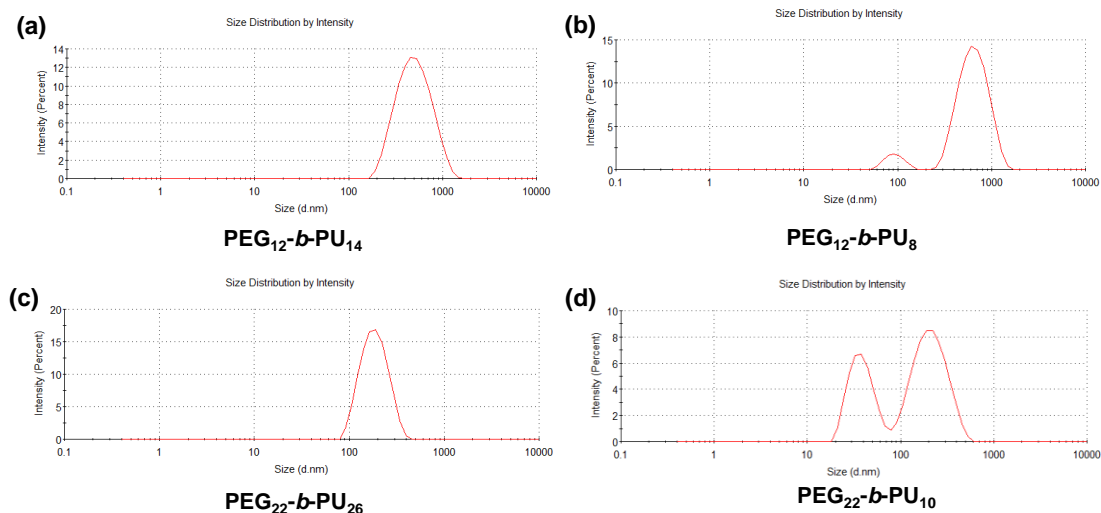
Figure 3.18. DLS characterizations of the self-assemblies of PEG$_{12}$-*b*-PU$_{14}$ (a), PEG$_{12}$-*b*-PU$_8$ (b), PEG$_{22}$-*b*-PU$_{26}$ (c) and PEG$_{22}$-*b*-PU$_{10}$ (d).

The self-assemblies of the four PEG-*b*-PU samples were characterized carefully by DLS, SEM and cryo-EM measurements. The DLS characterization results are shown

in Figure 3.18. We can see that there are two types of size distributions for the self-assemblies of PEG$_{12}$-b-PU$_8$ and PEG$_{22}$-b-PU$_{10}$ copolymers, while there is only one type of size distribution for the self-assemblies of PEG$_{12}$-b-PU$_{14}$ and PEG$_{22}$-b-PU$_{26}$ copolymers. The hydrodynamic diameters (D$_h$) of the two kinds of nanoparticles of PEG$_{12}$-b-PU$_8$ were about 96 nm and 568 nm, respectively. For PEG$_{12}$-b-PU$_{14}$, D$_h$ of the nanoparticles was about 530 nm. For PEG$_{22}$-b-PU$_{26}$, D$_h$ of the nanoparticles was about 190 nm. For PEG$_{22}$-b-PU$_{10}$, D$_h$ of the two kinds of nanoparticles were about 40 nm and 220 nm, respectively.
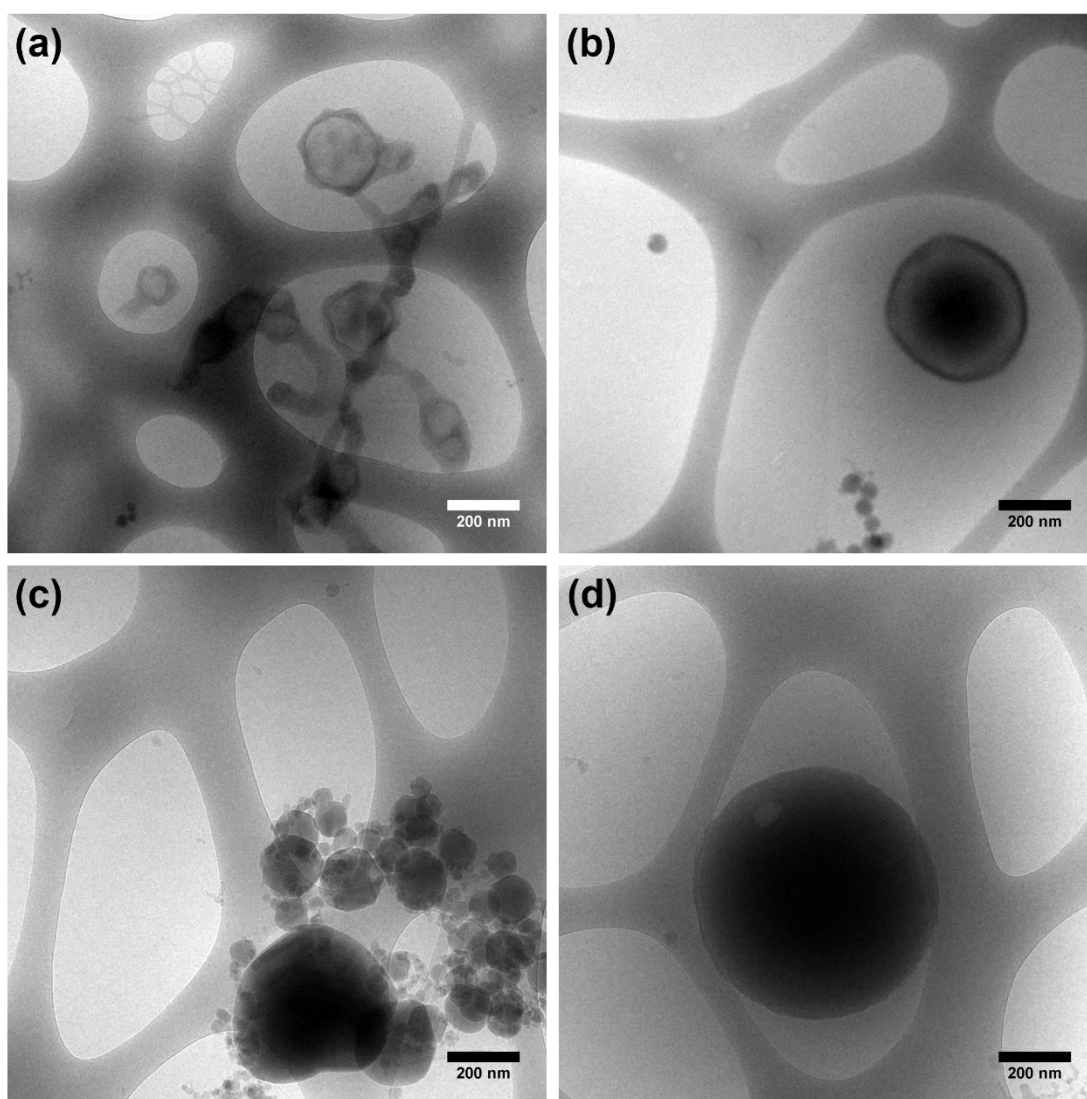
Figure 3.19. Cryo-EM images of the self-assemblies of PEG$_{12}$-b-PU$_{14}$ (a, b) and PEG$_{12}$-b-PU$_8$ (c, d).

The morphologies of the self-assemblies of PEG_{12}-b-PU_{14} and PEG_{12}-b-PU_8 were
characterized by cryo-EM (Figure 3.19). For PEG_{12}-b-PU_{14} ($f_{wt\%}$ = 17.7%), vesicles
with irregular shapes were observed (Figure 3.19a, b). The diameter of the irregular
vesicles was around 200 nm. The membrane thickness of the vesicles was determined
to be 15.1 ± 0.8 nm by statistical analysis of the cryo-EM images of 30 different vesicles.
Also, small nanoparticles with diameters less than 100 nm were observed (Figure 3.19
b). For PEG_{12}-b-PU_8 ($f_{wt\%}$ = 26.1%), solid spherical micelles with a diameter of less
than 100 nm to 500 nm were observed (Figure 3.19c, d), which might correspond to a
hydrophobic PU core surrounded by the hydrophilic PEG corona.
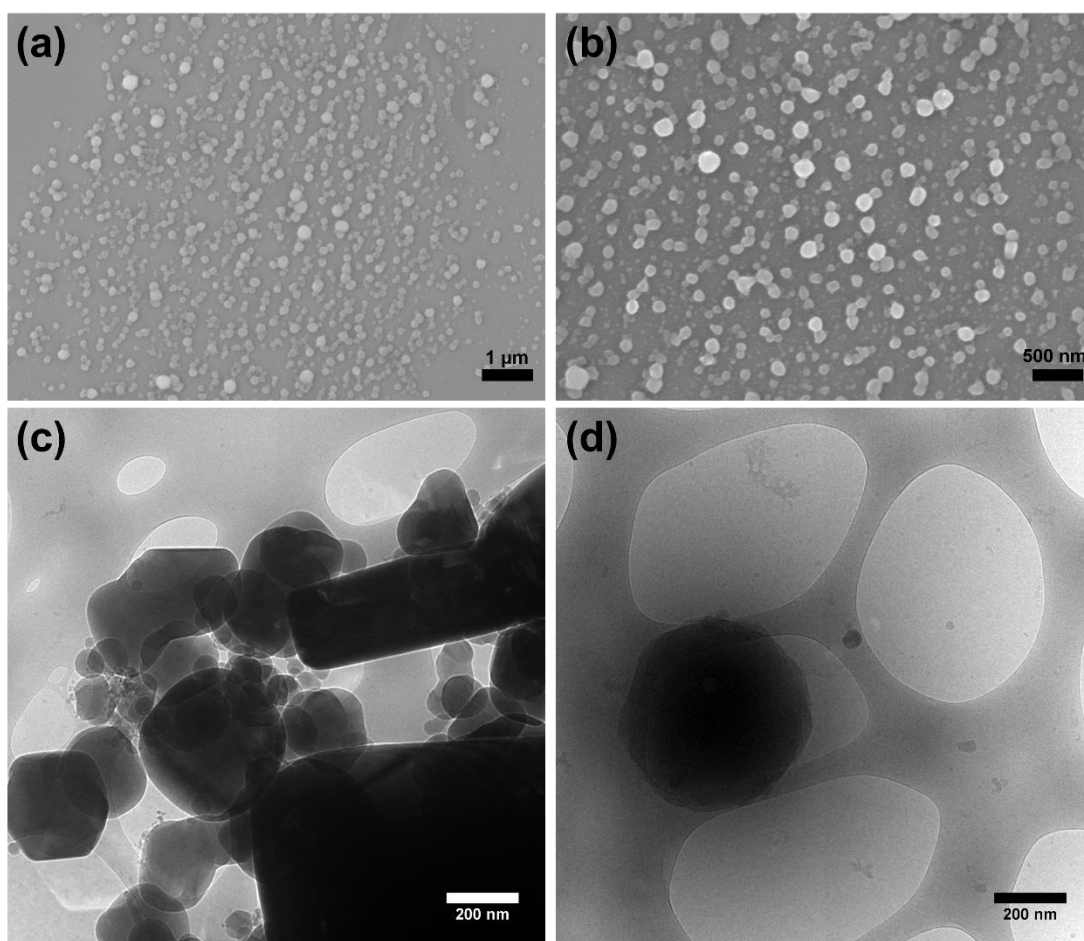
Figure 3.20. SEM (a, b) and cryo-EM (c, d) images of the self-assemblies of PEG_{22}-b-PU_{26}.

The morphologies of the self-assemblies of PEG_{22}-b-PU_{26} and PEG_{22}-b-PU_{10} were
characterized by SEM and cryo-EM (Figure 3.20 and 3.21). For PEG_{22}-b-PU_{26} ($f_{wt\%}$ =

17.9%), many nanoparticles with diameters ranging from less than 100 nm to 300 nm were observed by SEM (Figure 3.20a, b). Cryo-EM images showed that they were solid micelles with irregular shapes (Figure 3.20c, d). These micelles seemed to have polygonal morphologies like hexagons with many corner angles (Figure 3.20c). For PEG$_{22}$-b-PU$_{10}$ ($f_{wt\%}$ = 34.5%), nanoparticles with heterogeneous sizes were also observed by SEM (Figure 3.21a, b). Cryo-EM images evidenced the presence of micelles with spherical shapes (Figure 3.21c, d). These micelles tended to adhere to each other to form necklace-like fibers or other hierarchical aggregates.
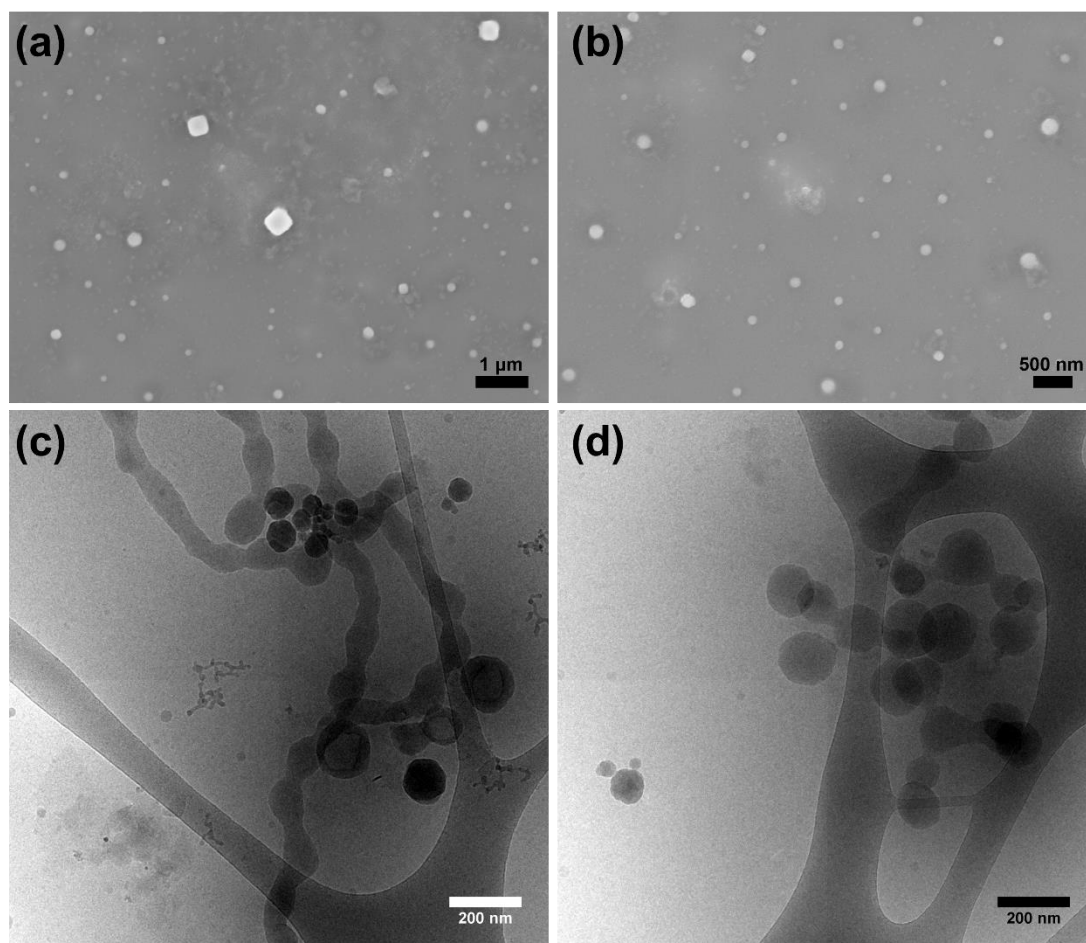
Figure 3.21. SEM (a, b) and cryo-EM (c, d) images of the self-assemblies of PEG$_{22}$-b-PU$_{10}$.

During the study of the self-assembly behaviors of our PEG-b-PU linear diblock copolymers, we found that the self-assembly solution of the two PEG$_{22}$-b-PU copolymers could emit strong fluorescence under the UV light (λ = 365 nm) while it

was not the case for the solution of the two PEG_{12}-b-PU copolymers. The photographs
of the aqueous solution of the self-assemblies of the four PEG-b-PU samples under
visible light and UV light are shown in Figure 3.22. We can see that the self-assembly
solution of both PEG_{22}-b-PU_{26} ($f_{wt\%}$ = 17.9%) and PEG_{22}-b-PU_{10} ($f_{wt\%}$ = 34.5%)
samples emit strong cyan fluorescence under the UV light (λ = 365 nm) and the
fluorescence of the former was stronger, while there is no fluorescence observed for the
self-assembly solution of the two PEG_{12}-b-PU copolymers. In addition, the
fluorescence of the self-assembly solution of the two PEG_{22}-b-PU copolymers were
characterized by fluorescence spectroscopy, as shown in Figure 3.23. The maximum
emission wavelength for the two self-assembly solutions is around 465 nm, although
the fluorescence intensity of the self-assembly solution of PEG_{22}-b-PU_{26} sample is
much higher than that of PEG_{22}-b-PU_{10} under the same characterization conditions.
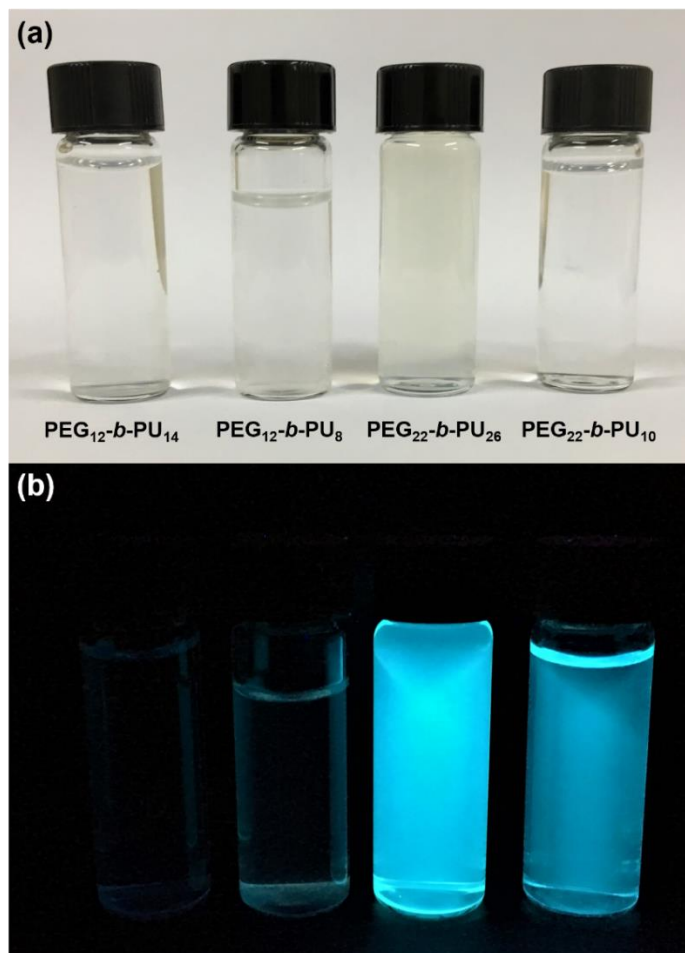
Figure 3.22. Photographs of the self-assembly solution of PEG-b-PUs under visible
light (a) and UV light (λ = 365 nm) (b).
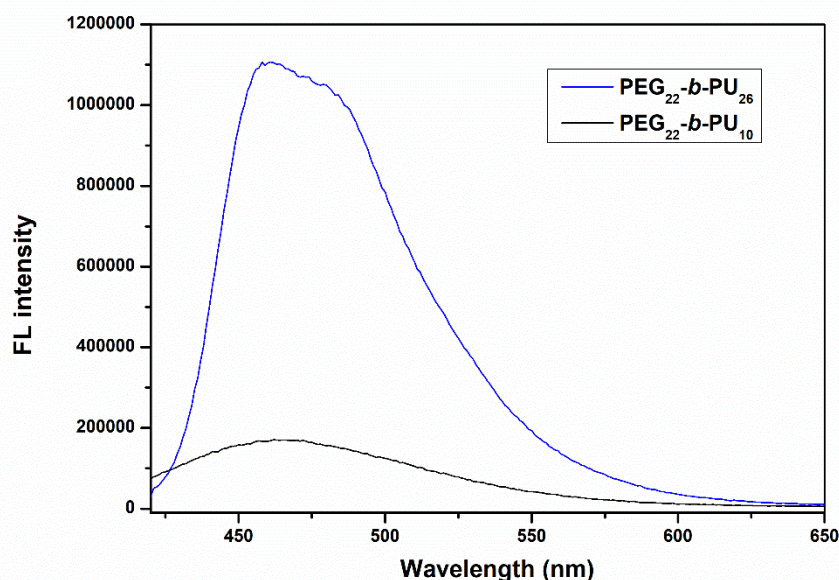
Figure 3.23. Fluorescence spectra of the self-assembly solution of PEG_{22}-b-PU_{26} and PEG_{22}-b-PU_{10}. The excitation wavelengths were 396 nm and 335 nm separately, which were the maximum excitation wavelengths for them separately.

The reason of the fluorescence emission exhibited by the self-assemblies of PEG_{22}-b-PU copolymers might be the same as in the case of the PU homopolymers, described in the second chapter, after heating at 180 °C. We hypothesize that it also belongs to the clustering-triggered emission. In detail, the clustering of urethane groups which contain electron-rich atoms N and O in the ordered and condensed nanoparticles induces the appearance of cyan fluorescence. In addition, the degree of clustering of urethane groups in the self-assemblies of PEG_{22}-b-PU_{26} ($f_{wt\%}$ = 17.9%) might be higher than that in the self-assemblies of PEG_{22}-b-PU_{10} ($f_{wt\%}$ = 34.5%) because of the longer PU chain length. Therefore, stronger fluorescence was emitted by the self-assemblies of PEG_{22}-b-PU_{26} upon UV irradiation.

3.4 Conclusion

In this chapter, a series of novel PU based amphiphilic PEG-b-PU linear diblock copolymers with different sequence lengths of PEG and PU was prepared *via* the AROP of 5-membered cyclic carbamate monomer (CHU) in the presence of mPEG based

macromolecular co-initiators (mPEG-CHU). Three types of mPEG-CHU with different molecular weights of PEG were synthesized successfully by esterification between mPEG-OH and carboxylic acid functionalized CHU (CHU-COOH). Two PEG_{12}-*b*-PU diblock copolymers and two PEG_{22}-*b*-PU diblock copolymers with different hydrophilic ratios were chosen for the self-assembly study using the nanoprecipitation technique. Cryo-EM characterizations showed that PEG_{12}-*b*-PU_{14} diblock copolymer with a hydrophilic ratio of 17.7% could self-assemble into vesicles with irregular shapes. SEM and cryo-EM characterizations showed that PEG_{22}-*b*-PU_{26} diblock copolymer with a hydrophilic ratio of 17.9% could self-assemble into solid micelles with polygonal morphologies. The self-assemblies of the PEG_{12}-*b*-PU_8 copolymer with a hydrophilic ratio of 26.1% and the PEG_{22}-*b*-PU_{10} copolymer with a hydrophilic ratio of 34.5% were spherical solid micelles. In addition, the self-assemblies of the two PEG_{22}-*b*-PU diblock copolymers could emit strong cyan fluorescence when they were excited by UV light. Also, the self-assemblies of the PEG_{22}-*b*-PU_{26} copolymer with a hydrophilic ratio of 17.9% emitted stronger fluorescence than those of the PEG_{22}-*b*-PU_{10} copolymer with a hydrophilic ratio of 34.5%. In summary, these prepared PEG-*b*-PU linear diblock copolymers could self-assemble into nanoparticles that could emit fluorescence, which might have potential applications for drug delivery and bioimaging.

References

1. Riess, G.; Hurtrez, G.; Bahadur, P. Block copolymers, In *Encyclopedia of polymer science and engineering* (second edition), vol. 2, Wiley, New York, **1985**, pp. 324-434.

2. Riess, G. *Prog. Polym. Sci.* **2003**, *28*, 1107-1170.

3. Mai, Y.; Eisenberg, A. *Chem. Soc. Rev.* **2012**, *41*, 5969-5985.

4. Karayianni M.; Pispas, S. In *Fluorescence Studies of Polymer Containing Systems*, edited by K. Procházka, Springer International Publishing, **2016**, pp. 27-63.

5. Zhang, L.; Eisenberg, A. *J. Am. Chem. Soc.* **1996**, *118*, 3168-3181.

6. Feng, H. B.; Lu, X. Y.; Wang, W. Y.; Kang, N. G.; Mays, J. W. *Polymers* **2017**, *9*, 494.

7. Hawker, C.J.; Wooley, K.L. *Science* **2005**, *309*, 1200-1205.

8. Wang, J.-S.; Matyjaszewski, K. *J. Am. Chem. Soc.* 1995, 117, 5614-5615.

9. Chiefari, J.; Chong, Y. K.; Ercole, F.; Krstina, J.; Jeffery, J.; Le, T. P. T.; Mayadunne, R. T. A.; Meijs, G. F.; Moad, C. L.; Moad, G.; Rizzardo, E.; Thang, S. H. *Macromolecules* **1998**, *31*, 5559-5562.

10. Georges, M. K.; Veregin, R. P. N.; Kazmaier, P. M.; Hamer, G. K. *Macromolecules* **1993**, *26*, 2987-2988.

11. Braunecker, W.A.; Matyjaszewski, K. *Prog. Polym. Sci.* **2007**, *32*, 93-146.

12. Wei, X. W.; Gong, C. Y.; Gou, M. Y.; Fu, S. Z.; Guo, Q. F.; Shi, S.; Luo, F.; Guo, G.; Qiu, L. Y.; Qian, Z. Y. *Int. J. Pharm.* **2009**, *381*, 1-18.

13. Huang, M. H.; Li, S. M.; Hutmacher, D. W.; Schantz, J. T.; Vacanti, C. A.; Braud, C.; Vert, M. *J. Biomed. Mater. Res. A.* **2004**, *69A*, 417-427.

14. Oh, J. K. *Soft Matter* **2011**, *7*, 5096-5108.

15. Wu, X. H.; El Ghzaoui, A.; Li, S. M. *Langmuir* **2011**, *27*, 8000-8008.

16. Steinbach, T.; Wurm F. R. *Angew. Chem., Int. Ed.* **2015**, *54*, 6098-6108.

17. Zhang, S. Y.; Zou, J.; Zhang, F. W.; Elsabahy, M.; Felder, S. E.; Zhu, J. H.; Pochan, D. J.; Wooley, K. L. *J. Am. Chem. Soc.* **2012**, *134*, 18467-18474.

18. Sun, C. Y.; Ma, Y. C.; Cao, Z. Y.; Li, D. D.; Fan, F.; Wang, J. X.; Tao, W.; Yang, X. Z. *ACS Appl. Mater. Interfaces* **2014**, *6*, 22709-22718.

19. Wang, Y. C.; Tang, L. Y.; Li, Y.; Wang, J. *Biomacromolecules* **2009,** *10,* 66-73.

20. Zhou, L.; Zhang, D.; Hocine, S.; Pilone, A.; Trépout, S.; Marco, S.; Thomas, C. M.; Guo, J.; Li, M.-H. *Polym. Chem.* **2017**, *8*, 4776-4780.

21. Venkataraman, S.; Lee, A. L.; Maune, H. T.; Hedrick, J. L.; Prabhu, V. M.; Yang, Y. Y. *Macromolecules* **2013**, *46*, 4839-4846.

22. Bellomo, E. G.; Wyrsta, M. D.; Pakstis, L.; Pochan D. J.; Deming, T. J. *Nat. Mater.* **2004**, *3*, 244-248.

23. Holowka, E. P.; Pochan D. J.; Deming, T. J. *J. Am. Chem. Soc.* **2005**, *127*, 12423-12428.

24. Lin, X.; He X.; Hu, C.; Chen, Y.; Mai, Y.; Lin, S. *Polym. Chem.* **2016**, *7*, 2815-2820.

Chapter IV. Synthesis and self-assembly of polyurethane-based amphiphilic graft copolymers

4.1 Introduction

4.1.1 General introduction of graft copolymers

Graft copolymers, also known as cylindrical polymer brushes or brush-like polymers, are polymers with unique topology.[1] Composed of a high amount of side chains chemically linked to a linear backbone, graft copolymers possess fascinating properties including wormlike conformation, compact molecular dimension and specific chain end effects, in comparison with their linear counterparts with similar molecular weights.[1-3] They can be either flexible or stiff, depending on the grafting density and molecular length of the side chains. Steric repulsions between the densely grafted side chains enhance the stiffness of the main chain, hamper overlapping and entanglement with adjacent macromolecules, and promote ordering.[1]

Brush-like macromolecules are well-known in biology where they are responsible of various significant biological functions. For example, proteoglycans are polyelectrolyte brush-like macromolecules consisting of a protein backbone with numerous carbohydrate side chains. They are able to perform several functions including cell signaling, cell surface protection, joint lubrication and lung clearance.[4,5] Inspired by nature, development of artificial brush-like macromolecules to explore their potential functionalities and properties is important and necessary. Studies on graft copolymers have attracted much interest, and are mainly focused on the control of molecular structures, the understanding of the relationship between architectures and distinctive properties, and their potential applications.[6-8]

Three main strategies were developed to synthesize graft copolymers: "grafting onto" (the addition of previously prepared side chains to a backbone), "grafting through" (the polymerization of macromonomers) and "grafting from" (the polymerization of side chains with the linear main chain as the macroinitiator), as shown in Figure 4.1.[1] Below will be introduced briefly the three different synthetic strategies as well as examples of

self-assembly of amphiphilic graft copolymers. Particular attention will be paid to the "grafting onto" strategy as the synthesis of our amphiphilic PU-*g*-PEG graft copolymers will be based on this strategy.
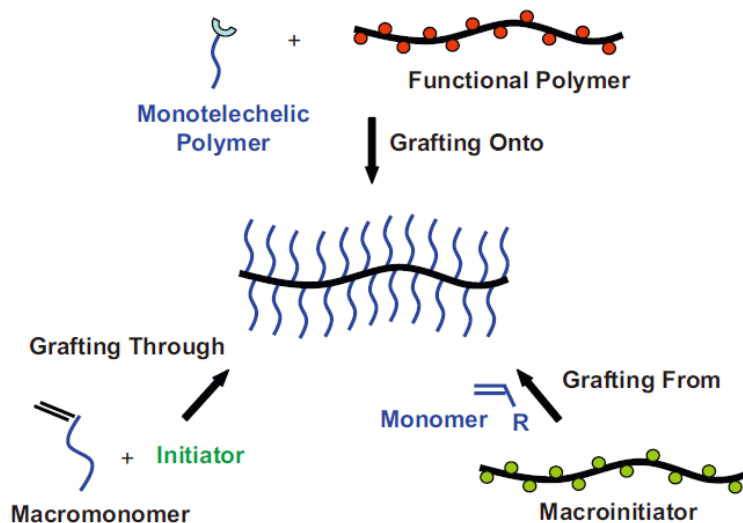

Figure 4.1. Three main strategies developed to synthesize graft copolymers.[1]

4.1.2 Synthetic strategies of graft copolymers

4.1.2.1 Grafting onto strategy

The "grafting onto" strategy is based on the coupling reaction of end-functionalized polymers with a linear polymer backbone precursor containing complimentary functionality on each repeating unit. In this strategy, both the linear polymer backbone and side chains are prepared in advance and their chain lengths and structures can be easily tuned. However, the removal of unreacted side chains and highly efficient coupling methods such as nucleophilic substitution and click-type coupling reactions are required for preparing graft copolymers with high grafting densities and narrow molecular weight distributions.[2]

As one of the most efficient click-type coupling reactions, copper-catalyzed azide-alkyne cycloaddition (CuAAC) reaction has been widely used in the synthesis of graft copolymers through the reaction of polymer backbone and side chains bearing the two complimentary functional groups.[9,10] For example, Matyjaszewski and coworkers have reported a "grafting onto" strategy to graft copolymers by the combination of ATRP and
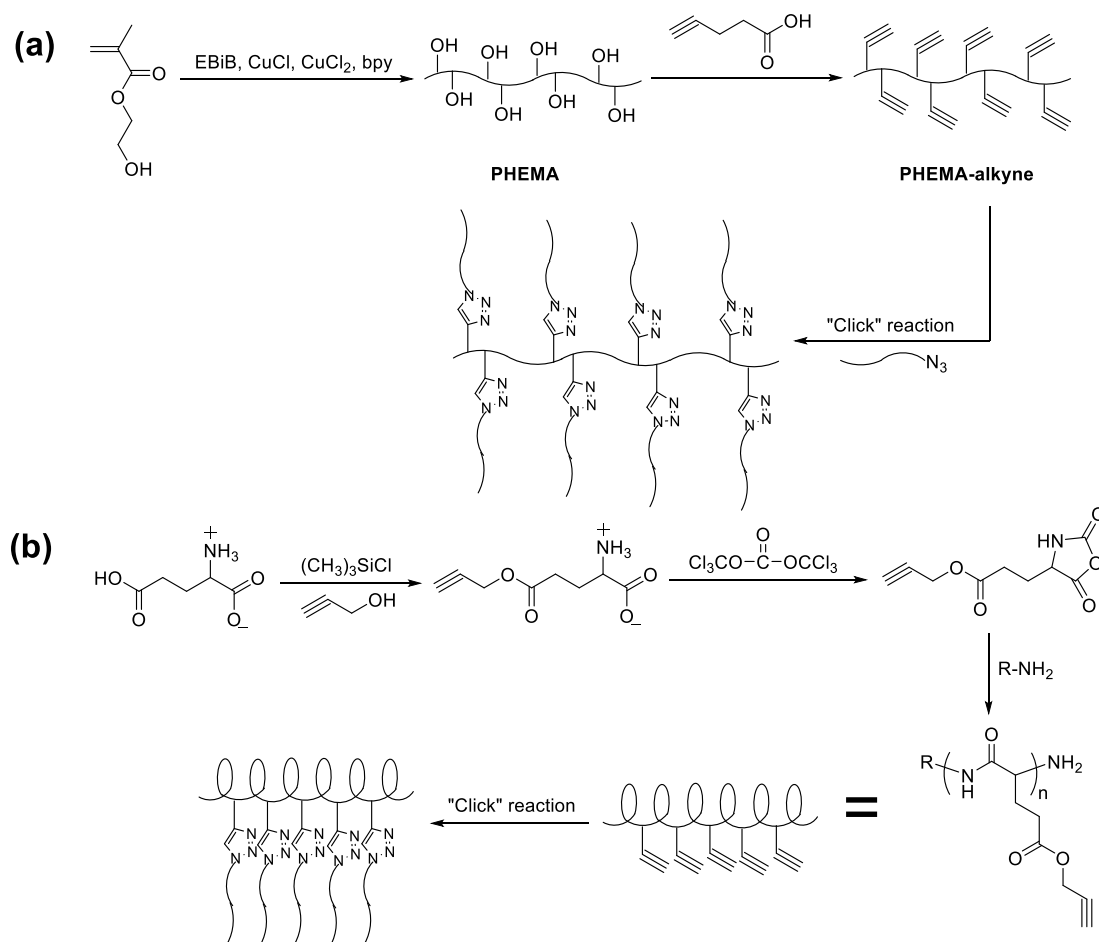
Figure 4.2. Synthesis of graft copolymers (a) containing PEG, PS, PBA and PBA-b-PS side chains; (b) consisting of PPLG backbone and PEG side chains through a CuAAC "click" reaction.[11,12]

CuAAC as shown in Figure 4.2a.[11] Alkynyl side groups were attached to each repeating unit by esterification of poly(2-hydroxymenhyl methacrylate) (PHEMA) backbone, previously prepared by ATRP. Different azido-terminated side chains such as poly(ethylene glycol)-N$_3$ (PEG-N$_3$), polystyrene-N$_3$ (PS-N$_3$), poly(n-butyl acrylate)-N$_3$ (PBA-N$_3$) and poly(n-butyl acrylate)-b-polystyrene-N$_3$ (PS-b-PBA-N$_3$) were connected to the PHEMA backbone to prepare graft copolymers by reacting alkynyl groups on the backbone with azido groups on the side chains. The authors observed that the grafting densities of the obtained graft copolymers depended on the chemical structures of side chains. For bulky side chains such as PS, PBA and PBA-b-PS, grafting densities were lower than 50% since the steric hindrance of linked side chains blocked the diffusion

of unreacted side chains to the reactive sites on the backbone. By contrast, for less sterically encumbered PEG chains, grafting density reached up to 88.4%.[11]

Hammond and coworkers have reported the synthesis of graft copolymers consisting of poly(γ-propargyl-L-glutamate) (PPLG) backbone and PEG side chains through the combination of ROP of *N*-carboxyanhydrides and CuAAC reaction (Figure 4.2b).[12] The authors found that the alkynyl groups on the backbone protruded outward due to the rigid α-helical structure of the PPLG backbone, which increased their reactivity with the azido groups on PEG side chains. As a result, nearly perfect grafting densities ranging from 95.8% to 98.9% were achieved.
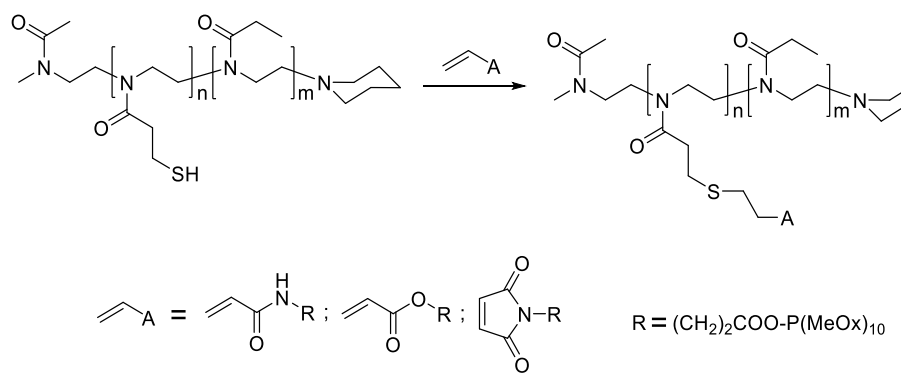
Figure 4.3. Synthesis of poly(2-oxazoline) based graft copolymers through the thiol-ene coupling reaction.[14]

Thiol-ene coupling reaction is a highly efficient "click" reaction between an alkene and a thiol to form an alkyl sulfide. It can proceed by a radical-mediated or a base/nucleophile-initiated process under various conditions without any metal catalyst.[13] Moreover, this kind of coupling reaction is usually tolerant to the presence of air/oxygen, moisture and various functional groups, exhibits extremely rapid reaction rate and can form the corresponding thioether in a quantitative and regioselective fashion.[13] Therefore, it has been used for the synthesis of graft copolymers based on the "grafting onto" strategy. For example, Nuyken and coworkers have reported the synthesis of poly(2-oxazoline) based graft copolymers through the thiol-ene coupling reaction (Figure 4.3).[14] They firstly synthesized poly[2-(4-methoxybenzylsulfanyl)ethyl-2-oxazoline]-*co*-poly-(ethyl-2-oxazoline) biocompatible

copolymers with different molecular weights and functional group densities *via* the cationic ROP of 2-oxazoline based monomers. After a quantitative deprotection to form pendant thiol groups along the backbone, a thiol-ene coupling reaction can occur between the resulting SH groups and acrylamide or maleimide groups at the end of poly(2-methyl-2-oxazoline)s, therefore allowing the quantitative formation of a series of poly(2-oxazoline) based graft copolymers with different lengths of side chains.[14]

4.1.2.2 Grafting through strategy

The "grafting through" strategy involves the polymerization of macromonomers with a polymerizable end group (Figure 4.1).[15,16] Using this strategy, graft copolymers with well-defined composition and grafting density can be prepared. Meanwhile, by tuning the degree of polymerization of backbone and side chains, graft copolymers with different backbone lengths and side chain lengths can be readily obtained.[2] However, this strategy might suffer from slow polymerization rate and low conversion of monomers due to the necessarily low concentration of polymerizable end groups and high steric hindrance between the propagating chain ends.[1,17] Nonetheless, there have been many successful reports on the preparation of graft copolymers by using this strategy. Different polymerization approaches such as living anionic polymerization, "living" / controlled radical polymerization (CRP), ROP, ROMP, and the combination of them have been utilized.[2]

For example, ROMP was proposed to be an efficient approach for polymerization of macromonomers since the ring strain and large spacing between side chains of the cycloalkenes (such as norbornene) functionalized macromonomers provide a kinetically and thermodynamically favorable environment for polymerization. Grubbs and coworkers have reported the efficient synthesis of narrowly dispersed graft copolymers *via* living ROMP of macromonomers (Figure 4.4).[18] The authors firstly prepared several macromonomers by the copper-catalyzed azide-alkyne ''click'' coupling of a norbornene moiety bearing an alkynyl group to the azido-terminated PS, PMMA and P*t*BA that were prepared *via* ATRP (Figure 4.4). Then ROMP of these

macromonomers were carried out using the highly active, fast-initiating ruthenium

catalyst (H_2IMes)-$(pyr)_2(Cl)_2RuCHPh$ in THF at room temperature, producing a series

of graft copolymers with very narrow PDIs of 1.01-1.07 and high molecular weights of

200-2600 kDa. The ROMP reaction was found to be living with almost quantitative

conversions (> 90%) of the corresponding macromonomers. The authors thought that

the efficient ROMP of these macromonomers overcomes previous difficulties in the

controlled polymerization of macromonomers and provides facile access to the

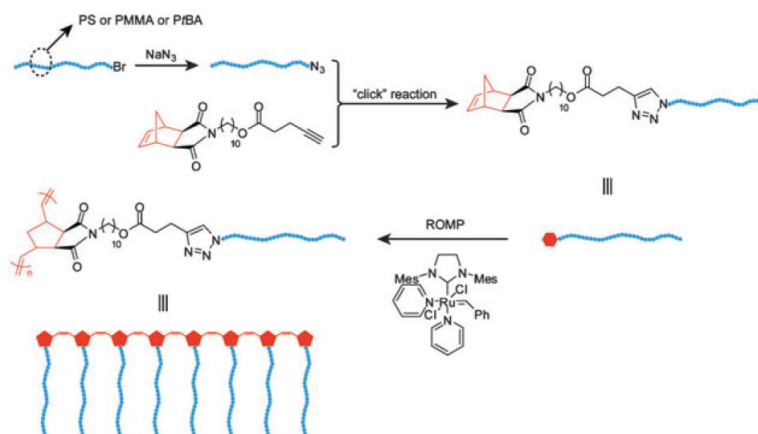synthesis of graft copolymers with various molecular structures.[18]

Figure 4.4. Synthesis of graft copolymers containing PS, P*t*BA and PMMA side chains
by combining ATRP, ''click'' reaction, and ROMP.[18]

4.1.2.3 Grafting from strategy

The "grafting from" strategy for the synthesis of graft copolymers starts with the

preparation of initiation-group-containing backbone polymer (macroinitiator) with a

predetermined number of initiation sites which are subsequently used to initiate the

polymerization of side chains (Figure 4.1). The macroinitiator can be prepared directly

from the polymerization of initiation-group-containing monomers or by the post-

functionalization of backbone polymers with initiating functional groups. In this

strategy, the gradual growth of the side chains alleviates the steric effect which is the

inevitable limitation of either ''grafting onto'' or "grafting through" strategy. Moreover,

the instantaneous concentration of radical species is usually low in grafting from

strategy using the CRP technique, which limits effectively the termination events during

the synthesis of graft copolymers since intramolecular termination can produce pendant macrocycles and intermolecular coupling can lead to macroscopic gelation.[1]

As stated above, the "grafting from" strategy enables preparation of long-backbone graft copolymers with high grafting densities and narrow molecular weight distributions. However, in comparison with the grafting through strategy, the grafting from strategy allows less control of side chain lengths and grafting densities. Both parameters are dependent on the initiation efficiency, as it was reported for the ATRP of BA (butyl acrylate) and MMA (methyl methacrylate) monomers from a poly(2-2-bromopropionyloxy(ethyl methacrylate)) (PBPEM) macroinitiator backbone.[19,20]

4.1.3 Self-assembly of amphiphilic graft copolymers

Amphiphilic graft copolymers consisting of immiscible linear backbone and pendant side chains are interesting polymer architectures for self-assembly studies. Compared to the linear block copolymers, graft copolymers exhibit distinct self-assembly behavior due to the effect of grafting densities and molecular lengths of side chains.[2] For example, graft copolymers present spherical molecule shape, when the length of backbone is similar to the one of the side chains; or wormlike shape, when the length of backbone is significantly longer than the one of the side chains.[2] Therefore, it is important to study the self-assembly of graft copolymers, especially amphiphilic graft copolymers, to precisely explore the relationship between complex architectures and the corresponding properties as well as the potential applications.

Lin and coworkers have reported the self-assembly of amphiphilic poly(γ-benzyl-L-glutamate)-g-poly(ethylene glycol) (PBLG-g-PEG) graft copolymers containing rigid polypeptide backbone and soft PEG side chains, which were synthesized by the transesterification of PBLG with mPEG-OH (M_w = 750 Da) (Figure 4.5a).[21] The self-assembly technique they used was nanoprecipitation and the initial common solvent was removed by dialysis against deionized water. The authors observed that the grafting density of PEG chains and the nature of the initial common solvent played an important role on the self-assembly behavior of PBLG-g-PEG graft copolymers. When THF was

used as the initial solvent, vesicles were formed by the graft copolymers with lower grafting density and the aggregate morphology transformed from vesicles to spindle-like micelles then to spherical micelles with the increasing of grafting density of the PBLG-*g*-PEG graft copolymers. The authors also found that when DMF (*N,N'*-dimethylformamide) was introduced into the initial solvent, the vesicles also transformed into spindles and increasing the fraction of DMF in the initial solvent led to a spindle to connected-spindle transition (Figure 4.5b). They claimed that the obtained polypeptide-based polymeric aggregates, especially the vesicles, might be potential drug carriers.[21]
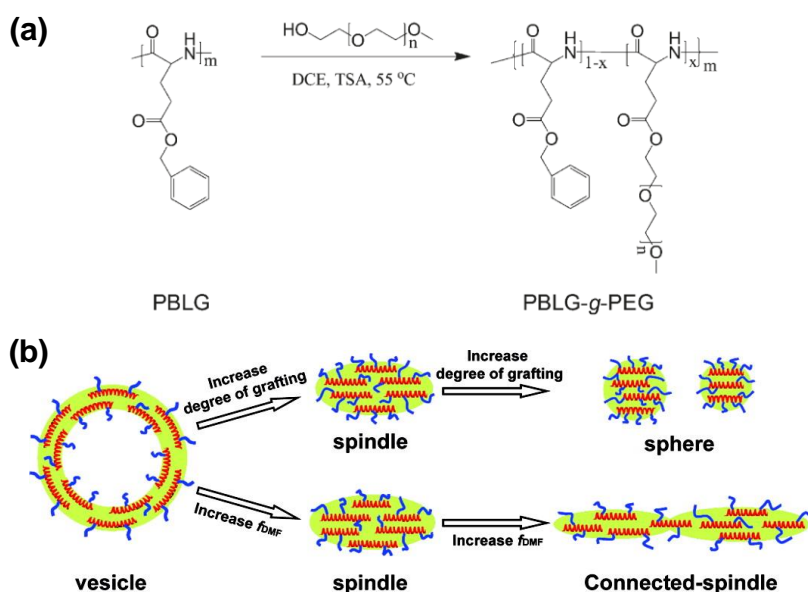

Figure 4.5. (a) Synthesis of PBLG-*g*-PEG graft copolymer by ester exchange reaction. DCE: 1,2-dichloroethane; TSA: *p*-toluenesulfuric acid. (b) Schematic representation of the morphology transition from vesicles to spindles, and then to spheres.[21]

Six and coworkers have reported the synthesis and self-assembly of amphiphilic Dextran-g^N-poly(diethylene glycol cholesteryl ether acrylate)^F (Dex-g^N-PDEGCholA^F, N and F are the number of PDEGCholA grafts per 100 glucopyranosic units of dextran backbone and the weight fraction of PDEGCholA in glycopolymer separately) graft glycopolymers (Figure 4.6).[22] In these graft copolymers, dextran was the hydrophilic polysaccharidic backbone and PDEGCholA was the hydrophobic side chains with

liquid crystalline property. They were synthesized by the ATRP of DEGCholA monomers using the initiation-group-containing dextran as the macroinitiator. The self-assembly was performed using the nanoprecipitation technique and the initial good solvent (THF or DMSO) was removed by dialysis against deionized water.

The authors found that the self-assembly behaviors of these graft glycopolymers depended on the number and length of the grafted PDEGCholA chains. For copolymers with a high number of short PDEGCholA chains, only precipitates were formed during the dialysis process. While for copolymers with a moderate number of long PDEGCholA chains, nanoobjects were produced. Cryo-EM characterizations showed that these nanoobjects were polymersomes with a hollow vesicular structure (Figure 4.6b). These results seemed to indicate that a moderate number of long PDEGCholA chains allowed a suitable copolymer folding and formation of a bilayer membrane, which was stabilized due to the liquid-crystal properties of PDEGCholA chains.[22]
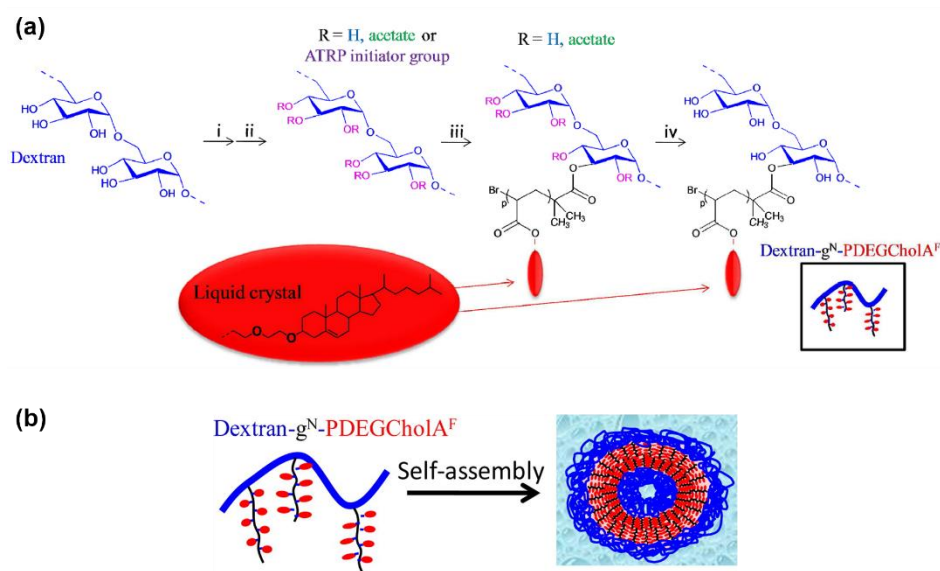
Figure 4.6. (a) Synthesis of amphiphilic Dex-g^N-PDEGCholA^F graft glycopolymers using a "grafting from" strategy. (b) Schematic illustration of the self-assembly of graft glycopolymers into polymersomes.[22]

Huang and coworkers have reported the self-assembly of an amphiphilic graft copolymer containing poly(6-methyl-1,2-heptadien-4-ol) (PMHDO) backbone and PEG side chains.[23] The graft copolymers were synthesized by a grafting onto strategy

through the coupling reaction between PMHDO homopolymer with pendant hydroxy
groups and acyl chloride-terminated mPEG with DMAP as the catalyst. The self-
assembly was carried out using the nanoprecipitation technique and the initial common
solvent THF was removed by dialysis against deionized water. Diverse micellar
morphologies including spheres, cylinders, spirally twisted cylinders, wormlike
micelles and super-rings were observed by changing the water content, the initial
copolymer concentration in THF and the ion strength (Figure 4.7). Particularly, the
authors found that chiral helical twisted cylinders were formed under given conditions,
even though no chiral center was present on the PMHDO-*g*-PEG graft copolymer. The
presence of a chiral source was further confirmed by CD spectrum characterization of
the corresponding self-assembly solution, which showed a strong peak at 227 nm
attributed to the double bond on the PMHDO backbone (Figure 4.7D). The authors
thought that the rigid "perpendicular" double bonds on the backbone might force the
backbone into an isotactic and/or a syndiotactic configuration (Figure 4.7E).
Meanwhile, a specific THF/water mixture (33 wt% of water) can be used as a
solvophobic solvent to help the PMHDO backbone keeping the helical conformation.
As a result, the formation of ribbon-like cylinders was induced by these factors.[23]
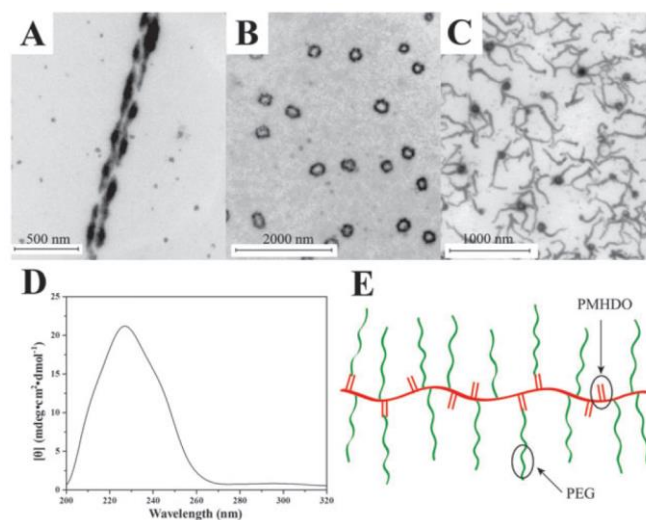

Figure 4.7. TEM images of aggregates formed by PMHDO$_{45}$-*g*-PEG$_{125}$ copolymers
with different water contents, (A) 33 wt%, (B) 25 wt%, and (C) 63 wt%; (D) CD
spectrum of the self-assembly solution of PMHDO$_{45}$-*g*-PEG$_{125}$ with a water content of
33 wt%; (E) schematic illustration of the molecular structure of PMHDO-*g*-PEG.[23]

4.2 Research subjects

We have prepared amphiphilic PU-*g*-PEG graft copolymers *via* the thiol-ene coupling reaction of PU homopolymers with pendant double bonds that were prepared by AROP of the 5-membered cyclic carbamate monomer (CHU) and thiol-terminated mPEG (mPEG-SH) based on a grafting onto strategy. mPEG-SH was prepared by esterification of mPEG-OH (M_n = 550 Da) with thioglycolic acid. Two types of PU-*g*-PEG graft copolymers with different backbone lengths and hydrophilic ratios were obtained. The critical micelle concentration (CMC) of the amphiphilic PU-*g*-PEG graft copolymers in water was measured by fluorescence technique since the aqueous solution of the PU-*g*-PEG graft copolymers could emit fluorescence (excited by UV light) and the fluorescence behavior changed along with micellization.[24-26] The self-assembly of PU-*g*-PEG copolymers was performed using the nanoprecipitation technique. The obtained self-assemblies were carefully characterized by DLS (dynamic light scattering), fluorescence microscopy, SEM (scanning electron microscopy) and cryo-EM (cryo-electron microscopy).

4.3 Results and Discussion

4.3.1 Synthesis of thiol-terminated mPEG (mPEG-SH)

Thiolation of linear poly(ethylene glycol) monomethyl ether with a molecular weight of 550 Da ($mPEG_{12}$-OH) was carried out by reaction with thioglycolic acid using sulfuric acid as the catalyst (Figure 4.8). The water produced in the reaction was removed by azeotropic distillation with toluene to force the chemical equilibrium to the product side. Pure mPEG-SH was then obtained by recrystallization of the crude product from a THF/diethyl ether mixture, as confirmed by the ^{1}H NMR spectrum (Figure 4.8).

We can distinguish two resonances at 2.02 and 3.29 ppm, which were attributed to the thioglycolyl end group. In addition, the appearance of a triplet signal at δ 4.28 ppm (peak c, Figure 4.8) attributed to protons of CH_2 group indicated the formation of ester bond. The singlet signal at δ 3.37 ppm (peak a, Figure 4.8) was attributed to the methyl

group at the other chain end of mPEG$_{12}$-SH. The degree of functionalization of the obtained mPEG-SH could then be calculated by comparing the integration area of peak d with the one of peak a in the ^{1}H NMR spectrum of mPEG$_{12}$-SH, and was determined to be approximately 99%.
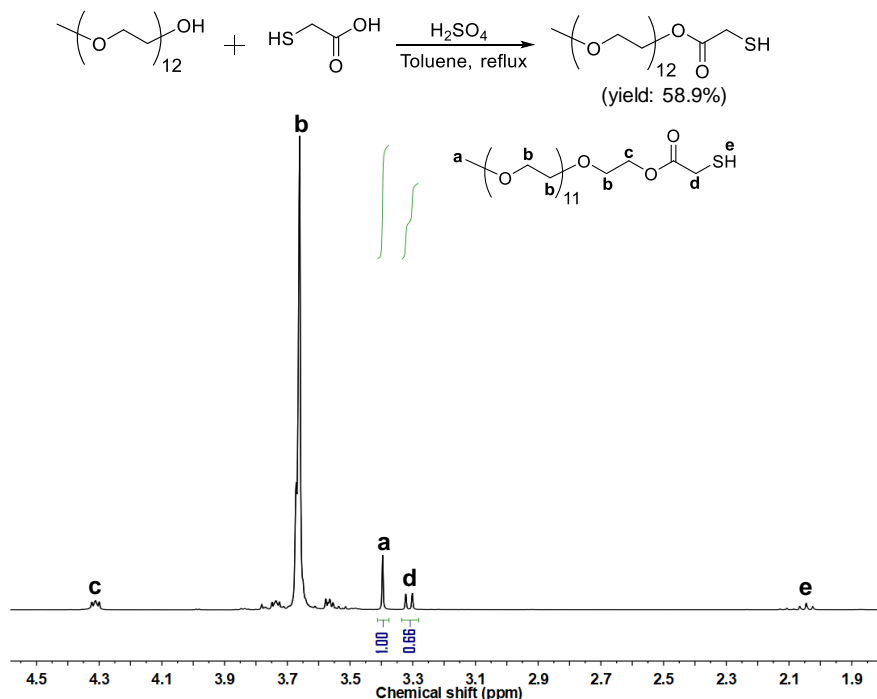

Figure 4.8. Synthetic scheme and ^{1}H NMR spectrum of mPEG$_{12}$-SH.

The prepared mPEG-SH was not air stable since the oxidative coupling reaction between two thiol groups at the chain end of PEG could produce PEG-S-S-PEG side product,[24] which was unfavorable for the next thiol-ene coupling reaction to prepare PU-*g*-PEG graft copolymers. Therefore, the prepared mPEG-SH needed to be used rapidly or stored carefully under inert conditions and darkness.

4.3.2 Synthesis of amphiphilic PU-*g*-PEG graft copolymers

The amphiphilic PU-*g*-PEG graft copolymers were prepared by the radical-mediated thiol-ene reaction of a linear PU homopolymer functionalized with vinyl groups and mPEG-SH, using a grafting onto strategy (Figure 4.9). The PU homopolymer was prepared *via* the AROP method as described in the second chapter. The thiol-ene coupling reaction was performed using 2,2'-azobis(isobutyronitrile) (AIBN) as the

radical initiator in THF at 65 °C. Excess mPEG-SH (4-fold molar of the vinyl groups
on PU chains) was added to the reaction mixture in order to obtain high grafting density
of PEG chains and avoid possible cross-linking reaction caused by radical coupling.
After completion of the reaction, the crude product was purified by dialysis against
ethanol in a 3500 Da cut off cellulose bag for 5 days to remove unreacted mPEG-SH,
and the ethanol solution was changed twice a day.

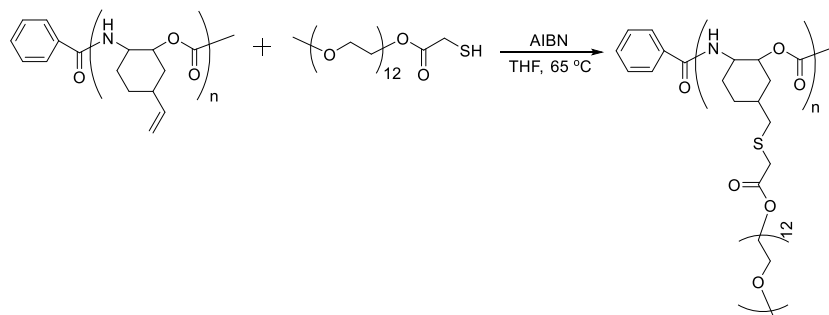**Figure 4.9**. Synthesis of amphiphilic PU-*g*-PEG graft copolymers *via* the thiol-ene
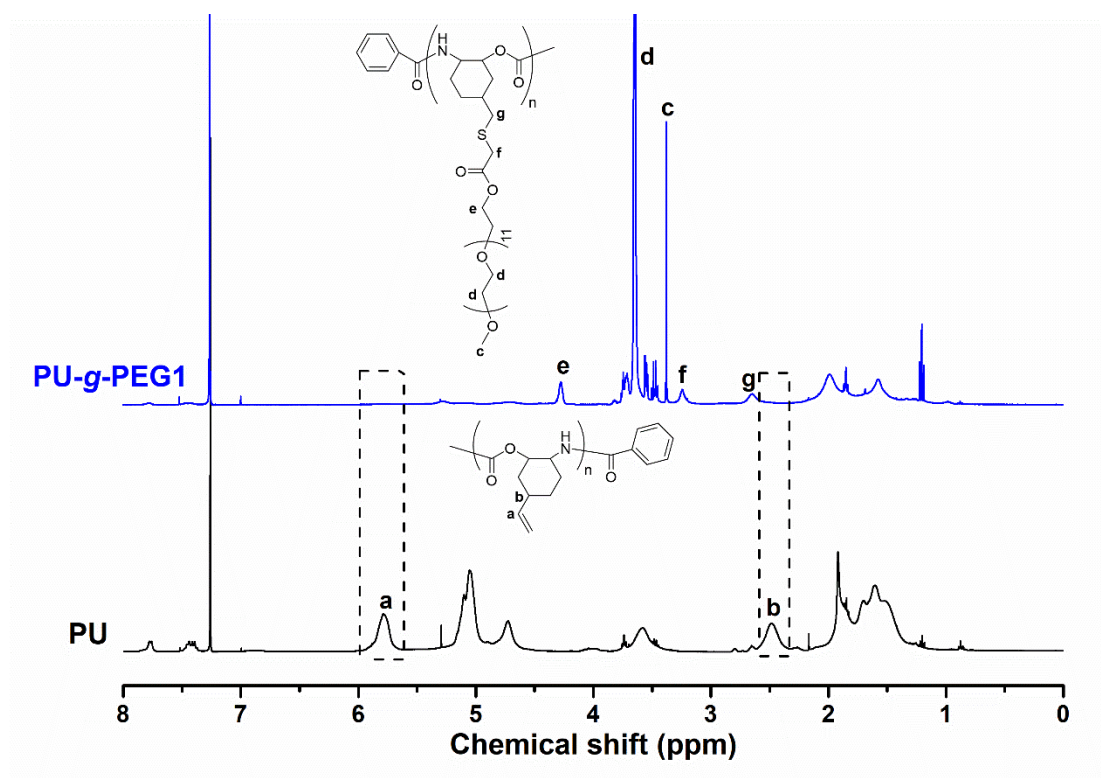coupling reaction. PU was prepared by AROP of CHU monomer.

Figure 4.10. ^{1}H NMR spectra of the amphiphilic graft copolymer PU-*g*-PEG1 and PU
backbone.

The pure product was carefully characterized by ^{1}H NMR spectroscopy and GPC (Figure 4.10 and 4.11). By comparing the ^{1}H NMR spectra of PU and PU-*g*-PEG, the proton signals at δ 5.78 (peak a) and 2.48 ppm (peak b) attributed respectively to "CH" groups on the vinyl moiety and cyclohexane completely disappeared after the reaction (Figure 4.10). This result indicated that the grafting ratio of PEG side chains was 100%. In addition, new ^{1}H resonances at δ 4.28 ppm (peak e), 3,64 ppm (peak d), 3.37 ppm (peak c), 3.24 ppm (peak f) and 2.64 ppm (peak g) appeared on the ^{1}H NMR spectrum of the obtained PU-*g*-PEG product, which were assigned to the protons of the PEG side chains. Finally, the GPC curve of PU-*g*-PEG showed a unimodal distribution and the retention time shifted to the left compared to the GPC curve of PU (Figure 4.11). All these characterization results confirm that pure amphiphilic graft copolymer PU-*g*-PEG with high grafting density was obtained by the thiol-ene coupling reaction of PU and mPEG-SH.
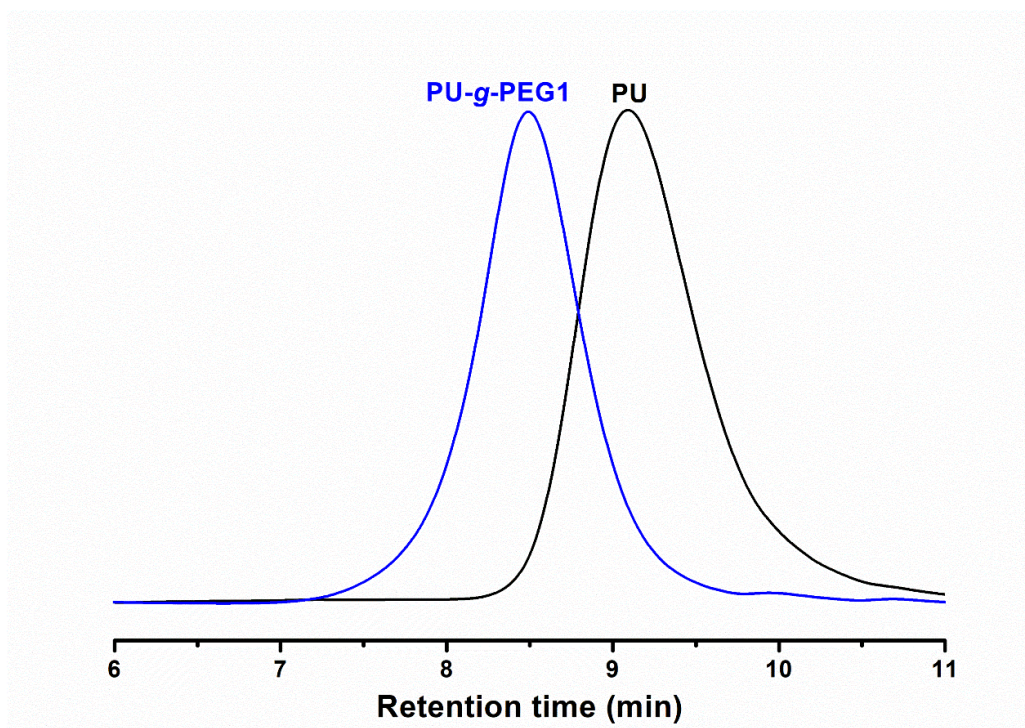

Figure 4.11. GPC traces of the amphiphilic graft copolymer PU-*g*-PEG1 and PU backbone with THF as the eluent.

Based on this grafting onto strategy, two amphiphilic PU-*g*-PEG copolymers with different backbone lengths and molecular weights were prepared by using PU with different molecular weights. Consequently, the resulting PU-*g*-PEG copolymers showed different self-assembly behaviors in water, as described below. Their molecular weights and molecular weight distributions are listed in Table 4.1.

Table 4.1. Synthesis of PU based amphiphilic graft copolymer PU-*g*-PEG with 100% grafting density.

Sample[a]	DP of PU[b]	$M_{n,PU}$[b]	M_n[b]	PDI[c]	$f_{PEG,wt\%}$
PU-*g*-PEG1	14	2400	13600	1.41	56.6%
PU-*g*-PEG2	24	4000	19100	1.60	69.1%

a. All the graft copolymers were synthesized through the thiol-ene coupling reaction between PU and mPEG$_{12}$-SH in THF at 65 °C; reaction time: 24 h; Purification: dialysis against ethanol for 5 days.

b. Conversion of monomers, degree of polymerization (DP) and M_n were calculated by ^{1}H NMR;

c. PDI was obtained by GPC with THF as eluent and PS as standards.

4.3.3 Self-assembly of amphiphilic PU-*g*-PEG graft copolymers

Since the obtained PU-*g*-PEG copolymers have relatively high hydrophilic ratios (Table 4.1), they might have good solubility in water if their concentrations are not high. Therefore, it is possible to measure their critical micelle concentration (CMC) by following the change of the properties of the polymer solution along with concentration increase. The common CMC measurement method is to look for the intersection or crossover region of some measured properties of amphiphilic molecules including electrical conductivity, surface tension, absorption, NMR chemical shifts, self-diffusion coefficients, fluorescence intensity *versus* the molecular concentration.
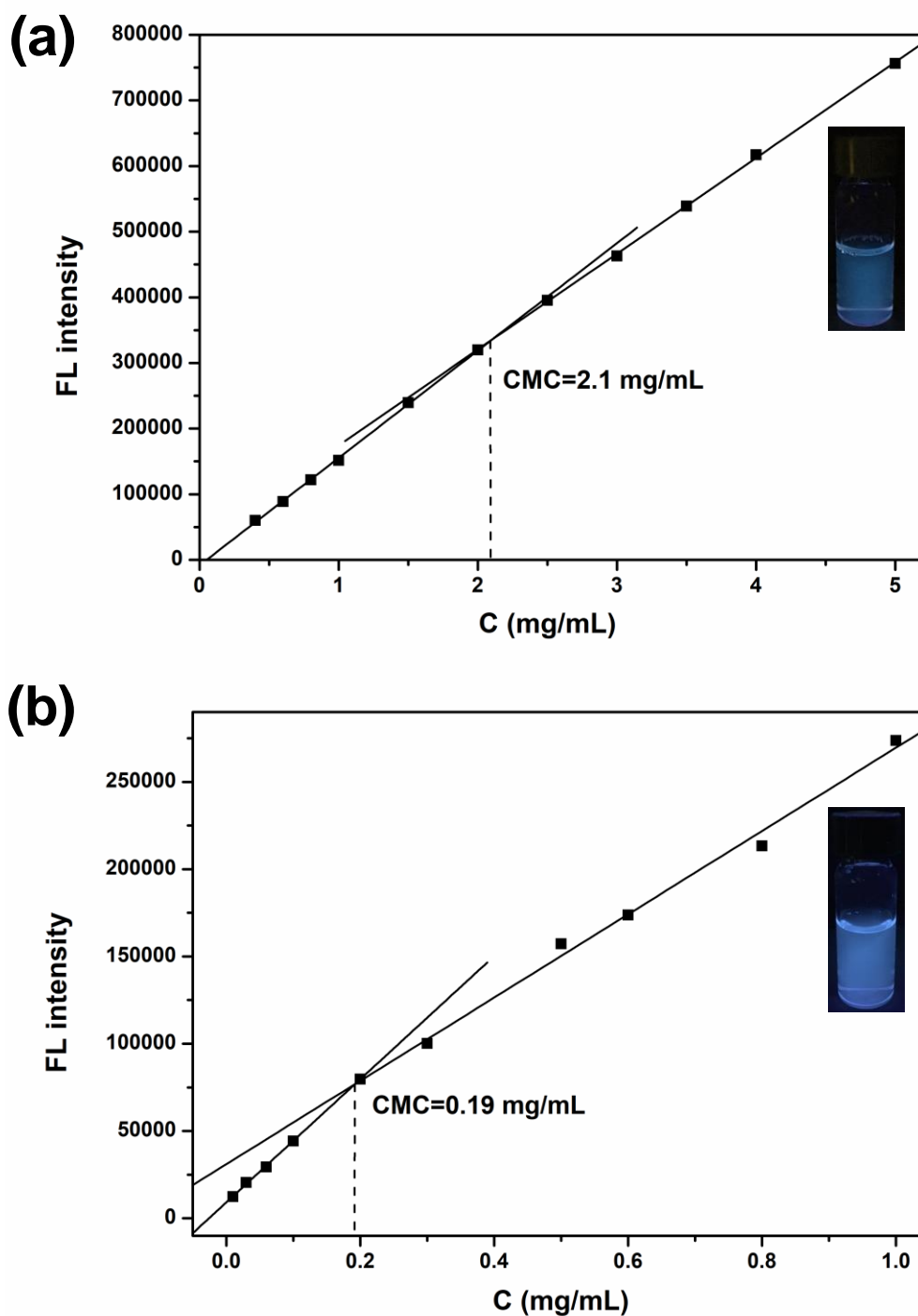
Figure 4.12. CMC measurements of amphiphilic graft copolymers by fluorescence technique. (a) Plot of fluorescence intensity at 403 nm *versus* the concentration of PU-*g*-PEG1 in water (λ_{ex} = 327 nm); (b) Plot of fluorescence intensity at 418 nm *versus* the concentration of PU-*g*-PEG2 in water (λ_{ex} = 323 nm). The insets in (a) and (b) are the photographs of the aqueous solution of PU-*g*-PEG copolymers with a concentration of 2 mg/mL under UV light (λ = 365 nm).

Here, we chose the fluorescence technique to measure the CMCs of PU-*g*-PEG graft copolymers since their aqueous solution could emit fluorescence when excited by UV light. Firstly, the excitation and emission spectra of the aqueous solution of the two PU-*g*-PEG graft copolymers were characterized by fluorescence spectroscopy. For PU-*g*-PEG1, the maximum excitation and emission wavelengths of its aqueous solution are 327 nm and 403 nm, respectively. For PU-*g*-PEG2, the maximum excitation and emission wavelengths of its aqueous solution are 323 nm and 418 nm, respectively. Then we measured the variation of fluorescence intensity at maximum emission wavelength of the aqueous solution of PU-*g*-PEG copolymers *versus* the concentrations under the same characterization conditions (Figure 4.12).

Figure 4.12a showed the plot of fluorescence intensity at 403 nm *versus* the concentration of PU-*g*-PEG1 in water (λ_{ex} = 327 nm). We can see that the fluorescence intensity of the PU-*g*-PEG1 aqueous solution increased gradually as the PU-*g*-PEG1 concentration increased. One intersection appeared at around 2.1 mg/mL, which indicated a change in the aggregation state from surfactant unimers to micelles. The possible reason of the slope decrease after the intersection might be due to the environment changes of PU-*g*-PEG molecules, that is, from single molecules surrounded by water molecules to aggregates surrounded by copolymer molecules. So, the luminescent property like the fluorescence intensity also changed.

Based on the intersection of the fluorescence intensity-concentration plot, we obtained the CMC of PU-*g*-PEG1 graft copolymer in water, which was 2.1 mg/mL. For PU-*g*-PEG2, plot of fluorescence intensity at 418 nm *versus* the concentration of PU-*g*-PEG2 in water (λ_{ex} = 323 nm) showed intersection at around 0.19 mg/mL (Figure 4.12b), which represented the CMC of PU-*g*-PEG2 in water. The CMC of PU-*g*-PEG2 was lower than the one of PU-*g*-PEG1, although the hydrophilic ratio of PU-*g*-PEG2 (69.1%) was higher than the one of PU-*g*-PEG1 (56.6%). The reason might be that PU-*g*-PEG2 had a longer linear PU backbone (M_n = 4000 Da) than PU-*g*-PEG1 (M_n = 2400 Da), which had a greater influence on the CMC of PU-*g*-PEG graft copolymers than the hydrophilic ratios.

After CMC measurements of the two PU-*g*-PEG graft copolymers, their self-assembly in water was carried out by using the nanoprecipitation technique. In a typical self-assembly experiment, PU-*g*-PEG was firstly dissolved in THF (concentration 3.5 mg/mL for PU-*g*-PEG1 and 1 mg/mL for PU-*g*-PEG2), which was a good solvent for both PEG and PU. Then deionized water was added gradually (around 0.5 uL/min) until it reached 50 wt% of the whole solution. The solution was shaked gently during the addition of water. THF was then removed by dialysis against deionized water for 3 days in a 3500 Da cut off cellulose bag. Finally, the aqueous solution of the self-assemblies of PU-*g*-PEG1 with a concentration of about 3 mg/mL and PU-*g*-PEG2 with a concentration of about 0.8 mg/mL in the dialysis bag was collected.
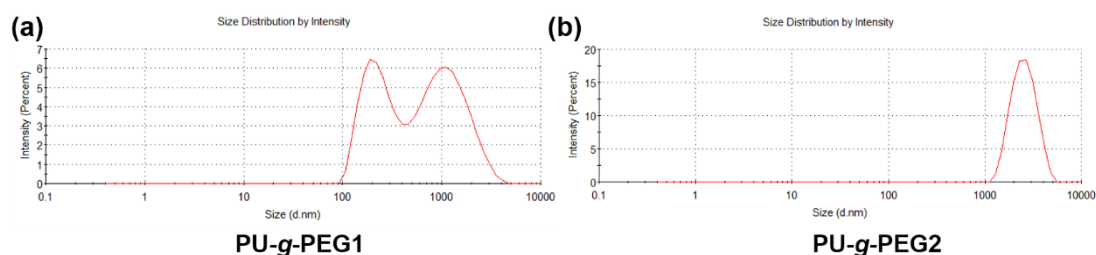

Figure 4.13. DLS characterizations of the self-assemblies of PU-*g*-PEG1 (a) and PU-*g*-PEG2.

The self-assemblies of the two PU-*g*-PEG samples were characterized carefully by DLS, SEM and cryo-EM. The DLS characterization results are shown in Figure 4.13. We can observe that there are two types of size distributions for the self-assemblies of PU-*g*-PEG1 graft copolymer, while there is only one type of size distributions for the self-assemblies of PU-*g*-PEG2 graft copolymer. The hydrodynamic diameters (D_h) of the two types of nanoparticles of PU-*g*-PEG1 were about 240 nm and 1230 nm, respectively. For PU-*g*-PEG2, D_h of the nanoparticles was around 2.6 μm, which suggested that the obtained self-assemblies had a relatively large size.

The morphology of the self-assemblies of PU-*g*-PEG1 ($f_{wt\%} = 56.6\%$) copolymer was characterized by SEM and cryo-EM (Figure 4.14). SEM images (Figure 4.14a, b) showed that micelles with rough surface were obtained. The diameter of the formed micelles varied from 500 nm to 4 μm. Cryo-EM images (Figure 4.14c, d) also showed

micelles with different sizes and the shape of the observed micelles was not spherical. The observed surface also seemed to be rough. All these results may suggest that the PU-*g*-PEG1 graft copolymer firstly self-assembled into small micelles with diameters around dozens of nanometers and then large micelles were formed by aggregation of the small micelles, which resulted in the rough and irregular surface of the large micelles.
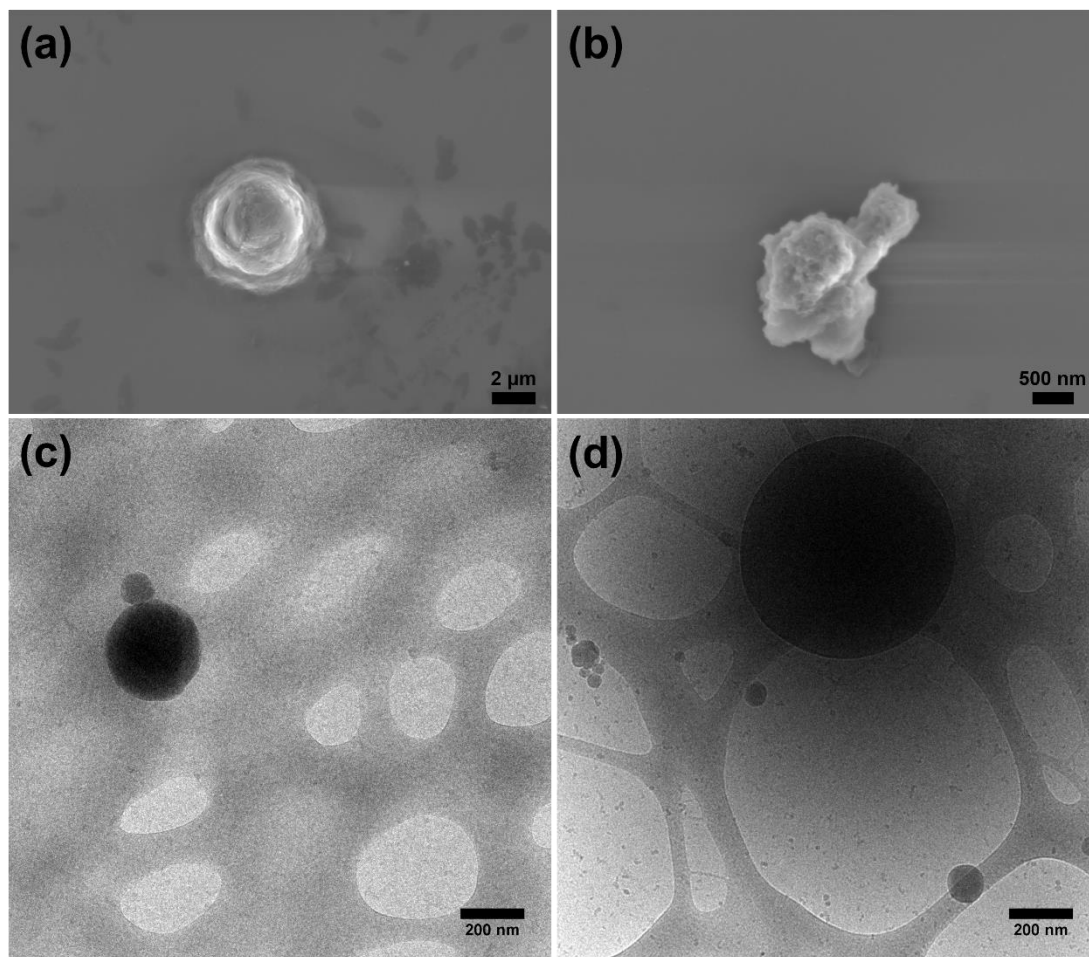

Figure 4.14. SEM (a, b) and cryo-EM (c, d) images of the self-assemblies of PU-*g*-PEG1.

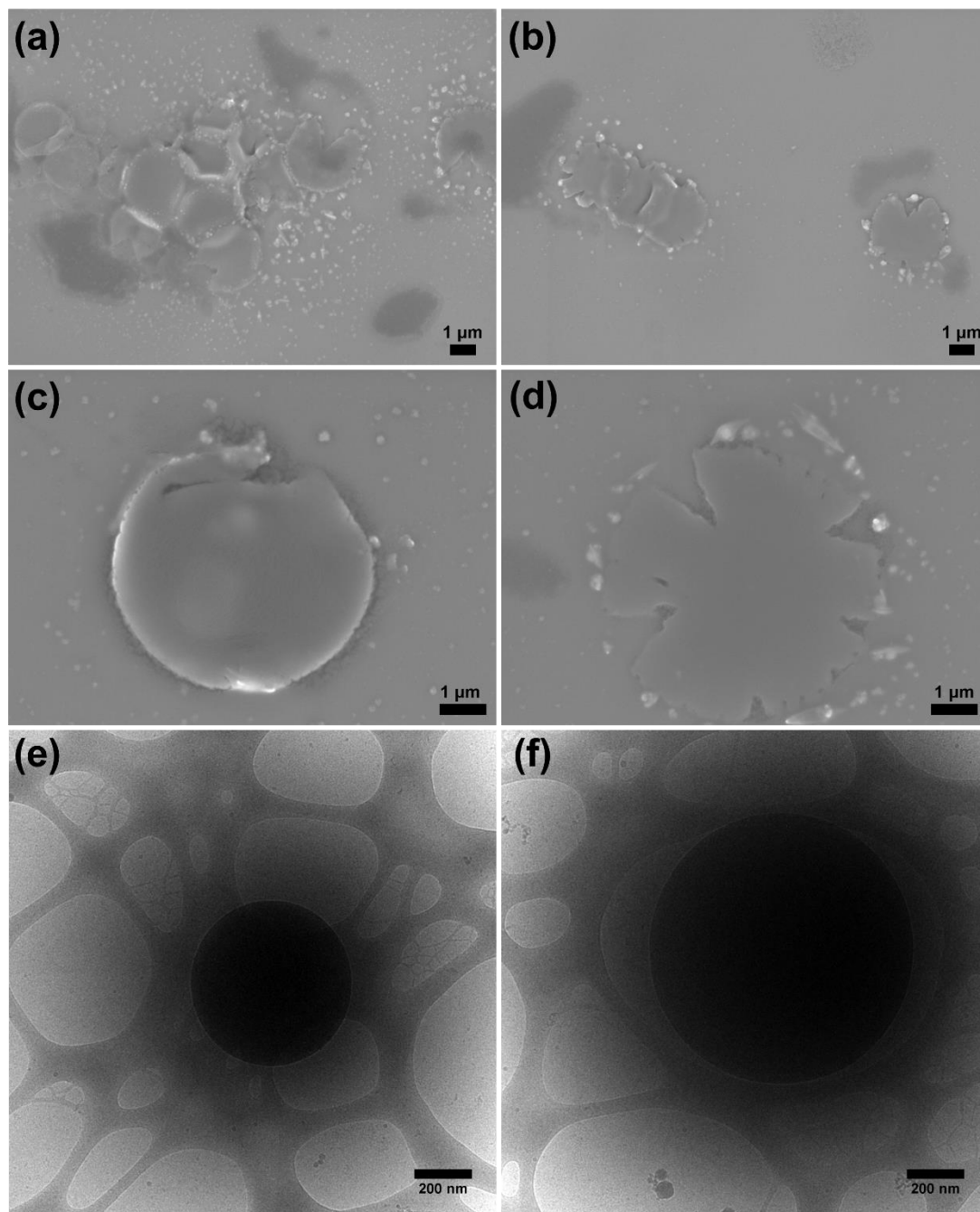**Figure 4.15**. SEM (a-d) and cryo-EM (e, f) images of the self-assemblies of PU-*g*-PEG2.

For the self-assemblies of PU-*g*-PEG2 ($f_{wt\%} = 69.1\%$) copolymer, their morphologies were also characterized by SEM and cryo-EM (Figure 4.15). From the SEM images (Figure 4.15a-d), numerous disk-like micelles were observed. The diameter of the disk-like surface was around 5 μm. The corresponding thickness in the range of 10 to 20 nm

was rather small. Moreover, some disk-like micelles were broken and splited from the outer edge to the center along the radius (Figure 4.15b, d). Many small nanoparticles scattered around the disk-like micelles, which might originate from the broken parts of the splitted disk-like micelles. The scission of the micelles might be caused by the drying of the self-assembly solution of PU-*g*-PEG2 graft copolymer during the sample preparation for the SEM characterization.

Cryo-EM images (Figure 4.15e, f) also showed disk-like micelles but the diameters of the observed micelles were less than 1 μm, as cryo-EM had better resolution for objects whose sizes are less than 1 μm. Self-assemblies with a micron size usually could not be observed clearly. So, small disk-like micelles with nanometer scale sizes were observed by cryo-EM for the self-assemblies of PU-*g*-PEG2 graft copolymer. In addition, the aggregation mode in the disk-like micelles formed by PU-*g*-PEG2 graft copolymer might be that the hydrophobic PU backbone arranged side by side with an extended chain conformation to form the two-dimensional disk-like core which were surrounded by the hydrophilic PEG side chains. The PU bakbones possibly formed a rigid and compact core thanks to the strong intramolecular and intermolecular hydrogen bonding interactions.
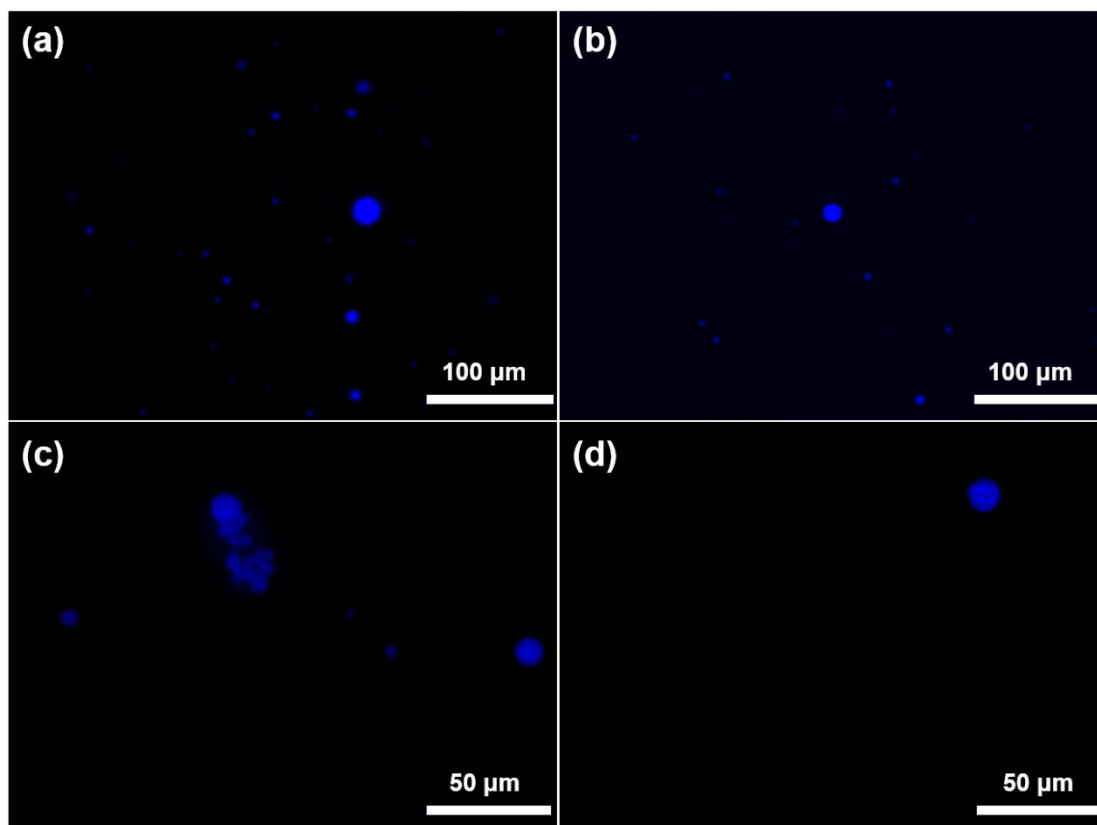
Figure 4.16. Fluorescence microscopy images of the self-assemblies of PU-*g*-PEG2.

The disk-like micelles formed by PU-*g*-PEG2 graft copolymer were also characterized by fluorescence microscopy (Figure 4.16). Blue circular particles with different sizes were observed under the excitation of UV light ($\lambda = 365$ nm) from the fluorescence microscopy. It was difficult to determine whether the particles were disk-like or spherical by the fluorescence microscopy images. However, by combining/comparing SEM and cryo-EM images, the observed blue nanoparticles should be disk-like. Moreover, large blue micelles with several small black spots were observed (Figure 4.16d), suggesting that the fluorescence emitted by the micelles was not homogeneous and the obtained disk-like micelles might therefore be heterogeneous.

4.4 Conclusion

In this chapter, novel PU based amphiphilic PU-*g*-PEG graft copolymers were prepared *via* the thiol-ene coupling reaction of PU homopolymer prepared by the AROP of CHU and thiol-terminated mPEG (mPEG-SH) based on a grafting onto strategy.

mPEG-SH was prepared by the esterification of mPEG-OH (M_n = 550 Da) with thioglycolic acid catalyzed by sulfuric acid. Two PU-g-PEG graft copolymers with different backbone lengths and hydrophilic ratios were prepared. The CMC of the amphiphilic PU-g-PEG graft copolymers in water was measured by fluorescence technique. The self-assembly of PU-g-PEG graft copolymers was performed using the nanoprecipitation technique. SEM and cryo-EM characterizations showed that PU-g-PEG graft copolymer with a hydrophilic ratio of 56.6% could self-assemble into micelles with rough and irregular surfaces, possibly resulting from the aggregation of small micelles. The self-assemblies of PU-g-PEG graft copolymer with a hydrophilic ratio of 69.1% were disk-like micelles with a large diameter and thin thickness. The fluorescence microscopy characterization of the disk-like micelles showed blue circle nanoparticles and the observation of heterogeneous fluorescence emission phenomenon suggested that the obtained disk-like micelles might be heterogeneous. In summary, we have synthesized novel amphiphilic PU-g-PEG graft copolymers and found that disk-like micelles that could emit fluorescence under UV light were formed by self-assembly of these graft copolymers with specific composition, which enriched our knowledge about the self-assembly of amphiphilic graft copolymers and provided more novel functionalized nanostructural materials.

References

1. Sheiko, S. S.; Sumerlin, B. S.; Matyjaszewski, K. *Prog. Polym. Sci.* **2008**, *33*, 759-785.

2. Feng, C.; Li, Y. J.; Yang, D.; Hu, J. H.; Zhang, X. H.; Huang, X. Y. *Chem. Soc. Rev.* **2011**, *40*, 1282-1295.

3. Zhang, M. F.; Müller, A. H. E. *J. Polym. Sci. Part A: Polym. Chem.* **2005**, *43*, 3461-3481.

4. Kaneider, N. C.; Dunzendorfer, S.; Wiedermann, C. J. *Biochemistry* **2004**, *43*, 237-244.

5. Scott, J. E. *Biochemistry* **1996**, *35*, 8795-8799.

6. Sheiko, S. S.; Sun, F. C.; Randall, A.; Shirvanyants, D.; Rubinstein, M.; Lee, H.; Matyjaszewski, K. *Nature* **2006**, *440*, 191-194.

7. Park, I.; Sheiko, S. S.; Nese, A.; Matyjaszewski, K. *Macromolecules* **2009**, *42*, 1805-1807.

8. Runge, M. B.; Bowden, N. B. *J. Am. Chem. Soc.* **2007**, *129*, 10551-10560.

9. Mynar, J. L.; Choi, T. L.; Yoshida, M.; Kim, V.; Hawker, C. J.; Fréchet, J. M. J. *Chem. Commun.* **2005**, 5169-5171.

10. Helms, B.; Mynar, J. L.; Hawker, C. J.; Fréchet, J. M. J. *J. Am. Chem. Soc.* **2004**, *126*, 15020-15021.

11. Gao, H. F.; Matyjaszewski, K. *J. Am. Chem. Soc.* **2007**, *129*, 6633-6639.

12. Engler, A. C.; Lee, H. I.; Hammond, P. T. *Angew. Chem., Int. Ed.* **2009**, *48*, 9334-9338.

13. Lowe, A. B. *Polym. Chem.* **2010**, *1*, 17-36.

14. Cesana, S.; Auernheimer, J.; Jordan, R.; Kessler, H.; Nuyken, O. *Macromol. Chem. Phys.* **2006**, *207*, 183-192.

15. Cheng, G. L.; Böker, A.; Zhang, M. F.; Krausch, G.; Müller, A. H. E. *Macromolecules* **2001**, *34*, 6883-6888.

16. Wintermantel, M.; Gerle, M.; Fischer, K.; Schmidt, M.; Wataoka, I.; Urakawa, H.; Kajiwara, K.; Tsukahara, Y. *Macromolecules* **1996**, *29*, 978-983.

17. Yamada, K.; Miyazaki, M.; Ohno, K.; Fukuda, T.; Minoda, M. *Macromolecules* **1999**, *32*, 290-293.

18. Xia, Y.; Kornfield, J. A.; Grubbs, R. H. *Macromolecules* **2009**, *42*, 3761-3766.

19. Sumerlin, B. S.; Neugebauer, D.; Matyaszewski, K. *Macromolecules* **2005**, *38*, 702-708.

20. Neugebauer D, Sumerlin BS, Matyaszewski K. *Polymer* **2004**, *45*, 8173-8179.

21. Cai, C. H.; Lin, J. P.; Chen, T.; Tian, X. H. *Langmuir* **2010**, *26*, 2791-2797.

22. Ferji, K.; Nouvel, C.; Babin, J.; Li, M.-H.; Gaillard, C.; Nicol, E.; Chassenieux, C.; Six, J.-L. *ACS Macro Lett.* **2015**, *4*, 1119-1122.

23. Zhang, X. H.; Shen, Z.; Feng, C.; Yang, D.; Li, Y. G.; Hu, J. H.; Lu, G. L.; Huang, X. Y. *Macromolecules* **2009**, *42*, 4249-4256.

24. Wan, D. C.; Pu, H. T.; Yang, G. J. *React. Funct. Polym.* **2008**, *68*, 431-435.

Chapter V. Materials and methods

All the synthesis and characterization procedures used in this work are summarized in this chapter. The first section is the instruments and measurements information. The following sections include the materials and synthesis information of the corresponding chapters: controlled anionic ring opening polymerization of 5-membered cyclic carbamates to polyurethanes, synthesis and self-assembly of polyurethane-based amphiphilic linear diblock copolymers, and synthesis and self-assembly of polyurethane-based amphiphilic graft copolymers.

5.1 General procedures

5.1.1 Nuclear Magnetic Resonance (NMR)

^{1}H NMR spectra were recorded either on Bruker Avance 300 MHz, Avance III HD 400 MHz spectrometer at 298 K. ^{13}C NMR spectra were recorded on Bruker Avance 300 MHz, Avance III HD 400 MHz or NEO 500 MHz at 298 K. 2D NMR (COSY, NOESY, HSQC and HMBC) spectra were recorded on Bruker NEO 500 MHz at 298 K. Deuterated chloroform (CDCl$_3$) was used as the solvent. NMR chemical shifts were recorded in parts per million referenced to the residual solvent proton (δ = 7.26 ppm) for ^{1}H NMR and carbon (δ = 77.1 ppm) for ^{13}C NMR.

5.1.2 Gas chromatography (GC)

GC was used to characterize the ratios of diastereomers in the starting vinyl cyclohexeneoxide and the final CHU monomer. The GC spectra were recorded on a GC-2010 Plus (SHIMADZU) instrument. Samples were prepared by dissolving in diethyl ether with a concentration of about 2 mg/mL and 2 μL sample solution was injected into the instrument for the analysis.

5.1.3 Size Exclusion Chromatography (SEC)

The number-average molecular weights (M_n) and molecular weight distributions of polymers (polydispersity index, PDI) were evaluated by size exclusion chromatography (SEC), using Agilent 1260 Infinity Series GPC (ResiPore 3 μm, 300 ×7.5 mm, 1.0 mL min^{-1}, UV (250 nm) and refractive index (RI, PLGPC 220) detector. All measurements were performed with THF as the eluent at a flow rate of 1.0 mL/min at 35 °C. Monodisperse poly(styrene) polymers were used as calibration standards.

5.1.4 Matrix-assisted laser desorption ionization-time of flight mass spectrometry (MALDI-TOF MS)

MALDI-TOF-MS characterization of polymers was performed on UltrafleXtreme mass spectrometer (Bruker Daltonics, Bremen) using *trans*-2-[3-(4-*tert*-Butylphenyl)-

2-methyl-2-propenylidene]malononitrile (DCTB) as the matrix. All data were processed using FlexAnalysis software (Bruker Daltonics, Bremen). Polymer samples for MALDI analysis were prepared at a concentration of 5 mg/mL in THF. The matrix solution was prepared at a concentration of 10 mg/mL in THF. The sample was prepared by mixing the polymer solution with matrix solution at a volume ratio of 1:5 and allowed to dry at room temperature before analysis.

5.1.5 Attenuated total reflection infrared spectroscopy (ATR-IR)

ATR-IR was used to characterize the infrared absorption spectra of PU samples. The spectra were recorded on a Magna – IR^{TM} 550 spectrometer equipped with a diamond probe. Solid PU samples were put under the probe with pressure and then characterized directly by the instrument.

5.1.6 In situ infrared spectroscopy (*In situ* IR)

In situ IR characterization was performed on METTLER TOLEDO ReactIR 15 analyzer using an attenuated total reflection (ATR) diamond probe in the range 3000-650 cm^{-1}. The reaction mixture containing monomer, co-initiator and THF was added to a 15 mL Schlenk tube in the argon-purged glovebox firstly and cooled to 0 °C. Then the initiator (*n*-butyllithium) was added to the above solution quickly under argon and sealed with a special cap equipped with the IR probe. IR spectra were recorded by using the iC IR software with a sampling interval of 2 min.

5.1.7 Thermogravimetric analysis (TGA)

TGA measurements were carried out on SDT Q600 TA instrument to analyze the thermal properties of the polyurethane (PU) samples. Samples (5-10 mg) were characterized under a nitrogen atmosphere over the temperature range of 25 to 650 °C, with a heating rate of 20 °C/min.

5.1.8 Differential Scanning Calorimetry (DSC)

Calorimetric measurements of polymers were performed using a Perkin Elmer DSC7 device. The reference cell was kept empty and the sample cell was filled with polymer sample (5 to 10 mg). Samples were scanned over a temperature range between -20 °C and 200 °C with a scanning rate of 5 °C/min or 10 °C/min. Glass temperature (T_g) was measured at the second heating scan.

5.1.9 Polarized optical microscopy (POM)

The morphology and polarity of PU samples before and after heat treatment were characterized by polarized optical microscopy. Samples were observed directly by a Leitz Ortholux microscopy.

5.1.10 Fluorescence microscopy

The morphology and fluorescence properties of PU samples after heat treatment and self-assemblies of amphiphilic PU-g-PEG graft copolymer with a hydrophilic ratio of 69.1% were characterized by fluorescence microscopy. Samples were observed directly by a Leica DMIL LED Fluo inverted microscopy.

5.1.11 Dynamic light scattering (DLS)

Hydrodynamic diameters (D_h) of the self-assemblies of amphiphilic PEG-b-PU linear diblock copolymers and PU-g-PEG graft copolymers and their size distributions in deionized water were measured at 25 °C by dynamic light scattering (DLS, Malvern zetasizer 3000HS, UK) with a 633 nm laser. All measurements were performed with a 90 ° scattering angle. The sample solution in the scattering cell was equilibrated for 10 min before measurements.

5.1.12 Scanning electron microscopy (SEM)

Morphologies of the self-assemblies of amphiphilic PEG-b-PU linear diblock copolymers and PU-g-PEG graft copolymers were characerized by Field-Emission

SEM (LEO GEMINI-1530). Samples were prepared by depositing one or two drops of the self-assembly solution onto the surface of a clean silicon chip, and the samples were dried at room temperature for 24 hours. A thin film of gold was coated on the samples before measurement.

5.1.13 Cryo-electron microscopy (Cryo-EM)

Morphologies of copolymer colloids were also characterized by cryo-EM. Images were acquired on a JEOL 2200FS energy-filtered (20 eV) field emission gun electron microscopy operating at 200 kV using a Gatan ssCCD 2048 × 2048 pixels. Samples were prepared by deposition of 5 µL sample solution onto a 200 mesh holey copper grid (Ted Pella Inc., U.S.A.) and the samples were flash-frozen in liquid ethane which were cooled down at liquid nitrogen temperature.

5.1.14 Fluorescence emission spectroscopy

The fluorescence emission measurements of self-assembly solution of amphiphilic PEG-*b*-PU linear diblock copolymers and aqueous solution of PU-*g*-PEG graft copolymers were carried out on a FluoroMax spectrofluorometer. Samples were added to a 1cm quartz cuvette with all flanks transparent.

5.2 Controlled anionic ring opening polymerization of 5-membered cyclic carbamates to polyurethanes

5.2.1 Materials

4-vinyl-1-cyclohexene-1,2-epoxide (mixture of isomers, 98%, TCI), ethyl chloroformate (97%, Sigma-Aldrich), triethylamine (99%, Alfa Aesar), sodium hydride (60 % dispersion in mineral oil, Sigma-Aldrich), benzoyl chloride (98%, TCI) and *n*-butyllithium (2.0 M in cyclohexane, Sigma-Aldrich) were used as received. THF used for polymerization was distilled over sodium and carefully degassed by three freeze-pump-thaw cycles prior to use.

5.2.2 Synthesis of CHU monomer

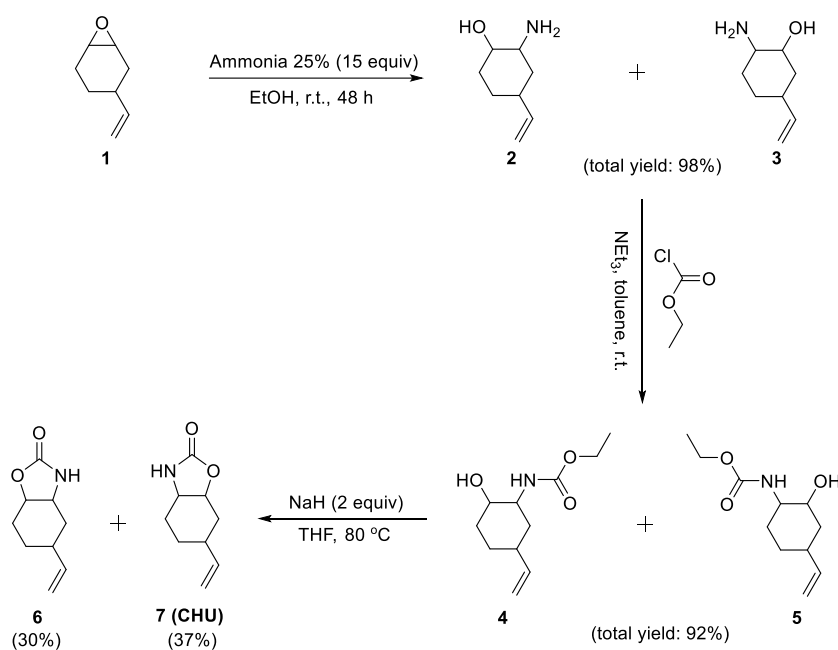The synthetic process included three steps, as shown in Figure 5.1.

Figure 5.1. Synthetic route to CHU.

Firstly, 4-vinyl-1-cyclohexene-1,2-epoxide (**1**, 10 g, 0.08 mol) and 25% ammonia (81 mL, 1.20 mol) were added into a 500 mL round-bottom flask and stirred. Ethanol (c.a. 70 mL) was added into the above mixture gradually until the solution became clear. After stirring at room temperature for 48 h, ethanol was removed by rotary evaporation. Then the solution was extracted by dichloromethane (DCM, 3 × 50 mL) and the

combined organic layers were dried over anhydrous magnesium sulfate. The solvent was evaporated, and the resulting material was a mixture of compounds **2** and **3** (11.14 g, yield: 98%). ^{1}H NMR (CDCl$_3$): δ 5.73-5.95 (m, 1H, -C*H*=CH$_2$), 4.94-5.10 (m, 2H, -CH=C*H*$_2$), 2.07-2.61 (m, 3H, -CH$_2$-CH(CH-)-O*H* and -CH$_2$-CH(CH-)-N*H*$_2$).

Secondly, mixture of **2** and **3** (11.14 g, 79 mmol) was dissolved in 80 mL toluene and triethylamine (TEA, 9.98 g, 99 mmol) was added dropwise at 0 °C. Then ethyl chloroformate (10.70 g, 99 mmol) was added dropwise at 0 °C. The mixture was stirred at room temperature for 3 h. Then, toluene was removed by rotary evaporation under vacuum and 120 mL water was added. Then the aqueous solution was extracted with DCM (3 × 50 mL) and the combined organic layers were dried over anhydrous magnesium sulfate. The solvent was evaporated to afford the crude product, as a mixture of compounds **4** and **5** (15.47 g, yield: 92%). The two products could be separated by column chromatography on a silica gel using toluene and tetrahydrofuran (THF) (40/1,20/1 and 10/1) as the eluent. However, the corresponding mixture can also be used directly for the third step and the separation can be done at last. ^{1}H NMR of **4** (CDCl$_3$): δ 5.68-5.95 (m, 1H, -C*H*=CH$_2$), 4.96-5.22 (m, 2H, -CH=C*H*$_2$), 4.61-4.88 (m, 1H, -N*H*-COOCH$_2$CH$_3$), 3.94-4.26 (2H, -NH-COOC*H*$_2$CH$_3$), 1.11-1.37 (3H, -NH-COOCH$_2$C*H*$_3$). ^{1}H NMR of **5** (CDCl$_3$): δ 5.70-5.88 (1H, -C*H*=CH$_2$), 4.97-5.11 (2H, -CH=C*H*$_2$), 4.64-4.89 (1H, -N*H*-COOCH$_2$CH$_3$), 4.01-4.18 (2H, -NH-COOC*H*$_2$CH$_3$), 1.14-1.30 (3H, -NH-COOCH$_2$C*H*$_3$). ^{13}C{^{1}H} NMR of **5** (CDCl$_3$): δ 157.61 (-NH-*C*OOCH$_2$CH$_3$), 141.55 (-*C*H=CH$_2$), 114.01 (-CH=*C*H$_2$), 69.97 (-CH$_2$*C*H(OH)CH-), 61.12 (-CH$_2$*C*H(NH-)CH-), 55.02 (-NH-COO*C*H$_2$CH$_3$).

Thirdly, mixture of **4** and **5** (10 g, 47 mmol) was dissolved in 80 mL THF and sodium hydride (60 % dispersion in mineral oil, 3.75 g, 94 mmol) was added to the solution. The mixture was heated at reflux overnight. After stopping the reaction, THF was removed by rotary evaporation and 80 mL water was added. Then the aqueous solution was extracted by ethyl acetate (3 × 50 mL). The combined organic layers were dried over anhydrous magnesium sulfate and evaporated under vacuum. Then the resulting crude product was chromatographed on a silica gel using hexane and ethyl acetate with

a volume ratio of 20/1 to 4/1 as the eluent. Finally, pure products **6** (white solid, 2.35 g, yield: 30%) and **7** (white solid, 2.90 g, yield: 37%) were obtained. Then compound **7** (50 °C, 0.6 mbar) sublimated to get pure 5-membered cyclic carbamate monomer (CHU). ^{1}H NMR (CDCl$_3$): δ 5.75-5.97 (1H, -C*H*=CH$_2$), 5.31-5.70 (1H, -N*H*-COO-), 5.02 -5.24 (2H, -CH=C*H$_2$*), 4.06 (1H, -CH$_2$-C*H*(OCONH)-CH-), 3.34 (1H, -CH$_2$-C*H*(NHCOO)-CH-), 2.77 (1H, -CH$_2$-C*H*(CH=CH$_2$)-CH$_2$-). ^{13}C{^{1}H} NMR (CDCl$_3$): δ 161.00 (-NH*C*OO-), 140.48 (-*C*H=CH$_2$), 115.09 (-CH=*C*H$_2$), 80.26 (-CH$_2$*C*H(OCONH-)CH-), 61.26 (-CH$_2$*C*H(NHCOO-)CH-), 35.82 (-CH(NHCOO-)CH-*C*H$_2$-).

GC spectrum of 4-vinyl-1-cyclohexene-1,2-epoxide (mixture of isomers)

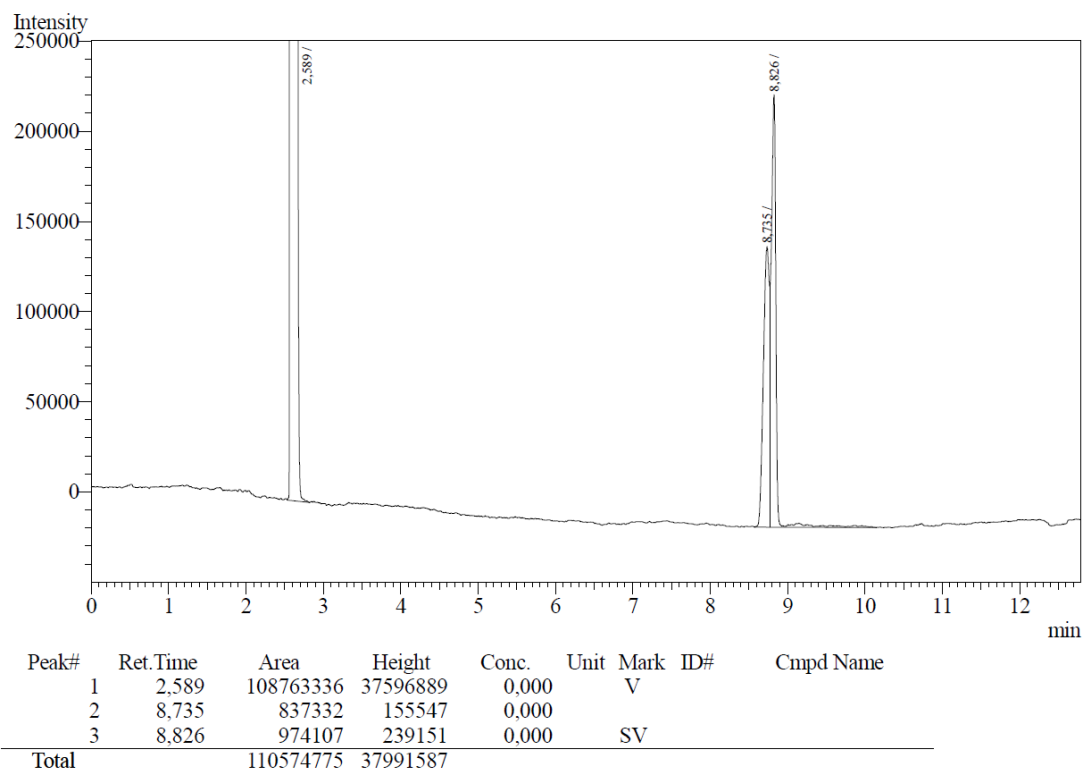| Peak#	Ret.Time	Area	Height	Conc.	Unit	Mark	ID#	Cmpd Name
1	2,589	108763336	37596889	0,000		V		
2	8,735	837332	155547	0,000				
3	8,826	974107	239151	0,000		SV		
Total		110574775	37991587					

Figure 5.2. GC spectrum of 4-vinyl-1-cyclohexene-1,2-epoxide (mixture of isomers). Injection temperature: 260 °C. The column temperature was increased from 80 °C to 160 °C with a rate of 2 °C/min.
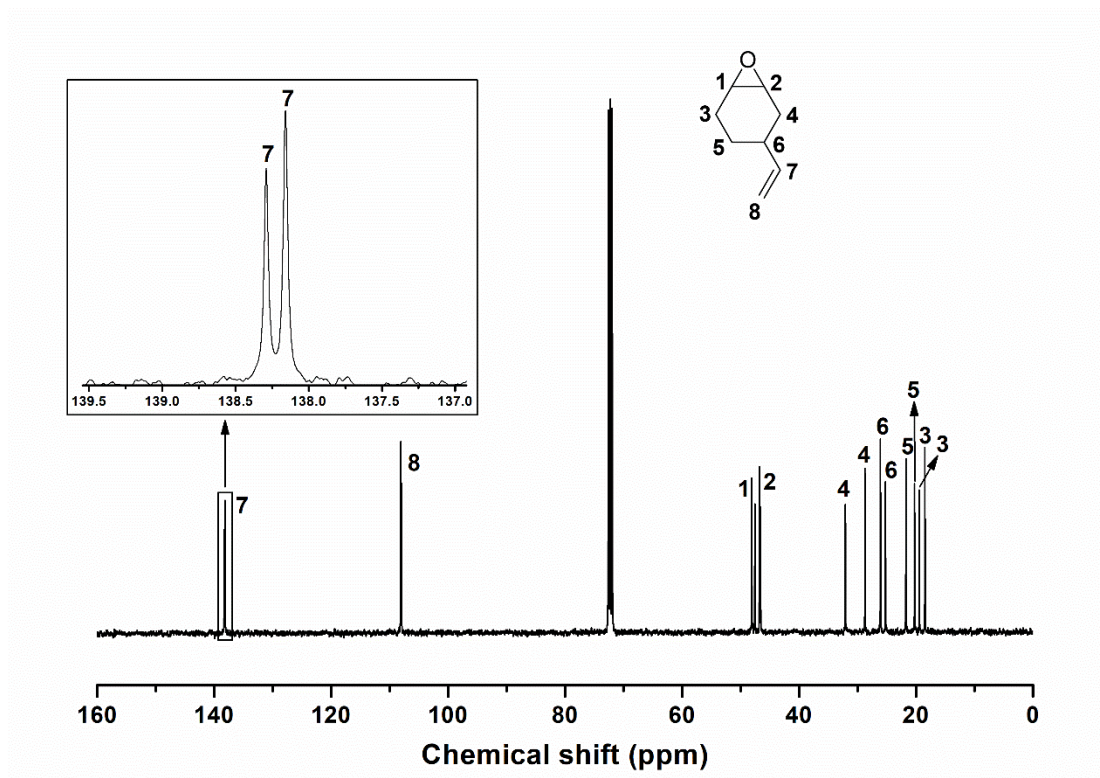
^{13}C NMR spectrum of 4-vinyl-1-cyclohexene-1,2-epoxide (mixture of isomers)

Figure 5.3. ^{13}C NMR spectrum of 4-vinyl-1-cyclohexene-1,2-epoxide (mixture of isomers). CDCl$_3$, 400 MHz, 297 K.
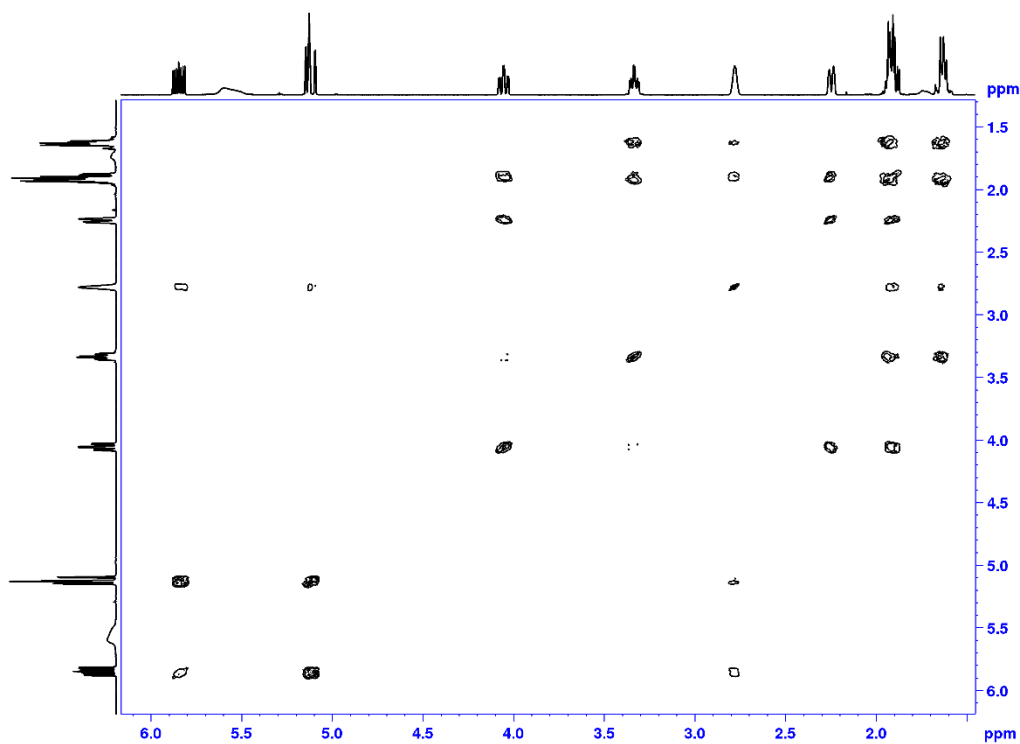
2D NMR spectra of CHU

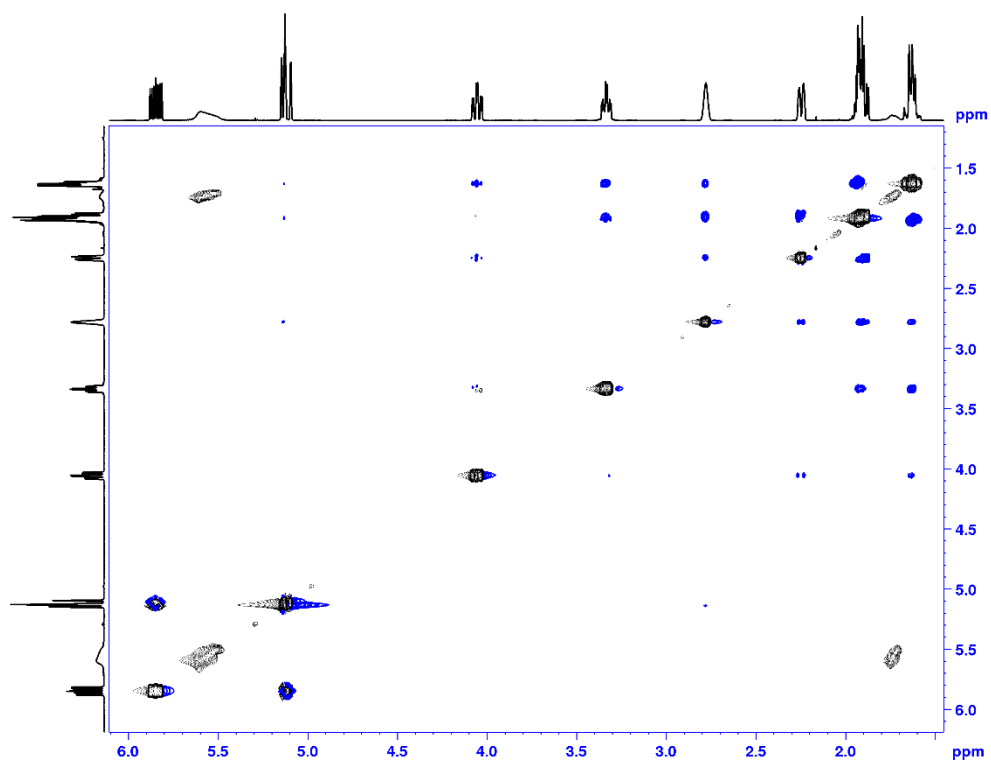**Figure 5.4**. 2D COSY spectrum of CHU monomer. CDCl$_3$, 500 MHz, 297 K.

Figure 5.5. 2D NOESY spectrum of CHU monomer. CDCl$_3$, 500 MHz, 297 K.
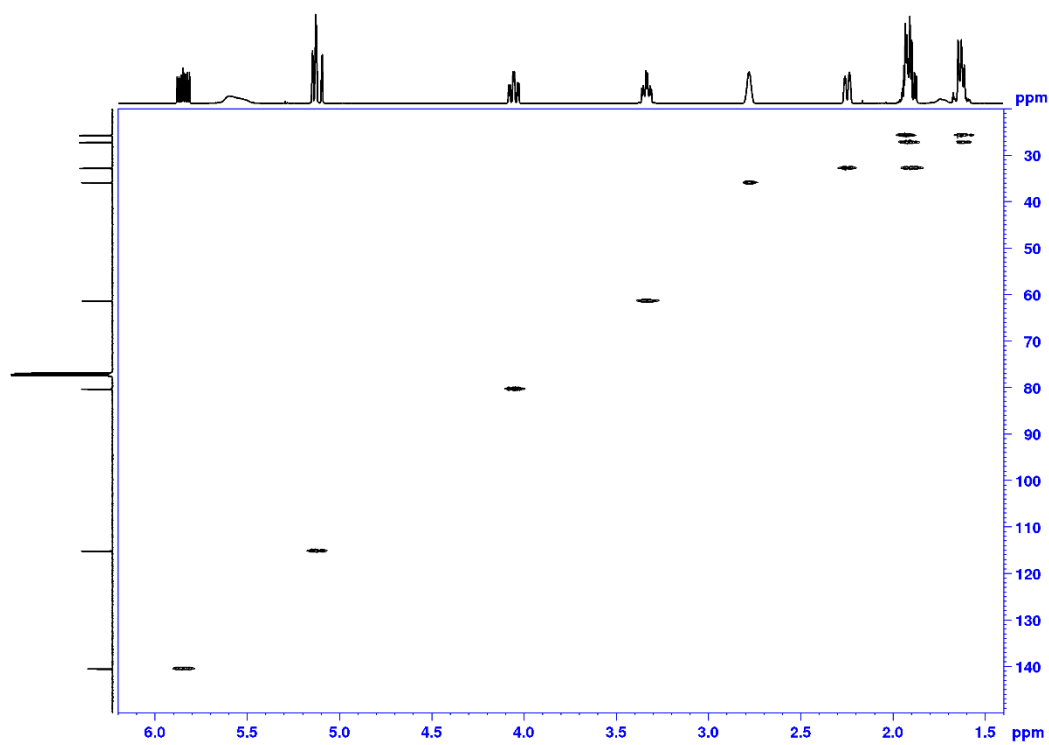
169

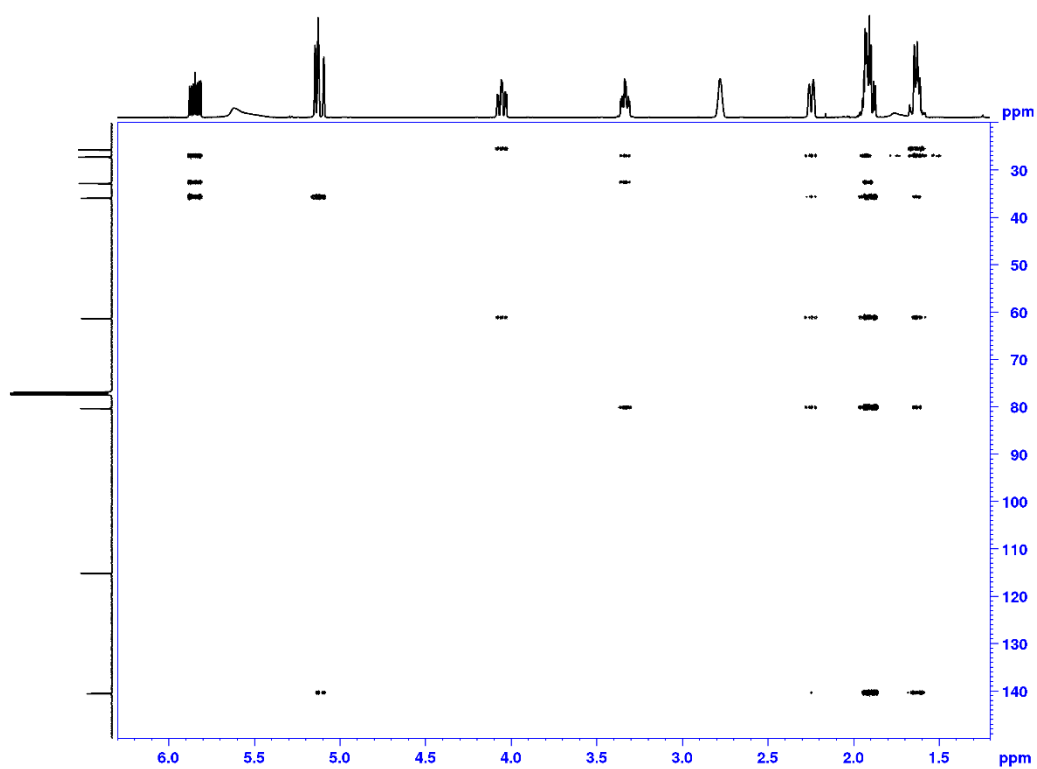**Figure 5.6**. 2D HSQC spectrum of CHU monomer. CDCl$_3$, 500 MHz, 297 K.

Figure 5.7. 2D HMBC spectrum of CHU monomer. CDCl$_3$, 500 MHz, 297 K.

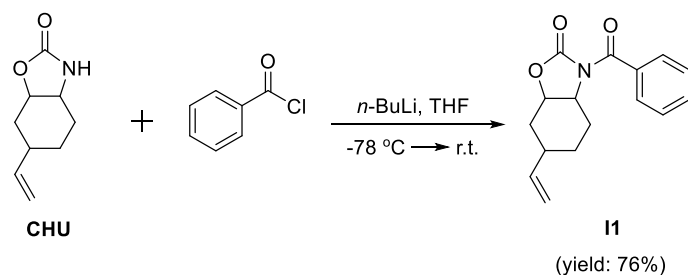**5.2.3 Synthesis of CHU-derived imide I1 (co-initiator)**

Figure 5.8. Synthetic route to CHU-derived imide **I1**.

The CHU-derived imide **I1** (co-initiator) was synthesized through the one step reaction between CHU monomer and benzoyl chloride (Figure 5.8). The typical synthesis process was as follows: CHU (0.50 g, 3.0 mmol) was dissolved in dry THF (10 mL) and the solution was cooled to -78 °C. Then *n*-butyllithium (2.0 M in cyclohexane, 1.65 mL, 3.3 mmol) was added slowly and the mixture was stirred at -78 °C for 30 min. A solution of benzoyl chloride (0.51 g, 3.6 mmol) in dry THF (20 mL) was subsequently added dropwise to the above mixture and the reaction mixture was stirred overnight while warming to the room temperature. After stopping the reaction, silica gel was added directly into the reaction mixture. Removed the solvent by rotary evaporation to afford the dried silica gel with crude product adhered to. Then the crude product was chromatographed on a silica gel using petroleum ether and ethyl acetate with a volume ratio of 1/1 as the eluent. Finally, pure CHU-derived imide **I1** (white solid, 0.62 g, yield: 76 %) was obtained after recrystallization from acetone. The ^{1}H NMR and ^{13}C NMR spectra of **I1** were shown in Figure 5.9.
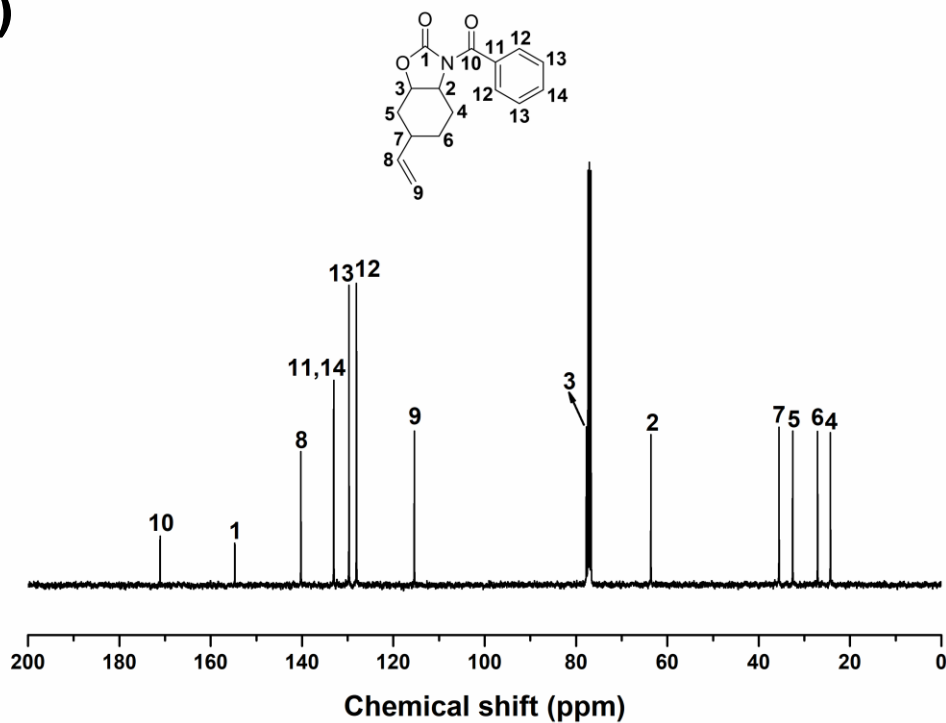
(a)
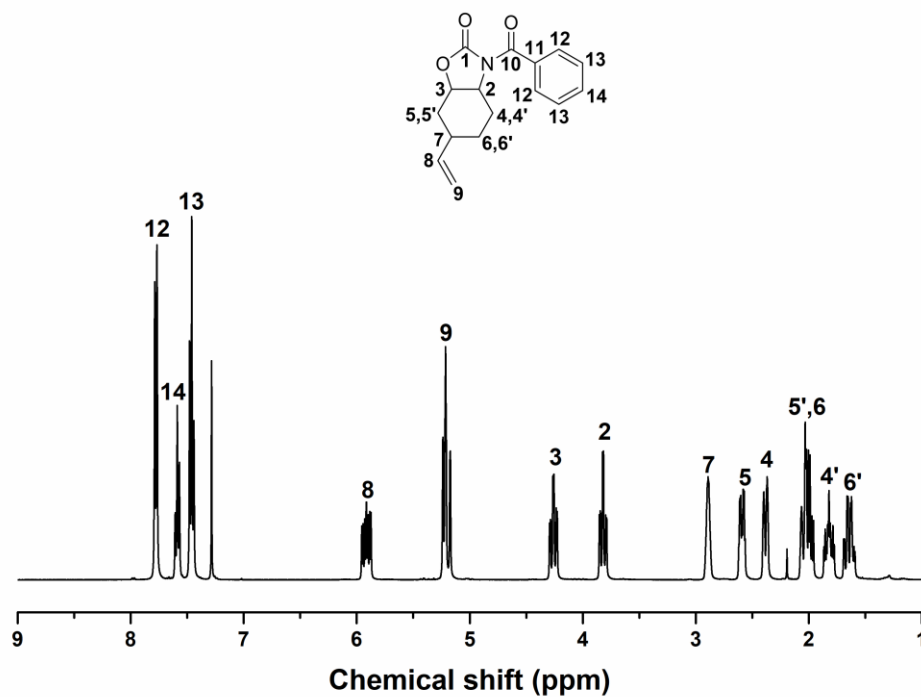
(b)

Figure 5.9. ^{1}H NMR (a) and ^{13}C NMR (b) spectra of CHU-derived imide **I1**. CDCl$_3$, 400 MHz, 297 K.
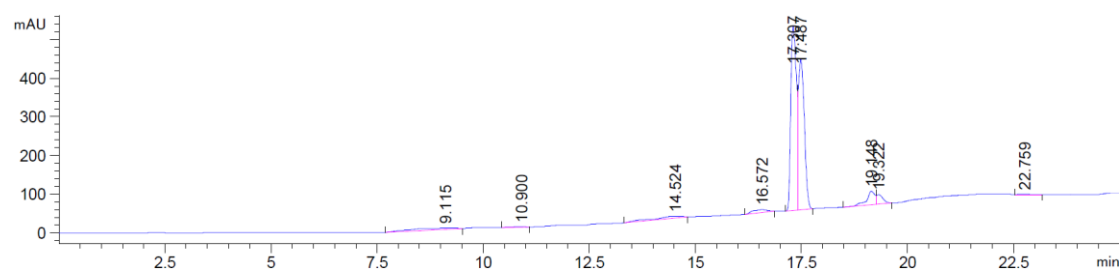
HPLC spectrum of CHU-derived imide I1

Figure 5.10. HPLC spectrum of CHU-derived imide **I1**. The eluent was the mixture of acetonitrile and water.
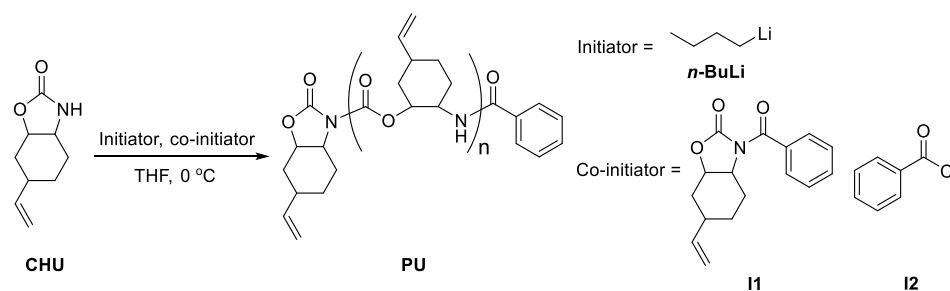
5.2.4 Polymerization

Figure 5.11. Synthetic scheme of PU by AROP of CHU.

The AROP scheme to prepare PU homopolymer is shown in Figure 5.11. All polymerizations were carried out under argon in a 15 mL Schlenk tube equipped with a Teflon coated stirring bar. The typical polymerization process was as follows: In the glove box, the Schlenk tube was charged with appropriate amounts of CHU monomer, co-initiator and THF to reach the desired monomer to co-initiator ratio and monomer concentration. The Schlenk tube was kept for 20 min in the refrigerator of -40 °C in the glove box. Then appropriate amount of *n*-butyllithium was added and the Schlenk tube was transferred outside of the glove box quickly. The mixture was stirred at 0 °C for a certain time. The polymerization was stopped by adding a small amount of methanol. The mixture was then poured drop-by-drop into *n*-hexane (15 mL) to precipitate the crude PU polymer. The precipitate was collected by centrifugation. After being re-dissolved in THF and reprecipitated in *n*-hexane twice more, the pure polymer was collected and dried under vacuum at room temperature for 24 h.

5.3 Synthesis and self-assembly of polyurethane-based amphiphilic linear diblock copolymers

5.3.1 Materials

Cyclohexene oxide (98%, Sigma-Aldrich), ethyl chloroformate (97%, Sigma-Aldrich), triethylamine (99%, Alfa Aesar), sodium hydride (60 % dispersion in mineral oil, Sigma-Aldrich), succinic anhydride (99%, Sigma-Aldrich), 1-(3-dimethylaminopropyl)-3-ethylcarbodiimide hydrochloride (EDC•HCl, 99%, Sigma-Aldrich), poly(ethylene glycol) monomethyl ether (mPEG, M_n = 550, 1000, 2000 Da, TCI), 4-(dimethylamino)pyridine (DMAP, 99%, Sigma-Aldrich) and n-butyllithium (2.0 M in cyclohexane, Sigma-Aldrich) were used as received. THF used for polymerization was distilled over sodium and carefully degassed by three freeze-pump-thaw cycles prior to use.

5.3.2 Synthesis of cyclohexane urethane compound without vinyl group

The synthetic process included three steps, as shown in Figure 5.12.
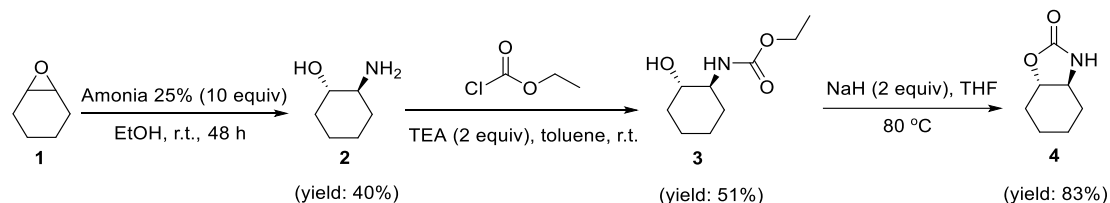
Figure 5.12. Synthetic route of cyclohexane urethane compound without vinyl group (also termed as CHU in the synthesis of mPEG-CHU).

Firstly, cyclohexene oxide (**1**, 9.80 g, 0.10 mol) and 25% ammonia (112 mL, 1.50 mol) were added into a 250 mL round-bottom flask and stirred. Ethanol (50 mL) was added into the above mixture gradually and the solution became clear. After stirred at room temperature for 48 h, ethanol was removed by rotary evaporation. Then the solution was extracted by dichloromethane (DCM, 3 × 50 mL). After drying over anhydrous magnesium sulfate and rotary evaporation to remove DCM, compound **2** was isolated (4.60 g, yield: 40%). ^{1}H NMR (CDCl$_3$): δ 5.23 (1H, -OH), 3.07 (1H, OH-CH-CH(CH$_2$)), 2.34 (1H, NH$_2$-CH-CH(CH$_2$)).

Secondly, 1-hydroxy-2-amino-cyclohexane (**2**, 4.60 g, 0.04 mol) was dissolved in 100 mL toluene and triethylamine (TEA, 5.06 g, 0.05 mol) was added dropwise in the ice-water bath. Then ethyl chloroformate (5.43 g, 0.05 mol) was added dropwise in the ice-water bath. The mixture was stirred at room temperature for 3 h. After stopping the reaction, toluene was removed by rotary evaporation and 120 mL water was added. Then the aqueous solution was extracted by DCM (3 × 50 mL). The crude product was chromatographed on a silica gel using n-hexane and ethyl acetate (EA) with a volume ratio of 1:1 as eluent, and the pure product was compound **3** (3.83 g, yield: 51%). ^{1}H NMR (CDCl$_3$): δ 4.60 (1H, -NH-), 4.05 (2H, COO-CH_2-CH$_3$), 3.26 (2H, CH$_2$(OH)-CH-CH-CH$_2$(NH)), 2.94 (1H, -OH). ^{13}C{^{1}H} NMR (CDCl$_3$): δ 157.60 (-NH-COOEt), 74.70 (CH$_2$$C$H(OH)CH), 61.07 (CH$_2$$C$H(NH-)CH), 56.55 (COO$CH_2CH_3$), 14.54 (COOCH$_2$$CH_3$).

Thirdly, 1-hydroxy-2-carbamate-cyclohexane (**3**, 3.00 g, 16 mmol) was dissolved in 75 mL tetrahydrofuran (THF) and sodium hydride (60 % dispersion in mineral oil, 1.28 g, 32 mmol) was added to the solution. The mixture was heated at reflux for 4 h. After stopping the reaction, THF was removed by rotary evaporation and 120 mL water was added. Then the aqueous solution was extracted by EA (3 × 30 mL). The crude product was chromatographed on a silica gel using DCM and EA with a volume ratio of 4:1 as eluent, and the pure product was cyclic urethane **4** (1.88 g, yield: 83%). ^{1}H NMR (CDCl$_3$): δ 5.15 (1H, -OCO-NH-CH), 3.91 (1H, -CH$_2$-CH-CH(OCO)), 3.33 (1H, -CH$_2$-CH-CH(NHCO)).

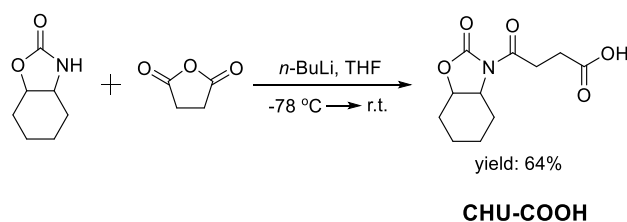### 5.3.3 Synthesis of carboxylic acid functionalized CHU (CHU-COOH)

Figure 5.13. Synthetic scheme of CHU-COOH.

The synthetic scheme of CHU-COOH is shown in Figure 5.13. The typical synthesis process was as follows: Cyclohexane urethane (CHU, 0.65 g, 4.61 mmol) was dissolved in dry THF (15 mL). The solution was cooled to -78 °C and *n*-butyllithium (2.0 M in cyclohexane, 2.54 mL, 5.08 mmol) was added dropwise. The reaction mixture was stirred at -78 °C for 30 min. Then a solution of succinic anhydride (0.55 g, 5.50 mmol) dissolved in dry THF (30 mL) was added dropwise to the above mixture. The reaction mixture was stirred overnight while warming to the room temperature. After quenching by addition of deionized water (30 mL), THF was removed by rotary evaporation. The residue aqueous mixture was basified to pH > 9 by addition of saturated aqueous solution of sodium bicarbonate. After extraction by ethyl acetate (2 × 10 mL), the aqueous phase was acified with conc. HCl to pH < 2, followed by extraction with DCM (4 × 20 mL). The combined DCM phase was dried over anhydrous magnesium sulfate. The solvent was evaporated to afford the oily crude product which was dried in high vacuum. Pure CHU-COOH (white solid, 0.74 g, yield: 67%) was obtained by recrystallization from acetone. The ^{1}H NMR and ^{13}C NMR spectra of CHU-COOH were shown in Figure 3.10 in the third chapter.

5.3.4 Synthesis of mPEG based macromolecular co-initiator mPEG-CHU
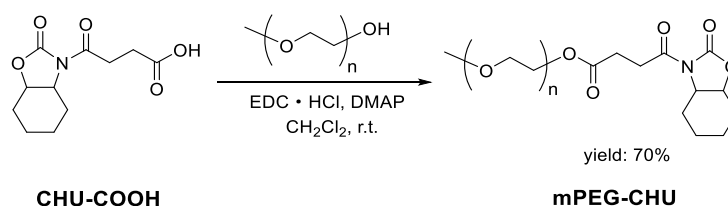
Figure 5.14. Synthetic scheme of mPEG-CHU.

The synthetic scheme of mPEG-CHU is shown in Figure 5.14. The typical synthesis of mPEG$_{12}$-CHU was as follows: mPEG$_{12}$-OH (0.356 g, 0.65 mmol), CHU-COOH (0.130g, 0.54 mmol), EDC•HCl (0.125 g, 0.65 mmol) and DMAP (0.033 g, 0.27 mmol) were added into a 100 mL round-bottom flask, followed by the addition of 20 mL dry DCM. The mixture was stirred for 20 h at room temperature. After stopping the reaction, the DCM was extracted by dilute HCl aqueous solution (3%) (3 × 10 mL) to remove

DMAP and water-soluble side products. The DCM phase was dried over anhydrous magnesium sulfate. Then concentrated the DCM solution to about 1 mL by rotary evaporation. Then the crude product was chromatographed on a silica gel using DCM and methanol with a volume ratio of 12/1 as the eluent to afford the pure mPEG$_{12}$-CHU (colorless viscous liquid, 0.332 g, yield: 79.6 %).

For the synthesis of mPEG$_{22}$-CHU and mPEG$_{45}$-CHU, all the synthetic procedures were similar to those of mPEG$_{12}$-CHU except that different volume ratios of DCM and methanol were used as the eluent for column chromatography.

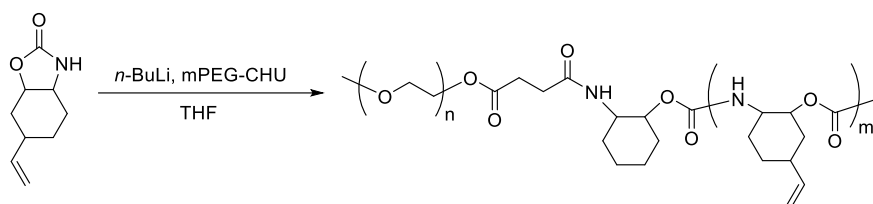### 5.3.5 Synthesis of amphiphilic PEG-*b*-PU linear diblock copolymers

Figure 5.15. Synthetic scheme of amphiphilic PEG-*b*-PU linear diblock copolymers.

The synthetic scheme of PU based amphiphilic PEG-*b*-PU linear diblock copolymers is shown in Figure 5.15. The copolymers were synthesized *via* the AROP of CHU monomer with *n*-butyllithium as the initiator and mPEG-CHU as the macromolecular co-initiator. All anionic ring opening polymerizations of CHU monomers were carried out under argon in a 15 mL Schlenk tube equipped with a Teflon coated stirring bar. The typical polymerization process was as follows: In the glove box, the Schlenk tube was charged with appropriate amounts of CHU monomer, macromolecular co-initiator mPEG-CHU and THF to reach the desired monomer to co-initiator ratio and monomer concentration. After the solution was clear, appropriate amount of *n*-butyllithium was added. Then the Schlenk tube was transferred outside of the glove box quickly and immersed into an oil bath of 40 °C. The mixture was stirred at 40 °C for a certain time. The polymerization was stopped by adding a small amount of methanol. The mixture was then poured drop-by-drop into the mixture of *n*-hexane and diethyl ether (2/1, v/v) to precipitate the crude PEG-*b*-PU polymer. The precipitate was collected by

centrifugation. After being re-dissolved in THF and reprecipitated in the mixture of *n*-hexane and diethyl ether twice more, the pure polymer was collected and dried under vacuum at room temperature for 24 h.

5.3.6 Self-assembly of amphiphilic PEG-*b*-PU linear diblock copolymers

Nanoparticles were prepared from PEG-*b*-PU diblock copolymers using a classical nanoprecipitation method. Briefly, the polymer was firstly dissolved in THF, which was a good solvent for both polymer blocks. The initial concentration of the polymer in THF was 2.5 mg/mL. Then deionized water was added slowly to the THF solution (around 3 uL/min) until it reached 50 wt% of the whole solution. The solution was shaked gently during the addition of water. THF was removed by dialysis against deionized water for 3 days in a 3500 Da cut off cellulose bag. Finally, the aqueous solution of the self-assemblies of PEG-*b*-PU with a concentration of about 2 mg/mL in the dialysis bag was obtained.

5.4 Synthesis and self-assembly of polyurethane-based amphiphilic graft copolymers

5.4.1 Materials

Poly(ethylene glycol) monomethyl ether (mPEG, M_n = 550 Da, TCI), thioglycolic acid (98%, Sigma-Aldrich) and 2,2'-Azobis(isobutyronitrile) (AIBN, 98%, Sigma-Aldrich, recrystallized from anhydrous ethanol) were used as received. Toluene and THF were dried by solvent purification system.

5.4.2 Synthesis of thiol-terminated mPEG (mPEG-SH)

yield: 58.9%
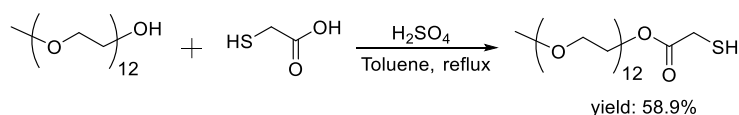
Figure 5.16. Synthetic scheme of mPEG-SH.

Thiol-terminated mPEG was prepared through the esterification reaction between mPEG$_{12}$-OH and thioglycolic acid with sulfuric acid as the catalyst (Figure 4.6). The typical synthesis process was as follows: mPEG$_{12}$-OH (3.30 g, 6 mmol) and thioglycolic acid (1.66 g, 18 mmol) were dissolved in dry toluene (10 mL). Then conc. sulfuric acid (2 drops) was added to the mixture and the reaction flask was equipped with an azeotropic distillation apparatus. The mixture was refluxed at 130 °C for 16 h. After stopping the reaction by cooling to the room temperature, toluene was removed under reduced pressure. Pure mPEG$_{12}$-SH (colorless viscous liquid, 2.20 g, yield: 58.9%) was obtained by recrystallization of the crude product once from the mixture of THF and diethyl ether.

5.4.3 Synthesis of amphiphilic PU-*g*-PEG graft copolymers

Figure 5.17. Synthetic scheme of amphiphilic PU-*g*-PEG graft copolymer.
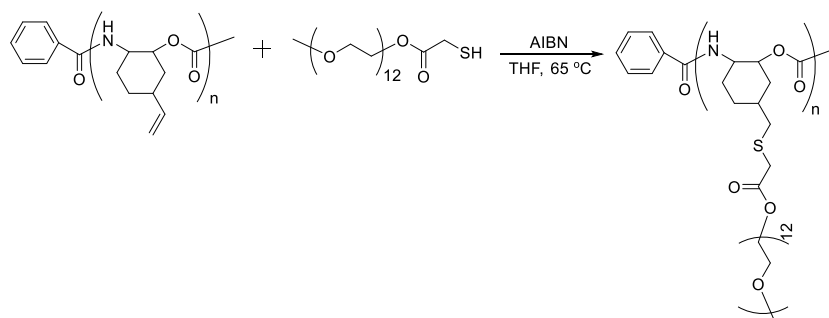
The amphiphilic PU-*g*-PEG graft copolymers were prepared by the radical-mediated thiol-ene reaction of a linear PU homopolymer backbone with vinyl groups attached on each repeating unit and mPEG$_{12}$-SH, which was a grafting onto strategy to prepare graft copolymers (Figure 5.17). The PU homopolymer was prepared *via* the AROP of CHU monomer as described in the second chapter. The typical synthesis of PU-*g*-PEG graft copolymer with a hydrophilic ratio of 56.6% by thiol-ene coupling reaction was as follows: PU (M_n = 2400 Da, 30 mg, c.a. 0.175 mmol vinyl groups), mPEG$_{12}$-SH (437 mg, 0.7 mmol), AIBN (34.5 mg, 0.21 mmol) and 2 mL dry THF were added to a 15 mL Schlenk tube equipped with a Teflon coated stirring bar. After deoxygenation by three freeze-pump-thaw cycles, the reaction mixture was stirred at 65 °C for 24 h. The reaction was stopped by cooling to the room temperature. The crude product was purified by dialysis against ethanol in a 3500 Da cut off cellulose bag for 5 days to remove unreacted mPEG$_{12}$-SH, and the ethanol was changed twice a day. The ethanol solution in the dialysis bag was collected and pure PU-*g*-PEG graft copolymer (colorless viscous liquid, 82 mg, yield: 59.0 %) was obtained by removing the ethanol under high vacuum.

5.4.4 Self-assembly of amphiphilic PU-*g*-PEG graft copolymers

Nanoparticles were prepared from PU-*g*-PEG graft copolymers using a classical nanoprecipitation method. In a typical self-assembly experiment, PU-*g*-PEG was firstly dissolved in THF (concentration 3.5 mg/mL for PU-*g*-PEG1 and 1 mg/mL for PU-*g*-

PEG2), which was a good solvent for both PEG and PU. Then deionized water was added gradually (around 0.5 uL/min) until it reached 50 wt% of the whole solution. The solution was shaked gently during the addition of water. THF was removed by dialysis against deionized water for 3 days in a 3500 Da cut off cellulose bag. Finally, the self-assembly solution of PU-*g*-PEG1 with a concentration of about 3 mg/mL and self-assembly solution of PU-*g*-PEG2 with a concentration of about 0.8 mg/mL in the dialysis bags were collected.

General Conclusions and Perspectives

1. General Conclusions

The thesis describes the synthesis of isocyanate-free PUs through the AROP technique and study of the self-assembly behavior of PU based amphiphilic linear block copolymers and graft copolymers. A series of PU homopolymers with different molecular weights and narrow polydispersity indexes has been synthesized. In addition, a series of PU based amphiphilic linear block copolymers PEG-*b*-PUs and graft copolymers PU-*g*-PEGs has also been prepared. The self-assembly behaviors of these PU based amphiphilic copolymers have been studied carefully. The present thesis manuscript mainly includes three chapters (chapter II, III and IV):

In the second chapter, a new isocyanate-free method to prepare PUs has been reported. Non-isocyanate and well-defined PUs with novel structures were prepared *via* the AROP of a 5-membered cyclic carbamate bearing a vinyl group (CHU) with using *n*-butyllithium as the initiator and CHU-derived imide as the co-initiator. The monomer was synthesized in three steps at 80 °C with a good yield. A series of PUs with different molecular weights was synthesized by changing the feeding ratios of monomer, initiator and co-initiator. The AROP mechanism was proposed and characterized by *in situ* IR and ^{13}C NMR. The ROP kinetics in the polymerization system was studied and the polymerization could present the characteristics of the first order kinetics in some cases. The preliminary study of the properties of the obtained PUs showed that they could emit blue fluorescence upon UV irradiation after thermal treatment. We believe the present work will provide more options and inspirations for people to prepare isocyanate-free PUs.

In the third chapter, a series of novel PU based amphiphilic PEG-*b*-PU linear diblock copolymers with different sequence lengths of PEG and PU were prepared *via* the AROP of CHU in the presence of mPEG based macromolecular co-initiators (mPEG-CHU). Three types of mPEG-CHU with different molecular weights of PEG were synthesized successfully by esterification between mPEG-OH and carboxylic acid

functionalized CHU (CHU-COOH). Two types of PEG$_{12}$-*b*-PU diblock copolymers and two types of PEG$_{22}$-*b*-PU diblock copolymers with different hydrophilic ratios were chosen for the self-assembly study using the nanoprecipitation technique. We found that PEG$_{12}$-*b*-PU diblock copolymers could self-assemble into vesicles or spherical micelles in water and PEG$_{22}$-*b*-PU$_{26}$ diblock copolymers could self-assemble into micelles with spherical or polygonal morphologies in water. In addition, the self-assemblies of the two PEG$_{22}$-*b*-PU diblock copolymers could emit strong cyan fluorescence when they were excited by UV light, which might have potential applications in biomedical areas such as drug delivery or bioimaging.

In the fourth chapter, novel PU based amphiphilic PU-*g*-PEG graft copolymers were prepared *via* the thiol-ene coupling reaction of PU homopolymer prepared by the AROP of CHU and thiol-terminated mPEG (mPEG-SH). mPEG-SH was prepared by the esterification of mPEG-OH (M_n = 550 Da) and thioglycolic acid catalyzed by sulfuric acid. Two PU-*g*-PEG graft copolymers with different backbone lengths and hydrophilic ratios were prepared. The CMC of the amphiphilic PU-*g*-PEG graft copolymers in water was measured by fluorescence technique. The self-assembly of PU-*g*-PEG graft copolymers was performed using the nanoprecipitation technique. We found that the PU-*g*-PEG graft copolymers could self-assemble into micelles with rough and irregular or disk-like micelles with a large diameter and thin thickness in water. The fluorescence microscopy characterization of the disk-like micelles showed blue circle nanoparticles with heterogeneous fluorescence emission phenomenon. All these findings enriched our knowledge about the self-assembly of amphiphilic graft copolymers and provided more novel functionalized nanostructural materials.

In conclusion, we have disclosed a new route of AROP of cyclic carbamates to prepare isocyanate-free PUs which represents a highly promising approach in PU production. PU homopolymers, PEG-*b*-PU linear diblock copolymers and PU-*g*-PEG graft copolymers have been prepared based on the AROP approach. The obtained copolymers are amphiphilic and can self-assemble into various defined aggregates with fluorescence emission property, which provides more novel PU based functionalized

nanostructural materials with potential applications.

2. Perspectives

In the present manuscript, we have successfully carried out the synthesis of PU homopolymers and copolymers as well as the self-assembly study of the corresponding PU-based copolymers. Nevertheless, more experimental and theoretical work is required to get deeper insight into the synthesis of PUs *via* AROP. Fox example, it will be interesting to prepare PUs with molecular weight higher than 10000 Da in the future. The AROP process needs to be optimized further in order to have a "living" process, enabling the polymer structure and properties to be easily tuned. It will also be crucial to explore and explain the fluorescence emission mechanism of PU samples after thermal treatment more precisely, which might have interesting applications in the area of optical materials.

In addition, it is necessary to study the self-assembly of PU-based amphiphilic copolymers further. For example, more PEG-*b*-PU block copolymers and PU-*g*-PEG graft copolymers with different hydrophilic ratios or grafting ratios need to be prepared to explore the effects of copolymer composition and structure on the self-assembly behavior. The self-assembly mechanisms of linear PEG-*b*-PU block copolymers and PU-*g*-PEG graft copolymers need to be described more precisely. Finally, more work is also needed to study the properties of the self-assemblies such as fluorescence property as well as their potential applications.

Publications

1. Zhou, L.; **<u>Zhang, D.</u> (Co-first author)**; Hocine, S.; Pilone, A.; Trépout, S.; Marco, S.; Thomas, C.; Guo, J.; Li, M.-H., Transition from smectic nanofibers to smectic vesicles in the self-assemblies of PEG-*b*-liquid crystal polycarbonates. *Polym. Chem.* **2017,** *8*, 4776-4780.

2. **<u>Zhang, D.</u>** et al. *Polymerization of Cyclic Carbamates: A Practical Route to Aliphatic Polyurethanes*. Submitted.

3. **<u>Zhang, D.</u>** et al. *Synthesis and self-assembly of polyurethane-based amphiphilic linear diblock copolymers.* In preparation.

4. **<u>Zhang, D.</u>** et al. *Synthesis and self-assembly of polyurethane-based amphiphilic graft copolymers*. In preparation.

RÉSUMÉ

   Le présent travail décrit la synthèse de polyuréthanes (PUs) sans isocyanate par la technique de polymérisation par ouverture de cycle anionique (AROP) et l'étude du comportement d'auto-assemblage de copolymères diblocs linéaires amphiphiles à base de PU et de copolymères greffés. Généralement, les PUs sont préparés par polyaddition de diols (ou polyols) sur des diisocyanates (ou polyisocyanates). Cette méthode nécessite des conditions drastiques pour conduire la réaction vers une conversion élevée et utilise des isocyanates très sensibles à l'humidité et toxiques, limitant ainsi leurs applications médicales. Dans ce travail, nous utilisons une nouvelle stratégie, basée sur la polymérisation par ouverture de cycle (ROP), pour obtenir des polyuréthanes aliphatiques à partir de carbamates cycliques. Une série d'homopolymères de PU ayant des poids moléculaires différents et des indices de polydispersité étroits ont été synthétisés. Par ailleurs, une série de copolymères diblocs linéaires amphiphiles à base de PU, PEG-*b*-PUs (polyéthylène glycol-*b*-polyuréthanes) et des copolymères greffés (PU-*g*-PEGs) ont été préparés. Les comportements d'auto-assemblage de ces copolymères amphiphiles à base de PU ont été étudiés en détails. La thèse se compose de cinq chapitres, dont le dernier est constitué par la partie expérimentale. Nous croyons que le présent travail fournira plus d'options et d'inspirations pour que les personnes puissent préparer des PUs sans isocyanate et des matériaux nanostructuraux fonctionnalisés à base de PU avec des applications potentielles.

MOTS CLÉS

Polyuréthane, polymérisation par ouverture de cycle anionique, auto-assemblage, copolymère dibloc, copolymère greffé

ABSTRACT

   The present work describes the synthesis of isocyanate-free polyurethanes (PUs) through the anionic ring-opening polymerization (AROP) technique and study of the self-assembly behavior of PU based amphiphilic linear diblock copolymers and graft copolymers. Generally, PUs are prepared by the polyaddition of diols (or polyols) with diisocyanates (or polyisocyanates). This method requires drastic conditions to drive the reaction toward high conversion and uses highly moisture sensitive and toxic isocyanates, thus limiting their medical applications. In this work, we use a new strategy, based on ring-opening polymerization (ROP), to obtain aliphatic polyurethanes from cyclic carbamates. A series of PU homopolymers with different molecular weights and narrow polydispersity indexes has been synthesized. Also, a series of PU based amphiphilic linear diblock copolymers PEG-*b*-PUs (polyethylene glycol-*b*-polyurethanes) and graft copolymers (PU-*g*-PEGs) has been prepared. The self-assembly behaviors of these PU based amphiphilic copolymers have been studied carefully. The present thesis manuscript consists of five chapters, in which the last chapter is the experimental part. We believe the present work will provide more options and inspirations for people to prepare isocyanate-free PUs and PU based functionalized nanostructural materials with potential applications.

KEYWORDS

Polyurethane, anionic ring-opening polymerization, self-assembly, diblock copolymer, graft copolymer